USGS
science for a changing world

Terrestrial Lidar Monitoring of the Effects of Glen Canyon Dam Operations on the Geomorphic Condition of Archaeological Sites in Grand Canyon National Park, 2010–2020

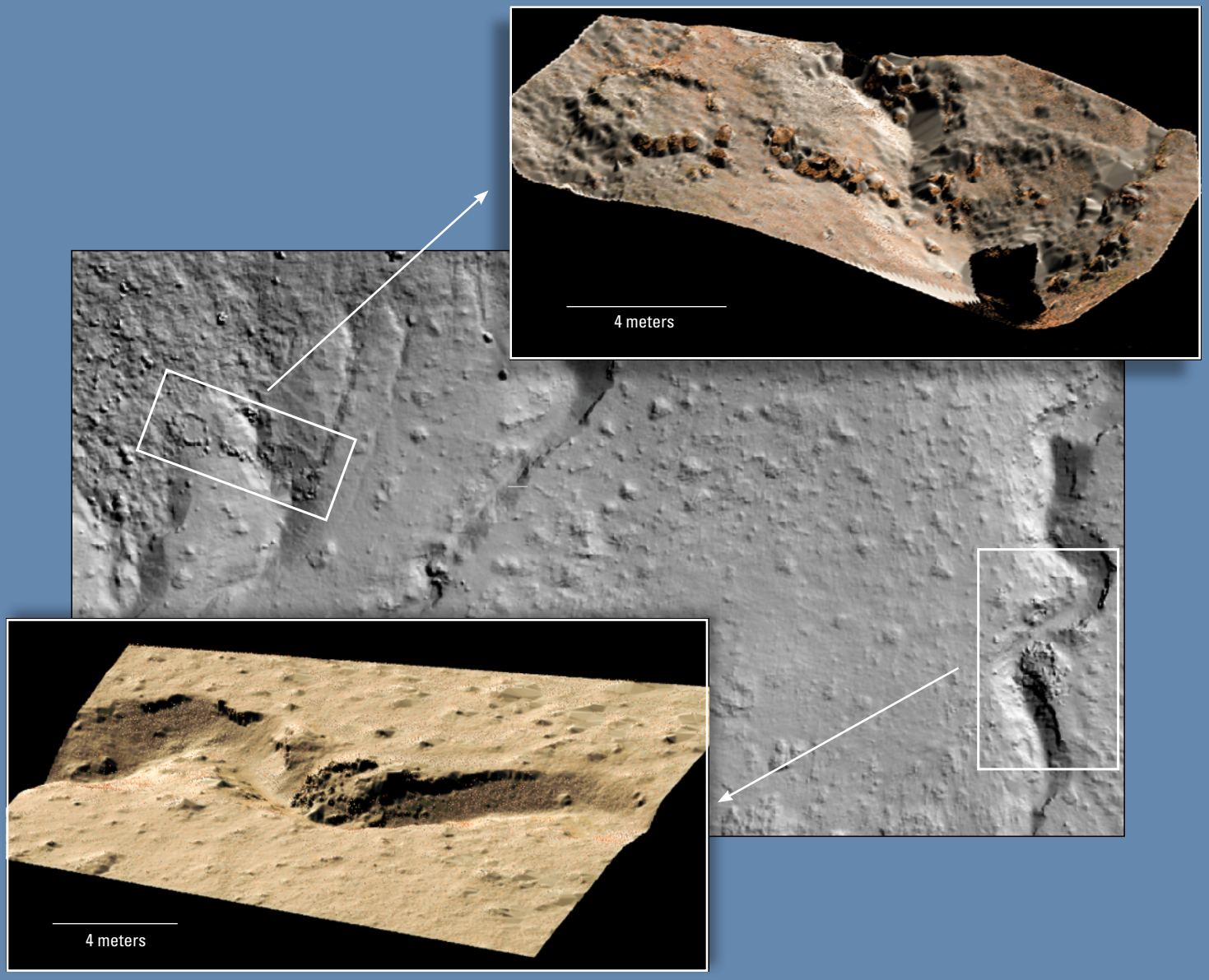

Open-File Report 2022–1097

U.S. Department of the Interior
U.S. Geological Survey

Cover. Shaded-relief images depicting three-dimensional topographic models from an archaeological site survey conducted in June 2020 within Grand Canyon National Park, Arizona.

Terrestrial Lidar Monitoring of the Effects of Glen Canyon Dam Operations on the Geomorphic Condition of Archaeological Sites in Grand Canyon National Park, 2010–2020

By Joshua Caster, Joel B. Sankey, Helen Fairley, and Alan Kasprak

Open-File Report 2022–1097

U.S. Department of the Interior
U.S. Geological Survey

U.S. Geological Survey, Reston, Virginia: 2022

Suggested citation:
Caster, J., Sankey, J.B., Fairley, H., and Kasprak, A., 2022, Terrestrial lidar monitoring of the effects of Glen Canyon Dam operations on the geomorphic condition of archaeological sites in Grand Canyon National Park, 2010–2020: U.S. Geological Survey Open-File Report 2022–1097, 100 p., https://doi.org/10.3133/ofr20221097.

ISSN 2331-1258 (online)

Acknowledgments

This study was supported by Glen Canyon Dam Adaptive Management Program funding from the Bureau of Reclamation through the U.S. Geological Survey (USGS) Grand Canyon Monitoring and Research Center and was conducted in collaboration with the National Park Service (NPS) in Grand Canyon National Park. We thank Jennifer Dierker for valuable guidance in the field and discussions regarding landscape processes and archeological sites. The ideas of Amy East and Brian Collins were instrumental to our conceptual understanding of landscape processes discussed herein. Aaron Borling, Nat Bransky, Skye Corbett, Joe Hazel, Keith Kohl, Mark Mastin, Paul Rauss, and Lauren Tango provided survey support. Carol Fritzinger and Ann-Marie Bringhurst coordinated field logistics; boat operators Carolyn Alvord, Don Bacco, Kirk Burnett, Jeremy Draper, Seth Felder, Dave Foster, Don Massman, Mark Perkins, Dennis Harris, and Dom Zanzucchi contributed in numerous ways to the field operations and data collection. We thank Jennifer Dierker, Ellen Brennan, and Michael Moran for reviewing previous drafts of this report.

Contents

Figures

Tables

Conversion Factors

International System of Units to U.S. customary units

Multiply	By	To obtain
	Length	
centimeter (cm)	0.3937	inch (in.)
millimeter (mm)	0.03937	inch (in.)
meter (m)	3.281	foot (ft)
kilometer (km)	0.6214	mile (mi)
meter (m)	1.094	yard (yd)
	Area	
square meter (m^2)	0.0002471	acre
square kilometer (km^2)	247.1	acre
square meter (m^2)	10.76	square foot (ft^2)
square kilometer (km^2)	0.3861	square mile (mi^2)
	Volume	
cubic meter (m^3)	264.2	gallon (gal)
cubic meter (m^3)	0.0002642	million gallons (Mgal)
cubic centimeter (cm^3)	0.06102	cubic inch (in^3)
cubic meter (m^3)	35.31	cubic foot (ft^3)
cubic meter (m^3)	1.308	cubic yard (yd^3)
cubic meter (m^3)	0.0008107	acre-foot (acre-ft)
	Flow rate	
meter per second (m/s)	3.281	foot per second (ft/s)
meter per minute (m/min)	3.281	foot per minute (ft/min)
meter per hour (m/hr)	3.281	foot per hour (ft/hr)
meter per day (m/d)	3.281	foot per day (ft/d)
meter per year (m/yr)	3.281	foot per year (ft/yr)
cubic meter per second (m^3/s)	35.31	cubic foot per second (ft^3/s)

Datum

Vertical coordinate information is referenced to the North American Vertical Datum of 1988 (NAVD 88). Horizontal coordinate information is referenced to the North American Datum of 1983 (NAD 83) and projected into the State Plane Arizona Central system. Elevation, as used in this report, refers to distance above the vertical datum.

Abbreviations

DEM	digital elevation model
DoD	DEM of difference
FIS	fuzzy inference system
GCD	geomorphic change detection
GCDAMP	Glen Canyon Dam Adaptive Management Program
GCMRC	Grand Canyon Monitoring and Research Center
HFE	high-flow experiment
lidar	light detection and ranging
NPS	National Park Service
TLS	terrestrial laser scanning (synonymous with ground-based lidar and terrestrial lidar)
USGS	U.S. Geological Survey

Terrestrial Lidar Monitoring of the Effects of Glen Canyon Dam Operations on the Geomorphic Condition of Archaeological Sites in Grand Canyon National Park, 2010–2020

By Joshua Caster, Joel B. Sankey, Helen Fairley, and Alan Kasprak

Abstract

The U.S. Geological Survey's Grand Canyon Monitoring and Research Center, in coordination with the Glen Canyon Dam Adaptive Management Program, has monitored the geomorphic condition of select archaeological sites along the Colorado River in Grand Canyon using high-resolution terrestrial light detection and ranging (lidar) topographic surveys. Many of these sites are vulnerable to degradation by natural erosional processes. Regulation of the Colorado River by some operations of Glen Canyon Dam has been shown to affect archaeological resources by directly or indirectly causing degradation of site condition. Conversely, some specific operations of Glen Canyon Dam, such as controlled flood releases (termed high flow experiments), can potentially be used to slow or stop erosion at some degraded archaeological sites. Results of monitoring conducted with terrestrial lidar surveys from 2006 to 2010 have been synthesized in previous reports and publications. Here, we present and summarize results of monitoring conducted at 30 archaeological sites within 23 monitoring locations from 2010 to 2020. This report presents a sample of a much larger population of Colorado River archaeological sites in Grand Canyon that are being qualitatively monitored by the National Park Service (NPS). To ensure relevance to the NPS monitoring program, the quantitative high-resolution topographic monitoring presented in this report focused on sites binned by geomorphic context, using two previously published geomorphic classification frameworks to identify important changes in geomorphic condition within archaeological sites that can be related to operations of Glen Canyon Dam. We found that 22 archaeological sites changed within one or both of the previously determined geomorphic classifications, and changes at 21 of those 22 sites were interpreted as a transition to a more degraded geomorphic condition. The monitoring records contained within this report represent the foundation for future monitoring of these and other archaeological sites with high-resolution topographic surveys and change detection. These monitoring results provide benchmarks for managers of cultural resources along the Colorado River in Grand Canyon to assess significant changes to cultural resource integrity, aid in future risk management at these locations, and illustrate methods relevant for assessing geomorphic condition changes within other river valleys.

Introduction and Purpose

The U.S. Geological Survey's (USGS) Grand Canyon Monitoring and Research Center (GCMRC), in conjunction with the Glen Canyon Dam Adaptive Management Program (GCDAMP), monitors landscape change along the Colorado River in Grand Canyon associated with the operations of Glen Canyon Dam (U.S. Department of the Interior, 2016). Monitoring efforts are focused on a variety of resources within the regulated active river channel, which is defined as the area inundated by the maximum regulated river discharge. Dam operations can also affect areas outside of the active river channel, which can affect cultural, environmental, and recreational resources (U.S. Department of the Interior, 1996, 2016). Potential effects on archaeological and other cultural resources outside of the regulated active river channel have been linked to reduced river sediment supply and increased riparian vegetation (Fairley and Sondossi, 2010; Draut, 2012; Collins and others, 2016; East and others, 2016; Sankey and others, 2018a; Cook and others, 2019). Long-term reduction in river sandbar area and volume caused by erosion, loss of sediment supply owing to trapping by Lake Powell reservoir upstream, increased baseflows inundating contemporary sand deposits, and vegetation encroachment associated with dam operations have affected sediment transport (exchange) between the contemporary and historical active river channel (Draut, 2012; East and others, 2016; Sankey and others, 2018a; Cook and others, 2019). As a result, bare, unvegetated sand resources have decreased in area throughout the river corridor since dam completion in 1963 (Kasprak and others, 2018, 2021). The decreases in the areal coverage of bare sand, and the decreased exchange of sediment between the contemporary and historical active river channels have affected the condition of archaeological sites and other cultural resources that are dependent on burial by river-derived sand to provide a protective barrier against erosional processes (Collins and others, 2016; East and others, 2016).

Implementation of periodic high-flow releases from the dam to promote flood deposition onto channel bars, termed high-flow experiments (HFE), have been conducted annually since 2012 as environmental conditions have allowed. HFEs are implemented in response to specific criteria, such as sedimentary inputs to the Colorado River by tributaries downstream of the dam, and, as occurred in 2015 and 2017,

these criteria are not always met during the annual cycle and thus a flood is not implemented (fig. 1). HFEs are intended to resupply sandbars with sediment, increasing sandbar area and volume, and thereby increasing sand storage within the river corridor. Sandbars that are rebuilt by HFEs have been shown to subsequently provide sand via aeolian (wind-driven) processes to resupply dune fields throughout Marble and Grand Canyons. These dune field areas commonly contain archaeological sites (Sankey and others, 2018b). Such aeolian dune fields with archaeological sites were resupplied with sand from HFE deposits in many of the instances monitored after the 2012, 2013, 2014, and 2016 HFEs (Sankey and others, 2018b). There is also evidence that HFEs with annual frequency have a cumulative effect on sediment resupply of dune fields (Sankey and others, 2018b).

As a method of assessing normal and experimental dam operation effects on cultural resources, high-resolution, laser-based, light detection and ranging (lidar) topographic surveys have been used to assess local landscape change at archaeological sites by GCMRC since 2006. Prior to 2010, 13 sites had been surveyed with lidar, and 9 of these sites had been surveyed at least twice, allowing changes in surface condition through time to be documented and measured. Since 2010, as many as seven repeat topographic surveys have been conducted at monitoring locations within Grand Canyon National Park spanning five HFEs (fig. 1). Parts of these data have been published previously (Collins and others, 2008, 2009, 2012, 2016; East and others, 2016; Sankey and others, 2018b). Collins and others (2012, 2016) synthesized survey results between 2006 and 2010 at 13 monitoring locations (Collins and others, 2008, 2009, 2012). This report is intended to synthesize monitoring efforts within Grand Canyon between 2010 and 2020 at 30 archaeological sites; surveys conducted prior to 2010 are not examined herein. Where repeat survey data are available since 2010, the results of the change detection analyses are presented to illustrate how archaeological sites have changed and whether changes have caused site geomorphic condition to become more degraded or less degraded. The findings presented within this document are expected to be useful for land managers to identify patterns of change within the surveyed sites that can be applied to a broader understanding of the physical processes affecting archaeological and cultural resources within Grand Canyon National Park. A secondary goal of this report is to provide a baseline dataset for future quantitative monitoring of archaeological site geomorphic condition in the park. Finally, this report may add to the scientific understanding of linkages between fluvial, aeolian, and alluvial (hillslope and rainfall-runoff) geomorphic processes that are relevant in river valleys beyond the setting of this study.

Methods

Monitoring Site Selection and Classification

Archaeological monitoring sites in Grand Canyon National Park, Arizona (fig. 2), were selected for topographic surveying using several criteria, including (1) potential for sites to be affected by dam operations, (2) availability of previous records, and (3) low potential for surveyor impacts during site visits. The potential

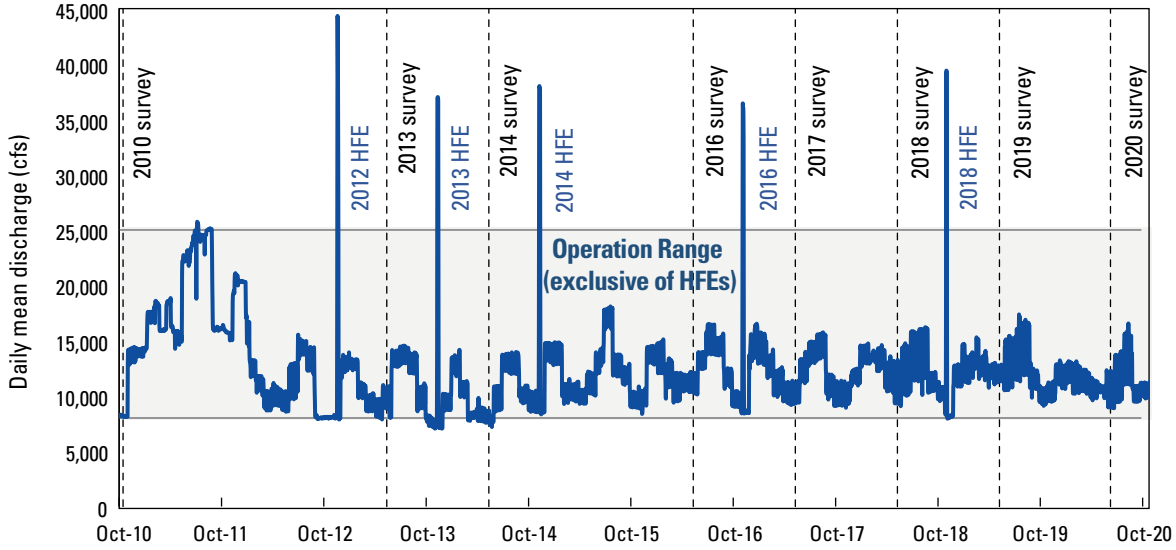

Figure 1. Plot of daily mean discharge recorded at U.S. Geological Survey streamgage 09380000 in the Colorado River at Lees Ferry, Arizona. Dates of eight high-resolution topographic survey campaigns (dashed lines) and discharges of five high-flow experiments (HFEs; solid lines) are labeled for reference. The Glen Canyon Dam flow operation range, excluding HFEs, was approximately 8,000 to 25,000 cubic feet per second (cfs). Mean discharge data were acquired from https://waterdata.usgs.gov on February 1, 2021.

for dam operational effects to archaeological sites within Grand Canyon has been extensively described (Draut, 2012; Collins and others, 2016; East and others, 2016, 2017) and can be summarized into two general classification schemes that are focused on geomorphic processes that erode, transport, and deposit sediment. The first classification scheme was proposed by Hereford and others (1993) and binned sites based on potential for sediment loss by erosion owing to excess rainfall runoff and gullying. In this classification, sites are ranked numerically from 1 to 4 as follows.

- *Drainage type 1*.— Sites are not dissected by rills, gullies, or arroyos.
- *Drainage type 2*.—Sites are dissected by rills, gullies, or arroyos that do not grade to the active river channel or a side canyon tributary.
- *Drainage type 3*.—Sites are dissected by rills, gullies, or arroyos that grade to a side canyon tributary.
- *Drainage type 4*.—Sites are dissected by rills, gullies, or arroyos that grade to the active river channel.

Implicit in this classification is the hypothesis that drainages that grade to a lower base level (that is, the mainstem Colorado River) have a greater propensity to cause erosion of adjacent upland areas given their relatively higher slope and stream power. In this system, higher ranking drainage classes (drainage types 3 and 4) represent mature gullies and lower ranking classes (drainage types 1 and 2) represent less developed drainage networks (East and others, 2017). This system, termed the "drainage classification," has been recently updated for sites within Glen and Grand Canyons as a metric for assessing change in the maturity of drainage networks (East and others, 2017).

East and others (2016, 2017) developed a separate site classification for characterizing sediment connectivity between the active Colorado River channel and the surrounding landscape through aeolian sediment transport. In this system, termed the "aeolian classification," sites are ranked by the availability of river sediment from fluvial sandbars and potential obstructions to wind-driven sediment transport from these fluvial sandbars to the archaeological site. Sites are classified as follows.

- *Aeolian type 1*.— Sites have an adjacent, upwind sandbar with no substantial barriers to impede sediment transport by wind.
- *Aeolian type 2*.—Sites have an adjacent, upwind sandbar but have a barrier that could impede sediment transport by wind. These are divided into three barrier types.
  - *Type 2a*.—A vegetative barrier is present.
  - *Type 2b*.—A topographic barrier is present (for example, a tributary channel or bedrock outcrop).
  - *Type 2c*.—Both vegetative and topographic barriers are present.
- *Aeolian type 3*.—Sites have an adjacent, upwind shoreline but no modern sandbar is present.
- *Aeolian type 4*.—Sites are situated in river-derived sediment but do not have an adjacent upwind shoreline or sandbar present.
- *Aeolian type 5*.—River-derived sediment is nonexistent or only incidental to site setting.

Aeolian type 1 sites are expected to have the greatest sediment connectivity with the active river channel. Impediments to sediment transport (aeolian type 2) and loss of upwind fluvial sandbars (aeolian type 3) reduce this connectivity, potentially limiting sediment supply that may ameliorate some runoff erosion and gullying within archaeological sites (Sankey and Draut, 2014).

Monitoring sites were selected to include a larger proportion of aeolian type 1 and 2 sites than types 3–5. Though a diversity of classes is important for quantitatively testing for site type effects, aeolian types 1 and 2 represent the greatest potential to be affected by dam operations (East and others, 2016, 2017), as changes in river flow regime could lead to increases or decreases in sediment supply (that is, upwind sandbars) or encroachment of riparian vegetation onto those areas. Thus, initial site selection emphasized aeolian types 1 and 2 to monitor system sensitivity. Some of the selected monitoring locations contained more than one archaeological site with different aeolian or drainage classifications. These locations permit more robust analyses of site type effects under similar weather conditions and substrate characteristics.

Survey Methods and Topographic Data Analysis

We conducted high-resolution topographic surveys at 23 monitoring locations containing 30 individual archaeological sites within Grand Canyon (fig. 2; appendix 1) using terrestrial laser scanning (TLS or lidar) between September 2010 and June 2020. TLS is a ground-based, line-of-sight survey method that uses infrared lasers to measure distance to objects readily visible by the instrument. Because of the line-of-sight requirement, TLS survey protocol used multiple scan positions to achieve maximum survey coverage by reducing survey gaps owing to topographic or vegetative barriers to laser measurements from one or more survey positions. To ensure accurate registration of the data from multiposition surveys, ground control targets were stationed within the lidar survey area and then surveyed using a total station referenced to the USGS geodesic network within Grand Canyon. Referenced ground control targets are used to assess proper alignment of topographic measurements and to geographically reference the survey within the Arizona State Plane coordinate projection system.

During September 2010 and May 2013, USGS scientists Brian Collins and Skye Corbett conducted surveys using a RIEGL VZ-400 TLS instrument. These procedures were carried forward to surveys conducted by Skye Corbett in May 2014 and later by the authors of this report in May 2016 through June 2020 using a RIEGL VZ-1000 TLS instrument (fig. 3). TLS surveys generate a dense set of point measurements, termed a point cloud, that can be used to create a topographic model. A topographic model, such as a digital elevation model (DEM), represents continuous elevation

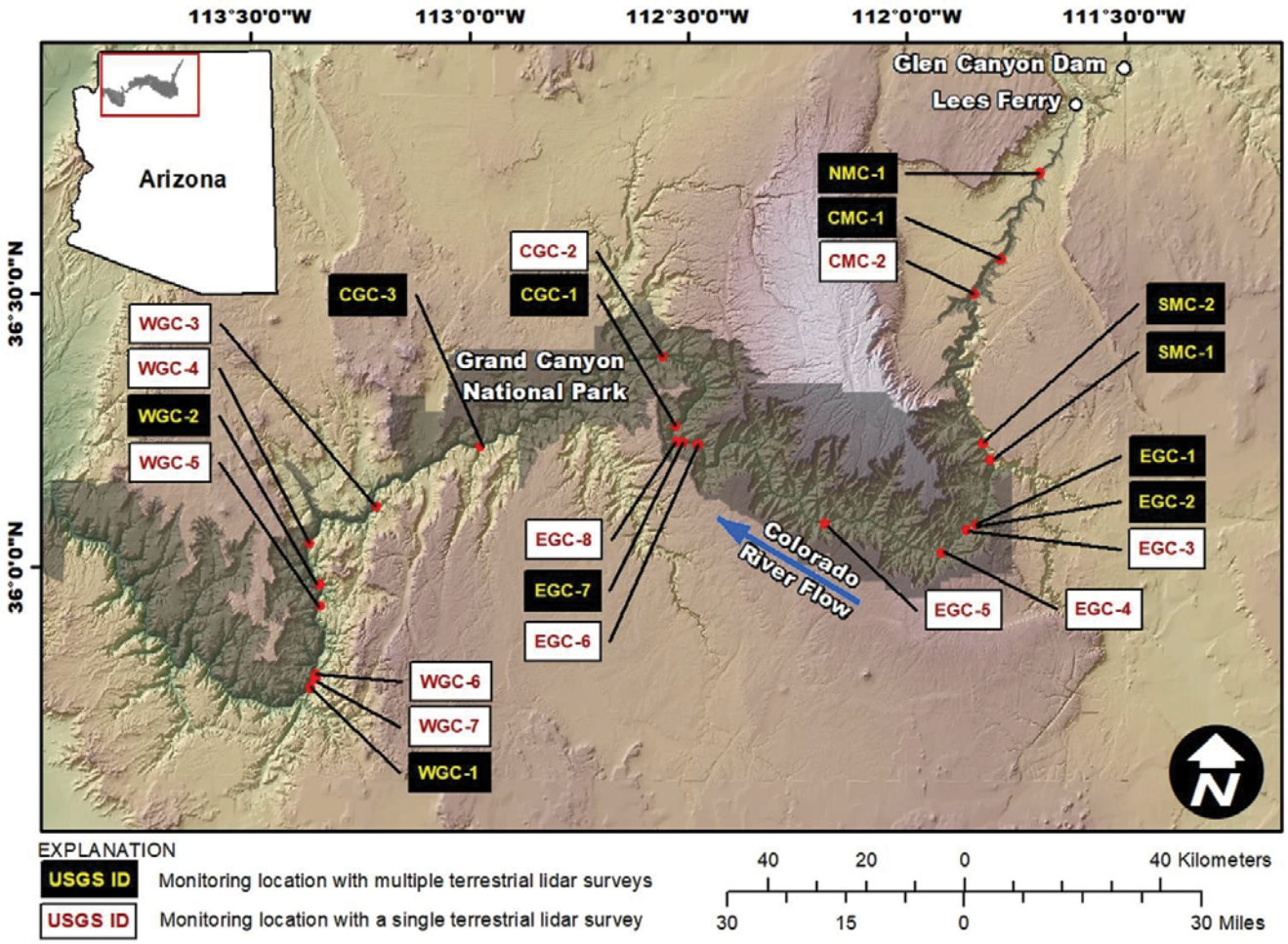

Figure 2. Map of Grand Canyon, Arizona, showing monitoring locations along the Colorado River. Location labels are color coded to identify sites with one, as opposed to more than one, terrestrial light detection and ranging (lidar) survey. The locations of Glen Canyon Dam and Lees Ferry streamgage as well as the Grand Canyon National Park (dark gray) are provided for reference. Base from U.S. Geological Survey's The National Map 30-meter digital data, 2018.

Figure 3. Photograph of a survey being conducted using the RIEGL VZ-1000 terrestrial laser scanner (TLS) in Grand Canyon, Arizona. TLS instrument and reflective survey ground control target are identified on the image. Photograph by Alan Fairley, U.S. Geological Survey volunteer.

data summarized into raster cells, or pixels, of a given spatial resolution. The resolution of the topographic model is user-defined but is generally based on point density of the point cloud, with the mean point density used to inform appropriate raster cell size. Point density within the overlapping survey areas for all periods were ≥400 points per square meter. This minimum point density provided sufficient data to produce 5-centimeter (cm) pixel resolution DEMs.

We processed TLS point cloud datasets to separate vegetation and ground surface topographic measurements, termed the bare earth surface, using Maptek's I-Site Studio v. 7.0.5 software topographic filters. The bare-earth surface point cloud was used to generate DEMs for all 23 monitoring locations within Esri's ArcGIS v. 10.5 software. For this report, the 23 monitoring locations are organized into two groups: (1) locations with a single TLS survey and (2) locations with more than one TLS survey between 2010 and 2020 (fig. 2). At each monitoring site, we established a baseline survey area that represents the highest quality data within the area surrounding a resource of interest.

Monitoring Locations with a Single Survey

Between 2016 and 2020, we surveyed a total of 16 new monitoring locations that had no previous TLS survey (fig. 2). For these new locations, we used field and aerial photograph observations of the distribution of unconsolidated (that is, non-bedrock) sediment along with measurement point density and topographic variability to establish a baseline survey area to be compared with future survey campaigns. The baseline survey area within the DEMs for these monitoring locations represents the highest quality data available at 5-cm resolution and suitable for use in geomorphic change detection. However, a large extent of topographic data are also available at each site that could be used at lower resolutions (25 cm to 1 meter [m]) suitable for other applications not covered within this report, such as rainfall runoff characterization, debris flow roughness estimations, or vegetative canopy analysis.

Monitoring Locations with Repeat Surveys

Six monitoring sites were surveyed using TLS in 2010 and then were resurveyed at least once between 2013 and 2020. Four of the six monitoring locations (CMC-1, EGC-1, CGC-1, and WGC-1; fig. 2; appendix 1) have four or more repeat TLS survey datasets. For these areas as well as monitoring location EGC-2, we determined the baseline survey areas by the extent of the earliest survey period (2010) and its overlap with subsequent surveys. For monitoring location SMC-1, we conducted a single repeat TLS survey in May 2018 that covered a substantially larger portion of the area than the 2010 survey. For this reason, we established a larger baseline survey area at SMC-1 following the methods described for the monitoring locations with a single survey.

In addition to the six monitoring locations with 2010 TLS datasets, we also collected two or more surveys at five other monitoring locations. Baseline data at the monitoring locations NMC-1, SMC-2, EGC-7, CGC-1, and CGC-3 were collected between 2016 and 2019 and repeat datasets were collected between 2018 and 2020. The monitoring location WGC-2 had a previous 2007 TLS survey that preceded the 2010 baseline date; that dataset covered much of the 2020 survey area and is included in this report to assess geomorphic changes.

Geomorphic Change Detection with Repeat Surveys

Some of the topographic data collected at the repeat survey locations along with analyses of topographic changes have been presented in previous reports (Collins and others, 2016; East and others, 2016; Sankey and others, 2018b). Here we expand these analyses to include the 2017, 2018, 2019, and 2020 surveys and interpretation of topographic change using an automated geomorphic attribution process that has not yet been presented in previous reports for the entirety of these data prior to this study.

We conducted topographic change detection between each consecutive pair of repeat DEMs using Wheaton and others' (2010) geomorphic change detection tool (GCD 7; available at http://gcd.riverscapes.xyz) to create a DEM of difference (DoD) that spatially represents inter-survey landscape change as elevation shifts between two survey DEMs. As error exists within all modeled surfaces, we assessed topographic uncertainty within the GCD software to assign confidence to measured differences in the DoD. We accounted for survey uncertainty using a fuzzy inference system (FIS) model within GCD 7. In this FIS, uncertainty is defined by elevation differences between coincident points or points with the same x- and y-coordinates after rounding to the nearest meter, centimeter, or millimeter. To parameterize the FIS model, we compared elevations of coincident points rounded to the nearest centimeter as a function of TLS point density, DEM slope, and topographic roughness (standard deviation of slope). These data can then be translated to a spatially continuous estimation of measurement uncertainty using fuzzy logic, a system that uses descriptive categorical relations between multiple input variables and translates these to an output response variable (here, elevation error on a pixel-by-pixel basis). We summarized DoD change results at the 95-percent confidence interval for all repeat survey locations and survey intervals using the FIS error models to define the threshold for significant topographic change. In addition to this confidence threshold, a minimum detection limit was set as the data registration error, representing the root mean square error of coincident points between different TLS surveys. Following Collins and others' (2012, 2016) protocol, this detection limit was typically ≤3 cm and represented the smallest elevation change that we could reliably detect. Vegetation can impede measurement density and increase elevation uncertainty, so we removed changes identified within areas of dense vegetation—defined as one standard deviation above classified mean TLS vegetation point density (Norman and others, 2017). The DoDs presented here therefore represent high confidence estimates of topographic change within the survey area that provide a minimum estimate of total geomorphic change.

We identified a subset of areas of significant topographic change within each DoD by the most probable geomorphic mechanism of change using Kasprak and others' (2017)

automated geomorphic attribution software. This method uses survey topography and DoDs to generate as many as three different geomorphic mechanisms of topographic change for each pixel within the baseline study area. These mechanisms are then ranked and assigned a dominant process according to probability based on field validation and mechanism agreement. Geomorphic mechanisms considered in this software include fluvial, alluvial, colluvial, and aeolian processes (table 1). Where the probability of one of these mechanisms was low, topographic change was classified as indeterminate, meaning no geomorphic mechanism could be confidently identified (table 1). This provided a conservative estimate of classified topographic change but may underestimate the reported volume of aeolian, alluvial, and colluvial change in sediment storage. Fluvial processes were less influenced by indeterminate classifications owing to the nature of the automated attribution process. In general, the automated attribution process matched field observations and was considered reliable for assessing temporal changes within each mechanism.

Results

In the following sections, results are presented by survey group, first for monitoring locations with a single survey and then for monitoring locations with repeat surveys. For both survey groups, we segregated the baseline survey area by the extent of the modeled maximum regulated flood inundation area at 45,000 cubic feet per second (ft^3/s) (Magirl and others, 2008), termed maximum flood elevation, and the National Park Service (NPS)-documented archaeological site boundary (table 1). For monitoring locations with repeat surveys, we used additional spatial divisions, including archaeological features within defined cultural resource sites and mechanisms of change defined by the automated geomorphic attribution software. For archaeological features, the mapped extents have been excluded (see explanation in table 1). Table 1 provides a detailed explanation of each spatial division. Within the group of locations with repeat surveys, change detection and geomorphic attribution are summarized for as many as six DoD intervals designated by the years evaluated. For example,

Table 1. Survey area subdivisions and descriptions.

[The first three spatial subdivisions apply to monitoring locations with a single survey and with repeat surveys. The archaeological features, geomorphic processes, and change areas are used solely for segregating topographic change within monitoring locations with repeat surveys. DEM, digital elevation model; ft^3/s, cubic feet per second]

Spatial subdivision	Description
Baseline survey area	Area of interest showing the maximum extent of survey data with sufficient resolution to detect change. At sites where multiple DEMs exist from repeat surveys and survey coverage extent differed between DEMs, the baseline survey area was calculated as the maximum overlap between repeat surveys.
Above or below maximum flood elevation	Portion of survey area that is either above or below the maximum regulated flow elevation at a discharge of 45,000 ft^3/s based on Magirl and others' (2008) flow model.
Archaeological site boundary	Portion of the survey area that is within the mapped archaeological site and (or) feature boundaries. This area is included with the above maximum flood elevation spatial subdivision.
Archaeological features	Surveyed archaeological features associated with an archaeological site. Feature locations are not provided in this report as archaeological location information is protected from disclosure by Freedom of Information Act (b)(3). For further information please contact the National Park Service Cultural Resources Program.
Feature + buffer	A 1-meter buffer surrounding all surveyed archaeological features was included for summarizing topographic change. This additional buffer area is intended to capture near-feature changes that could pose future geomorphic effects.
Automated geomorphic attribution products	
Fluvial	Geomorphic change within the active channel by Colorado River flow.
Aeolian	Geomorphic change by wind-driven sediment transport.
Alluvial	Geomorphic change by rainfall runoff or gully processes.
Colluvial	Geomorphic change by gravity or slope failure.
Indeterminate	Geomorphic change that did not fit criteria for inclusion in other classes.
Summarized cumulative results	
Single change area	All pixels that have significant topographic changes documented in only one DEM of difference for the entire monitoring period to date.
Repeat change area	All pixels that have significant topographic changes documented in at least two DEMs of difference for the entire monitoring period to date.

$DoD_{2016–2017}$ represents a DoD created from May 2016 and May 2017 surveys. Three monitoring locations (CMC-1, EGC-1, and WGC-1) have six DoDs, monitoring location CGC-1 has four DoDs, monitoring location EGC-7 has two DoDs, and monitoring locations NMC-1, SMC-1, SMC-2, EGC-2, CGC-3, and WGC-2 have one DoD. Results for each DoD within a single monitoring location are presented graphically and summarized within tables containing areal and volumetric differences between topographic surveys. For sites with multiple survey intervals, cumulative results are presented as net volumetric changes in sediment storage since the baseline survey, where spatio-temporal continuity in topographic change is represented by measured erosion and deposition within the same areas over multiple DoDs (table 1).

Monitoring Locations with a Single Survey

Monitoring Location CMC-2

Monitoring location CMC-2 is located in central Marble Canyon on river right. In May 2017, we conducted TLS surveys for two separate baseline areas. The upstream area (fig. 4) includes the archaeological site C:05:0037 and surrounding landscape leading to a fluvial sandbar that is connected to a debris fan (fig. 4). The downstream area (fig. 4) is a section of the sandbar that is separated from the upstream site by water at a Colorado River discharge of 8,000 ft^3/s. The downstream area sandbar is a potential sediment source for wind transport to the upstream area and has been previously monitored as part of a USGS sandbar monitoring program (Hazel and others, 2010; Grams and others, 2013). A total of 4,991 square meters (m^2) are included in the combined baseline survey area, approximately half of which is below the maximum flood elevation (table 2). Almost all of the mapped archaeological site is contained within the upstream baseline survey area. This site was classified as aeolian type 2a owing to extensive riparian vegetation that grows between the sandbar and archaeological site. Gullies within the archaeological site connect to larger gullies downslope that have incised to the river. Hence, the site is classified as drainage type 4. Three features within the site were surveyed conventionally using a prism rod and total station to define their locations for future assessments of change. Table 2 provides a summary of the survey divisions in figure 4.

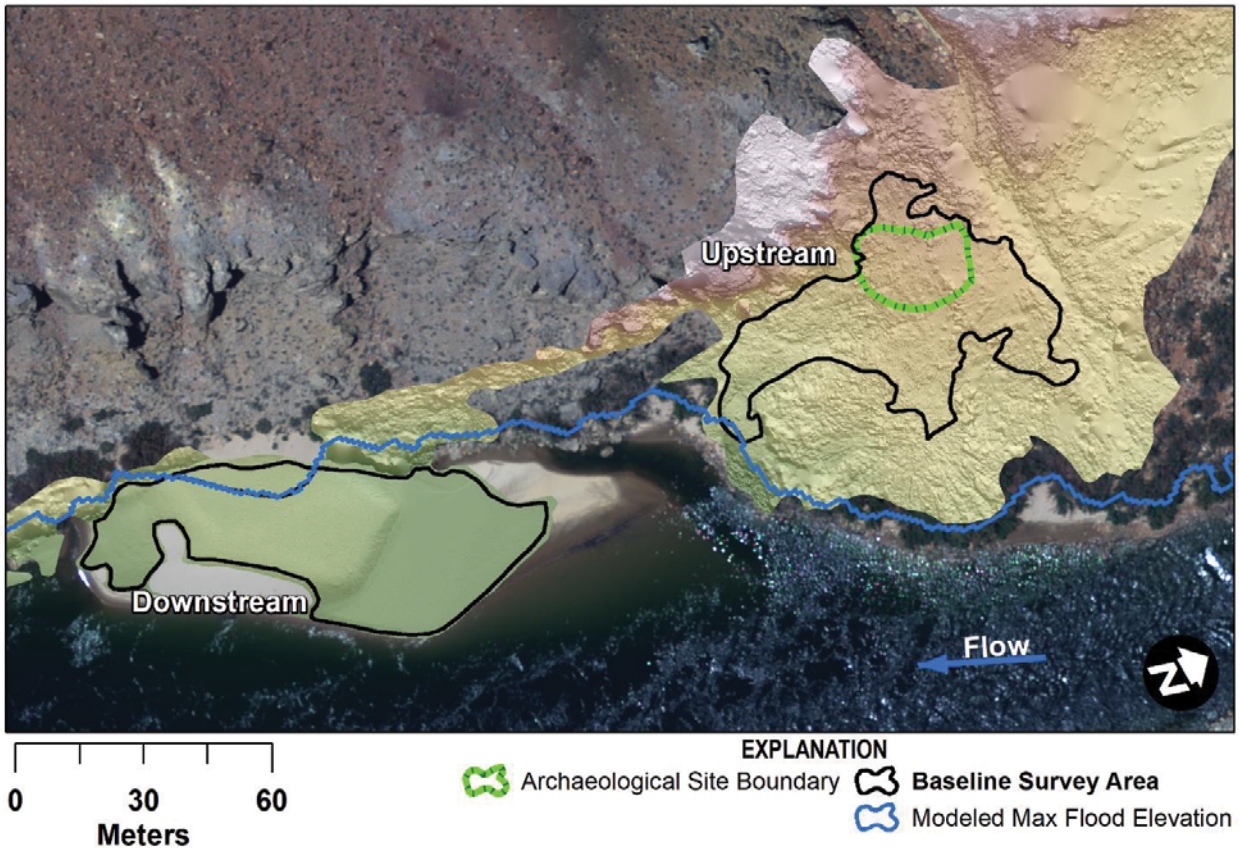

Figure 4. Digital elevation model and shaded-relief map for the survey conducted in May 2017 at monitoring location CMC-2, central Marble Canyon, Arizona. Aerial image collected by Grand Canyon Monitoring and Research Center (Durning and others, 2018).

Table 2. Summary of survey coverage at monitoring location CMC-2, central Marble Canyon, Arizona.

[Divisions within and outside of the survey represent the area of the archaeological site either within or outside of the baseline survey area, respectively. Below maximum flood elevation represents the portion of the baseline survey area that is potentially inundated by controlled floods. Archaeological site boundary information provided by the National Park Service. m^2, square meter; NA, not applicable]

Spatial subdivision	Area (m^2)	
	Within survey	Outside of survey
Baseline survey (upstream)	2,288.89	NA
Baseline survey (downstream)	2,701.83	NA
Below maximum flood elevation	2,548.17	NA
Archaeological site boundary (C:05:0037)	418.96	2.68
Feature 1	29.20	0.00
Feature 2	25.51	0.00
Feature 3	8.11	0.00

Monitoring Location EGC-3

Monitoring location EGC-3 is located in eastern Grand Canyon on river left. In May 2018, we surveyed the downstream part of a vegetated debris fan with one archaeological site (C:13:0069) located upslope of a prominent sand dune. In addition to the archaeological site, this location also contains a National Park Service vegetation restoration area at the river margin that was partially included within the survey (fig. 5). The baseline survey area was spatially divided into two parts. The upstream part contains the archaeological site and associated upwind sediment source (fig. 5). The downstream part contains an area of recent vegetation restoration activity (fig. 5). A total of 22,932 m^2 are included in the baseline survey area (table 3). All of the mapped archaeological site is contained within the baseline survey area. Site C:13:0069 is classified as aeolian type 2a because of an extensive riparian vegetative barrier to aeolian sediment transport between the active river channel and the site. The site is classified as drainage type 4 owing to a gully extending through the western part of the site that has incised to the Colorado River channel. No features were mapped during the survey to minimize effects on the site. Table 3 provides a summary of the survey divisions in figure 5.

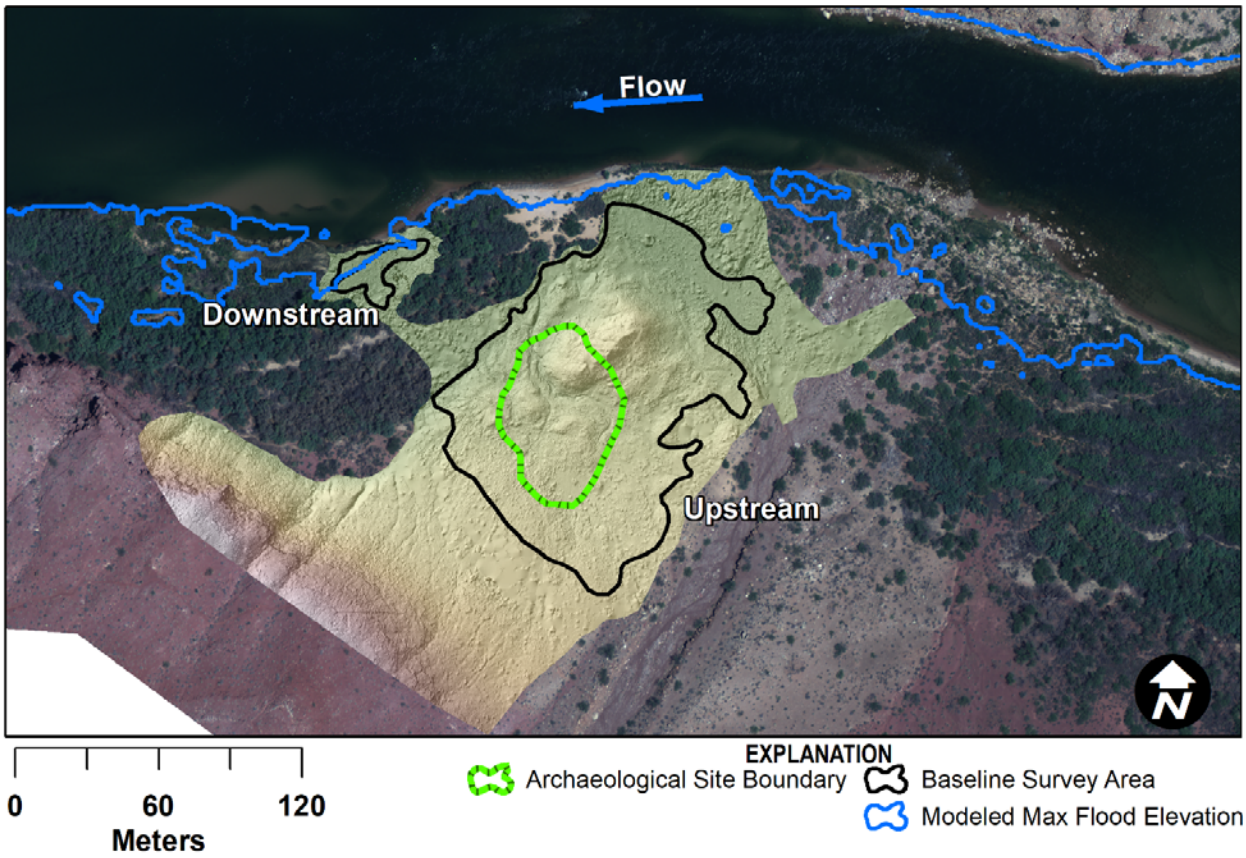

Figure 5. Digital elevation model and shaded-relief map for the survey conducted in May 2018 at monitoring location EGC-3, eastern Grand Canyon, Arizona. Aerial image collected by Grand Canyon Monitoring and Research Center (Durning and others, 2018).

Table 3. Summary of survey coverage at monitoring location EGC-3, eastern Grand Canyon, Arizona.

[Divisions within and outside of the survey represent the area of the archaeological site either within or outside of the baseline survey area, respectively. Below maximum flood elevation represents the portion of the baseline survey area that is potentially inundated by controlled floods. Archaeological site boundary information provided by the National Park Service. m^2, square meter; NA, not applicable]

Spatial subdivision	Area (m^2)	
	Within survey	Outside of survey
Baseline survey (upstream)	12,555.70	NA
Baseline survey (downstream)	376.53	NA
Below maximum flood elevation	114.75	NA
Archaeological site boundary (C:13:0069)	2,706.53	0.00

Monitoring Location EGC-4

Monitoring location EGC-4 is located in eastern Grand Canyon on river left. In May 2018, we surveyed a large aeolian sand dune superimposed on a boulder-rich debris fan. The area surveyed contained three archaeological sites; sites C:13:0005 and C:13:0392 are upstream of a side canyon tributary channel that bisects the survey area and site C:13:0393 is downstream of the tributary channel (fig. 6). The baseline survey area extends from the downstream active river channel, which represents the historical windblown sediment source for the aeolian dune on the debris fan (East and others, 2016), to the largest archaeological site C:13:0005 upstream of the tributary channel (fig. 6). A total of 25,668 m^2 are included in the baseline survey area (table 4). Approximately 49 percent of site C:13:0005 (table 4) is contained within the baseline survey area as well as most of the other two sites (88 percent of site C:13:0392 and 99.7 percent of site C:13:0393). No sandbar is present along the upwind shoreline, making all three sites aeolian type 3. Site C:13:0005 contains some small gullies that have not incised to the side canyon tributary; the site is classified as drainage type 2. The other two archaeological sites are classified as drainage type 1 because they have no gullies (fig. 6). Individual features were not mapped during the survey. Table 4 provides a summary of the survey divisions in figure 6.

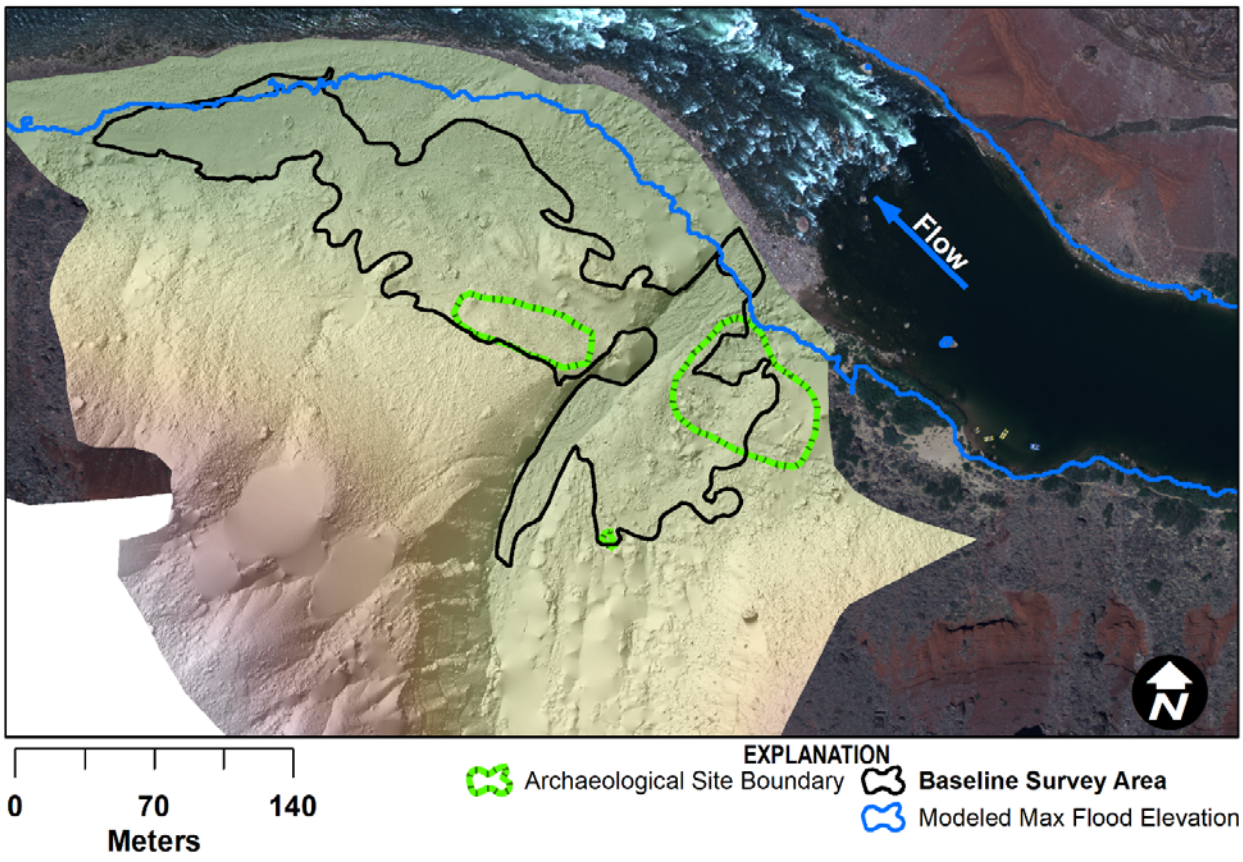

Figure 6. Digital elevation model and shaded-relief map for the survey conducted in May 2018 at monitoring location EGC-4, eastern Grand Canyon, Arizona. Aerial image collected by Grand Canyon Monitoring and Research Center (Durning and others, 2018).

Table 4. Summary of survey coverage at monitoring location EGC-4, eastern Grand Canyon, Arizona.

[Divisions within and outside of the survey represent the area of the archaeological site either within or outside of the baseline survey area, respectively. Below maximum flood elevation represents the portion of the baseline survey area that is potentially inundated by controlled floods. Archaeological site boundary information provided by the National Park Service. m^2, square meter; NA, not applicable]

Spatial subdivision	Area (m^2)	
	Within survey	Outside of survey
Baseline survey	25,668.11	NA
Below maximum flood elevation	799.11	NA
Archaeological site boundary 1 (C:13:0005)	1,695.80	1,757.81
Archaeological site boundary 2 (C:13:0392)	24.97	3.29
Archaeological site boundary 3 (C:13:0393)	1,446.19	4.17

Monitoring Location EGC-5

Monitoring location EGC-5 is located in eastern Grand Canyon on river left. In June 2020, we surveyed the downstream part of a rocky debris fan and side canyon tributary that has one archaeological site (B:16:0911). The baseline survey area covered 8,090 m^2 that included a portion of the downstream sandbar, the bed and banks of the side canyon tributary, and historical flood and windblown sand deposited on a low bluff of metamorphic basement rock (fig. 7; table 5). The archaeological site was not previously digitized, and the location has been estimated from documentation of a partial excavation conducted previously by the NPS and a formal survey of one identified feature within the excavated area during the June 2020 field expedition. Most of the mapped archaeological site is contained within the baseline survey area and is located along alluvial benches within the side canyon tributary. Site B:16:0911 is aeolian type 2c because of vegetative and topographic barriers to aeolian sediment transport between the active river channel and the site. The site is drainage type 3 owing to a gully that extends through the southwest part of the site that has incised to the side canyon tributary. Table 5 provides a summary of the survey divisions in figure 7.

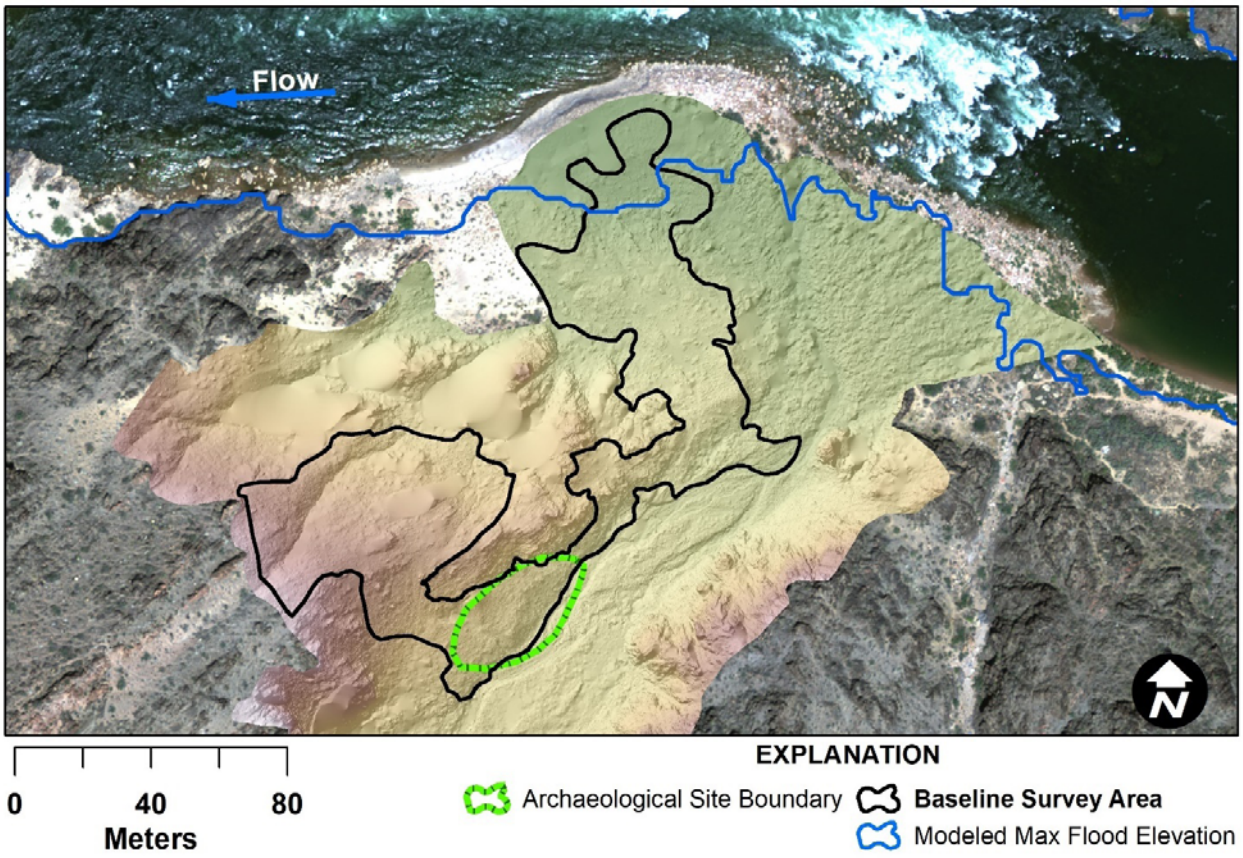

Figure 7. Digital elevation model and shaded-relief map for the survey conducted in June 2020 at monitoring location EGC-5, eastern Grand Canyon, Arizona. Aerial image collected by Grand Canyon Monitoring and Research Center (Durning and others, 2018).

Table 5. Summary of survey coverage at monitoring location EGC-5, eastern Grand Canyon, Arizona.

[Divisions within and outside of the survey represent the area of the archaeological site either within or outside of the baseline survey area, respectively. Below maximum flood elevation represents the portion of the baseline survey area that is potentially inundated by controlled floods. Archaeological site boundary information provided by the National Park Service. m^2, square meter; NA, not applicable]

Spatial subdivision	Area (m^2)	
	Within survey	Outside of survey
Baseline survey	8,090.30	NA
Below maximum flood elevation	501.60	NA
Archaeological site boundary (B:16:0911)	678.40	122.20

Monitoring Location EGC-6

Monitoring location EGC-6 is located in eastern Grand Canyon on river right. In May 2016, we surveyed the downstream part of an aeolian-sand-covered, boulder-rich debris fan with one archaeological site (B:15:0138) located at the base of exposed sandstone ledges just downstream of the side canyon tributary (fig. 8). Part of the survey extended into the side canyon tributary below the maximum flood elevation to capture a fluvial bench that could potentially preserve cultural material (fig. 8). A total of 2,278 m^2 are included in the baseline survey area (table 6). Eighty-five percent of the mapped archaeological site is contained in the baseline survey area. The remaining 15 percent is located on and within rock ledges that are inaccessible and obscured TLS returns from more distal scan positions. This site was classified as aeolian type 1 and drainage type 4 owing to the presence of an upwind sandbar and a gully extending from the site southwest to the river. Individual archaeological features were not mapped during the survey. Table 6 provides a summary of the survey divisions in figure 8.

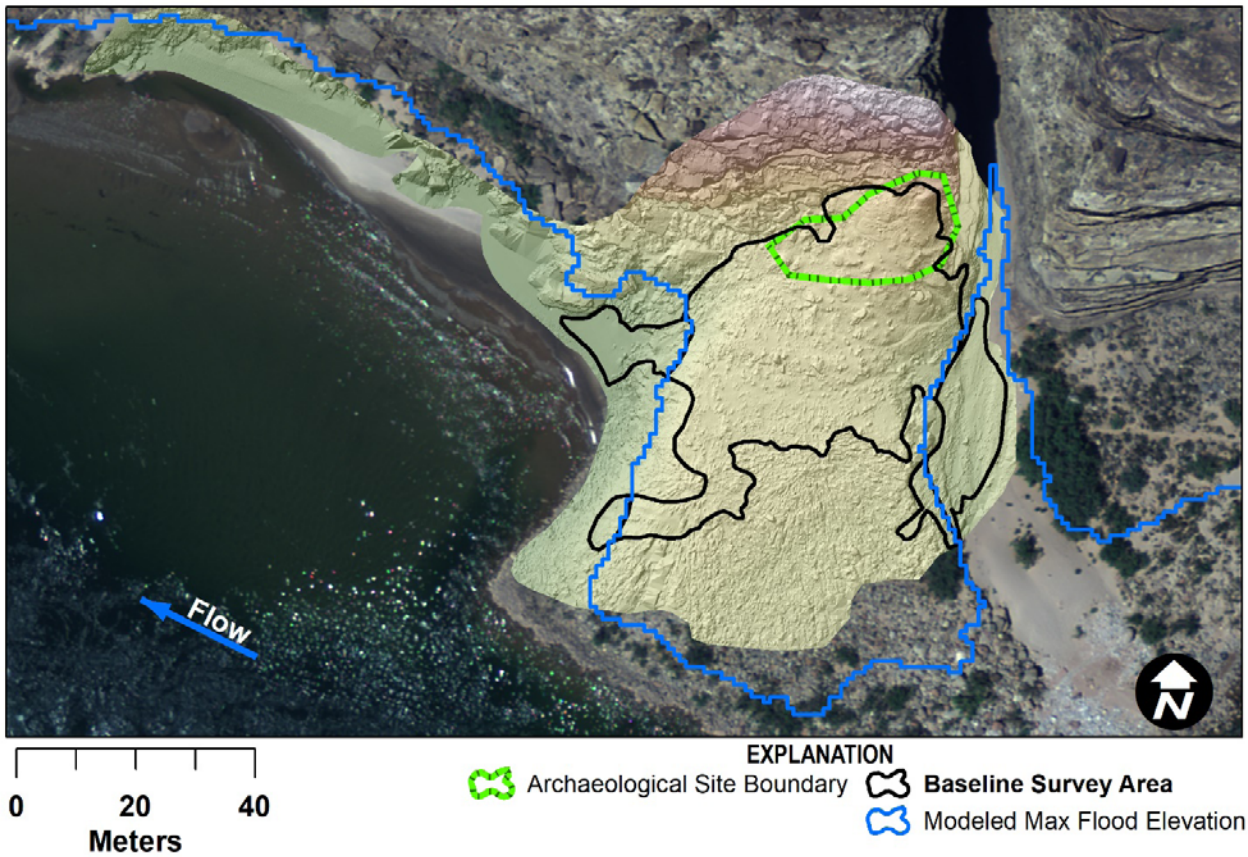

Figure 8. Digital elevation model and shaded-relief map for the survey conducted in May 2016 at monitoring location EGC-6, eastern Grand Canyon, Arizona. Aerial image collected by Grand Canyon Monitoring and Research Center (Durning and others, 2018).

Table 6. Summary of survey coverage at monitoring location EGC-6, eastern Grand Canyon, Arizona.

[Divisions within and outside of the survey represent the area of the archaeological site either within or outside of the baseline survey area, respectively. Below maximum flood elevation represents the portion of the baseline survey area that is potentially inundated by controlled floods. Archaeological site boundary information provided by the National Park Service. m^2, square meter; NA, not applicable]

Spatial subdivision	Area (m^2)	
	Within survey	Outside of survey
Baseline survey	2,277.96	NA
Below maximum flood elevation	459.04	NA
Archaeological site boundary (B:15:0138)	318.50	52.85

Monitoring Location EGC-8

Monitoring location EGC-8 is located in eastern Grand Canyon on river left. In May 2018, we surveyed a large portion of the EGC-8 debris fan, including multiple migrating dunes and two archaeological sites. Site B:14:0095 is proximal to the river and is separated into two spatially distinct loci, with the upstream locus contained within the depression of a dune blowout. Site B:14:0094 is distal to the active river channel on the downstream edge of the side canyon tributary channel (fig. 9). Both site B:14:0095 loci are aeolian type 1 and drainage type 2. Site B:14:0094 is aeolian type 2b, where the distance from the sandbar provides a barrier to aeolian sand transport. Despite the proximity of site B:14:0094 to the side canyon tributary, no discernable runoff pathways were present, making it drainage type 1. Both sites were entirely contained within the baseline survey area that extends from the downstream sandbar to the base of the canyon wall (fig. 9). A total of 28,292 m^2 are included in the baseline survey area (table 7). Individual archaeological features were not mapped during the survey. Table 7 provides a summary of the survey divisions in figure 9.

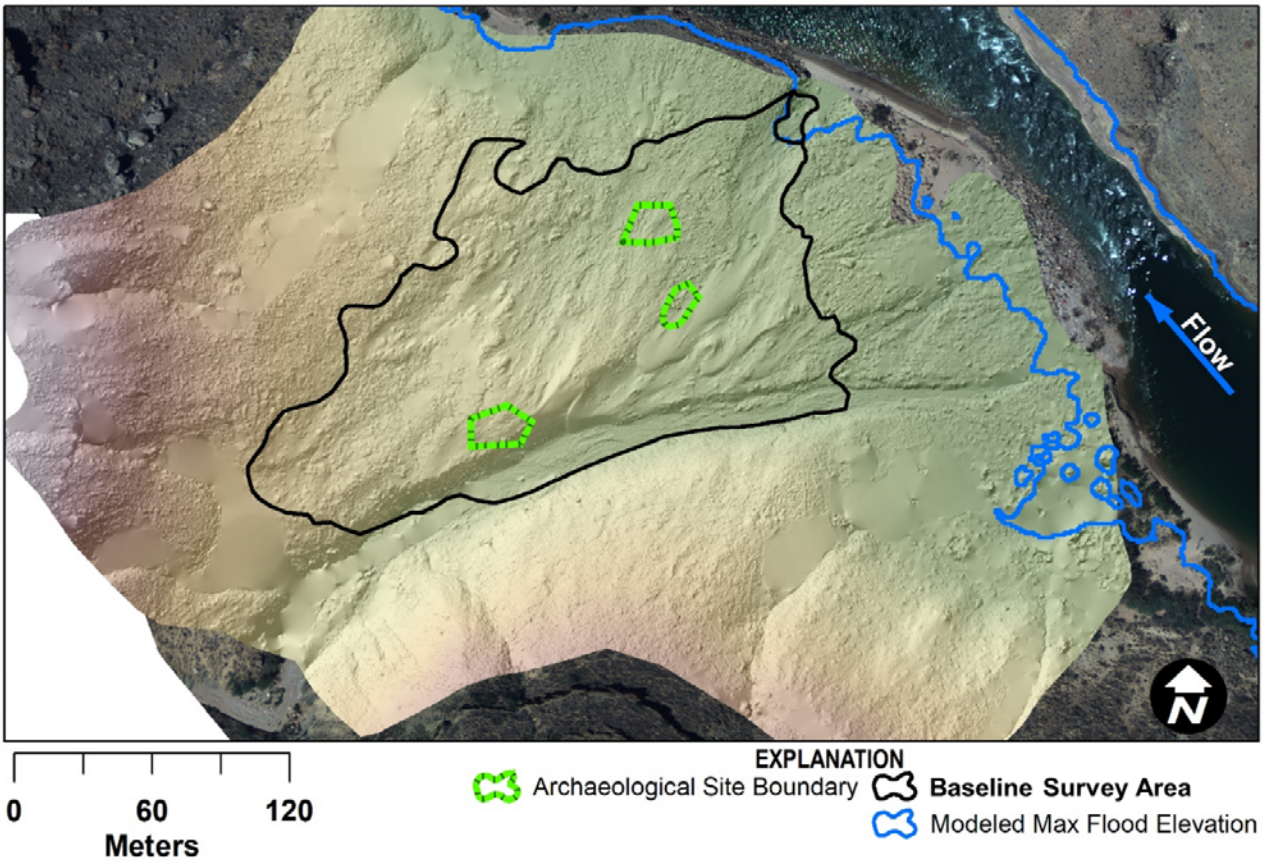

Figure 9. Digital elevation model and shaded-relief map for the survey conducted in May 2018 at monitoring location EGC-8, eastern Grand Canyon, Arizona. Aerial image collected by Grand Canyon Monitoring and Research Center (Durning and others, 2018).

Table 7. Summary of survey coverage at monitoring location EGC-8, eastern Grand Canyon, Arizona.

[Divisions within and outside of the survey represent the area of the archaeological site either within or outside of the baseline survey area, respectively. Below maximum flood elevation represents the portion of the baseline survey area that is potentially inundated by controlled floods. Archaeological site boundary information provided by the National Park Service. m^2, square meter; NA, not applicable]

Spatial subdivision	Area (m^2)	
	Within survey	Outside of survey
Baseline survey	28,292.05	NA
Below maximum flood elevation	222.88	NA
Archaeological site boundary 1 (B:14:0095; two loci)	477.02	0.00
Archaeological site boundary 2 (B:14:0094)	355.24	0.00

Monitoring Location CGC-2

Monitoring location CGC-2 is located in central Grand Canyon on river right. In May 2017, we surveyed the CGC-2 debris fan from the sandbar upstream of a side canyon tributary to archaeological site B:10:0237 (fig. 10). Site B:10:0237 is located at the north end of the survey area and approximately 92 percent of the archaeological site is included in the 6,637-m^2 baseline survey area (fig. 10; table 8). Within the site, three individual features were conventionally surveyed by total station to better characterize future changes (fig. 10). The site is downwind of the sandbar, upslope of recent riparian vegetation growth, and was designated aeolian type 2a. Rills within the site drain to the south and dissipate above the river and tributary, making it drainage type 2. Table 8 provides a summary of the survey divisions in figure 10.

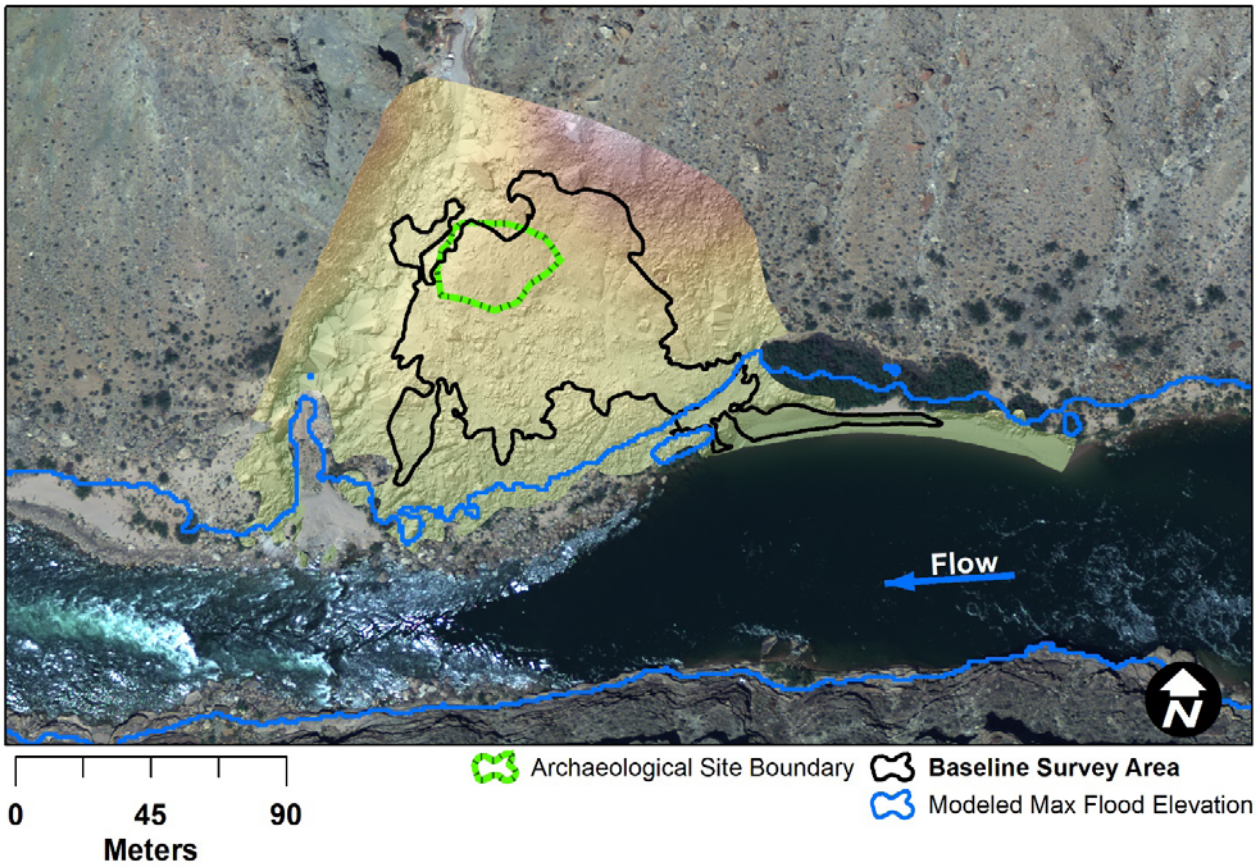

Figure 10. Digital elevation model and shaded-relief map for the survey conducted in May 2017 at monitoring location CGC-2, central Grand Canyon, Arizona. Aerial image collected by Grand Canyon Monitoring and Research Center (Durning and others, 2018).

Table 8. Summary of survey coverage at monitoring location CGC-2, central Grand Canyon, Arizona.

[Divisions within and outside of the survey represent the area of the archaeological site either within or outside of the baseline survey area, respectively. Below maximum flood elevation represents the portion of the baseline survey area that is potentially inundated by controlled floods. Archaeological site boundary information provided by the National Park Service. m^2, square meter; NA, not applicable]

Spatial subdivision	Area (m^2)	
	Within survey	Outside of survey
Baseline survey	6,637.13	NA
Below maximum flood elevation	618.09	NA
Archaeological site boundary (B:10:0237)	722.46	71.73
Feature 1	65.34	0.00
Feature 2	5.32	0.00
Feature 3	5.60	0.00

Monitoring Location WGC-3

Monitoring location WGC-3 is located in western Grand Canyon on river left. In May 2018, we surveyed almost the entire WGC-3 debris fan, from an archeological site (A:16:0004) on the upstream side of the side canyon tributary to the downstream sandbar near a river campsite (fig. 11). A total of 24,756 m^2 are included in the baseline survey area (table 9). Approximately 80 percent of the archaeological site is contained within the baseline survey area and, at present, no individual archaeological features have been mapped. The portion of the archaeological site that was not included within the surveyed area is situated on bedrock ledges overlooking the debris fan and therefore is not susceptible to effects from dam operations. Because the site is located on the downwind and upstream side of the side canyon tributary channel relative to the sandbar that serves as an aeolian sediment supply to the adjacent aeolian dunes and riparian vegetation stands as an additional barrier to sediment transport, it was designated aeolian type 2c. One major gully bisects the site and flows west by southwest, incising to the side canyon tributary down slope of several minor rills that drain the northeastern part of the site. Thus, the site is drainage type 3. Table 9 provides a summary of the survey divisions in figure 11.

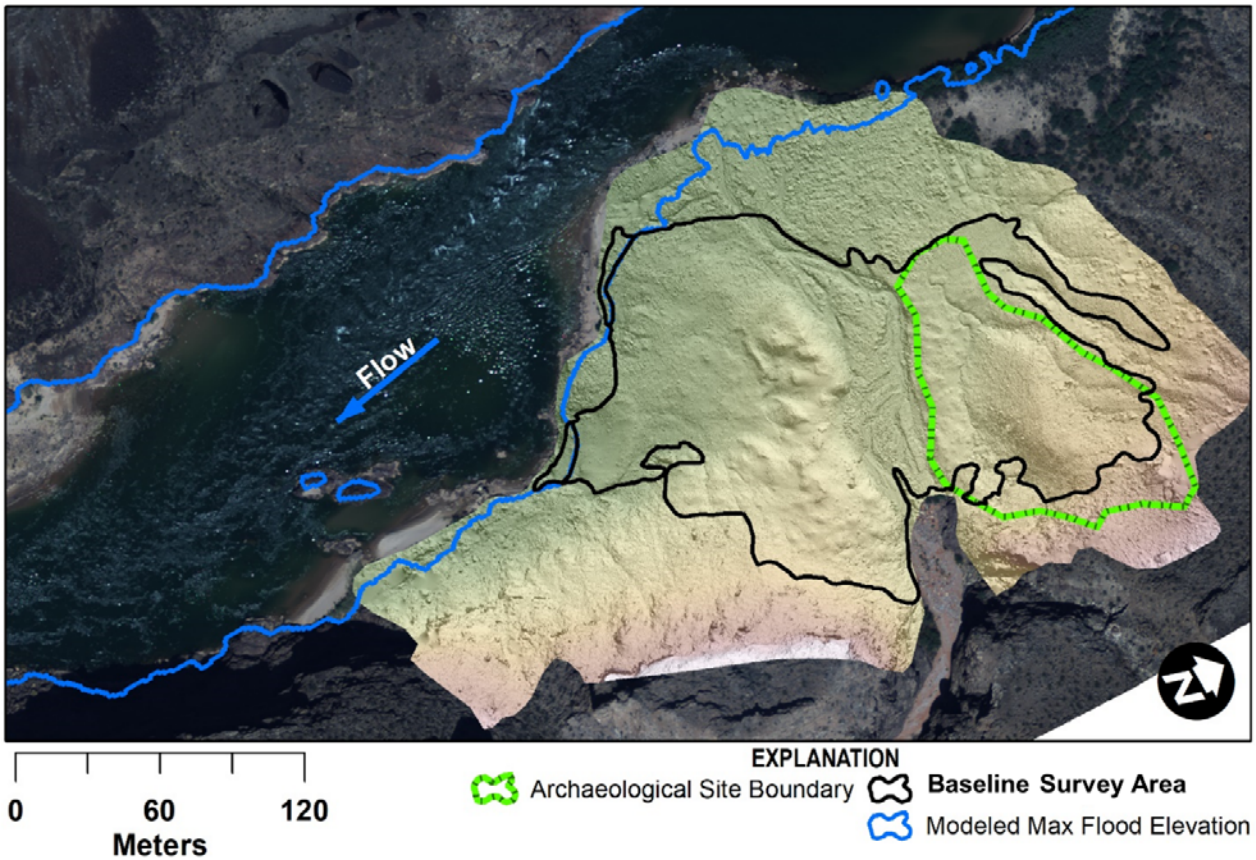

Figure 11. Digital elevation model and shaded-relief map for the survey conducted in May 2017 at monitoring location WGC-3, western Grand Canyon, Arizona. Aerial image collected by Grand Canyon Monitoring and Research Center (Durning and others, 2018).

Table 9. Summary of survey coverage at monitoring location WGC-3, western Grand Canyon, Arizona.

[Divisions within and outside of the survey represent the area of the archaeological site either within or outside of the baseline survey area, respectively. Below maximum flood elevation represents the portion of the baseline survey area that is potentially inundated by controlled floods. Archaeological site boundary information provided by the National Park Service. m^2, square meter; NA, not applicable]

Spatial subdivision	Area (m^2)	
	Within survey	Outside of survey
Baseline survey	24,756.35	NA
Below maximum flood elevation	356.58	NA
Archaeological site boundary (A:16:0004)	6,518.16	1,640.40

Monitoring Location WGC-4

Monitoring location WGC-4 is located in western Grand Canyon on river right. In May 2016, we surveyed much of the WGC-4 debris fan, from the river terrace that contains material from archaeological site A:15:0005, to the upwind sandbar near the associated river campsite (fig. 12). Site A:15:0005 is located at the north end of the survey area on the upstream side of the side canyon tributary and was entirely included in the baseline survey area (fig. 12). The site is classified as aeolian type 2c because the side canyon tributary functions as a barrier between the site and the upwind (downstream) sandbar, as does riparian and upland vegetation growing within the associated river campsite above the sandbar. There are several rills and gullies within the site that have incised into the side canyon tributary channel to the south, though the northernmost gully has incised to the river, making this site drainage type 4. A total of 10,632 m^2 are included in the baseline survey area (table 10). Individual archaeological features were not mapped during the survey. Table 10 provides a summary of the survey divisions in figure 12.

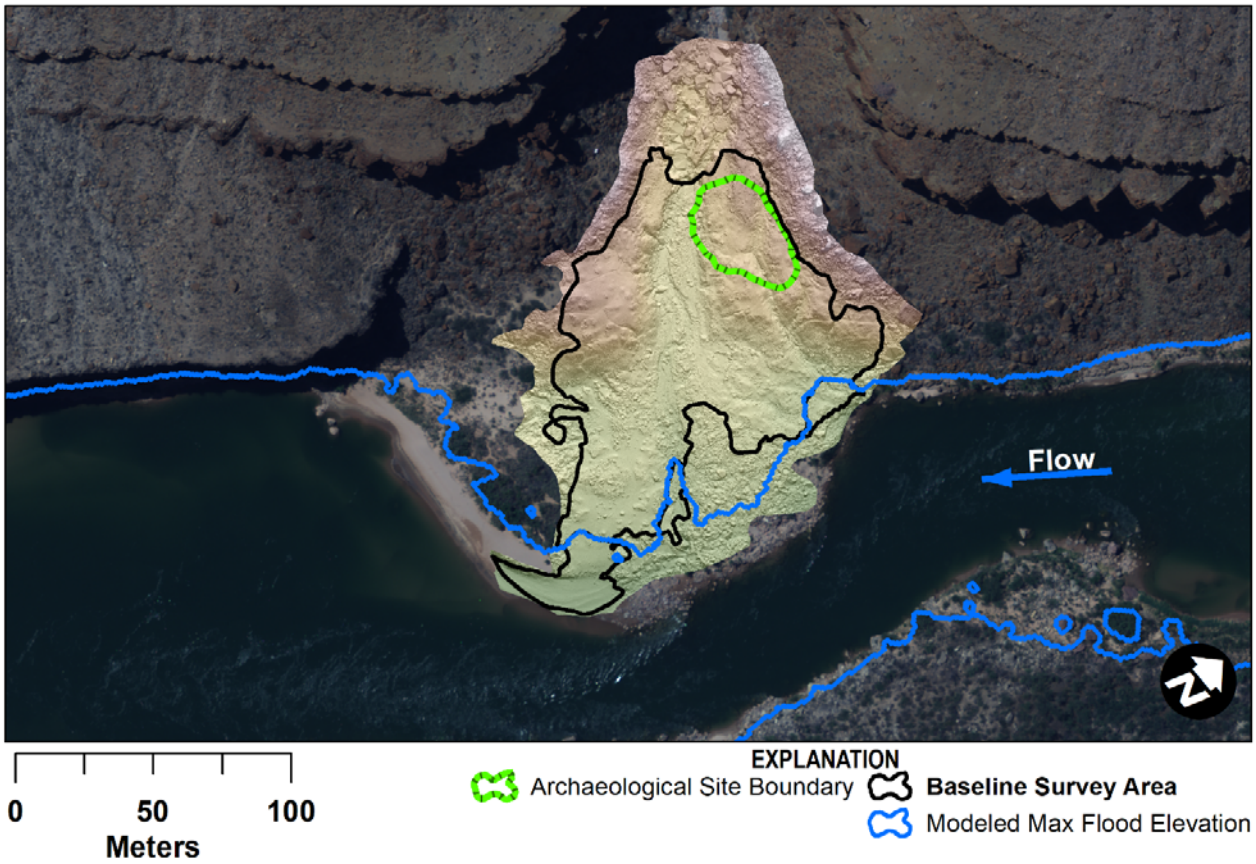

Figure 12. Digital elevation model and shaded-relief map for the survey conducted in May 2016 at monitoring location WGC-4, western Grand Canyon, Arizona. Aerial image collected by Grand Canyon Monitoring and Research Center (Durning and others, 2018).

Table 10. Summary of survey coverage at monitoring location WGC-4, western Grand Canyon, Arizona.

[Divisions within and outside of the survey represent the area of the archaeological site either within or outside of the baseline survey area, respectively. Below maximum flood elevation represents the portion of the baseline survey area that is potentially inundated by controlled floods. Archaeological site boundary information provided by the National Park Service. m^2, square meter; NA, not applicable]

Spatial subdivision	Area (m^2)	
	Within survey	Outside of survey
Baseline survey area	10,632.03	NA
Below maximum flood elevation	1,080.70	NA
Archaeological site boundary (A:15:0005)	1,001.84	0.00

Monitoring Location WGC-5

Monitoring location WGC-5 is located in western Grand Canyon on river left. In May 2018, we surveyed an area covering two archaeological sites, which are separated by a side canyon tributary, as well as much of the adjacent land toward the active river channel (fig. 13). Archaeological site G:03:0032 is located at the north end of the baseline survey area on the upstream side of the side canyon tributary (fig. 13). Site G:03:0044 is located downstream of the tributary and upwind of the associated sandbar. Site G:03:0044 is classified as aeolian type 3 as extensive riparian vegetation now covers the historical sandbar, though indicators of active wind transport (for example, wind ripples and sand shadows) were observed on the dune at the western edge of the site. A drainage running through the eastern part of the site has incised to the active Colorado River channel, making site G:03:0044 drainage type 4. The upstream site (G:03:0032) is also classified as aeolian type 3. Gullies in this site have incised to the side canyon tributary channel, making it drainage type 3. A total of 14,431 m^2 are included in the baseline survey area, including both archaeological sites (table 11). No archaeological features were mapped during the survey. Table 11 provides a summary of the survey divisions in figure 13.

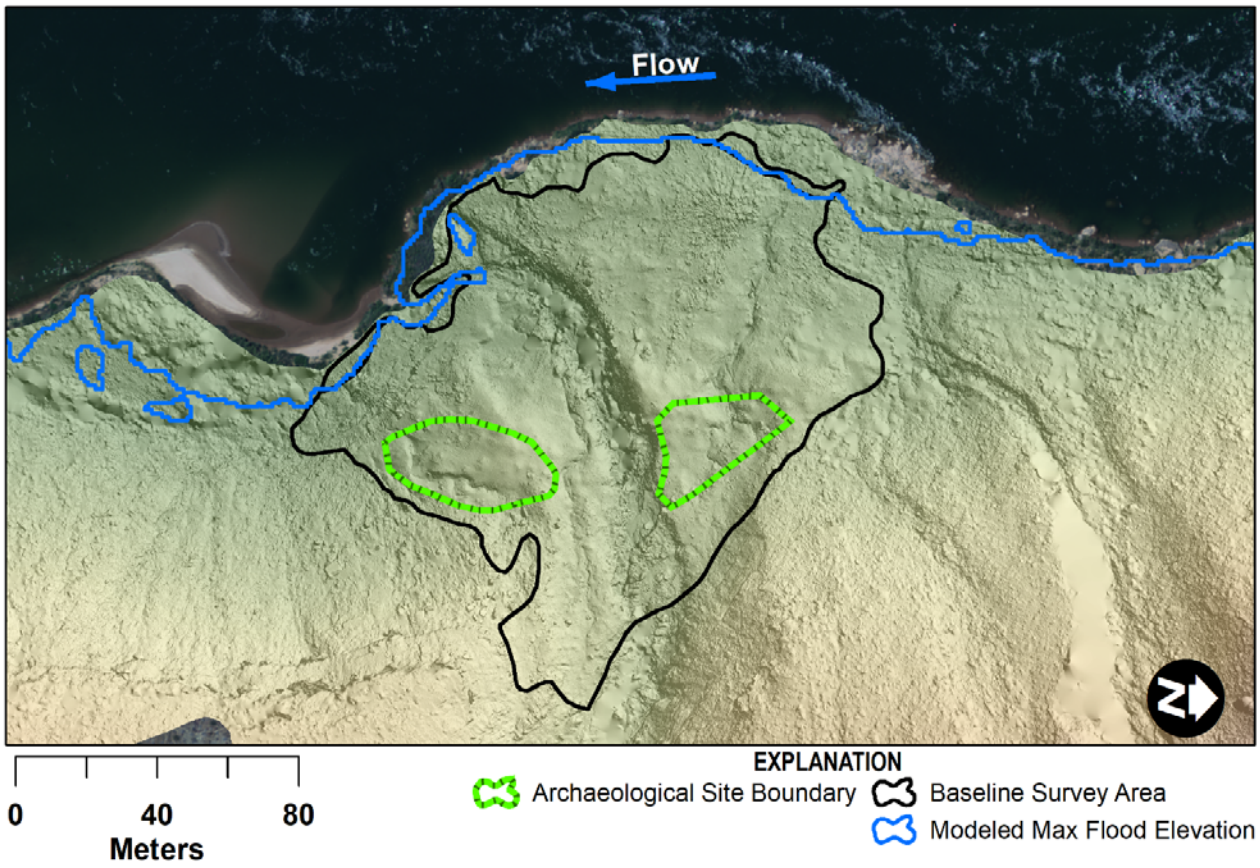

Figure 13. Digital elevation model and shaded-relief map for the survey conducted in May 2018 at monitoring location WGC-5, western Grand Canyon, Arizona. Aerial image collected by Grand Canyon Monitoring and Research Center (Durning and others, 2018).

Table 11. Summary of survey coverage at monitoring location WGC-5, western Grand Canyon, Arizona.

[Divisions within and outside of the survey represent the area of the archaeological site either within or outside of the baseline survey area, respectively. Below maximum flood elevation represents the portion of the baseline survey area that is potentially inundated by controlled floods. Archaeological site boundary information provided by the National Park Service. m^2, square meter; NA, not applicable]

Spatial subdivision	Area (m^2)	
	Within survey	Outside of survey
Baseline survey	14,430.60	NA
Below maximum flood elevation	234.67	NA
Archaeological site boundary 1 (G:03:0032)	677.76	0.00
Archaeological site boundary 2 (G:03:0044)	891.40	0.00

Monitoring Location WGC-6

Monitoring location WGC-6 is located in western Grand Canyon on river right. In May 2017, we surveyed almost the entire WGC-6 debris fan downstream of a side canyon tributary as well as an associated river campsite and one archaeological site (G:03:0058; fig. 14). Site G:03:0058 is located at the northwest end of the survey area and is entirely included in the baseline survey area (fig. 14). Nearly all of the upwind (downstream) sandbar is overgrown with vegetation and the site is thus aeolian type 3. Gullies exist within the site but have not incised to the river, making the site drainage type 2. A total of 13,504 m^2 are included in the baseline survey area (table 12). One archaeological feature was conventionally surveyed by total station (fig. 14). Table 12 provides a summary of the survey divisions in figure 14.

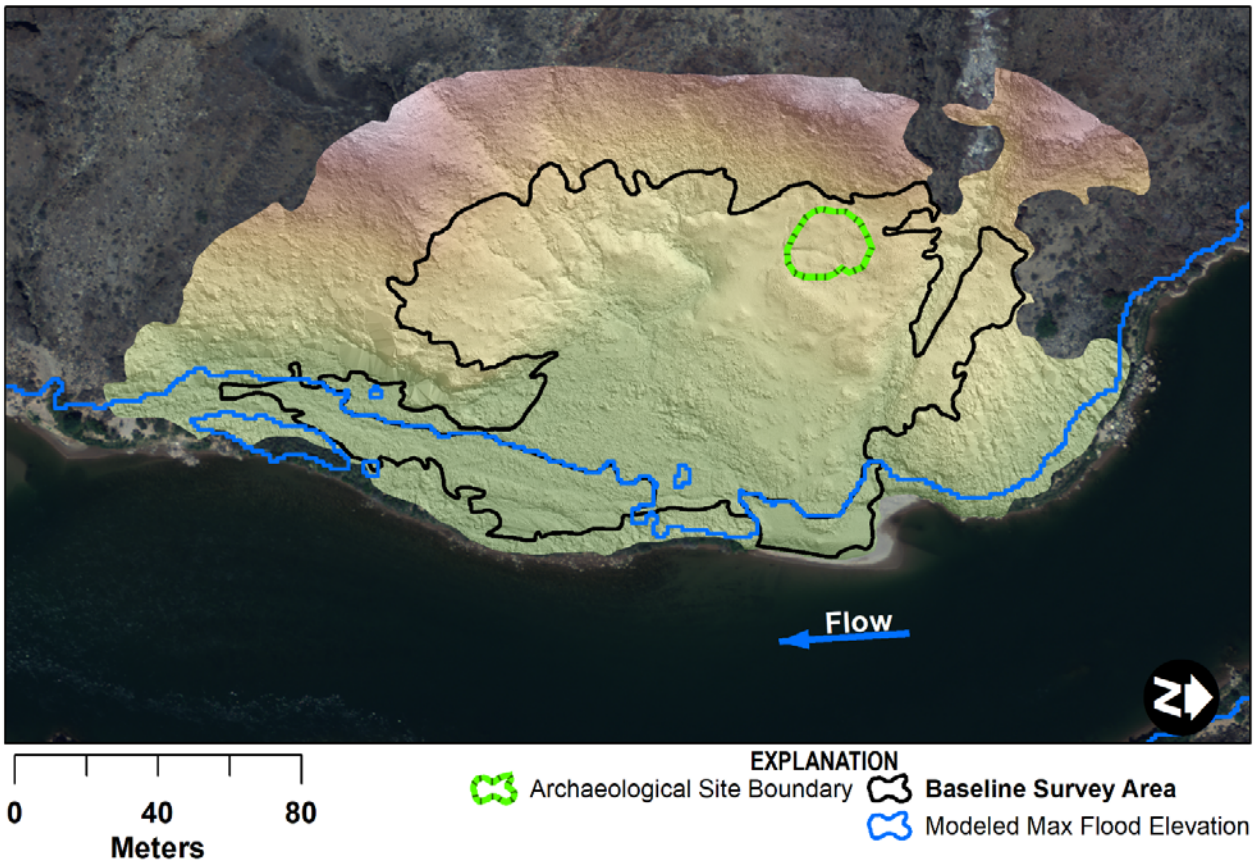

Figure 14. Digital elevation model and shaded-relief map for the survey conducted in May 2017 at monitoring location WGC-6, western Grand Canyon, Arizona. Aerial image collected by Grand Canyon Monitoring and Research Center (Durning and others, 2018).

Table 12. Summary of survey coverage at monitoring location WGC-6, western Grand Canyon, Arizona.

[Divisions within and outside of the survey represent the area of the archaeological site either within or outside of the baseline survey area, respectively. Below maximum flood elevation represents the portion of the baseline survey area that is potentially inundated by controlled floods. Archaeological site boundary information provided by the National Park Service. m^2, square meter; NA, not applicable]

Spatial subdivision	Area (m^2)	
	Within survey	Outside of survey
Baseline survey	13,503.86	NA
Below maximum flood elevation	2,092.62	NA
Archaeological site boundary (G:03:0058)	336.80	0.00
Feature 1	18.88	0.00

Monitoring Location WGC-7

Monitoring location WGC-7 is located in western Grand Canyon on river left. In May 2018, we surveyed both sides of a side canyon tributary channel that bisects the debris fan, extending from an upstream river terrace that contains archaeological site G:03:0080 to the downstream sandbar. There is extensive evidence of aeolian sediment transport in the survey area, including dunes, wind ripples, and sand shadows (fig. 15). Site G:03:0080 is located at the north end of the survey area on the upstream side of the side canyon tributary that, along with extensive riparian vegetation, creates a barrier to aeolian sediment transport from the sandbar; the site is classified as aeolian type 2c (fig. 15). This site is drainage type 3 owing to several south-sloping gullies that have incised to the side canyon tributary. A total of 19,264 m^2 are included in the baseline survey area (table 13). Individual archaeological features were not mapped during the survey. Table 13 provides a summary of the survey divisions in figure 15.

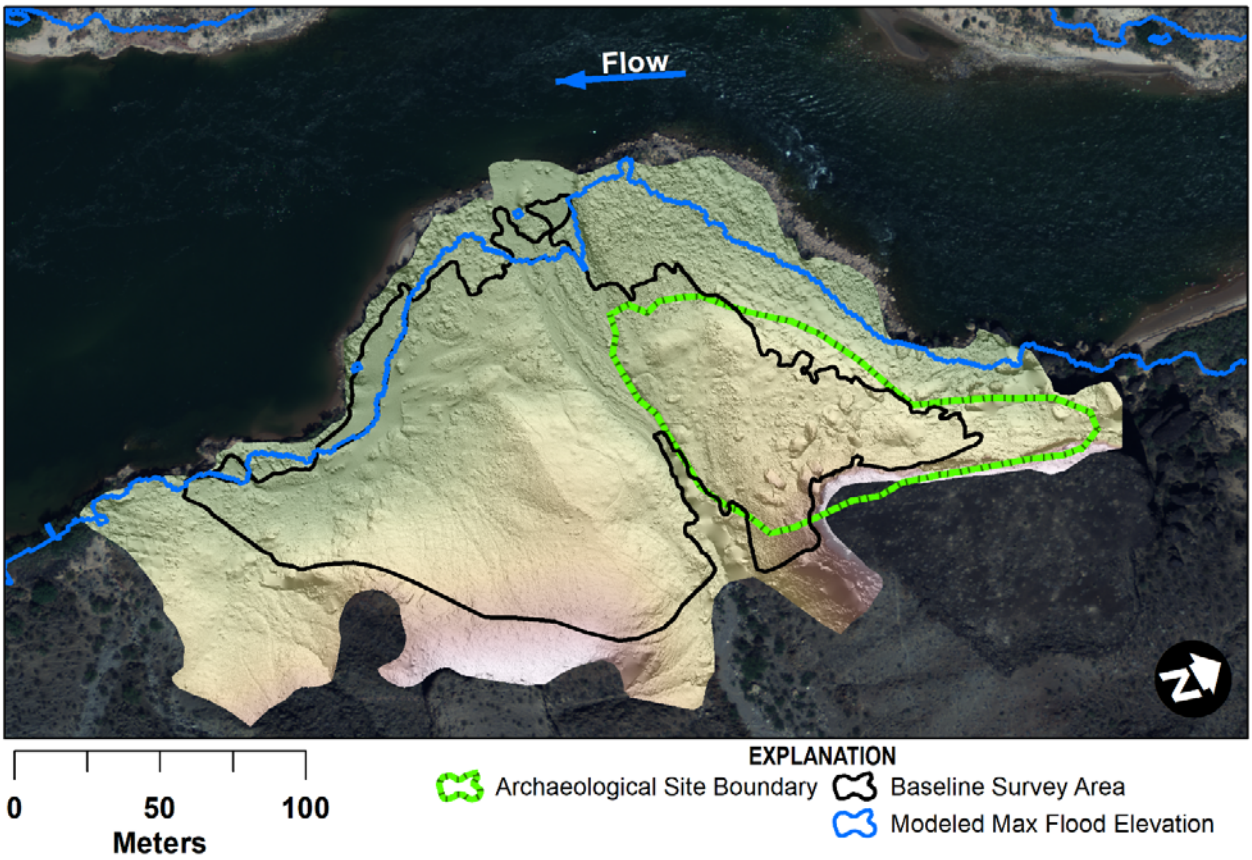

Figure 15. Digital elevation model and shaded-relief map for the survey conducted in May 2018 at monitoring location WGC-7, western Grand Canyon, Arizona. Aerial image collected by Grand Canyon Monitoring Research Center (Durning and others, 2018).

Table 13. Summary of survey coverage at monitoring location WGC-7, western Grand Canyon, Arizona.

[Divisions within and outside of the survey represent the area of the archaeological site either within or outside of the baseline survey area, respectively. Below maximum flood elevation represents the portion of the baseline survey area that is potentially inundated by controlled floods. Archaeological site boundary information provided by the National Park Service. m^2, square meter; NA, not applicable]

Spatial subdivision	Area (m^2)	
	Within survey	Outside of survey
Baseline survey	19,263.80	NA
Below maximum flood elevation	901.93	NA
Archaeological site boundary (G:03:0080)	4,916.07	1,909.85

Monitoring Locations with Repeat Surveys

Topographic change results were calculated for monitoring locations with more than one survey. We summarize topographic change as area, volume, and a sediment imbalance for each monitoring location using the spatial subdivisions in table 1. The subdivisions for archaeological site boundaries are approximated from NPS records. Locations of select archaeological features were surveyed using a total station.

Area and volume of topographic change is interpreted as erosion, where change values are negative, and deposition, where change values are positive. Changes in sediment storage within each detection interval are inferred by net volume change, representing the sum of erosion and deposition volumes. We then estimate the relative magnitude of the difference in sediment storage volume as the sediment imbalance percentage. The sediment imbalance is an index ranging from +50 to −50 percent, such that +50 percent indicates only deposition occurred, 0 percent indicates equal volumes of erosion and deposition, and −50 percent indicates only erosion occurred.

Monitoring Location NMC-1

Monitoring location NMC-1 is located in northern Marble Canyon on river right. In May 2017, we surveyed a large part of a debris fan formed by a side canyon tributary to the Colorado River and one archaeological site. Site C:06:0003 was split into two loci that are designated C:06:0003A and C:06:0003B. The baseline survey area, and the associated archaeological site, were divided into upstream and downstream units that were topographically separated by the side canyon tributary channel (fig. 16). A total of 36,448 square meters (m^2) are included in the baseline survey (table 14), though topographic data for more than 10,000 m^2 of additional area are available for use at lower resolutions (25 cm to 1 m). Both loci of the mapped archaeological site on the debris fan are contained within the baseline survey area. The upstream locus (site C:06:0003A) is classified as aeolian type 2b because it is located on the opposite side of the side canyon tributary relative to the upwind river sandbar. There is one gully that crosses through the site from the west. Though the most significant incision in the gully is below a knickpoint outside the southern boundary, the site was classified as a drainage type 3. The downstream locus (site C:06:0003B) is aeolian type 1 with clear evidence of aeolian sediment transport from the upwind river sandbar to the site. No gullies are located within the site and thus it is classified as drainage type 1. However, there is a gully located to the southeast of the site that may prograde into the site in the future. One feature, associated with the downstream part of the site, was surveyed using a stadia rod topped with a reflective prism and a total station to define its location for future assessments of change.

In 2019, a new weather station was installed at monitoring location NMC-1 and in June 2020 the survey was repeated to measure topographic changes within the 2017 baseline survey area. Between the 2017 and 2020 surveys, the net volumetric change for both the change detection area and the archaeological site loci was erosional (table 14). Both archaeological loci and the upstream survey area had a greater negative change imbalance (−24 to −34 percent) than the downstream survey area (−10 percent), though the overall net change volume was greater for the downstream side of the debris fan (table 14). Aeolian processes contributed to most topographic changes between the 2017 and 2020 surveys, though alluvial and indeterminate processes also significantly contributed to changes within the archaeological site boundaries (table 15). The greatest changes occurred within the dune field on the downstream side of the tributary, where alternating patterns of erosion and deposition were measured along the dominant wind direction from south to north (fig. 16). Topographic changes within the upstream archaeological site locus (C:06:0003A) were from wind-driven erosion and deposition measured along the northern edge of the site's boundary, along with alluvial erosion from a gully that runs through the center of the site into the tributary channel to the south. Topographic changes in the downstream locus (C:06:0003B) were primarily from diffuse wind scour and sheet wash, and the greatest changes occurred in the eastern part of the site.

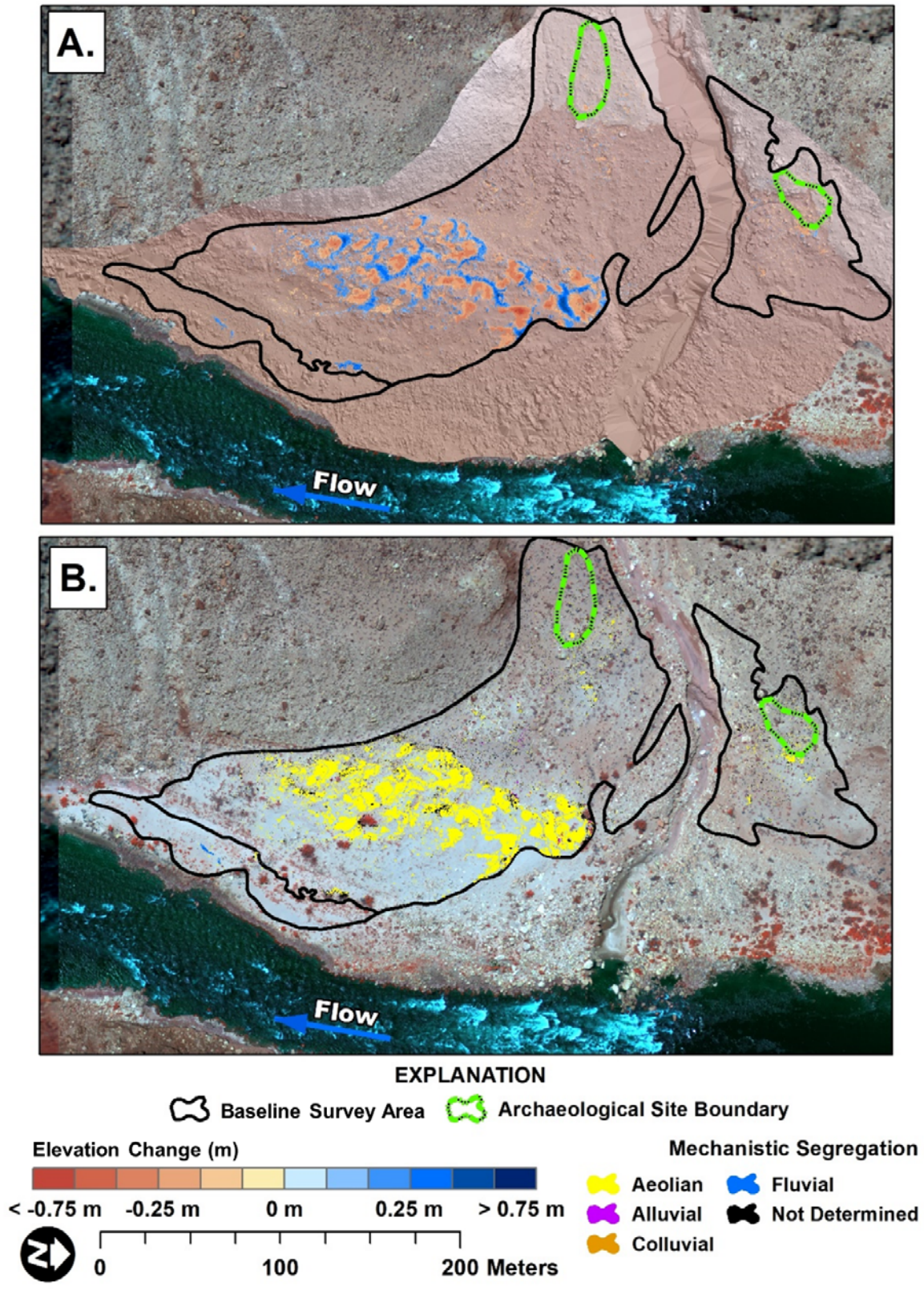

Figure 16. Maps showing change detection results between May 2017 and June 2020 for monitoring location NMC-1, northern Marble Canyon, Arizona. *A*, Shaded relief showing elevation change results, in meters (m). Changes are within the 95-percent confidence interval. *B*, Results of automated geomorphic classification changes after Kasprak and others (2017). Aerial image collected by Grand Canyon Monitoring and Research Center (Durning and others, 2018).

Table 14. Results of change detection between May 2017 and June 2020 for the change detection area at monitoring location NMC-1, northern Marble Canyon, Arizona.

[The archaeological site boundary is included in the above maximum flood elevation subdivision. m², square meter; m³, cubic meter; %, percent]

Spatial subdivision	Survey area (m²)	Area (m²)			Volume (m³)			Percent imbalance (%)
		Erosion	Deposition	Total	Erosion	Deposition	Net	
Baseline survey area	36,447.71	2,417.25	1,770.84	4,188.09	442.80	291.39	−151.41	−10.3
Below maximum flood elevation	2,820.84	10.10	17.69	27.79	1.21	2.77	1.56	19.6
Above maximum flood elevation (upstream)	6,425.32	146.71	58.34	205.04	12.48	4.20	−8.28	−24.8
Above maximum flood elevation (downstream)	27,201.55	2,260.45	1,694.81	3,955.26	429.11	284.41	−144.70	−10.1
Archaeological site boundary (C:06:0003A)	513.66	30.41	7.21	37.63	2.17	0.47	−1.70	−32.1
Archaeological site boundary (C:06:0003B)	834.24	27.83	7.72	35.55	2.37	0.44	−1.94	−34.4

Table 15. Results of change detection by geomorphic mechanism between May 2017 and June 2020 at monitoring location NMC-1, northern Marble Canyon, Arizona.

[NA indicates mechanisms not identified in the survey. m², square meter; m³, cubic meter; %, percent]

Spatial subdivision	Area (m²)			Volume (m³)			Percent imbalance (%)
	Erosion	Deposition	Total	Erosion	Deposition	Net	
Baseline survey area							
Fluvial	1.34	12.59	13.93	0.17	2.19	2.02	42.9
Aeolian	2,092.64	1,452.91	3,545.55	413.40	253.14	−160.26	−12.0
Alluvial	20.67	21.69	42.36	2.28	3.62	1.34	11.3
Colluvial	4.76	7.33	12.09	0.71	1.48	0.76	17.4
Indeterminate	297.83	275.81	573.64	26.23	30.96	4.73	4.1
Archaeological site boundary (C:06:0003A)							
Fluvial	NA	NA	NA	NA	NA	NA	NA
Aeolian	14.96	2.75	17.71	1.07	0.18	−0.89	−35.9
Alluvial	1.25	0.08	1.33	0.13	0.01	−0.12	−45.4
Colluvial	0.46	0.06	0.52	0.05	0.00	−0.04	−40.9
Indeterminate	13.75	4.33	18.07	0.93	0.29	−0.64	−26.3
Archaeological site boundary (C:06:0003B)							
Fluvial	NA	NA	NA	NA	NA	NA	NA
Aeolian	14.83	2.92	17.74	1.50	0.17	−1.33	−39.9
Alluvial	0.25	0.05	0.30	0.02	0.00	−0.02	−38.6
Colluvial	0.02	0.02	0.03	0.00	0.00	0.00	3.6
Indeterminate	12.74	4.74	17.48	0.86	0.27	−0.59	−26.3

Monitoring Location CMC-1

Monitoring location CMC-1 is an aeolian type 1 and drainage type 4 site located in central Marble Canyon on river left with one archaeological site, C:05:0031. It is one of several long-term monitoring sites with previous lidar surveys and weather station records (Draut and others, 2009, 2010; Collins and others, 2012, 2016; Dealy and others, 2014; Caster and others, 2014, 2018; Caster and Sankey, 2016; East and others, 2016; Sankey and others, 2018b). It was previously surveyed using lidar in April and September 2010 and those results are described and synthesized by Collins and others (2012, 2016), who showed that site changes were predominantly erosional during that time. Monitoring location CMC-1 has a baseline survey area of 5,844 m² that was collected during each of seven surveys between September 2010 and June 2020 (figs. 17–23; tables 16–33). In 2019, the NPS began

conducting annual vegetation management at monitoring location CMC-1 to remove riparian plants that create a barrier to aeolian transport of sand from the sandbar toward the archaeological site. In May 2019 we resurveyed monitoring location CMC-1 following that year's vegetation management effort, and we resurveyed again in June 2020 prior to that year's vegetation management effort.

In the $DoD_{2010–2013}$, net volumetric change within the baseline survey area was erosional, with the greatest negative imbalance (−47 percent) below the maximum regulated flood inundation elevation (fig. 17; table 16). However, net volumetric change in the archaeological site was depositional (table 16). Aeolian processes were the most common geomorphic process that occurred in and around the individual

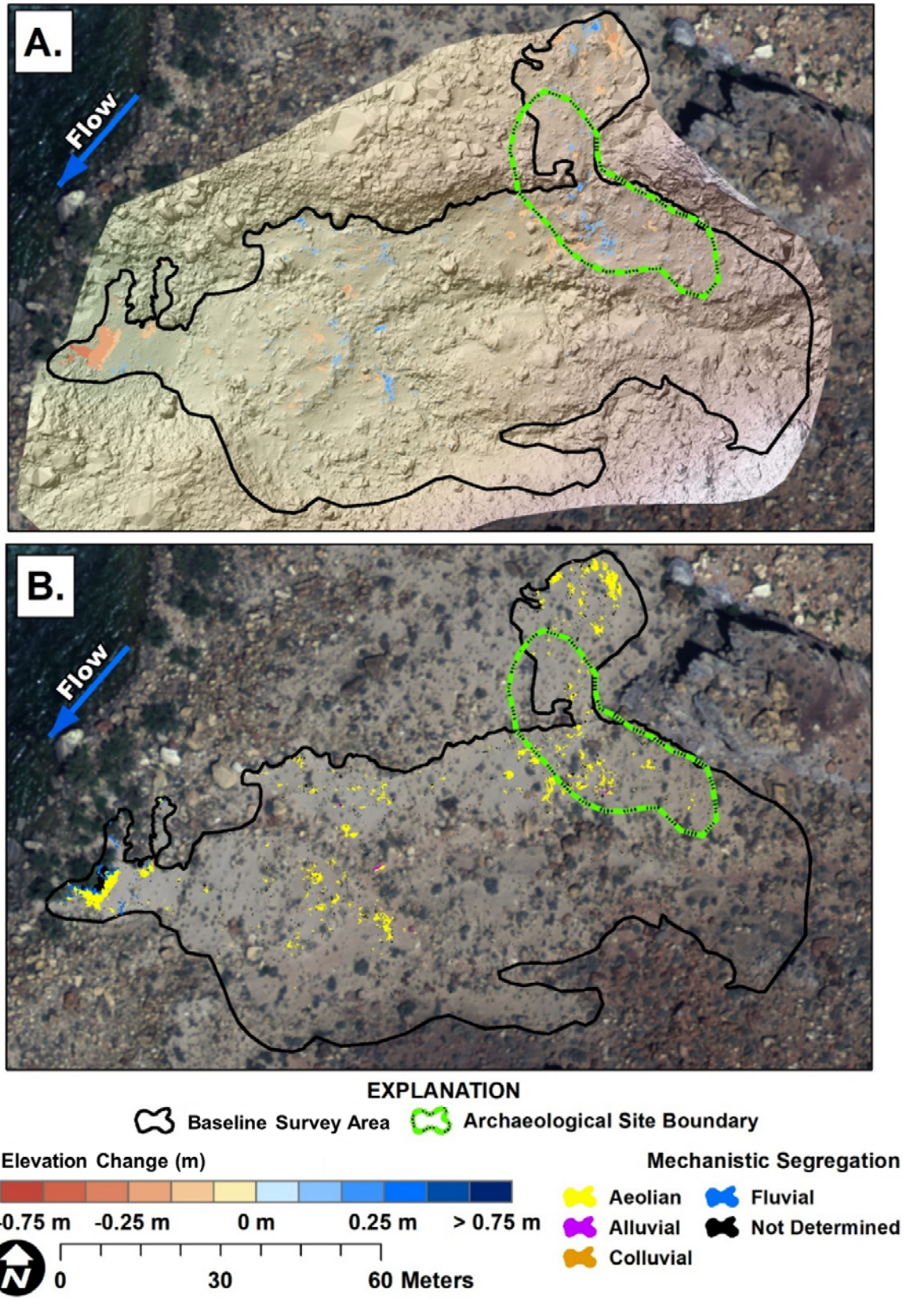

Figure 17. Maps showing change detection results between September 2010 and May 2013 for monitoring location CMC-1, central Marble Canyon, Arizona. *A*, Shaded relief showing elevation change results, in meters (m). Changes are within the 95-percent confidence interval. *B*, Results of automated geomorphic classification changes after Kasprak and others (2017). Aerial image collected by Grand Canyon Monitoring and Research Center (Durning and others, 2018).

mapped archaeological features (fig. 17; table 17). Within the larger archaeological site boundary and surrounding survey area, aeolian processes were also the dominant mechanism of change (table 18). Erosion was most pronounced in the western part of the survey area near the river (fluvial and aeolian) and along the edge of the side canyon tributary banks to the north (aeolian and colluvial). Much of the interior part of the survey area exhibited deposition, which indicates that sand was blown by wind from the river sandbar toward the archaeological site (fig. 17).

Table 16. Results of change detection between September 2010 and May 2013 for the baseline survey area at monitoring location CMC-1, central Marble Canyon, Arizona.

[The archaeological site boundary is included in the above maximum flood elevation subdivision. m^2, square meter; m^3, cubic meter; %, percent]

Spatial subdivision	Survey area (m^2)	Area (m^2)			Volume (m^3)			Percent imbalance (%)
		Erosion	Deposition	Total	Erosion	Deposition	Net	
Baseline survey area	5,843.74	124.03	72.72	196.75	16.65	7.13	−9.52	−20.0
Below maximum flood elevation	234.78	40.90	2.65	43.55	7.28	0.18	−7.10	−47.6
Above maximum flood elevation	5,612.23	83.14	70.08	153.22	9.37	6.96	−2.41	−7.4
Archaeological site boundary	617.86	11.45	19.68	31.13	1.23	1.58	0.35	6.2

Table 17. Results of change detection between September 2010 and May 2013 for mapped archaeological features at site C:05:0031, central Marble Canyon, Arizona.

[Feature + buffer is inclusive of the feature area and a surrounding 1-meter-wide buffer. m^2, square meter; m^3, cubic meter; %, percent]

Spatial subdivision	Survey area (m^2)	Area (m^2)			Volume (m^3)			Percent imbalance (%)
		Erosion	Deposition	Total	Erosion	Deposition	Net	
Feature 2	19.96	0.07	0.06	0.13	0.01	0.00	0.00	−2.6
Feature 2 + buffer	40.18	0.10	0.11	0.21	0.01	0.01	0.00	1.4
Feature 4	30.05	0.87	0.06	0.93	0.06	0.00	−0.06	−44.5
Feature 4 + buffer	58.15	1.05	0.99	2.04	0.08	0.07	−0.01	−2.3
Feature 5	24.84	0.06	0.02	0.08	0.00	0.00	0.00	−30.0
Feature 5 + buffer	50.52	0.06	0.22	0.28	0.00	0.01	0.01	31.0

Table 18. Results of change detection by geomorphic mechanism between September 2010 and May 2013 at monitoring location CMC-1, central Marble Canyon, Arizona.

[NA indicates mechanisms not identified in the survey. m^2, square meter; m^3, cubic meter; %, percent]

Spatial subdivision	Area (m^2)			Volume (m^3)			Percent imbalance (%)
	Erosion	Deposition	Total	Erosion	Deposition	Net	
Baseline survey area							
Fluvial	10.92	1.28	12.20	2.52	0.09	−2.43	−46.6
Aeolian	80.48	38.51	118.99	8.13	3.09	−5.04	−22.5
Alluvial	0.29	1.83	2.12	0.03	2.11	2.08	48.6
Colluvial	0.17	0.06	0.23	0.03	0.02	−0.01	−10.0
Indeterminate	26.32	26.61	52.93	2.93	2.28	−0.65	−6.2
Archaeological site boundary							
Fluvial	NA	NA	NA	NA	NA	NA	NA
Aeolian	8.15	13.53	21.68	0.64	1.08	0.44	12.8
Alluvial	0.00	0.50	0.50	0.00	0.04	0.04	50.0
Colluvial	0.08	0.00	0.08	0.01	0.00	−0.01	−50.0
Indeterminate	2.76	5.62	8.38	0.25	0.46	0.21	14.8

In the $DoD_{2013–2014}$, net volumetric change was depositional within the baseline survey area (fig. 18; table 19), but erosional within the archaeological site boundary, particularly at feature 4 (table 20). Fluvial and indeterminate deposition were the dominant geomorphic processes in the survey area, with fluvial changes constrained to the river margins and indeterminate change classified throughout the survey area where sediment was deposited at the base of vegetation and boulders (fig. 18; table 21). Aeolian erosion was the dominant process in the archaeological site.

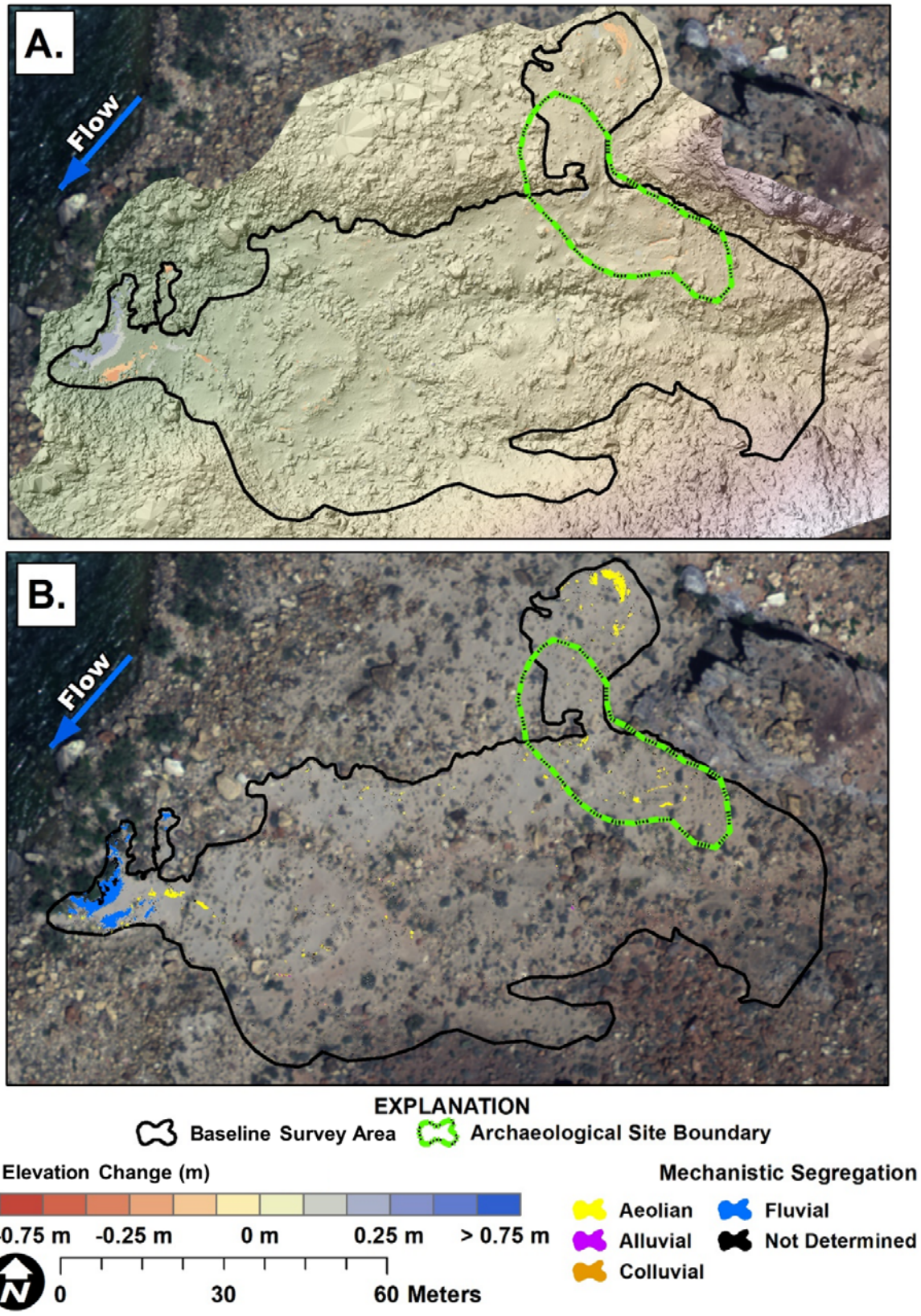

Figure 18. Maps showing change detection results between May 2013 and May 2014 for monitoring location CMC-1, central Marble Canyon, Arizona. *A*, Elevation change results, in meters (m). Changes are with the 95-percent confidence interval. *B*, Results of automated geomorphic classification changes after Kasprak and others (2017). Background aerial imagery collected by Grand Canyon Monitoring and Research Center (Durning and others, 2018).

Table 19. Results of change detection between May 2013 and May 2014 for the baseline survey area at monitoring location CMC-1, central Marble Canyon, Arizona.

[The archaeological site boundary is included in the above maximum flood elevation subdivision. m^2, square meter; m^3, cubic meter; %, percent]

Spatial subdivision	Survey area (m^2)	Area (m^2)			Volume (m^3)			Percent imbalance (%)
		Erosion	Deposition	Total	Erosion	Deposition	Net	
Baseline survey area	5,843.74	46.93	73.72	120.65	3.93	8.54	4.61	18.5
Below maximum flood elevation	234.78	14.53	40.41	54.94	1.31	5.00	3.69	29.2
Above maximum flood elevation	5,612.23	32.41	33.31	65.72	2.62	3.54	0.92	7.5
Archaeological site boundary	617.86	4.66	4.62	9.28	0.41	0.37	−0.04	−2.6

Table 20. Results of change detection between the May 2013 and May 2014 for mapped archaeological features at site C:05:0031, central Marble Canyon, Arizona.

[Feature + buffer is inclusive of the feature area and a surrounding 1-meter-wide buffer. m^2, square meter; m^3, cubic meter; %, percent]

Spatial subdivision	Survey area (m^2)	Area (m^2)			Volume (m^3)			Percent imbalance (%)
		Erosion	Deposition	Total	Erosion	Deposition	Net	
Feature 2	19.96	0.04	0.00	0.04	0.00	0.00	0.00	−50.0
Feature 2 + buffer	40.18	0.04	0.03	0.07	0.00	0.00	0.00	8.0
Feature 4	30.05	0.35	0.02	0.37	0.03	0.00	−0.03	−45.7
Feature 4 + buffer	58.15	0.79	0.22	1.01	0.09	0.01	−0.08	−36.2
Feature 5	24.84	0.01	0.00	0.01	0.00	0.00	0.00	−50.0
Feature 5 + buffer	50.52	0.02	0.00	0.02	0.00	0.00	0.00	−50.0

Table 21. Results of change detection by geomorphic mechanism between May 2013 and May 2014 at monitoring location CMC-1, central Marble Canyon, Arizona.

[NA indicates mechanisms not identified in the survey. m^2, square meter; m^3, cubic meter; %, percent]

Spatial subdivision	Area (m^2)			Volume (m^3)			Percent imbalance (%)
	Erosion	Deposition	Total	Erosion	Deposition	Net	
Baseline survey area							
Fluvial	11.90	30.74	42.64	1.11	3.72	2.61	27.0
Aeolian	21.79	10.54	32.33	1.74	0.81	−0.93	−18.2
Alluvial	0.05	0.31	0.36	0.04	0.04	0.00	0.9
Colluvial	0.00	0.12	0.12	0.00	0.05	0.05	50.0
Indeterminate	12.72	32.05	44.77	1.04	3.93	2.89	29.1
Archaeological site boundary							
Fluvial	NA	NA	NA	NA	NA	NA	NA
Aeolian	0.83	0.11	0.94	0.08	0.01	−0.08	−41.3
Alluvial	0.00	0.00	0.00	0.00	0.00	0.00	50.0
Colluvial	NA	NA	NA	NA	NA	NA	NA
Indeterminate	0.40	0.16	0.56	0.04	0.01	−0.03	−27.8

The $DoD_{2014–2016}$ exhibited net volumetric change near equilibrium with some areas of deep, localized erosion, and other areas of shallow, widespread deposition throughout the baseline survey area (fig. 19; table 22). The most significant deposition occurred below the maximum controlled flood elevation owing to fluvial and aeolian processes. Erosion occurred primarily at or above the stage elevation inundated by the largest post-dam flows (97,000 ft^3/s; Magirl and others, 2008). In the archaeological site, net volumetric change was depositional at all surveyed features except for feature 5 (table 23). Feature 5 is located at a slightly higher elevation than the other features and exhibited minor wind erosion (fig. 19; table 24). Indeterminate mechanisms of change were classified throughout the survey area where sediment was deposited at the base of vegetation and boulders, but elsewhere fluvial and aeolian processes were the dominant mechanisms of change for the baseline survey area (table 24).

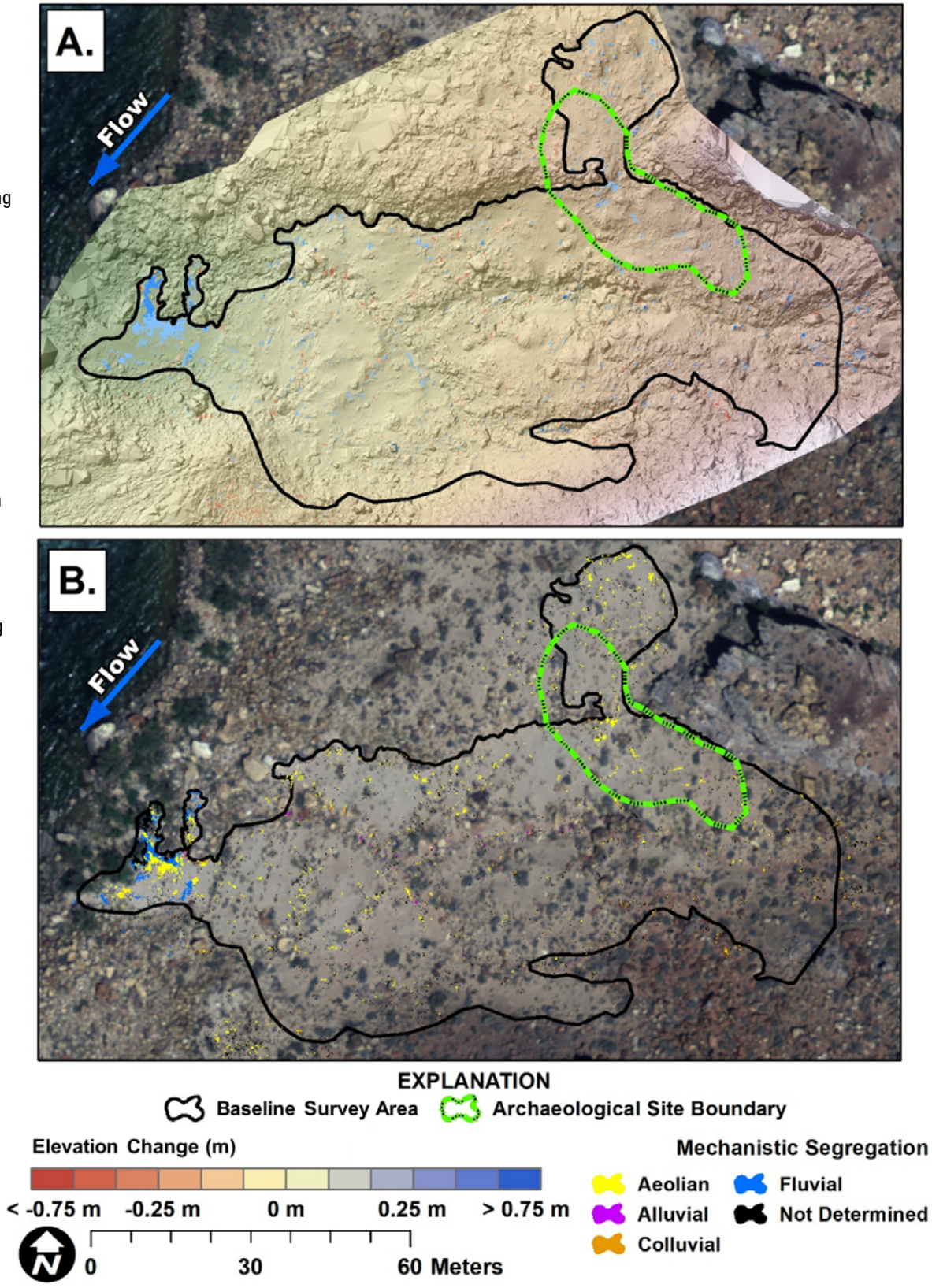

Figure 19. Maps showing change detection results between May 2014 and May 2016 for monitoring location CMC-1, central Marble Canyon, Arizona. *A*, Shaded relief showing elevation change results, in meters (m). Changes are within the 95-percent confidence interval. *B*, Results of automated geomorphic classification changes after Kasprak and others (2017). Aerial image collected by Grand Canyon Monitoring and Research Center (Durning and others, 2018).

Table 22. Results of change detection between May 2014 and May 2016 for the baseline survey area at monitoring location CMC-1, central Marble Canyon, Arizona.

[The archaeological site boundary is included in the Above max flood elevation subdivision. m^2, square meter; m^3, cubic meter; %, percent]

Spatial subdivision	Survey area (m^2)	Area (m^2)			Volume (m^3)			Percent imbalance (%)
		Erosion	Deposition	Total	Erosion	Deposition	Net	
Baseline survey area	5,843.74	64.30	142.31	206.61	12.98	12.92	−0.05	−0.1
Below maximum flood elevation	234.78	5.46	50.72	56.18	1.54	4.50	2.96	24.5
Above maximum flood elevation	5,612.23	58.84	91.59	150.43	11.43	8.42	−3.02	−7.6
Archaeological site boundary	617.86	3.14	13.88	17.02	0.32	1.09	0.78	27.4

Table 23. Results of change detection between May 2014 and May 2016 for mapped archaeological features at site C:05:0031, central Marble Canyon.

[Feature + buffer is inclusive of the feature area and a surrounding 1-meter-wide buffer. m^2, square meter; m^3, cubic meter; %, percent]

Spatial subdivision	Survey area (m^2)	Area (m^2)			Volume (m^3)			Percent imbalance (%)
		Erosion	Deposition	Total	Erosion	Deposition	Net	
Feature 2	19.96	0.00	0.87	0.87	0.00	0.07	0.07	50.0
Feature 2 + buffer	40.18	0.00	1.07	1.07	0.00	0.08	0.08	50.0
Feature 4	30.05	0.00	0.22	0.22	0.00	0.01	0.01	50.0
Feature 4 + buffer	58.15	0.12	1.47	1.59	0.01	0.14	0.13	43.5
Feature 5	24.84	0.10	0.15	0.25	0.03	0.01	−0.02	−20.4
Feature 5 + buffer	50.52	0.21	0.39	0.60	0.06	0.03	−0.03	−16.7

Table 24. Results of change detection by geomorphic mechanism between May 2014 and May 2016 at monitoring location CMC-1, central Marble Canyon, Arizona.

[NA indicates mechanisms not identified in the survey. m^2, square meter; m^3, cubic meter; %, percent]

Spatial subdivision	Area (m^2)			Volume (m^3)			Percent imbalance (%)
	Erosion	Deposition	Total	Erosion	Deposition	Net	
Baseline survey area							
Fluvial	1.92	20.74	22.66	0.44	1.89	1.45	31.1
Aeolian	16.48	55.79	72.27	3.49	4.79	1.30	50.0
Alluvial	1.93	2.17	4.10	0.41	0.37	−0.04	−2.6
Colluvial	3.80	1.58	5.38	1.53	0.41	−1.12	−28.9
Indeterminate	40.09	61.85	101.94	7.09	5.45	−1.64	−6.5
Archaeological site boundary							
Fluvial	NA	NA	NA	NA	NA	NA	NA
Aeolian	0.96	7.87	8.83	0.10	0.58	0.48	35.3
Alluvial	0.24	0.27	0.51	0.02	0.02	0.00	2.1
Colluvial	0.08	0.24	0.32	0.01	0.09	0.08	40.0
Indeterminate	1.87	5.52	7.39	0.19	0.40	0.21	−27.8

In the $DoD_{2016–2017}$, net volumetric change was erosional in the baseline survey area, particularly below the maximum regulated flood stage where erosion was more than 10 times greater than deposition (fig. 20; table 25). However, net volumetric change in the archaeological site and individual features was depositional, except for feature 2 (fig. 20; table 26). Fluvial processes were the dominant mechanism of topographic change, demonstrating that changes above the maximum flood elevation were minimal during this survey interval (fig. 20; table 27). Above the maximum flood elevation and within the archaeological site boundary, aeolian processes were the most significant contributor to topographic change.

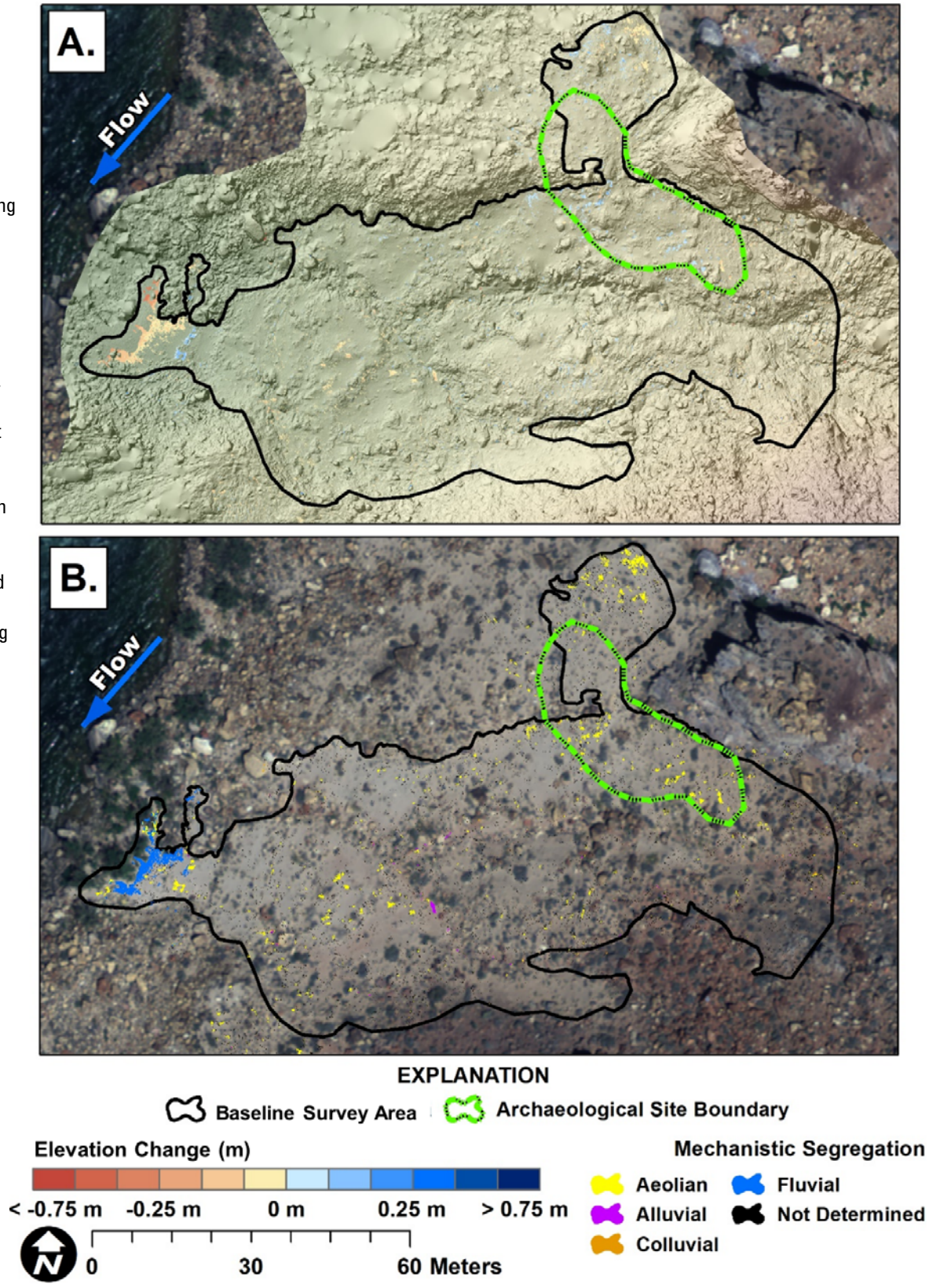

Figure 20. Maps showing change detection results between May 2016 and May 2017 for monitoring location CMC-1, central Marble Canyon, Arizona. *A*, Shaded relief showing elevation change results, in meters (m). Changes are within the 95-percent confidence interval. *B*, Results of automated geomorphic classification changes after Kasprak and others (2017). Aerial image collected by Grand Canyon Monitoring and Research Center (Durning and others, 2018).

Table 25. Results of change detection between May 2016 and May 2017 for the baseline survey area at monitoring location CMC-1, central Marble Canyon, Arizona.

[The archaeological site boundary is included in the above maximum flood elevation subdivision. m^2, square meter; m^3, cubic meter; %, percent]

Spatial subdivision	Survey area (m^2)	Area (m^2)			Volume (m^3)			Percent imbalance (%)
		Erosion	Deposition	Total	Erosion	Deposition	Net	
Baseline survey area	5,843.74	129.79	79.68	209.47	7.10	3.99	−3.11	−14.0
Below maximum flood elevation	234.78	40.83	4.42	45.25	2.93	0.25	−2.68	−42.1
Above maximum flood elevation	5,612.23	88.96	75.26	164.22	4.17	3.74	−0.43	−2.7
Archaeological site boundary	617.86	5.99	19.01	25.00	0.27	0.81	0.54	25.0

Table 26. Results of change detection between May 2016 and May 2017 for mapped archaeological features at site C:05:0031, central Marble Canyon, Arizona.

[Feature + buffer is inclusive of the feature area and a surrounding 1-meter-wide buffer. m^2, square meter; m^3, cubic meter; %, percent]

Spatial subdivision	Survey area (m^2)	Area (m^2)			Volume (m^3)			Percent imbalance (%)
		Erosion	Deposition	Total	Erosion	Deposition	Net	
Feature 2	19.96	0.94	0.05	0.99	0.04	0.00	−0.04	−50.0
Feature 2 + buffer	40.18	2.07	0.15	2.22	0.09	0.01	−0.08	−40.0
Feature 4	30.05	0.04	0.85	0.89	0.00	0.03	0.03	50.0
Feature 4 + buffer	58.15	0.13	1.59	1.72	0.01	0.06	0.05	35.7
Feature 5	24.84	0.03	0.39	0.42	0.00	0.01	0.01	50.0
Feature 5 + buffer	50.52	0.06	0.68	0.74	0.00	0.02	0.02	50.0

Table 27. Results of change detection by geomorphic mechanism between May 2016 and May 2017 at monitoring location CMC-1, central Marble Canyon, Arizona.

[NA indicates mechanisms not identified in the survey. m^2, square meter; m^3, cubic meter; %, percent]

Spatial subdivision	Area (m^2)			Volume (m^3)			Percent imbalance (%)
	Erosion	Deposition	Total	Erosion	Deposition	Net	
Baseline survey area							
Fluvial	33.06	1.15	34.21	2.13	0.06	−2.07	−47.3
Aeolian	34.73	28.27	63.00	1.98	1.26	−0.72	−23.7
Alluvial	3.19	0.53	3.72	0.16	0.03	−0.13	−34.2
Colluvial	0.61	0.32	0.93	0.08	0.04	−0.04	−16.7
Indeterminate	58.13	49.43	107.56	2.74	2.62	−0.12	−1.1
Archaeological site boundary							
Fluvial	NA	NA	NA	NA	NA	NA	NA
Aeolian	2.69	11.70	14.39	0.13	0.50	0.37	29.4
Alluvial	0.00	0.01	0.01	0.00	0.00	0.00	3.1
Colluvial	0.00	0.10	0.10	0.00	0.01	0.01	50.0
Indeterminate	3.32	7.21	10.53	0.14	0.31	0.17	18.9

In the $DoD_{2017–2019}$, net volumetric change was erosional in the baseline survey area, though the proportion of erosion to deposition was more balanced than between 2016 and 2017 (−6.5 percent imbalance; fig. 21; table 28). In this survey interval, the archaeological site received the largest net increase in sediment storage (1.22 cubic meters [m^3]) and all features increased in sediment cover (fig. 21; table 29). Upland topographic changes, including those in the archaeological site, were depositional as a result of aeolian and indeterminate processes that were interpreted as windblown sediment and sheetwash deposited at the base of vegetation (fig. 21; table 30). As in previous years, a portion of the wind-driven changes were in the northern part of the baseline survey area. However, a larger proportion of upland topographic changes were in the southern part of the baseline survey area along the toe of a steep rocky slope that is perpendicular to the river (fig. 21).

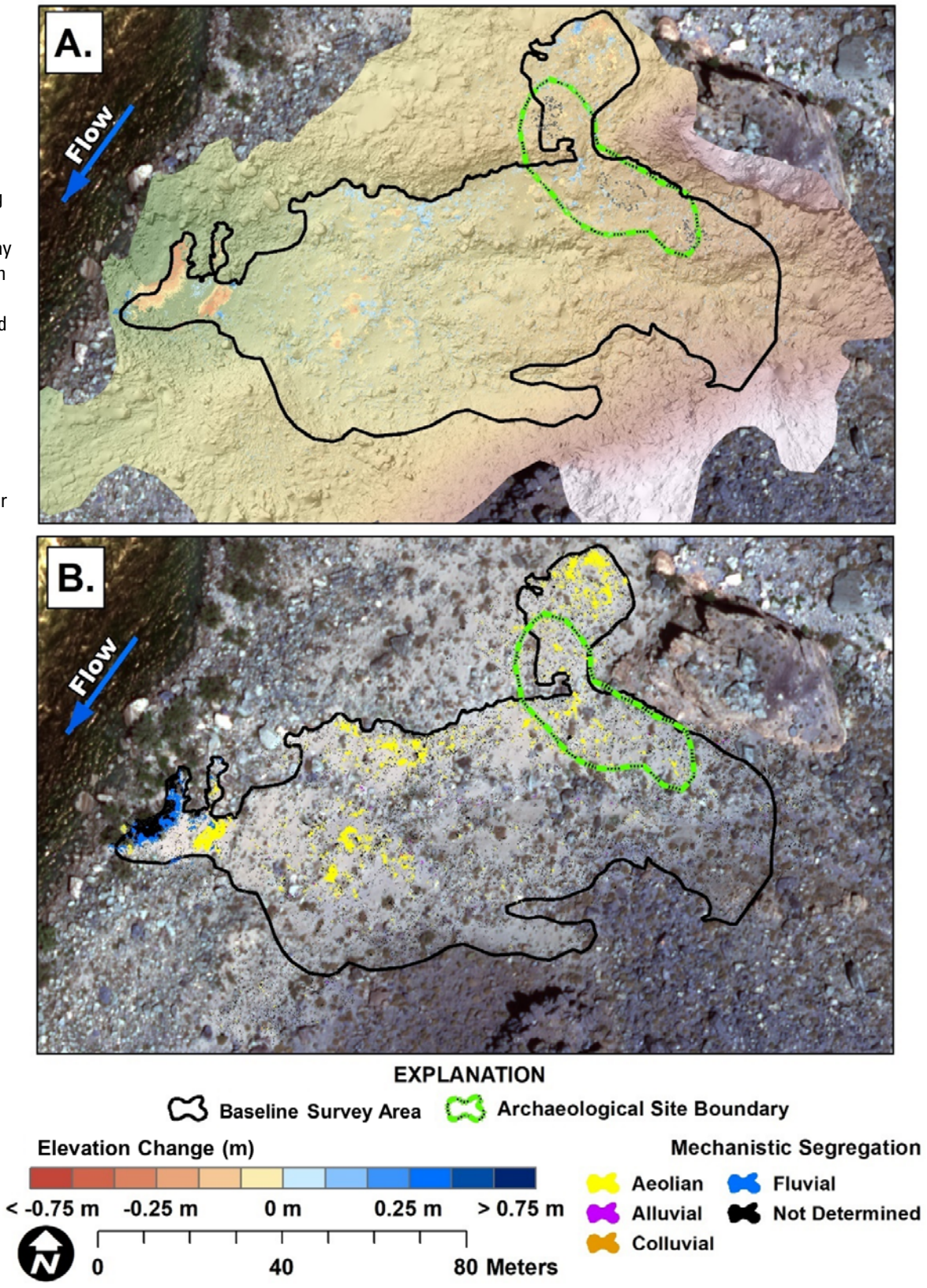

Figure 21. Maps showing change detection results between May 2017 and May 2019 for monitoring location CMC-1, central Marble Canyon, Arizona. *A*, Shaded relief showing elevation change results, in meters (m). Changes are within the 95-percent confidence interval. *B*, Results of automated geomorphic classification changes after Kasprak and others (2017). Aerial image collected by Grand Canyon Monitoring and Research Center (Durning and others, 2018).

Table 28. Results of change detection between May 2017 and May 2019 for the baseline survey area at monitoring location CMC-1, central Marble Canyon, Arizona.

[The archaeological site boundary is included above maximum flood elevation subdivision. m^2, square meter; m^3, cubic meter; %, percent]

Spatial subdivision	Survey area (m^2)	Area (m^2)			Volume (m^3)			Percent imbalance (%)
		Erosion	Deposition	Total	Erosion	Deposition	Net	
Baseline survey area	5,843.74	294.94	284.03	578.96	16.05	12.34	−3.72	−6.5
Below maximum flood elevation	234.78	78.76	8.93	87.69	6.07	0.46	−5.61	−43.0
Above maximum flood elevation	5,612.23	216.18	275.10	491.27	9.98	11.88	1.90	4.3
Archaeological site boundary	617.86	19.54	45.33	64.87	0.73	1.96	1.22	22.7

Table 29. Results of change detection between May 2017 and May 2019 for mapped archaeological features at site C:05:0031, central Marble Canyon, Arizona.

[Feature + buffer is inclusive of the feature area and a surrounding 1-meter-wide buffer. m^2, square meter; m^3, cubic meter; %, percent]

Spatial subdivision	Survey Area (m^2)	Area (m^2)			Volume (m^3)			Percent imbalance (%)
		Erosion	Deposition	Total	Erosion	Deposition	Net	
Feature 2	19.96	0.48	1.90	2.38	0.01	0.07	0.05	32.3
Feature 2 + buffer	40.18	2.11	2.91	5.02	0.07	0.11	0.04	10.8
Feature 4	30.05	0.06	2.53	2.59	0.00	0.09	0.09	48.1
Feature 4 + buffer	58.15	0.63	5.91	6.54	0.02	0.22	0.20	42.3
Feature 5	24.84	0.41	1.54	1.95	0.02	0.05	0.04	27.6
Feature 5 + buffer	50.52	1.83	2.29	4.12	0.07	0.08	0.00	1.3

Table 30. Results of change detection by geomorphic mechanism between May 2017 and May 2019 at monitoring location CMC-1, central Marble Canyon, Arizona.

[NA indicates mechanisms not identified in the survey. m^2, square meter; m^3, cubic meter; %, percent]

Spatial subdivision	Area (m^2)			Volume (m^3)			Percent imbalance (%)
	Erosion	Deposition	Total	Erosion	Deposition	Net	
Baseline survey area							
Fluvial	28.15	4.09	32.24	1.90	0.23	−1.67	−39.3
Aeolian	133.81	106.90	240.70	6.83	4.56	−2.27	−10.0
Alluvial	2.74	3.20	5.94	0.15	0.16	0.01	2.3
Colluvial	0.37	0.39	0.76	0.05	0.05	0.00	0.9
Indeterminate	129.97	169.42	299.39	7.13	7.34	0.21	0.7
Archaeological site boundary							
Fluvial	NA	NA	NA	NA	NA	NA	NA
Aeolian	11.42	21.78	33.20	0.43	0.94	0.52	18.8
Alluvial	0.03	0.44	0.47	0.00	0.02	0.02	44.4
Colluvial	0.00	0.15	0.15	0.00	0.01	0.01	50.0
Indeterminate	7.73	22.60	30.33	0.29	0.97	0.68	26.9

In the $DoD_{2019–2020}$, net volumetric change was erosional for both the baseline survey area and the archaeological site (fig. 22; table 31). Topographic change around the site features were net neutral except for the area immediately surrounding Features 4 and 5 (fig. 22; table 32). Fluvial and indeterminate processes were the dominant mechanisms of erosion for the baseline survey area, whereas aeolian and indeterminate processes were the dominant mechanisms in the archaeological site (fig. 22; table 33). Much of the indeterminate topographic change in both the baseline survey area and archaeological site was classified as such owing to its incoherent spatial distribution associated with rock and vegetation that may be representative of local wind scour.

Among the six repeat survey periods, volumetric changes in sediment storage for the baseline survey area at monitoring location CMC-1 showed significant erosion in $DoD_{2010–2013}$, followed by deposition in $DoD_{2013–2014}$, mixed erosion and deposition through

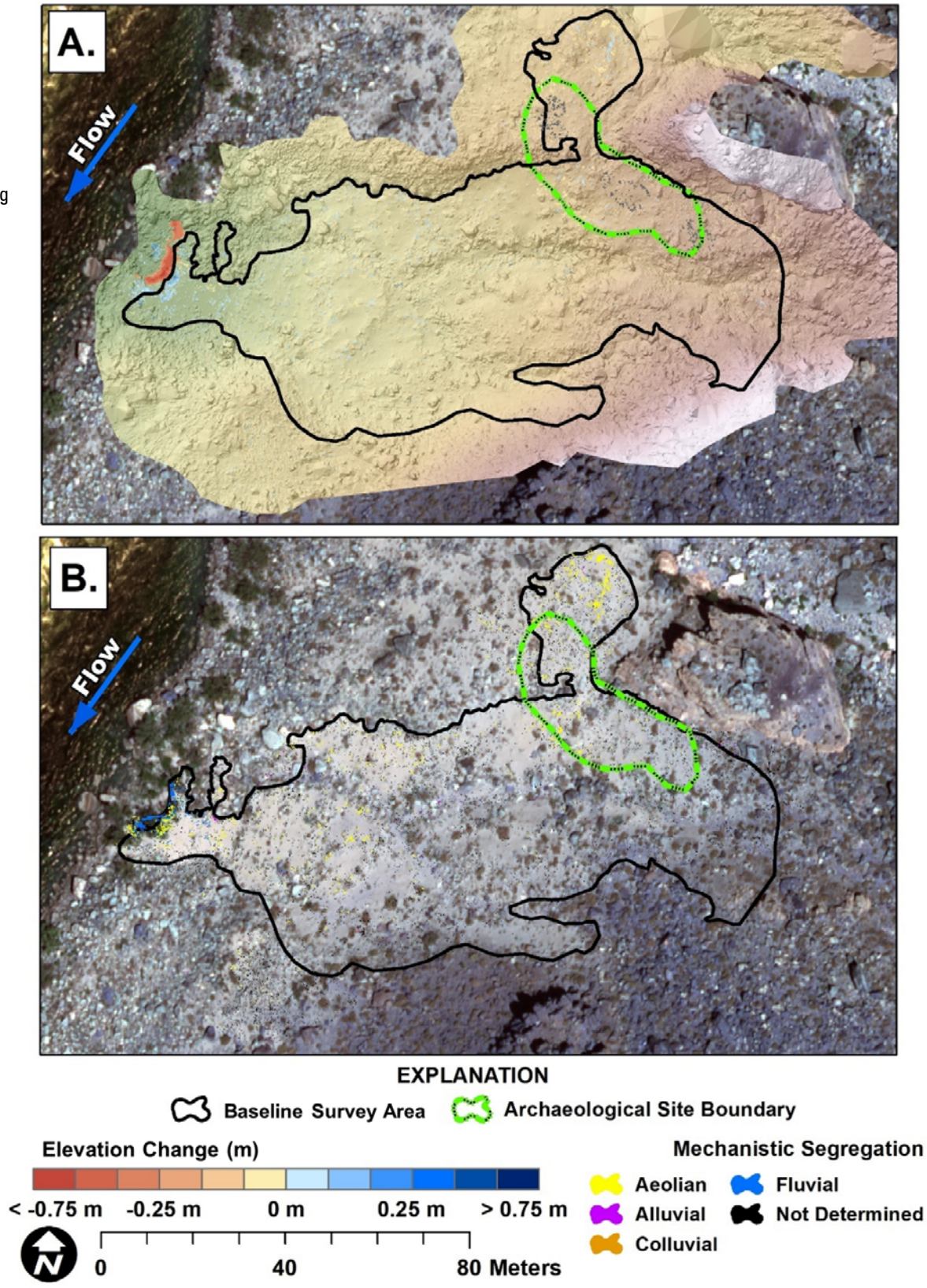

Figure 22. Maps showing change detection results between May 2019 and June 2020 for monitoring location CMC-1, central Marble Canyon, Arizona. *A*, Shaded relief showing elevation change results, in meters (m). Changes are within the 95-percent confidence interval. *B*, Results of automated geomorphic classification changes after Kasprak and others (2017). Aerial image collected by Grand Canyon Monitoring and Research Center (Durning and others, 2018).

Table 31. Results of change detection between May 2019 and June 2020 for the baseline survey area at monitoring location CMC-1, central Marble Canyon, Arizona.

[The archaeological site boundary is included in the above maximum flood elevation subdivision. m^2, square meter; m^3, cubic meter; %, percent]

Spatial subdivision	Survey area (m^2)	Area (m^2)			Volume (m^3)			Percent imbalance (%)
		Erosion	Deposition	Total	Erosion	Deposition	Net	
Baseline survey area	5,843.74	133.61	98.35	231.97	6.28	4.41	−1.87	−8.7
Below maximum flood elevation	234.78	7.62	22.09	29.71	0.95	1.12	0.17	4.2
Above maximum flood elevation	5,612.23	126.00	76.26	202.26	5.33	3.29	−2.04	−11.8
Archaeological site boundary	617.86	19.32	9.81	29.13	0.76	0.38	−0.39	−16.9

Table 32. Results of change detection between May 2019 and June 2020 for mapped archaeological features at site C:05:0031, central Marble Canyon, Arizona.

[Feature + buffer is inclusive of the feature area and a surrounding 1-meter-wide buffer. m^2, square meter; m^3, cubic meter; %, percent]

Spatial subdivision	Survey area (m^2)	Area (m^2)			Volume (m^3)			Percent imbalance (%)
		Erosion	Deposition	Total	Erosion	Deposition	Net	
Feature 2	19.96	0.40	0.27	0.67	0.01	0.01	0.00	−8.8
Feature 2 + buffer	40.18	0.28	0.23	0.51	0.01	0.01	0.00	2.6
Feature 4	30.05	0.18	0.21	0.39	0.01	0.01	0.00	3.1
Feature 4 + buffer	58.15	0.83	0.31	1.14	0.03	0.01	−0.02	−19.4
Feature 5	24.84	0.59	0.57	1.16	0.02	0.02	0.00	−1.5
Feature 5 + buffer	50.52	0.81	0.26	1.07	0.03	0.01	−0.02	−26.0

Table 33. Results of change detection by geomorphic mechanism between May 2016 and May 2017 at monitoring location CMC-1, central Marble Canyon, Arizona.

[NA indicates mechanisms not identified in the survey. m^2, square meter; m^3, cubic meter; %, percent]

Spatial subdivision	Area (m^2)			Volume (m^3)			Percent imbalance (%)
	Erosion	Deposition	Total	Erosion	Deposition	Net	
Baseline survey area							
Fluvial	5.38	6.06	11.45	0.86	0.30	−0.56	−24.2
Aeolian	33.60	30.25	63.85	1.31	1.31	0.00	−0.1
Alluvial	1.94	0.53	2.46	0.10	0.03	−0.07	−29.3
Colluvial	0.29	0.10	0.39	0.06	0.03	−0.03	−15.2
Indeterminate	92.40	61.42	153.83	3.95	2.75	−1.20	−9.0
Archaeological site boundary							
Fluvial	NA	NA	NA	NA	NA	NA	NA
Aeolian	7.73	2.36	10.08	0.30	0.09	−0.20	−26.1
Alluvial	0.05	0.00	0.05	0.00	0.00	0.00	−50.0
Colluvial	0.00	0.00	0.00	0.00	0.00	0.00	0.0
Indeterminate	11.54	7.45	18.99	0.46	0.28	−0.18	−12.1

$DoD_{2016–2017}$, significant deposition in $DoD_{2017–2019}$, and erosion in $DoD_{2019–2020}$ (fig. 23). This resulted in a net reduction in sediment storage between 2010 and 2020 of 12.2 m^3 for the baseline survey area. In the archaeological site, positive changes in sediment storage, indicating net sediment deposition or burial, occurred in four of the six repeat survey periods, resulting in a net gain of 2.8 m^3. In general, fluvial processes were the dominant mechanisms across the six survey periods, though aeolian processes were most common in the archaeological site and the area above the maximum regulated flood stage (fig. 23). Areas of repeat change were documented throughout the survey area, though they were particularly concentrated below the controlled flood elevation and along the northern part of the survey area, toward the side canyon tributary, with deposition noted along the toe of a rocky slope that crosses from the western edge of the baseline survey area into the archaeological site to the east (fig. 23). East and upslope of the sandbar deposit that is inundated by controlled floods is an area of alternating repeat and single period erosion and deposition that indicates aeolian dune migration in the dominant wind direction toward the archaeological site.

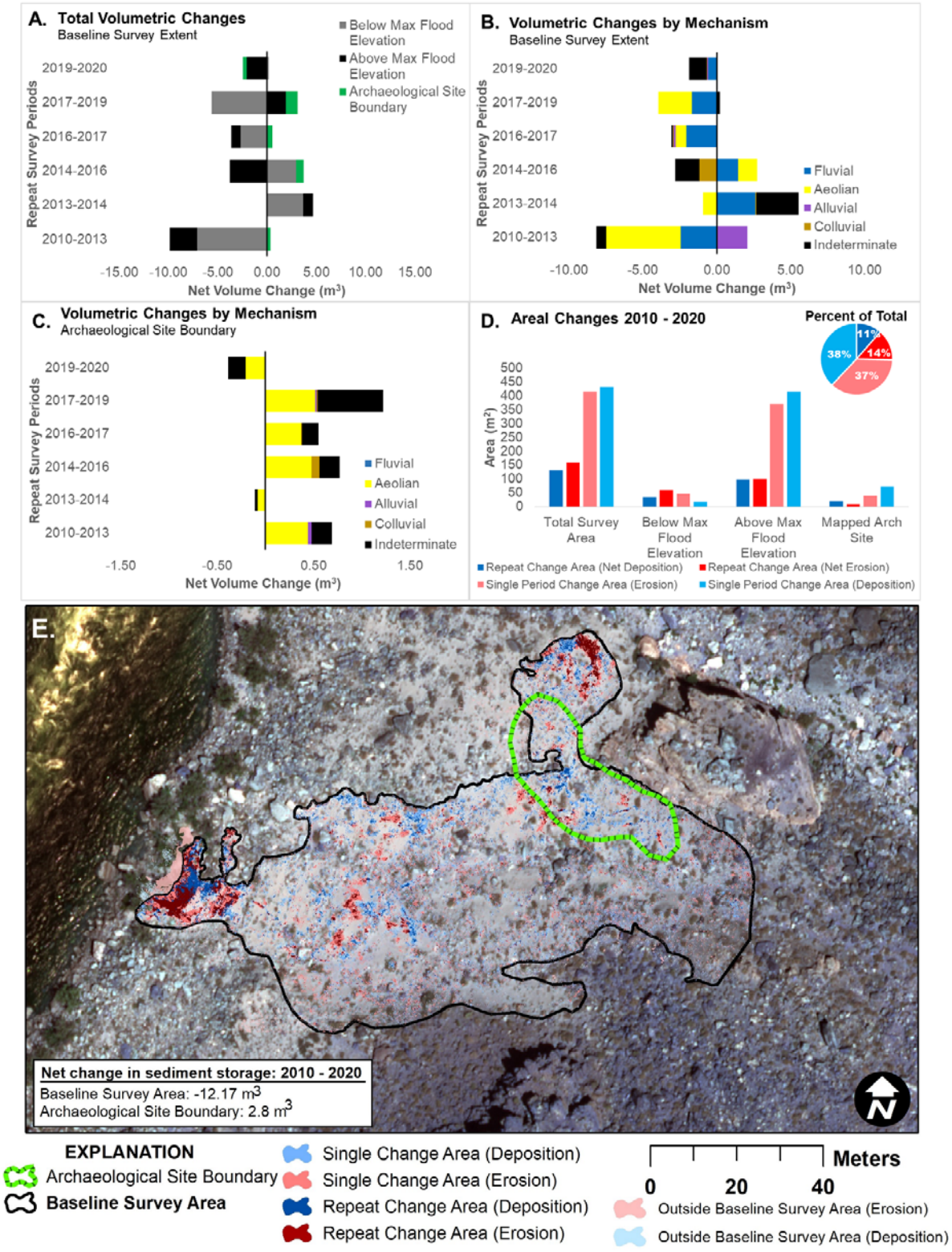

Figure 23. Plots of net volumetric (in cubic meters [m^3]) and areal (in square meters [m^2]) change in sediment storage between September 2010 and June 2020 for monitoring location CMC-1, central Marble Canyon, Arizona. *A*, Change results for the baseline survey area by spatial subdivision. *B*, Change results for the baseline survey area by geomorphic mechanism. *C*, Change results within the boundary of archaeological site C:05:0031 by geomorphic mechanism. Net volumetric changes to the left of the zero line indicate erosion and changes to the right of the zero line indicate deposition. *D*, Plot of change by location with regard to the regulated flood stage elevation (which occurs at a flow rate of 45,000 cubic feet per second) and the archaeological site. *E*, Map of areas that have repeat and single changes. Area of topographic change, net change direction (erosion or deposition), and net change in sediment storage were determined from the summation of all six digital elevation models of difference (DoDs). Repeat change area refers to pixels that have significant change in at least two DoDs. Single period change area refers to pixels that have significant change in only one DoD. Aerial image collected by Grand Canyon Monitoring and Research Center (Durning and others, 2018).

Monitoring Location SMC-1

Monitoring location SMC-1 is located in southern Marble Canyon on river right. This location was previously surveyed using TLS in May 2006, May 2007, September 2007, April 2010, and September 2010; those results are synthesized by Collins and others (2012, 2016). Meteorological data, including temperature, wind direction, wind speed, and rainfall, were collected at this location from February 2007 to June 2011 (Draut and others, 2009, 2010; Collins and others, 2012; Dealy and others, 2014; Caster and others, 2014). These data show that wind at this location originates from the southeast and blows from the downstream sandbar toward archaeological site C:13:0006 on the upstream side of the side canyon tributary (fig. 24). Collins and others (2016) reported that net topographic changes at site C:13:0006 were predominantly depositional from 2006 to 2007, and primarily erosional between 2007 and 2010.

We resurveyed the monitoring location in May 2018. This survey covered a significantly larger area than the previous surveys, allowing for a future baseline survey area of 10,257 m^2 that includes the downstream sandbar as well as archaeological site C:13:0006. The largest overlapping area between the 2010 and 2018 surveys permitted a change detection area of 5,221 m^2, which includes almost the entire mapped archaeological site (fig. 24). Site C:13:0006 is aeolian type 2c, where the side canyon tributary creates a barrier to sediment transport from the downstream sandbar as does riparian vegetation. This site is drainage type 3, as a portion of site C:13:0006 resides within the side canyon

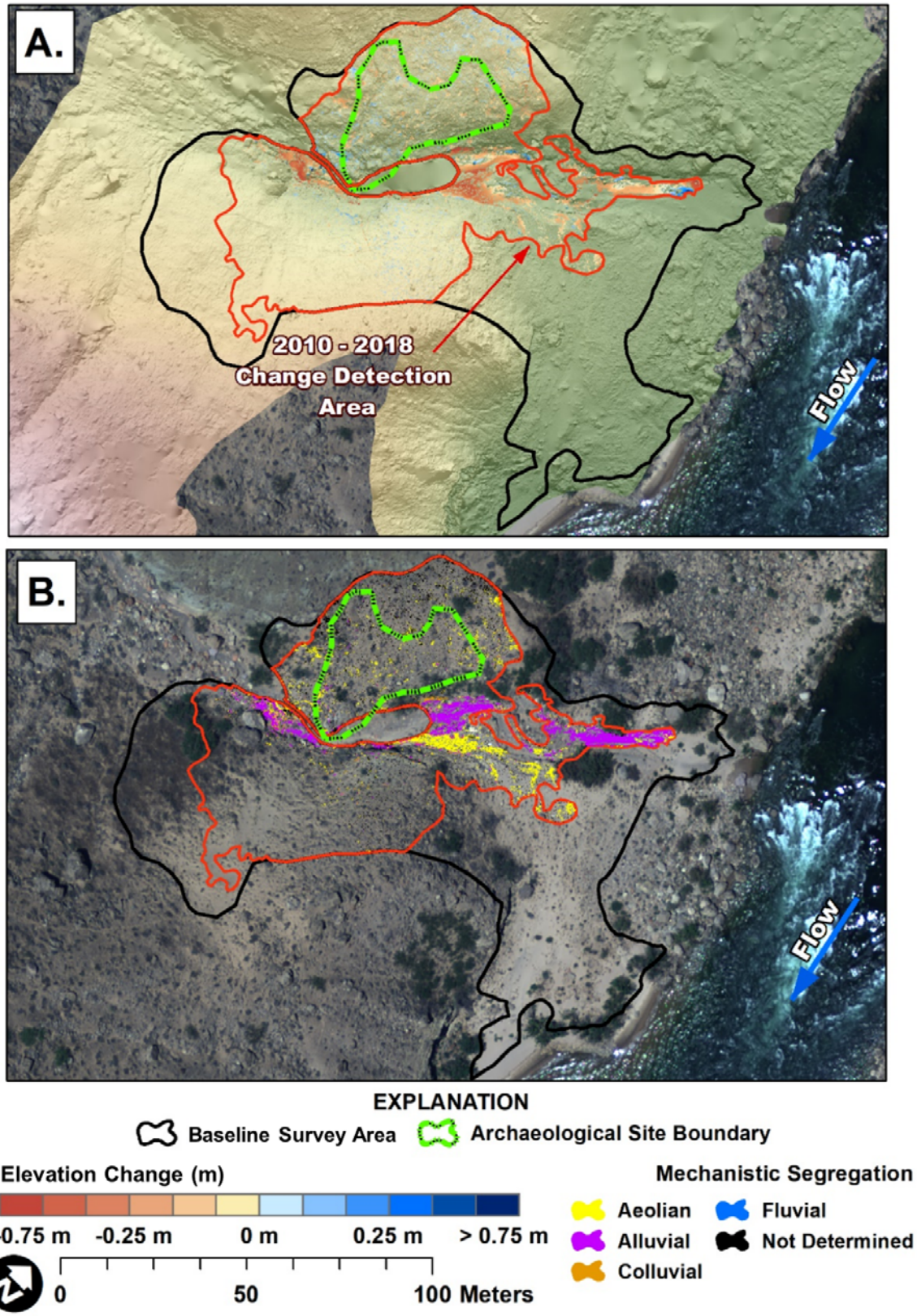

Figure 24. Maps showing change detection results between September 2010 and May 2018 for monitoring location SMC-1, southern Marble Canyon, Arizona. *A*, Shaded relief showing elevation change results, in meters (m). Changes are within the 95-percent confidence interval. *B*, Results of automated geomorphic classification changes after Kasprak and others (2017). Aerial image collected by Grand Canyon Monitoring and Research Center (Durning and others, 2018).

Table 34. Results of change detection between September 2010 and May 2018 for the change detection area at monitoring location SMC-1, southern Marble Canyon, Arizona.

[The archaeological site boundary is included in the above maximum flood elevation subdivision. m^2, square meter; m^3, cubic meter; %, percent; NA, not applicable]

Spatial subdivision	Survey area (m^2)	Area (m^2)			Volume (m^3)			Percent imbalance (%)
		Erosion	Deposition	Total	Erosion	Deposition	Net	
Change detection area	5,220.69	502.16	169.94	672.10	125.48	14.43	−111.05	−39.7
Below maximum flood elevation	0.00	NA	NA	NA	NA	NA	NA	NA
Above maximum flood elevation	5,220.69	502.16	169.94	672.10	125.48	14.43	−111.05	−39.7
Archaeological site boundary	915.30	63.09	37.05	100.14	7.63	2.84	−4.79	−22.9

Table 35. Results of change detection by geomorphic mechanism between September 2010 and May 2018 at monitoring location SMC-1, southern Marble Canyon, Arizona.

[NA indicates mechanisms not identified in the survey. m^2, square meter; m^3, cubic meter; %, percent]

Spatial subdivision	Area (m^2)			Volume (m^3)			Percent imbalance (%)
	Erosion	Deposition	Total	Erosion	Deposition	Net	
Baseline survey area							
Fluvial	NA	NA	NA	NA	NA	NA	NA
Aeolian	174.95	26.77	201.72	43.80	2.44	−41.36	−44.7
Alluvial	180.27	21.50	201.76	54.30	3.22	−51.07	−44.4
Colluvial	19.34	5.61	24.96	10.16	0.95	−9.22	−41.5
Indeterminate	127.32	115.98	243.29	17.17	7.81	−9.36	−18.7
Archaeological site boundary							
Fluvial	NA	NA	NA	NA	NA	NA	NA
Aeolian	20.83	6.94	27.76	2.70	0.66	−2.04	−30.4
Alluvial	3.52	1.24	4.76	0.65	0.11	−0.55	−36.1
Colluvial	1.48	0.32	1.80	0.32	0.02	−0.30	−44.1
Indeterminate	37.26	28.55	65.82	3.96	2.06	−1.91	−15.8

tributary channel. Individual archaeological features were not mapped during the TLS survey in 2018. Table 34 provides a summary of the survey divisions in figure 24.

Between 2010 and 2018, the net volumetric change for both the change detection area and the archaeological site was erosional (table 34). Indeterminate, aeolian, and alluvial processes contributed to most topographic changes between the 2010 and 2018 surveys (table 35). The greatest changes occurred along the side canyon tributary downslope of site C:13:0006 (fig. 24). This area incurred alluvial changes associated with widening of the side canyon channel as well as aeolian overprinting of alluvial processes associated with a depositional bench located on the right bank of the tributary (fig. 24). The left bank of the tributary, directly below the archaeological site, eroded and may contribute to future geomorphic changes in the site (fig. 24). Outside of the side canyon tributary, topographic changes in the archaeological site were driven by aeolian and indeterminate erosion (table 35).

Monitoring Location SMC-2

Monitoring location SMC-2 is located in southern Marble Canyon on river right. This location was previously monitored for weather parameters from February 2008 to July 2011 (Draut and others, 2009, 2010; Dealy and others, 2014; Caster and others, 2014) but no lidar data was collected prior to 2018. In May 2018, we surveyed most of the SMC-2 debris fan, including archaeological site C:13:0365 and the area between the site and the downstream sandbar. The large baseline survey area of 18,245 m^2 is oriented to match the interpretation of wind data from the weather monitoring records, which show wind originates from the south-southeast and blows from the downstream sandbar toward archaeological site C:13:0365 (fig. 25; Caster and others, 2014). Approximately 73 percent of the mapped archaeological site is contained within the baseline survey area. Site C:13:0365 is classified as aeolian type 2c owing to its position upstream of the side canyon tributary and the presence of a riparian vegetative barrier between the site and the upwind sandbar. Small rills within the site were noted in the field, but they have not incised to the tributary channel or the river and thus the site is classified as drainage type 2. Specific archaeological features were not mapped during the lidar survey.

We resurveyed the monitoring location in May 2019 covering all of the original survey area. In the $DoD_{2018–2019}$, both

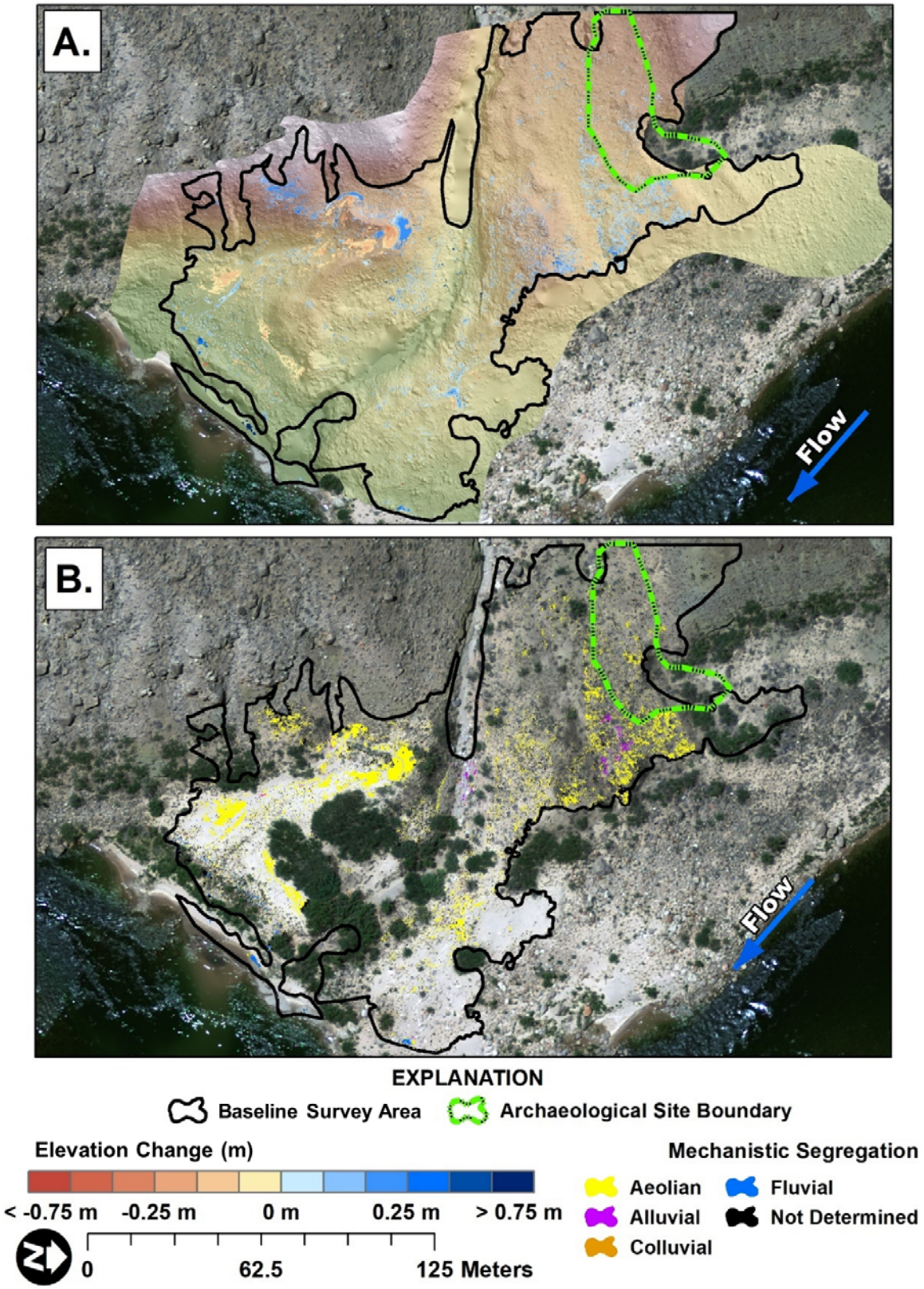

Figure 25. Maps showing change detection results between May 2018 and May 2019 for monitoring location SMC-2, southern Marble Canyon, Arizona. *A*, Shaded relief showing elevation change results, in meters (m). Changes are within the 95-percent confidence interval. *B*, Results of automated geomorphic classification changes after Kasprak and others (2017). Aerial image collected by Grand Canyon Monitoring and Research Center (Durning and others, 2018).

Table 36. Results of change detection between May 2018 and May 2019 for the change detection area at monitoring location SMC-2, southern Marble Canyon, Arizona.

[The archaeological site boundary is included in the above maximum flood elevation subdivision. m^2, square meter; m^3, cubic meter; %, percent]

Spatial subdivision	Survey area (m^2)	Area (m^2)			Volume (m^3)			Percent imbalance (%)
		Erosion	Deposition	Total	Erosion	Deposition	Net	
Baseline survey area	18,244.51	534.16	1,199.45	1,733.61	35.86	91.53	55.68	21.9
Below maximum flood elevation	1,033.94	44.61	64.64	109.25	3.32	13.45	10.13	30.2
Above maximum flood elevation	17,210.58	489.55	1,134.82	1,624.37	32.54	78.08	45.54	20.6
Archaeological site boundary	1,158.11	30.40	79.14	109.53	1.71	3.23	1.52	15.4

Table 37. Results of change detection by geomorphic mechanism between May 2018 and May 2019 at monitoring location SMC-2, southern Marble Canyon, Arizona.

[NA indicates mechanisms not identified in the survey. m^2, square meter; m^3, cubic meter; %, percent]

Spatial subdivision	Area (m^2)			Volume (m^3)			Percent imbalance (%)
	Erosion	Deposition	Total	Erosion	Deposition	Net	
Baseline survey area							
Fluvial	10.33	19.18	924.78	0.84	8.10	7.25	20.2
Aeolian	283.92	640.86	924.78	19.71	46.42	26.71	20.2
Alluvial	7.15	25.97	33.12	0.77	1.73	0.96	19.2
Colluvial	3.06	4.73	7.78	1.47	2.11	0.64	9.0
Indeterminate	131.99	342.32	474.31	10.60	28.98	18.38	23.2
Archaeological site boundary							
Fluvial	NA	NA	NA	NA	NA	NA	NA
Aeolian	7.06	33.34	40.40	0.58	1.59	1.00	23.1
Alluvial	0.00	0.11	0.11	0.00	0.01	0.01	50.0
Colluvial	0.21	0.02	0.23	0.03	0.00	−0.03	−46.7
Indeterminate	14.14	23.85	37.99	0.87	1.10	0.23	5.8

the baseline survey area and the archaeological site incurred net deposition (fig. 25; table 36). Aeolian sediment transport was the dominant process of topographic change, followed by indeterminant processes (fig. 25; table 37). Within the downstream part of the baseline survey area, aeolian sediment transport was interpreted as the process that produced alternating patterns of erosion and deposition in the downwind direction (northwest), consistent with dune migration. In the upstream part of the baseline survey area, there is also evidence of dune migration within the open sand to the east (riverward), with more dispersed aeolian and indeterminate topographic changes to the west and into the archaeological site (fig. 25). Indeterminate changes were primarily within areas of vegetation and sand covered with biological soil crust, possibly representing deposition from windblown sediment or sheetwash.

Monitoring Location EGC-1

Monitoring location EGC-1 is located in eastern Grand Canyon on river right. This is a long-term monitoring location centered on one archaeological site, C:13:0321, that was previously surveyed using TLS in April and September 2010. Collins and others (2012, 2016) synthesized the results of those surveys showing that topographic changes were predominantly erosional during that period. In addition to previous TLS surveys, the sandbar at this location has been surveyed as part of the USGS sandbar monitoring program (Hazel and others, 2010; Grams and others, 2013). On the opposite bank of the monitoring location, on river left, a weather monitoring station has recorded temperature, wind direction, wind speed, and rainfall since 2007 (Draut and others, 2009, 2010; Collins and others, 2012; Dealy and others, 2014; Caster and others, 2014, 2018; East and others, 2016). These data indicate that wind originates from the south by southwest and blows from the sandbar north by northeast to the archaeological site. In 2019, the NPS began conducting annual vegetation management at monitoring location EGC-1 to remove riparian plants that create a barrier to aeolian transport of sand from the sandbar toward the archaeological site. In May 2019, we resurveyed monitoring location EGC-1 following vegetation management efforts, and we resurveyed it again in June 2020 prior to that year's vegetation management effort.

Site C:13:0321 is classified as aeolian type 1 and drainage type 2 owing to the adjacent sandbar and a wide, but shallow, runoff channel that goes through the center of the baseline survey area. A baseline survey area of 3,056 m^2 was covered during seven surveys between 2010 and 2020 (figs. 26–32; tables 38–55). Additional area was surveyed after 2013 to include cultural features that were outside of

the 2010 survey area (tables 41–55). Beginning in May 2019, two additional archaeological sites were included within the survey: sites C:13:0009 and C:13:0092. Site C:13:0009 was classified as aeolian type 1 and drainage type 3 owing to the presence of an upwind sandbar and several gullies that connect directly to the side canyon tributary. Site C:13:0092 is an aeolian type 3 and a drainage type 1 site owing to the absence of an upwind sandbar or any concentrated runoff pathways. Change detection results focus on the previous baseline survey area, though topographic change associated with the areas added after 2010 are included in the cultural feature results (tables 42, 45, 48, 51, and 54) as well as the additional archaeological sites included after May 2019.

In the $DoD_{2010–2013}$, net volumetric change within the baseline survey area was erosional, particularly above the maximum regulated flood inundation elevation (fig. 26; table 38). Net erosion was also measured in the archaeological site and associated features (tables 38 and 39). Within the archaeological site boundary and the baseline survey area, aeolian processes were the dominant mechanism of change (table 40). Erosion was most pronounced on the sandbar above the maximum regulated flow stage elevation, and along the base of the dune west of features 5 and 6 (fig. 26).

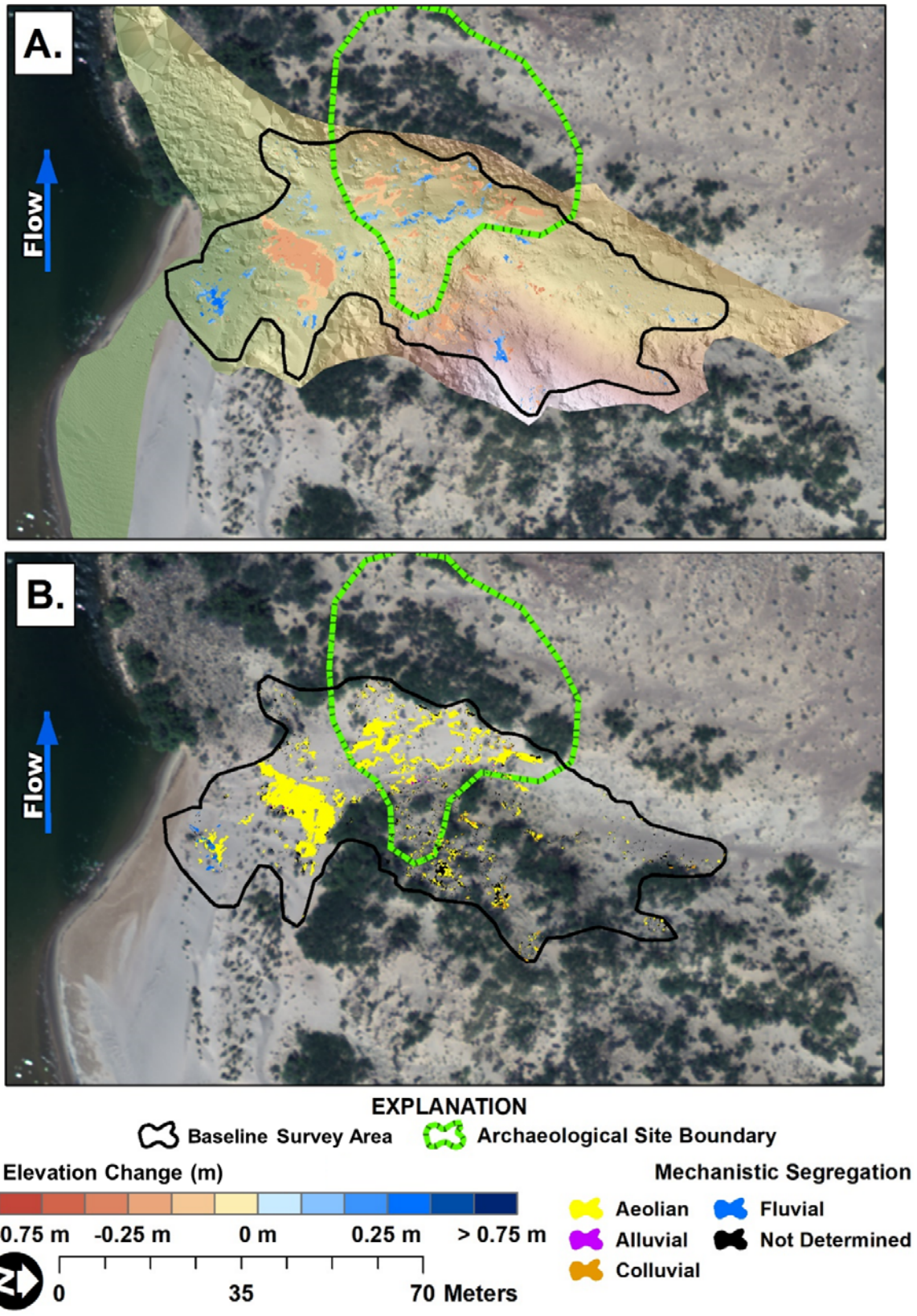

Figure 26. Maps showing change detection results between September 2010 and May 2013 for monitoring location EGC-1, eastern Grand Canyon, Arizona. *A*, Shaded relief showing elevation change results, in meters (m). Changes are within the 95-percent confidence interval. *B*, Results of automated geomorphic classification changes after Kasprak and others (2017). Aerial image collected by Grand Canyon Monitoring and Research Center (Durning and others, 2018).

Table 38. Results of change detection between September 2010 and May 2013 for the baseline survey area at monitoring location EGC-1, eastern Grand Canyon, Arizona.

[The archaeological site boundary is included in the above maximum flood elevation subdivision. m^2, square meter; m^3, cubic meter; %, percent]

Spatial subdivision	Survey area (m^2)	Area (m^2)			Volume (m^3)			Percent imbalance (%)
		Erosion	Deposition	Total	Erosion	Deposition	Net	
Baseline survey area	3,056.01	234.32	96.11	330.43	30.08	11.48	−18.60	−22.4
Below maximum flood elevation	176.05	0.56	15.00	15.55	0.07	3.17	3.11	48.0
Above maximum flood elevation	2,879.96	233.76	81.11	314.87	30.01	8.31	−21.70	−28.3
Archaeological site boundary	727.54	81.65	35.66	117.31	9.37	3.61	−5.76	−22.2

Table 39. Results of change detection between September 2010 and May 2013 for mapped archaeological features at site C:13:0321, eastern Grand Canyon, Arizona.

[Feature + buffer is inclusive of the feature area and a surrounding 1-meter-wide buffer. m^2, square meter; m^3, cubic meter; %, percent; NA, not applicable]

Spatial subdivision	Survey area (m^2)	Area (m^2)			Volume (m^3)			Percent imbalance (%)
		Erosion	Deposition	Total	Erosion	Deposition	Net	
Feature 1	12.24	NA	NA	NA	NA	NA	NA	NA
Feature 1 + buffer	28.85	NA	NA	NA	NA	NA	NA	NA
Feature 2	1.35	NA	NA	NA	NA	NA	NA	NA
Feature 2 + buffer	9.02	NA	NA	NA	NA	NA	NA	NA
Feature 3	3.93	NA	NA	NA	NA	NA	NA	NA
Feature 3 + buffer	14.72	NA	NA	NA	NA	NA	NA	NA
Feature 5	1.35	0.02	0.00	0.02	0.00	0.00	0.00	−50.0
Feature 5 + buffer	8.97	1.57	0.03	1.61	0.13	0.00	−0.12	−48.3
Feature 6	1.36	0.04	0.00	0.04	0.00	0.00	0.00	−50.0
Feature 6 + buffer	9.02	0.36	1.06	1.42	0.04	0.13	0.09	28.0
Feature 7	2.55	NA	NA	NA	NA	NA	NA	NA
Feature 7 + buffer	12.30	NA	NA	NA	NA	NA	NA	NA

Table 40. Results of change detection by geomorphic mechanism between September 2010 and May 2013 at monitoring location EGC-1, eastern Grand Canyon, Arizona.

[NA indicates mechanisms not identified in the survey. m^2, square meter; m^3, cubic meter; %, percent]

Spatial subdivision	Area (m^2)			Volume (m^3)			Percent imbalance (%)
	Erosion	Deposition	Total	Erosion	Deposition	Net	
Baseline survey area							
Fluvial	0.36	4.48	4.83	0.04	0.82	0.78	45.3
Aeolian	192.58	65.48	258.06	24.50	7.81	−16.68	−25.8
Alluvial	1.25	0.84	2.09	0.13	0.09	−0.04	−9.6
Colluvial	5.50	2.72	8.22	1.34	0.45	−0.89	−25.0
Indeterminate	34.63	22.60	57.23	4.06	2.31	−1.75	−13.7
Archaeological site boundary							
Fluvial	NA	NA	NA	NA	NA	NA	NA
Aeolian	67.53	28.91	96.44	7.52	2.98	−4.54	−21.6
Alluvial	0.85	0.72	1.57	0.08	0.06	−0.02	−5.4
Colluvial	1.34	0.21	1.56	0.49	0.03	−0.46	−44.9
Indeterminate	11.93	5.82	17.74	1.28	0.54	−0.74	−20.3

Net volumetric change for the $DoD_{2013–2014}$ was depositional in the baseline survey area (fig. 27; table 41). Within the archaeological site boundary, the net volumetric change was slightly erosional, and associated feature erosion was more pronounced outside of the baseline survey area (table 42; features 1 and 8) than inside (table 42; features 5 and 6). Wind was the most significant geomorphic agent both within the archaeological site and the baseline survey area (table 43). The greatest volume of change occurred in the southern (upwind) part of the baseline area (fig. 27).

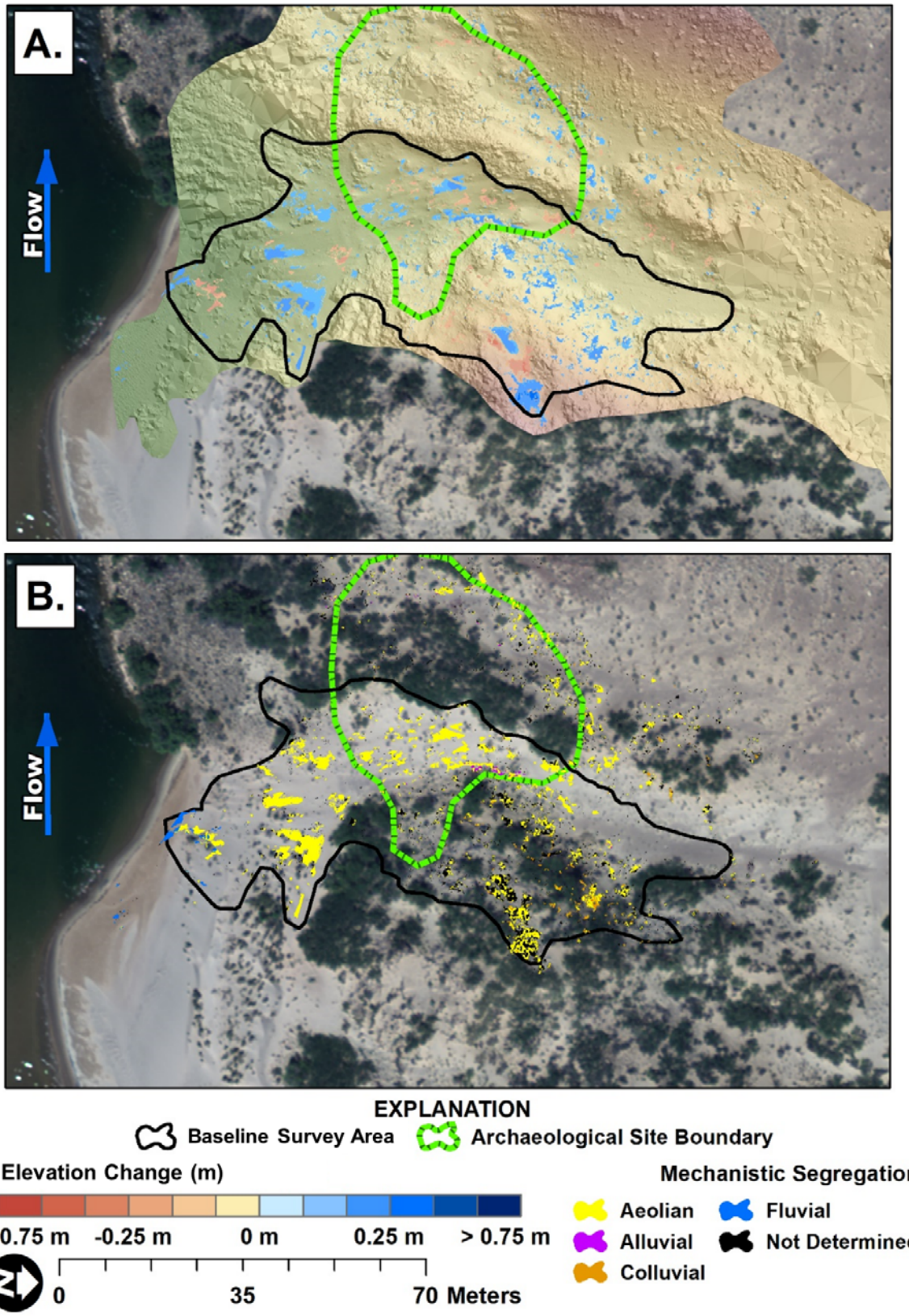

Figure 27. Maps showing change detection results between May 2013 and May 2014 for monitoring location EGC-1, eastern Grand Canyon, Arizona. *A*, Shaded relief showing elevation change results, in meters (m). Changes are within the 95-percent confidence interval. *B*, Results of automated geomorphic classification changes after Kasprak and others (2017). Aerial image collected by Grand Canyon Monitoring and Research Center (Durning and others, 2018).

Table 41. Results of change detection between May 2013 and May 2014 for the baseline survey area at monitoring location EGC-1, eastern Grand Canyon, Arizona.

[The archaeological site boundary is included in the above maximum flood elevation subdivision. m^2, square meter; m^3, cubic meter; %, percent]

Spatial subdivision	Survey area (m^2)	Area (m^2)			Volume (m^3)			Percent imbalance (%)
		Erosion	Deposition	Total	Erosion	Deposition	Net	
Baseline survey area	3,056.01	41.10	251.58	292.67	8.33	24.60	16.27	24.7
Below maximum flood elevation	176.05	11.33	8.75	20.08	1.20	1.17	−0.03	−0.6
Above maximum flood elevation	2,879.96	29.77	242.83	272.60	7.13	23.43	16.30	26.7
Archaeological site boundary	727.54	25.69	49.74	75.43	1.96	4.08	2.12	17.5

Table 42. Results of change detection between May 2013 and May 2014 for mapped archaeological features at site C:13:0321, eastern Grand Canyon, Arizona.

[Results are presented for two inclusive subdivisions. The largest overlapping area represents all significant topographic change in the DEM of difference and the baseline survey area represents a subset of significant changes relative to the baseline survey. Feature + buffer is inclusive of the feature area and a surrounding 1-meter-wide buffer. DEM, digital elevation model; m^2, square meter; m^3, cubic meter; %, percent; NA, not applicable]

Spatial subdivision	Survey area (m^2)	Area (m^2)			Volume (m^3)			Percent imbalance (%)
		Erosion	Deposition	Total	Erosion	Deposition	Net	
Largest overlapping area								
Feature 1	12.24	0.29	0.02	0.31	0.02	0.00	−0.02	−45.0
Feature 1 + buffer	28.85	1.15	0.03	1.18	0.07	0.00	−0.07	−47.7
Feature 2	1.35	0.00	0.00	0.00	0.00	0.00	0.00	0.0
Feature 2 + buffer	9.02	0.03	0.09	0.12	0.00	0.01	0.01	29.7
Feature 3	3.93	0.00	0.01	0.01	0.00	0.00	0.00	50.0
Feature 3 + buffer	14.72	0.00	0.47	0.47	0.00	0.03	0.03	50.0
Feature 5	1.35	0.00	0.12	0.12	0.00	0.01	0.01	50.0
Feature 5 + buffer	8.97	0.09	0.29	0.38	0.01	0.02	0.01	26.2
Feature 6	1.36	0.00	0.00	0.00	0.00	0.00	0.00	−50.0
Feature 6 + buffer	9.02	0.30	0.41	0.71	0.02	0.03	0.01	8.2
Feature 7	2.55	0.01	0.00	0.01	0.00	0.00	0.00	−50.0
Feature 7 + buffer	12.30	0.01	0.29	0.30	0.00	0.02	0.02	47.1
Baseline survey area								
Feature 1	12.24	NA	NA	NA	NA	NA	NA	NA
Feature 1 + buffer	28.85	NA	NA	NA	NA	NA	NA	NA
Feature 2	1.35	NA	NA	NA	NA	NA	NA	NA
Feature 2 + buffer	9.02	NA	NA	NA	NA	NA	NA	NA
Feature 3	3.93	NA	NA	NA	NA	NA	NA	NA
Feature 3 + buffer	14.72	NA	NA	NA	NA	NA	NA	NA
Feature 5	1.35	0.00	0.12	0.12	0.00	0.01	0.01	50.0
Feature 5 + buffer	8.97	0.09	0.29	0.38	0.01	0.02	0.01	26.2
Feature 6	1.36	0.00	0.00	0.00	0.00	0.00	0.00	−50.0
Feature 6 + buffer	9.02	0.30	0.41	0.71	0.02	0.03	0.01	8.2
Feature 7	2.55	NA	NA	NA	NA	NA	NA	NA
Feature 7 + buffer	12.30	NA	NA	NA	NA	NA	NA	NA

Table 43. Results of change detection by geomorphic mechanism between May 2013 and May 2014 at monitoring location EGC-1, eastern Grand Canyon, Arizona.

[NA indicates mechanisms not identified in the survey. m^2, square meter; m^3, cubic meter; %, percent]

Spatial subdivision	Area (m^2)			Volume (m^3)			Percent imbalance (%)
	Erosion	Deposition	Total	Erosion	Deposition	Net	
Baseline survey area							
Fluvial	2.24	6.29	8.53	0.20	0.87	0.67	31.2
Aeolian	54.28	164.94	219.21	5.26	15.32	10.06	24.4
Alluvial	0.38	2.99	3.37	0.05	0.36	0.31	38.2
Colluvial	1.94	11.48	13.42	0.30	1.36	1.06	32.0
Indeterminate	24.42	65.88	90.30	2.53	6.69	4.17	22.6
Archaeological site boundary							
Fluvial	NA	NA	NA	0.00	NA	NA	NA
Aeolian	20.51	40.19	60.70	1.55	3.27	1.72	17.9
Alluvial	0.31	2.73	3.04	0.04	0.33	0.29	38.3
Colluvial	0.24	0.20	0.44	0.03	0.02	−0.01	−10.4
Indeterminate	4.63	6.62	11.25	0.34	0.46	0.12	7.5

The $DoD_{2014–2016}$ exhibited a large amount of net deposition in the baseline survey area (table 44). Net volumetric change within the archaeological site was also depositional (table 44). Changes at the individual features were depositional except for at feature 5, located at the windward base of a dune (fig. 28; table 45). Similar to the previous DoD intervals, aeolian processes were the dominant mechanism of change, though both fluvial and alluvial processes were determined to be important contributors (table 46), particularly within the active Colorado River channel and in the northern part of the baseline survey area (fig. 28). Discrete areas of erosion and deposition associated with small dune troughs and crests, respectively, alternated from upwind to downwind (southwest to northeast) across the survey area (fig. 28). The greatest concentration of volumetric change in sediment storage was alluvial and aeolian sediment deposition in the northern part of the survey area (fig. 28).

Table 44. Results of change detection between May 2014 and May 2016 for the baseline survey area at monitoring location EGC-1, eastern Grand Canyon, Arizona.

[The archaeological site boundary is included in the above maximum flood elevation subdivision. m^2, square meter; m^3, cubic meter; %, percent]

Spatial subdivision	Survey area (m^2)	Area (m^2)			Volume (m^3)			Percent imbalance (%)
		Erosion	Deposition	Total	Erosion	Deposition	Net	
Baseline survey area	3,056.01	408.18	535.57	943.75	44.66	60.84	16.18	7.7
Below maximum flood elevation	176.05	53.22	1.72	54.94	16.21	0.11	−16.10	−49.3
Above maximum flood elevation	2,879.96	354.96	533.85	888.81	28.45	60.73	32.28	18.1
Archaeological site boundary	727.54	94.02	130.89	224.91	6.60	9.00	2.39	7.7

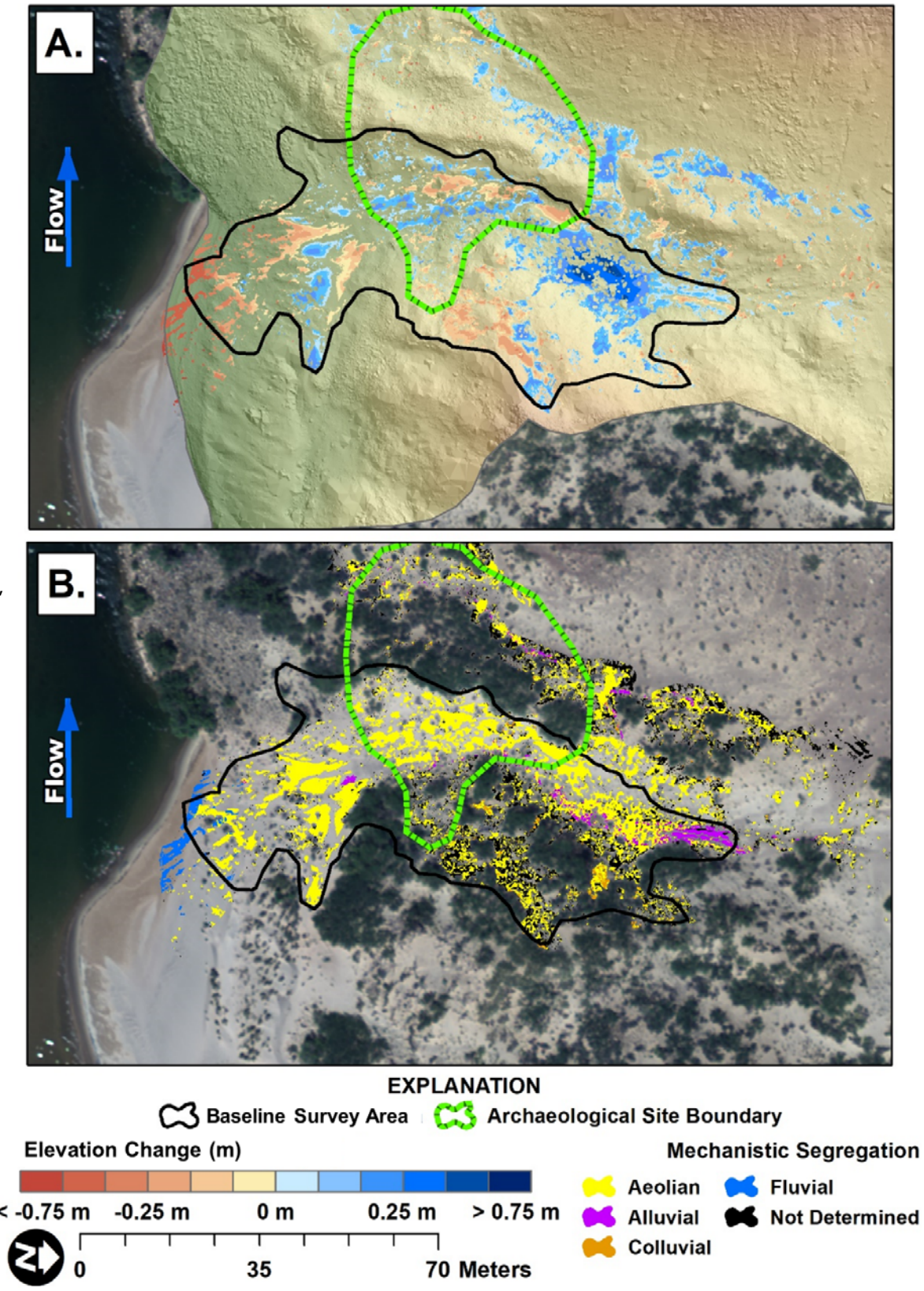

Figure 28. Maps showing change detection results between May 2014 and May 2016 for monitoring location EGC-1, eastern Grand Canyon, Arizona. *A*, Shaded relief showing elevation change results, in meters (m). Changes are within the 95-percent confidence interval. *B*, Results of automated geomorphic classification changes after Kasprak and others (2017). Aerial image collected by Grand Canyon Monitoring and Research Center (Durning and others, 2018).

Table 45. Results of change detection between May 2014 and May 2016 for mapped archaeological features at site C:13:0321, eastern Grand Canyon, Arizona.

[Results are presented for two inclusive subdivisions. The largest overlapping area represents all significant topographic change in the DEM of difference and the baseline survey area represents a subset of significant changes relative to the baseline survey. Feature + buffer is inclusive of the feature area and a surrounding 1-meter-wide buffer. DEM, digital elevation model; m^2, square meter; m^3, cubic meter; %, percent; NA, not applicable]

Spatial subdivision	Survey area (m^2)	Area (m^2)			Volume (m^3)			Percent imbalance (%)
		Erosion	Deposition	Total	Erosion	Deposition	Net	
Largest overlapping area								
Feature 1	12.24	0.79	1.15	1.94	0.04	0.05	0.01	7.3
Feature 1 + buffer	28.85	1.58	3.77	5.35	0.06	0.23	0.17	28.9
Feature 2	1.35	0.00	0.00	0.00	0.00	0.00	0.00	0.0
Feature 2 + buffer	9.02	0.80	0.46	1.26	0.03	0.02	−0.01	−10.4
Feature 3	3.93	0.01	1.23	1.24	0.00	0.04	0.04	49.3
Feature 3 + buffer	14.72	0.79	2.18	2.98	0.05	0.08	0.03	11.5
Feature 5	1.35	1.06	0.03	1.08	0.06	0.00	−0.06	−48.3
Feature 5 + buffer	8.97	2.66	0.88	3.54	0.16	0.05	−0.11	−24.9
Feature 6	1.36	0.01	0.34	0.34	0.00	0.01	0.01	48.0
Feature 6 + buffer	9.02	0.10	1.63	1.73	0.00	0.08	0.08	45.7
Feature 7	2.55	0.00	1.11	1.11	0.00	0.04	0.04	50.0
Feature 7 + buffer	12.30	0.00	4.59	4.59	0.00	0.25	0.25	50.0
Baseline survey area								
Feature 1	12.24	NA	NA	NA	NA	NA	NA	NA
Feature 1 + buffer	28.85	NA	NA	NA	NA	NA	NA	NA
Feature 2	1.35	NA	NA	NA	NA	NA	NA	NA
Feature 2 + buffer	9.02	NA	NA	NA	NA	NA	NA	NA
Feature 3	3.93	NA	NA	NA	NA	NA	NA	NA
Feature 3 + buffer	14.72	NA	NA	NA	NA	NA	NA	NA
Feature 5	1.35	1.06	0.03	1.08	0.06	0.00	−0.06	−48.3
Feature 5 + buffer	8.97	2.66	0.88	3.54	0.16	0.05	−0.11	−24.9
Feature 6	1.36	0.01	0.34	0.34	0.00	0.01	0.01	48.0
Feature 6 + buffer	9.02	0.10	1.63	1.73	0.00	0.08	0.08	45.7
Feature 7	2.55	NA	NA	NA	NA	NA	NA	NA
Feature 7 + buffer	12.30	NA	NA	NA	NA	NA	NA	NA

Table 46. Results of change detection by geomorphic mechanism between May 2014 and May 2016 at monitoring location EGC-1, eastern Grand Canyon, Arizona.

[NA indicates mechanisms not identified in the survey. m^2, square meter; m^3, cubic meter; %, percent]

Spatial subdivision	Area (m^2)			Volume (m^3)			Percent imbalance (%)
	Erosion	Deposition	Total	Erosion	Deposition	Net	
Baseline survey area							
Fluvial	16.78	0.24	17.03	7.43	0.01	−7.42	−49.9
Aeolian	279.46	375.18	654.64	28.21	45.67	17.46	11.8
Alluvial	12.85	34.91	47.76	0.76	4.84	4.08	36.4
Colluvial	8.99	10.68	19.67	0.95	0.89	−0.06	−1.5
Indeterminate	90.10	114.56	204.66	7.31	9.43	2.12	6.3
Archaeological site boundary							
Fluvial	NA	NA	NA	NA	NA	NA	NA
Aeolian	76.57	112.64	189.21	5.48	7.89	2.41	9.0
Alluvial	0.80	2.87	3.67	0.03	0.29	0.26	39.6
Colluvial	1.44	0.61	2.05	0.14	0.05	−0.09	−23.5
Indeterminate	15.34	14.76	30.10	0.95	0.76	−0.19	−5.6

In the $DoD_{2016–2017}$, net volumetric change was erosional in the baseline survey area but depositional in archaeological site C:13:0321 (fig. 29; table 47). Net deposition volume in the archaeological site was four times greater than the previous survey interval (fig. 29; table 47), though there were some areas of erosion around features 5 and 6 (fig. 29; table 48). Fluvial erosion was the dominant geomorphic mechanism of volumetric changes within the baseline survey area, though aeolian processes contributed to the largest amount of change by area (table 49). Beginning in 2016, TLS surveys captured a larger portion of the sandbar east of the baseline survey area. Within this extended survey area, changes on the sandbar were primarily depositional.

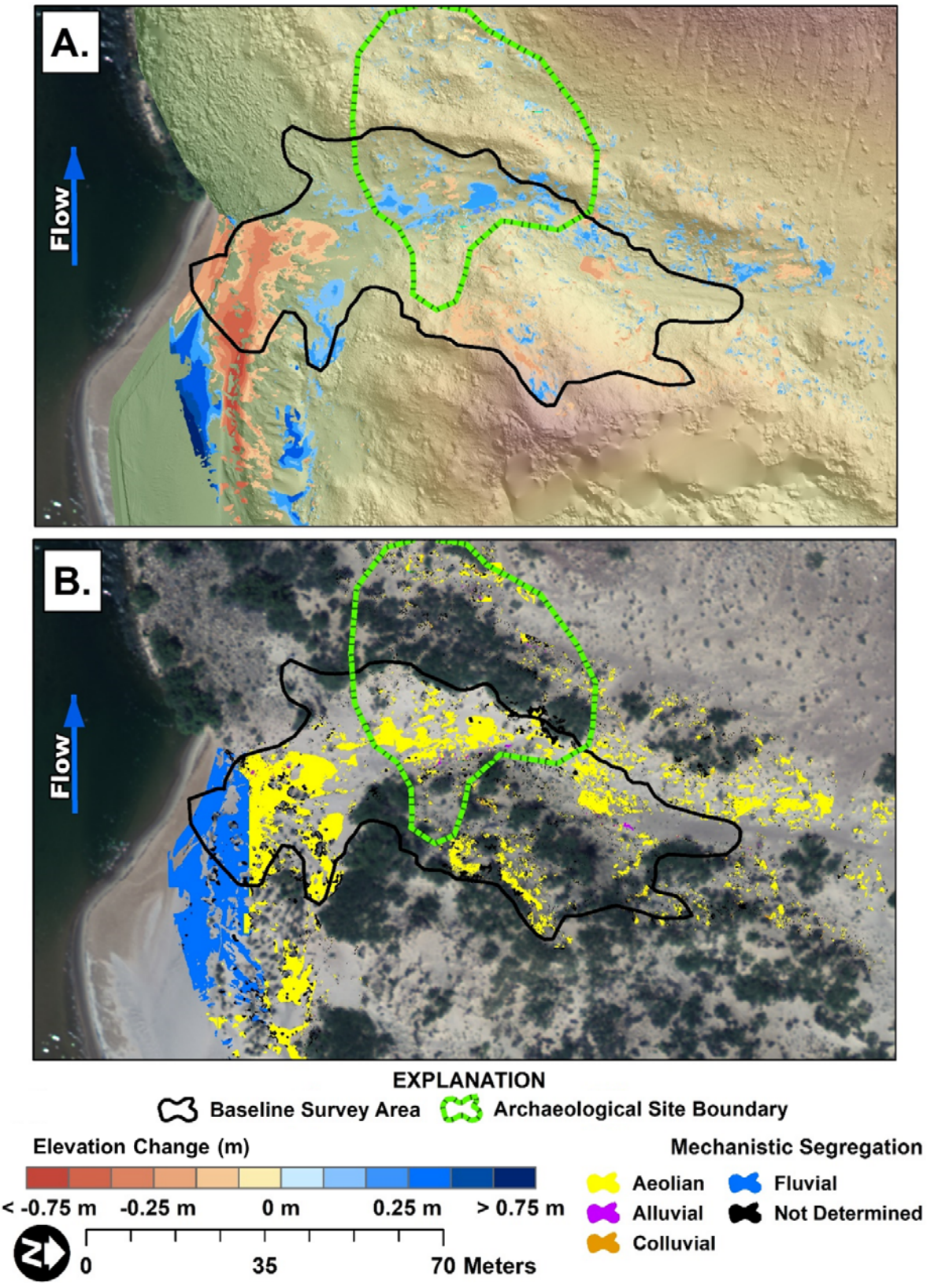

Figure 29. Maps showing change detection results between May 2016 and May 2017 for monitoring location EGC-1, eastern Grand Canyon, Arizona. *A*, Shaded relief showing elevation change results, in meters (m). Changes are within the 95-percent confidence interval. *B*, Results of automated geomorphic classification changes after Kasprak and others (2017). Aerial image collected by Grand Canyon Monitoring and Research Center (Durning and others, 2018).

Table 47. Results of change detection between May 2016 and May 2017 for the baseline survey area at monitoring location EGC-1, eastern Grand Canyon, Arizona.

[The archaeological site boundary is included in the above maximum flood elevation subdivision. m^2, square meter; m^3, cubic meter; %, percent]

Spatial subdivision	Survey area (m^2)	Area (m^2)			Volume (m^3)			Percent imbalance (%)
		Erosion	Deposition	Total	Erosion	Deposition	Net	
Baseline survey area	3,056.01	369.86	304.80	674.66	84.49	26.16	−58.33	−26.4
Below maximum flood elevation	176.05	0.95	0.95	1.90	39.95	0.06	−39.89	−49.9
Above maximum flood elevation	2,879.96	368.91	303.86	672.77	44.55	26.10	−18.44	−13.1
Archaeological site boundary	727.54	27.55	140.80	168.35	1.95	12.99	11.04	37.0

Table 48. Results of change detection between May 2016 and May 2017 for mapped archaeological features at site C:13:0321, eastern Grand Canyon, Arizona.

[Results are presented for two inclusive subdivisions. The largest overlapping area represents all significant topographic change in the DEM of difference and the baseline survey area represents a subset of significant changes relative to the baseline survey. Feature + buffer is inclusive of the feature area and a surrounding 1-meter-wide buffer. DEM, digital elevation model; m^2, square meter; m^3, cubic meter; %, percent; NA, not applicable]

Spatial subdivision	Survey area (m^2)	Area (m^2)			Volume (m^3)			Percent imbalance (%)
		Erosion	Deposition	Total	Erosion	Deposition	Net	
Largest overlapping area								
Feature 1	12.24	0.48	0.84	1.32	0.04	0.07	0.03	12.9
Feature 1 + buffer	28.85	0.60	1.41	2.01	0.05	0.10	0.05	16.5
Feature 2	1.35	0.00	0.00	0.00	0.00	0.00	0.00	0.0
Feature 2 + buffer	9.02	0.00	0.00	0.00	0.00	0.00	0.00	50.0
Feature 3	3.93	0.00	0.24	0.24	0.00	0.02	0.02	50.0
Feature 3 + buffer	14.72	0.00	0.26	0.26	0.00	0.11	0.11	50.0
Feature 5	1.35	0.03	0.00	0.04	0.00	0.00	0.00	−44.2
Feature 5 + buffer	8.97	0.77	0.85	1.62	0.05	0.06	0.01	3.7
Feature 6	1.36	0.00	0.00	0.00	0.00	0.00	0.00	0.0
Feature 6 + buffer	9.02	0.37	0.23	0.60	0.02	0.01	−0.01	−10.5
Feature 7	2.55	0.00	0.08	0.08	0.00	0.00	0.00	50.0
Feature 7 + buffer	12.30	0.00	0.72	0.72	0.00	0.05	0.05	50.0
Baseline survey area								
Feature 1	12.24	NA	NA	NA	NA	NA	NA	NA
Feature 1 + buffer	28.85	NA	NA	NA	NA	NA	NA	NA
Feature 2	1.35	NA	NA	NA	NA	NA	NA	NA
Feature 2 + buffer	9.02	NA	NA	NA	NA	NA	NA	NA
Feature 3	3.93	NA	NA	NA	NA	NA	NA	NA
Feature 3 + buffer	14.72	NA	NA	NA	NA	NA	NA	NA
Feature 5	1.35	0.03	0.00	0.04	0.00	0.00	0.00	−56.5
Feature 5 + buffer	8.97	0.77	0.85	1.62	0.05	0.06	0.01	3.7
Feature 6	1.36	0.00	0.00	0.00	0.00	0.00	0.00	0.0
Feature 6 + buffer	9.02	0.37	0.23	0.60	0.02	0.01	−0.01	−10.5
Feature 7	2.55	NA	NA	NA	NA	NA	NA	NA
Feature 7 + buffer	12.30	NA	NA	NA	NA	NA	NA	NA

Table 49. Results of change detection by geomorphic mechanism between May 2016 and May 2017 at monitoring location EGC-1, eastern Grand Canyon, Arizona.

[NA indicates mechanisms not identified in the survey. m^2, square meter; m^3, cubic meter; %, percentpercent]

Spatial subdivision	Area (m^2)			Volume (m^3)			Percent imbalance (%)
	Erosion	Deposition	Total	Erosion	Deposition	Net	
Baseline survey area							
Fluvial	123.81	0.88	124.69	38.02	0.06	−37.96	−49.9
Aeolian	295.51	232.73	528.24	37.82	20.38	−17.44	−15.0
Alluvial	3.84	0.93	4.77	0.49	0.09	−0.40	−34.6
Colluvial	2.54	0.44	2.98	0.28	0.05	−0.23	−35.1
Indeterminate	72.78	69.83	142.60	7.89	5.59	−2.30	−8.5
Archaeological site boundary							
Fluvial	NA	NA	NA	NA	NA	NA	NA
Aeolian	18.06	115.00	133.06	1.27	10.74	9.47	39.4
Alluvial	0.81	0.63	1.44	0.05	0.06	0.01	3.0
Colluvial	0.02	0.05	0.07	0.00	0.00	0.00	24.4
Indeterminate	8.68	25.13	33.81	0.63	2.19	1.56	27.7

In the $DoD_{2017–2019}$, net volumetric change was erosional in the baseline survey area but less so than $DoD_{2016–2017}$ (fig. 30; table 50). Within the archaeological site boundary, net deposition was slightly greater than in $DoD_{2016–2017}$ though depositional area increased by more than 100 m^2 (fig. 30; table 50). All archaeological features within the baseline survey area were depositional but features 1 and 3 in the 2016–2017 overlapping survey area were erosional (table 51). As in previous years, fluvial erosion was responsible for the greatest net change in sediment volume within the baseline survey area, but aeolian processes made up the majority of erosion and deposition within the largest overlapping area, baseline survey area, and archaeological site (table 52). Aeolian erosion was concentrated above the sandbar as well as along the upwind (southwest) side of the dune crests in the eastern and western parts of the baseline survey area and archaeological site. Deposition was concentrated just downwind of the sandbar outside of the baseline survey area and in the archaeological site as well as the northern part of the survey area (fig. 30).

Table 50. Results of change detection between May 2017 and May 2019 for the baseline survey area at monitoring location EGC-1, eastern Grand Canyon, Arizona.

[The archaeological site boundary is included in the above maximum flood elevation subdivision. m^2, square meter; m^3, cubic meter; %, percent]

Spatial subdivision	Survey area (m^2)	Area (m^2)			Volume (m^3)			Percent imbalance (%)
		Erosion	Deposition	Total	Erosion	Deposition	Net	
Baseline survey area	3,056.01	743.72	947.22	1,690.94	103.96	81.37	−22.59	−6.1
Below maximum flood elevation	176.05	189.00	1.87	190.87	47.80	0.07	−47.74	−49.9
Above maximum flood elevation	2,879.96	554.72	945.35	1,500.07	56.16	81.30	25.14	9.1
Archaeological site boundary	727.54	132.51	253.05	385.56	8.03	19.84	11.81	21.2

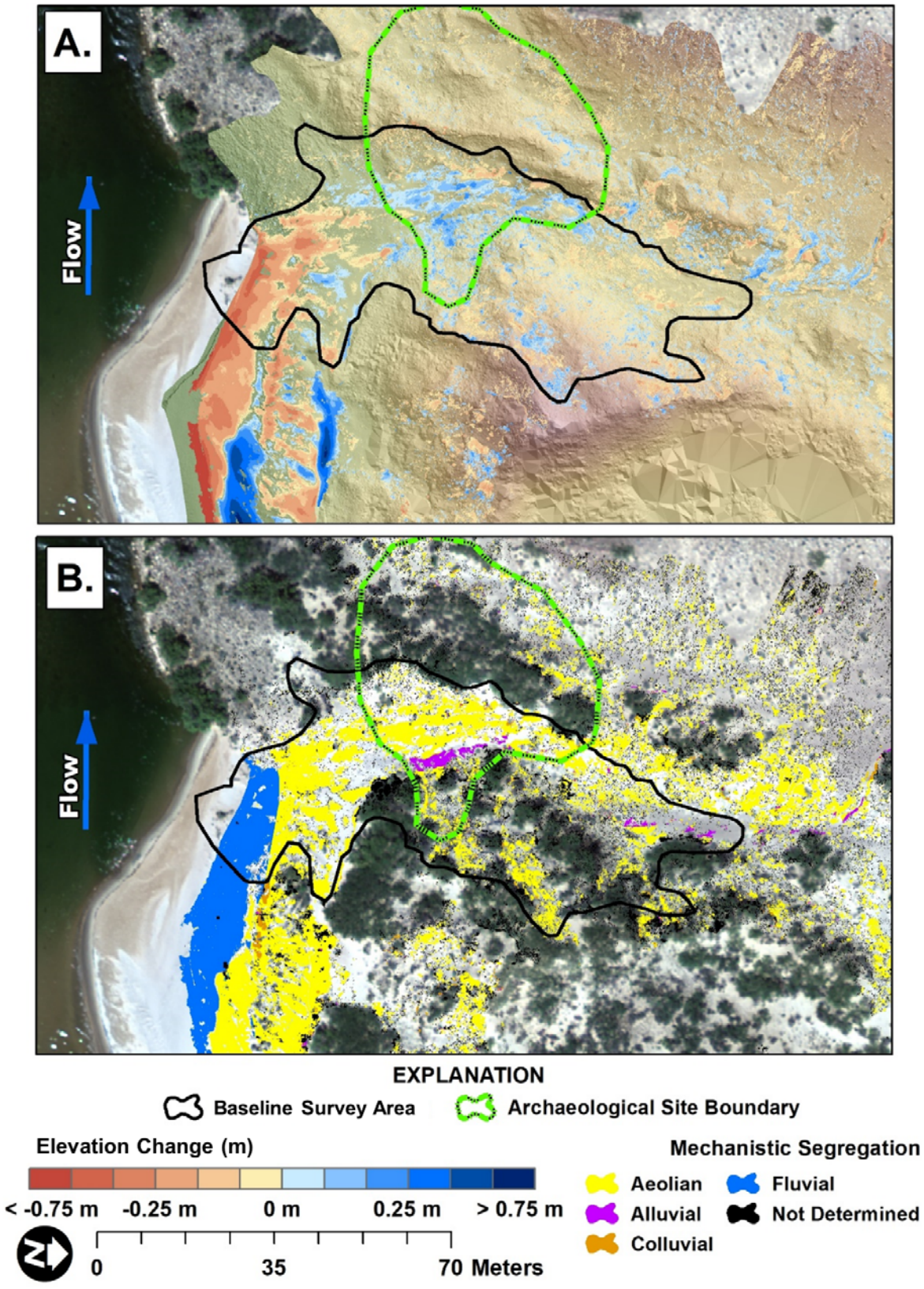

Figure 30. Maps showing change detection results between May 2017 and May 2019 for monitoring location EGC-1, eastern Grand Canyon, Arizona. *A*, Shaded relief showing elevation change results, in meters (m). Changes are within the 95-percent confidence interval. *B*, Results of automated geomorphic classification changes after Kasprak and others (2017). Aerial image collected by Grand Canyon Monitoring and Research Center (Durning and others, 2018).

Table 51. Results of change detection between May 2017 and May 2019 for mapped archaeological features at site C:13:0321, eastern Grand Canyon, Arizona.

[Results are presented for two inclusive subdivisions. The largest overlapping area represents all significant topographic change in the DEM of difference and the baseline survey area represents a subset of significant changes relative to the baseline survey. Feature + buffer is inclusive of the feature area and a surrounding 1-meter-wide buffer. DEM, digital elevation model; m^2, square meter; m^3, cubic meter; %, percent; NA, not applicable]

Spatial subdivision	Survey area (m^2)	Area (m^2)			Volume (m^3)			Percent imbalance (%)
		Erosion	Deposition	Total	Erosion	Deposition	Net	
Largest overlapping area								
Feature 1	12.24	3.16	0.43	3.59	0.15	0.02	−0.13	−37.4
Feature 1 + buffer	28.85	6.27	1.59	7.86	0.27	0.07	−0.20	−28.3
Feature 2	1.35	0.02	0.36	0.38	0.01	0.01	0.01	19.9
Feature 2 + buffer	9.02	0.48	1.25	1.72	0.02	0.05	0.03	20.9
Feature 3	3.93	0.13	0.12	0.25	0.01	0.00	0.00	−7.5
Feature 3 + buffer	14.72	1.35	0.95	2.29	0.08	0.03	−0.05	−21.1
Feature 5	1.35	0.11	1.01	1.12	0.00	0.08	0.07	44.3
Feature 5 + buffer	8.97	1.20	4.95	6.15	0.07	0.41	0.34	35.3
Feature 6	1.36	0.14	0.67	0.81	0.01	0.03	0.02	33.4
Feature 6 + buffer	9.02	0.70	4.15	4.84	0.03	0.25	0.22	39.8
Feature 7	2.55	0.19	0.35	0.55	0.01	0.01	0.01	16.8
Feature 7 + buffer	12.30	1.33	2.22	3.54	0.07	0.09	0.02	7.8
Baseline survey area								
Feature 1	12.24	NA	NA	NA	NA	NA	NA	NA
Feature 1 + buffer	28.85	NA	NA	NA	NA	NA	NA	NA
Feature 2	1.35	NA	NA	NA	NA	NA	NA	NA
Feature 2 + buffer	9.02	NA	NA	NA	NA	NA	NA	NA
Feature 3	3.93	NA	NA	NA	NA	NA	NA	NA
Feature 3 + buffer	14.72	NA	NA	NA	NA	NA	NA	NA
Feature 5	1.35	0.10	1.05	1.15	0.00	0.08	0.08	44.8
Feature 5 + buffer	8.97	1.17	5.05	6.21	0.07	0.42	0.35	35.9
Feature 6	1.36	0.11	0.71	0.81	0.00	0.03	0.02	36.8
Feature 6 + buffer	9.02	0.68	4.25	4.93	0.03	0.26	0.23	40.4
Feature 7	2.55	NA	NA	NA	NA	NA	NA	NA
Feature 7 + buffer	12.30	NA	NA	NA	NA	NA	NA	NA

Table 52. Results of change detection by geomorphic mechanism between May 2017 and May 2019 at monitoring location EGC-1, eastern Grand Canyon, Arizona.

[NA indicates mechanisms not identified in the survey. m^2, square meter; m^3, cubic meter; %, percent]

Spatial subdivision	Area (m^2)			Volume (m^3)			Percent imbalance (%)
	Erosion	Deposition	Total	Erosion	Deposition	Net	
Baseline survey area							
Fluvial	188.53	0.28	188.80	47.70	0.01	−0.25	−50.0
Aeolian	483.37	723.39	1,206.76	51.61	64.70	0.01	5.6
Alluvial	2.14	13.87	16.00	0.13	1.62	0.09	42.6
Colluvial	8.83	20.13	28.96	0.72	1.75	0.04	20.9
Indeterminate	60.80	189.54	250.34	3.77	13.28	0.04	27.9
Archaeological site boundary							
Fluvial	NA	NA	NA	NA	NA	NA	NA
Aeolian	112.66	216.44	329.09	6.96	17.58	10.62	21.6
Alluvial	1.71	3.02	4.72	0.08	0.23	0.15	23.2
Colluvial	1.68	2.25	3.93	0.12	0.19	0.07	11.9
Indeterminate	16.44	31.30	47.74	0.86	1.82	0.96	17.9

In the $DoD_{2019–2020}$, net volumetric change was erosional in the baseline survey area and depositional in archaeological site C:13:0321 (fig. 31; table 53). Beginning in 2019, additional sites were also included within the survey as well as additional area for site C:13:0321. Net erosion in site C:13:0092 was relatively minor compared to site C:13:0009, which lost approximately the same volume of sediment as the entire baseline survey area (table 53). Outside of the baseline survey area, site C:13:0321 along with the areas surrounding features 1, 3, and 7 were almost entirely erosional but the area surrounding feature 5 experienced the greatest recorded deposition (table 54). As with previous years, fluvial erosion was responsible for the greatest net volume

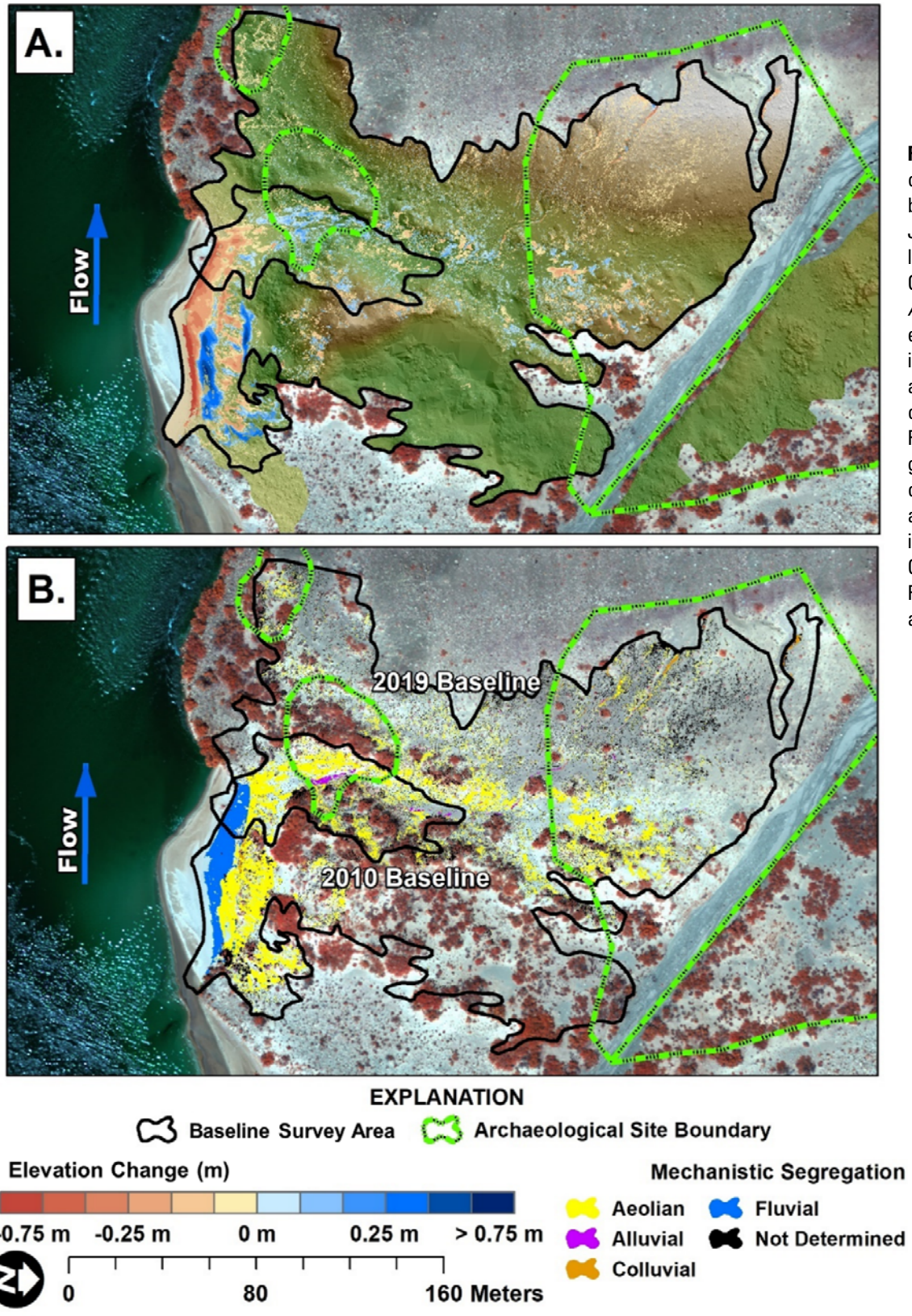

Figure 31. Maps showing change detection results between May 2019 and June 2020 for monitoring location EGC-1, eastern Grand Canyon, Arizona. *A*, Shaded relief showing elevation change results, in meters (m). Changes are within the 95-percent confidence interval. *B*, Results of automated geomorphic classification changes after Kasprak and others (2017). Aerial image collected by Grand Canyon Monitoring and Research Center (Durning and others, 2018).

Table 53. Results of change detection between May 2019 and June 2020 for the baseline survey area at monitoring location EGC-1, eastern Grand Canyon, Arizona.

[The archaeological site boundary is included in the above maximum flood elevation subdivision. Baseline indicates the portion of the archaeological site within the baseline survey area. Overlapping area indicates the portion of the site within the largest overlapping area between the May 2019 and June 2020 surveys. m^2, square meter; m^3, cubic meter; %, percent]

Spatial subdivision	Survey area (m^2)	Area (m^2)			Volume (m^3)			Percent imbalance (%)
		Erosion	Deposition	Total	Erosion	Deposition	Net	
Baseline survey area	3,056.01	613.97	545.20	1,159.17	64.31	27.37	−36.94	−20.1
Below maximum flood elevation	176.05	155.88	3.08	158.96	35.28	0.12	−35.16	−49.7
Above maximum flood elevation	2,879.96	458.08	542.13	1,000.21	29.03	27.25	−1.78	−1.6
Archaeological site boundary (baseline C:13:0321)	727.54	73.50	245.10	318.60	3.50	13.30	9.79	29.1
Newly included archaeological sites								
Archaeological site boundary (C:13:0009)	1,836.35	956.13	406.12	1,362.25	53.33	17.80	−35.53	−25.0
Archaeological site boundary (C:13:0092)	9,809.20	110.49	13.94	124.42	4.36	0.43	−3.93	−41.1
Archaeological site boundary (overlapping area C:13:0321)	605.65	150.89	304.36	455.25	6.99	15.73	8.75	19.3

Table 54. Results of change detection between May 2019 and June 2020 for mapped archaeological features at site C:13:0321, eastern Grand Canyon, Arizona.

[Results are presented for two inclusive subdivisions. The largest overlapping area represents all significant topographic change in the DEM of difference and the baseline survey area represents a subset of significant changes relative to the baseline survey. Feature + buffer is inclusive of the feature area and a surrounding 1-meter-wide buffer. DEM, digital elevation model; m^2, square meter; m^3, cubic meter; %, percent; NA, not applicable]

Spatial subdivision	Survey area (m^2)	Area (m^2)			Volume (m^3)			Percent imbalance (%)
		Erosion	Deposition	Total	Erosion	Deposition	Net	
Largest overlapping area								
Feature 1	12.24	1.65	0.32	1.97	0.07	0.02	−0.05	−29.9
Feature 1 + buffer	28.85	3.21	0.72	3.93	0.12	0.03	−0.09	−29.7
Feature 2	1.35	0.10	0.07	0.17	0.00	0.00	0.00	−3.1
Feature 2 + buffer	9.02	0.10	0.07	0.17	0.00	0.00	0.00	−3.1
Feature 3	3.93	0.06	0.19	0.25	0.00	0.01	0.00	28.5
Feature 3 + buffer	14.72	1.69	0.95	2.65	0.06	0.04	−0.02	−11.4
Feature 5	1.35	0.00	1.06	1.06	0.00	0.06	0.06	50.0
Feature 5 + buffer	8.97	0.02	7.19	7.21	0.00	0.46	0.46	49.8
Feature 6	1.36	0.02	0.57	0.59	0.00	0.02	0.02	47.2
Feature 6 + buffer	9.02	0.15	3.79	3.94	0.01	0.17	0.17	47.0
Feature 7	2.55	0.07	0.09	0.16	0.00	0.00	0.00	7.1
Feature 7 + buffer	12.30	1.70	0.62	2.32	0.07	0.02	−0.05	−26.3
Baseline survey area								
Feature 1	12.24	NA	NA	NA	NA	NA	NA	NA
Feature 1 + buffer	28.85	NA	NA	NA	NA	NA	NA	NA
Feature 2	1.35	NA	NA	NA	NA	NA	NA	NA
Feature 2 + buffer	9.02	NA	NA	NA	NA	NA	NA	NA
Feature 3	3.93	NA	NA	NA	NA	NA	NA	NA
Feature 3 + buffer	14.72	NA	NA	NA	NA	NA	NA	NA
Feature 5	1.35	0.00	1.06	1.06	0.00	0.06	0.06	50.0
Feature 5 + buffer	8.97	0.02	7.19	7.21	0.00	0.46	0.46	49.8
Feature 6	1.36	0.02	0.57	0.59	0.00	0.02	0.02	47.2
Feature 6 + buffer	9.02	0.15	3.79	3.94	0.01	0.17	0.17	47.0
Feature 7	2.55	NA	NA	NA	NA	NA	NA	NA
Feature 7 + buffer	12.30	NA	NA	NA	NA	NA	NA	NA

change in sediment storage but aeolian processes produced the greatest total area and volume of topographic change (table 55). Within the baseline survey area, erosion was most concentrated in the southern part of the monitoring location with alternating deposition and erosion in the northern part. For site C:13:0321, this followed patterns observed in previous years where erosion occurred along the dune crests on the east and west side of the baseline survey area and deposition occurred in the northern part of the baseline survey area. Within the extended 2019 survey area, site C:13:0009 exhibited erosion by indeterminate processes in the western part of the site along a rocky talus slope (fig. 31; table 55). Much of these indeterminate topographic changes, as well as classified colluvial topographic changes, are interpreted as being from rainfall runoff that transported sediment downslope toward the base of the main dune field as either sheetwash or concentrated flow by gullies (fig. 31; table 55). In the eastern part of the site, topographic changes were dominantly aeolian, with alternating erosion and deposition along the wind direction (southwest to northeast). At site C:13:0092, topographic changes were primarily from aeolian wind scour and indeterminate processes interpreted as sheetwash erosion (fig. 31; table 55).

Net change in sediment storage at monitoring location EGC-1 between 2010 and 2020 for the baseline survey area was −103.7 m^3, though for the baseline survey area above the maximum regulated flood inundation elevation, net volume change was depositional (56.1 m^3; fig. 32). Changes in sediment storage at archaeological site C:13:0321 were depositional and increased in magnitude over time, showing a net volume change between 2010 and 2020 of 31.4 m^3 (fig. 32). Aeolian processes were a consistently important mechanism of change throughout all DoD intervals, specifically above the maximum regulated flood elevation, though fluvial erosion was an important factor in recent intervals for the active Colorado River channel ($DoD_{2014–2016}$ to $DoD_{2019–2020}$; fig. 32). Areas of repeat change were documented throughout the baseline survey area, with single interval changes representing less areal coverage than repeat changes (fig. 32).

Table 55. Results of change detection by geomorphic mechanism between May 2019 and June 2020 at monitoring location EGC-1, eastern Grand Canyon, Arizona.

[Baseline indicates the portion of the archaeological site within the baseline survey area. Overlapping area indicates the portion of the site within the largest overlapping area between the May 2019 and June 2020 surveys. NA indicates mechanisms not identified in the survey. m^2, square meter; m^3, cubic meter; %, percent]

Spatial subdivision	Area (m^2)			Volume (m^3)			Percent imbalance (%)
	Erosion	Deposition	Total	Erosion	Deposition	Net	
Baseline survey area							
Fluvial	154.27	2.02	156.29	35.09	0.08	−35.01	−49.8
Aeolian	339.34	352.30	691.64	23.28	17.84	−5.45	−6.6
Alluvial	9.63	27.63	37.27	0.48	1.68	1.20	27.8
Colluvial	3.80	4.32	8.13	0.26	0.26	0.00	0.3
Indeterminate	106.92	158.93	265.85	5.20	7.51	2.31	9.1
Archaeological site boundary (baseline C:13:0321)							
Fluvial	NA	NA	NA	NA	NA	NA	NA
Aeolian	49.12	174.64	223.76	2.36	9.43	0.03	29.9
Alluvial	1.19	25.70	26.89	0.07	1.58	0.06	45.6
Colluvial	1.35	1.97	3.32	0.10	0.12	0.00	3.4
Indeterminate	21.84	42.81	64.64	0.96	2.17	0.02	19.2
Archaeological site boundary (overlapping area C:13:0321)							
Fluvial	NA	NA	NA	NA	NA	NA	NA
Aeolian	83.22	195.13	278.34	3.81	10.26	6.45	22.9
Alluvial	1.78	25.97	27.75	0.10	1.60	1.50	44.3
Colluvial	2.43	2.07	4.50	0.17	0.12	−0.04	−7.3
Indeterminate	63.46	81.20	144.66	2.91	3.74	0.83	6.3
Archaeological site boundary (C:13:0009)							
Fluvial	NA	NA	NA	NA	NA	NA	NA
Aeolian	381.82	222.06	603.87	22.07	10.30	−11.77	−18.2
Alluvial	5.86	3.81	9.66	0.46	0.20	−0.26	−19.6
Colluvial	49.38	2.34	51.72	8.70	0.16	−8.53	−48.2
Indeterminate	519.07	177.93	697.00	22.11	7.13	−14.97	−25.6
Archaeological site boundary (C:13:0092)							
Fluvial	NA	NA	NA	NA	NA	NA	NA
Aeolian	49.11	2.37	51.47	1.79	0.07	−1.72	−46.2
Alluvial	1.43	0.02	1.45	0.06	0.00	−0.06	−48.5
Colluvial	0.28	0.00	0.28	0.01	0.00	−0.01	−50.0
Indeterminate	59.67	11.55	71.22	2.49	0.35	−2.13	−37.6

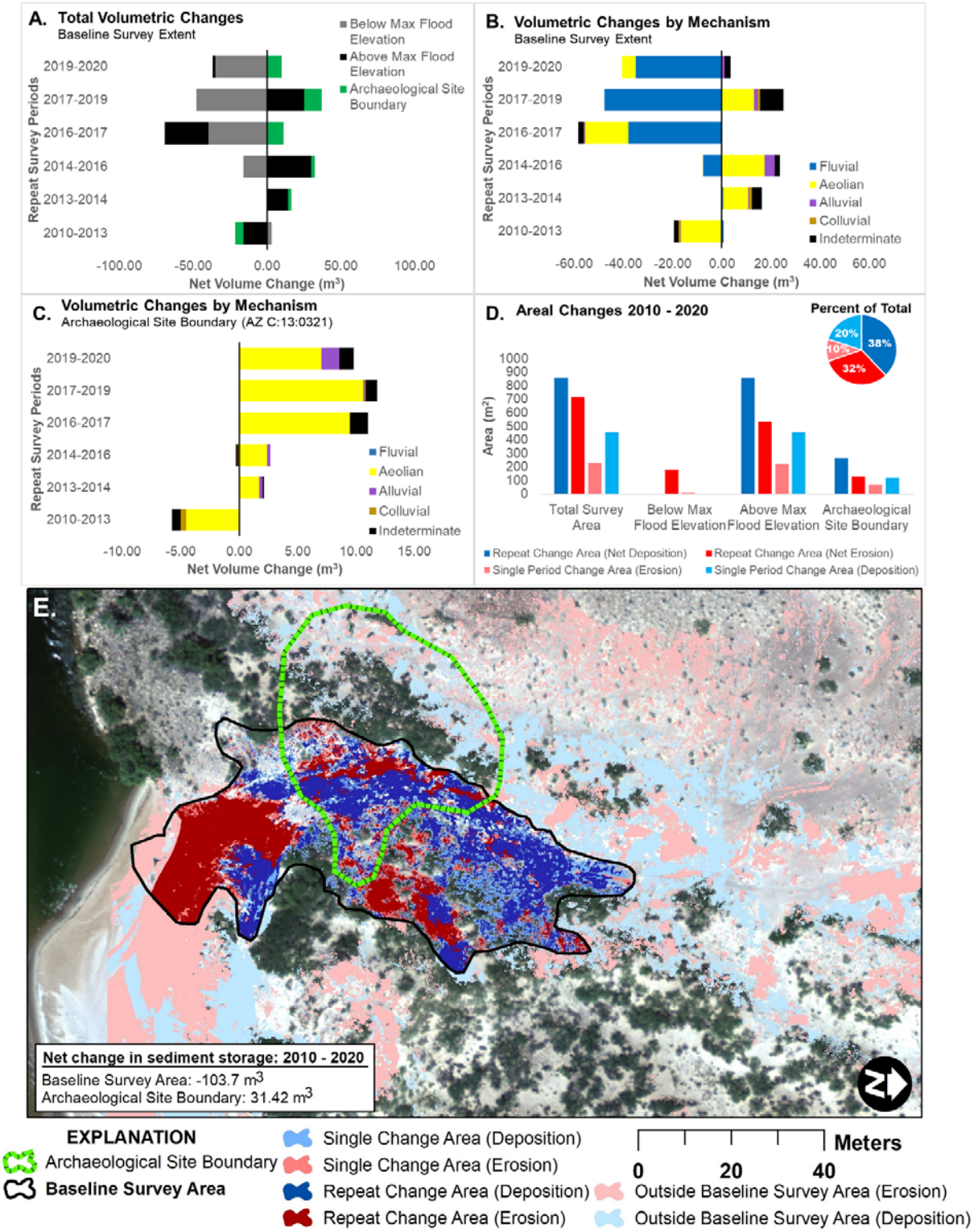

Figure 32. Plots of net volumetric (in cubic meters [m^3]) and areal (in square meters [m^2]) change in sediment storage between September 2010 and June 2020 for monitoring location EGC-1, eastern Grand Canyon, Arizona. *A*, Change results for the baseline survey area by spatial subdivision. *B*, Change results for the baseline survey area by geomorphic mechanism. *C*, Change results within the boundary of archaeological site C:13:0321 by geomorphic mechanism. Net volumetric changes to the left of the zero line indicate erosion and changes to the right of the zero line indicate deposition. *D*, Plot of change by location with regard to the regulated flood stage elevation (which occurs at a flow rate of 45,000 cubic feet per second) and the archaeological site. *E*, Map of areas that have repeat and single changes. Area of topographic change, net change direction (erosion or deposition), and net change in sediment storage were determined from the summation of all six digital elevation models of difference (DoDs). Repeat change area refers to pixels that have significant change in at least two DoDs. Single period change area refers to pixels that have significant change in only one DoD. Aerial image collected by Grand Canyon Monitoring and Research Center (Durning and others, 2018).

Repeat erosion was best expressed along the edge of the active channel and the crests of the two prominent dunes that frame the baseline survey area (fig. 32). Repeat deposition, which had a greater areal coverage than repeat erosion, was concentrated upwind of the sandbar in the southeastern part of the site and within the northern part of the baseline survey area (fig. 32).

Monitoring Location EGC-2

Monitoring location EGC-2 is located in eastern Grand Canyon on river left downstream from monitoring location EGC-1. Meteorological data, including temperature, wind direction, wind speed, and rainfall, have been collected at this location since 2007 Draut and others, 009, 2010; Collins and thers, 2012; Dealy and thers, 2014; Caster and thers, 2014). These ata indicate that wind riginates from the outh by southwest, lowing from the three rchaeological sites ithin the survey area n an upstream direction oward the river (fig. 33). wo archaeological ites, C:13:0346 and :13:0348, were reviously surveyed sing TLS in May 2006, ay 2007, September 007, and September 010; those results are ynthesized by Collins nd others (2012). opographic changes uring these survey ntervals were primarily rosion from wind scour roughout the survey rea as well as alluvial rosion and deposition ssociated with three

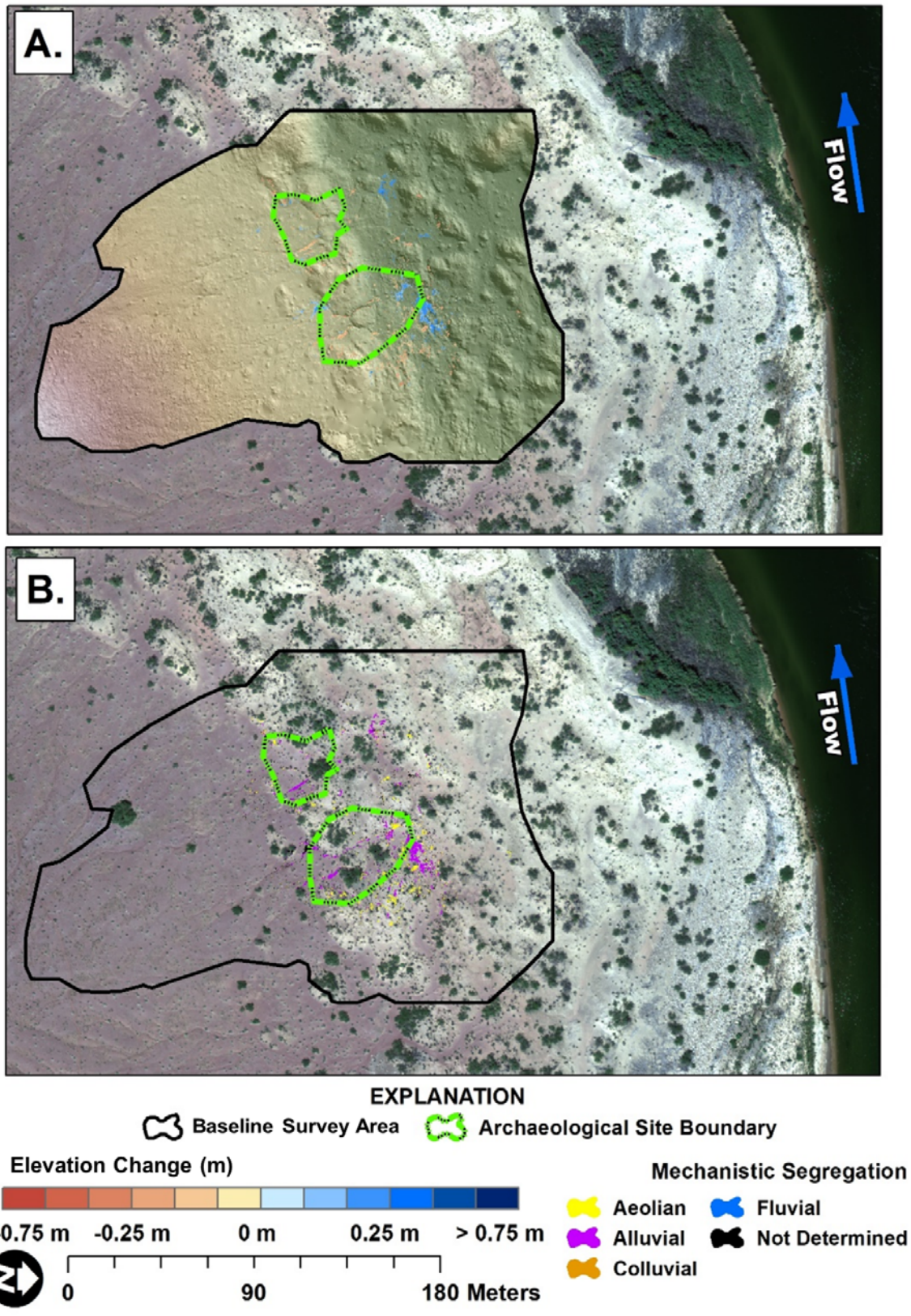

Figure 33. Maps showing change detection results between September 2010 and June 2020 for monitoring location EGC-2, eastern Grand Canyon, Arizona. *A*, Shaded relief showing elevation change results, in meters (m). Changes are within the 95-percent confidence interval. *B*, Results of automated geomorphic classification changes after Kasprak and others (2017). Aerial image collected by Grand Canyon Monitoring and Research Center (Durning and others, 2018).

Table 56. Results of change detection between September 2010 and June 2020 for the change detection area at monitoring location EGC-2, eastern Grand Canyon, Arizona.

[The archaeological site boundary is included in the above maximum flood elevation subdivision. NA indicates areas outside of the baseline survey. m^2, square meter; m^3, cubic meter; %, percent]

Spatial subdivision	Survey area (m^2)	Area (m^2)			Volume (m^3)			Percent imbalance (%)
		Erosion	Deposition	Total	Erosion	Deposition	Net	
Baseline survey area	33,598.40	316.18	212.44	528.63	32.36	22.86	−9.50	−8.6
Below maximum flood elevation	NA	NA	NA	NA	NA	NA	NA	NA
Above maximum flood elevation	30,048.28	200.47	149.65	350.12	20.65	17.03	−3.62	−4.8
Archaeological site boundary (C:13:0346)	1,684.67	83.88	53.23	137.10	8.42	5.09	−3.32	−12.3
Archaeological site boundary (C:13:0348)	886.14	31.84	9.57	41.41	3.13	0.74	−2.38	−30.8

Table 57. Results of change detection by geomorphic mechanism between September 2010 and June 2020 at monitoring location EGC-2, eastern Grand Canyon, Arizona.

[NA indicates mechanisms not identified in the survey. m^2, square meter; m^3, cubic meter; %, percent]

Spatial subdivision	Area (m^2)			Volume (m^3)			Percent imbalance (%)
	Erosion	Deposition	Total	Erosion	Deposition	Net	
Baseline survey area							
Fluvial	NA	NA	NA	NA	NA	NA	NA
Aeolian	122.93	23.23	146.16	15.17	2.56	−12.61	−35.6
Alluvial	93.84	126.65	220.49	10.15	15.40	5.25	10.3
Colluvial	0.04	0.00	0.04	0.00	0.00	0.00	−50.0
Indeterminate	99.38	62.56	161.94	7.04	4.90	−2.13	−8.9
Archaeological site boundary (C:13:0346)							
Fluvial	NA	NA	NA	NA	NA	NA	NA
Aeolian	23.73	9.95	33.68	2.75	0.94	−1.81	−24.5
Alluvial	36.04	30.87	66.92	4.09	3.36	−0.73	−4.9
Colluvial	0.00	0.00	0.00	0.00	0.00	0.00	0.0
Indeterminate	24.11	12.41	36.51	1.57	0.79	−0.78	−16.5
Archaeological site boundary (C:13:0348)							
Fluvial	NA	NA	NA	NA	NA	NA	NA
Aeolian	8.16	0.72	8.88	1.15	0.06	−1.09	−45.2
Alluvial	14.90	3.74	18.64	1.40	0.36	−1.04	0.0
Colluvial	0.00	0.00	0.00	0.00	0.00	0.00	0.0
Indeterminate	8.78	5.11	13.89	0.57	0.32	−0.25	−14.1

gullies, two in site C:13:0346 and one in site C:13:0348 (Collins and others, 2012). Both sites are aeolian type 3 and drainage type 2 owing to the lack of an adjacent upwind sandbar and the presence of gullies within the site that terminate on a low terrace of the historical Colorado River floodplain.

In June 2020, we repeated the topographic survey of monitoring location EGC-2. As with the previous results by Collins and others (2012), net topographic change was erosional for the baseline survey area and both archaeological sites (fig. 33; table 56). Aeolian erosion by wind scour had the greatest net effect on topographic changes, but alluvial processes, including gully erosion and alluvial fan deposition, had the greatest areal coverage (fig. 33; table 57). Indeterminate processes were also an important component of change for both the baseline survey area and the archaeological sites. The majority of these changes were concentrated along alluvial flow paths or on the upslope (south) side of vegetation and other barriers to alluvial sediment transport and are interpreted as resulting from erosion and deposition owing to excess rainfall runoff.

Monitoring Location EGC-7

Monitoring location EGC-7 is located in eastern Grand Canyon on river right. In May 2016, we surveyed the downstream part of a debris fan that contains one archaeological site, B:14:0105, and an associated downstream sandbar (fig. 34). A significant part of the downstream sandbar included in the survey has been previously monitored as part of the USGS sandbar monitoring program (Hazel and others, 2010; Grams and others, 2013). A total of 7,998 m^2 are included in the baseline survey area (table 58). Approximately 30 percent of the archaeological site is within the baseline survey area. The low survey coverage

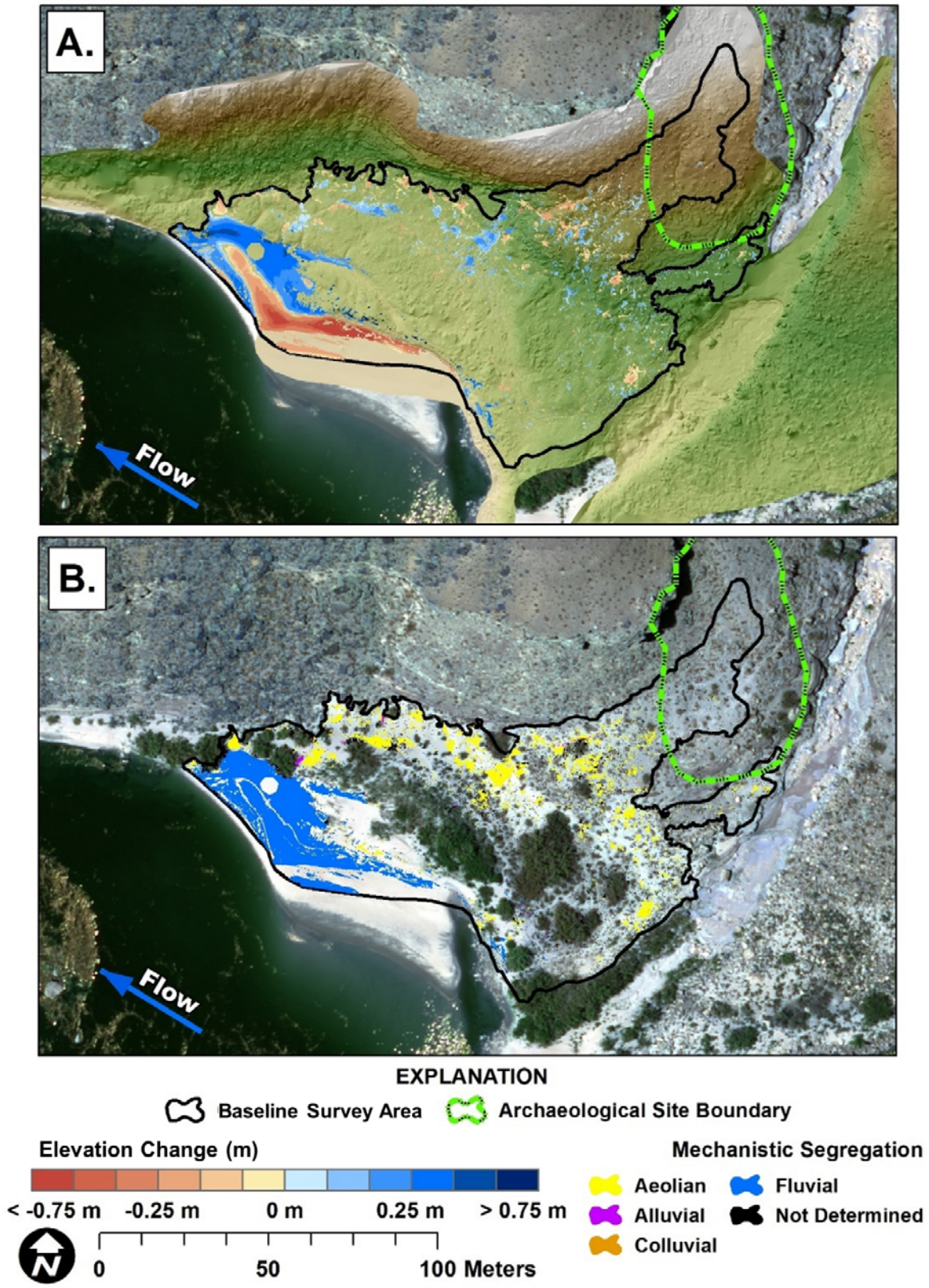

Figure 34. Maps showing change detection results between May 2016 and May 2019 for monitoring location EGC-7, eastern Grand Canyon, Arizona. *A*, Shaded relief showing elevation change results, in meters (m). Changes are within the 95-percent confidence interval. *B*, Results of automated geomorphic classification changes after Kasprak and others (2017). Aerial image collected by Grand Canyon Monitoring and Research Center (Durning and others, 2018).

of this site was due to two factors: (1) the northern part of the site is talus that likely will not be significantly affected by river fluctuations and (2) we limited the number of scan positions within the site to minimize effects (for example, trampling and trailing) of the survey on the archaeological site. This site was classified as aeolian type 2a and drainage type 3 based on the presence of riparian vegetation on and downwind of the sandbar and small gullies extending from the site to the side canyon tributary channel to the east. No individual archaeological features were mapped during the survey to minimize effects to the site.

In 2019, the NPS began conducting annual vegetation management at monitoring location EGC-7 to remove riparian plants on the sandbar that create a barrier to aeolian sand transport from the sandbar toward the site. In May 2019, we resurveyed monitoring location EGC-7 following vegetation management and we resurveyed it again in June 2020 prior to that year's vegetation management effort. As a result, there are two repeat change detection intervals. In the $DoD_{2016–2019}$, erosion and deposition were approximately equal (0.1 percent imbalance) for the baseline survey area, though topographic change in the archaeological site was erosional (fig. 34; table 58). Within the baseline survey area, the largest volume of changes was measured on the sandbar, where topographic changes were primarily a mix of fluvial and aeolian processes (fig. 34; table 59). Above the maximum regulated flood elevation, topographic changes in the baseline survey area resulted primarily from wind scouring of the open sand upwind of a dense stand of arrowweed (*Plucea sericea*), alluvial erosion of gullies below the archaeological site and the rock ledges to the west, and indeterminate processes interpreted as a mix of wind and runoff sediment capture around the base of vegetation stands (fig. 34; table 59). Within the archaeological site, topographic change was classified as indeterminate, though much of it occurred along old walking trails that appeared to function as concentrated runoff pathways and is interpreted as alluvial (fig. 34; table 59).

Table 58. Results of change detection between May 2016 and May 2019 for the baseline survey area at monitoring location EGC-7, eastern Grand Canyon, Arizona.

[The archaeological site boundary is included in the above maximum flood elevation subdivision. m^2, square meter; m^3, cubic meter; %, percent]

Spatial subdivision	Survey area (m^2)	Area (m^2)			Volume (m^3)			Percent imbalance (%)
		Erosion	Deposition	Total	Erosion	Deposition	Net	
Baseline survey area	9,008.71	634.93	911.09	1,546.02	164.20	164.54	0.34	0.1
Below maximum flood elevation	3,252.44	390.12	530.78	920.89	145.32	139.89	−5.44	−1.0
Above maximum flood elevation	5,756.26	244.81	380.32	625.13	18.87	24.65	5.77	6.6
Archaeological site boundary	820.88	8.72	4.25	12.97	0.54	0.22	−0.33	−21.4

Table 59. Results of change detection by geomorphic mechanism between May 2016 and May 2019 at monitoring location EGC-7, eastern Grand Canyon, Arizona.

[NA indicates mechanisms not identified in the survey. m^2, square meter; m^3, cubic meter; %, percent]

Spatial subdivision	Area (m^2)			Volume (m^3)			Percent imbalance (%)
	Erosion	Deposition	Total	Erosion	Deposition	Net	
Baseline survey area							
Fluvial	359.55	466.63	826.18	142.42	122.30	−20.12	−3.8
Aeolian	171.03	294.24	465.26	12.61	28.23	15.62	19.1
Alluvial	10.57	2.06	12.64	1.29	0.14	−1.15	−40.1
Colluvial	0.34	0.12	0.45	0.05	0.01	−0.05	−38.4
Indeterminate	93.45	148.04	241.50	7.82	13.85	6.03	13.9
Archaeological site boundary							
Fluvial	NA	NA	NA	NA	NA	NA	NA
Aeolian	0.91	0.99	1.90	0.06	0.06	0.00	−0.6
Alluvial	0.51	0.00	0.51	0.03	0.00	−0.03	−50.0
Colluvial	0.01	0.00	0.01	0.00	0.00	0.00	−50.0
Indeterminate	7.29	3.26	10.56	0.46	0.16	−0.30	−24.0

In the $DoD_{2019–2020}$, net volumetric change within the baseline survey area was erosional, with the greatest area and volume change occurring below the maximum regulated flood inundation elevation (fig. 35; table 60). As such, fluvial processes were interpreted as the dominant mechanism of change for the baseline survey area, though aeolian and other indeterminate processes were important contributors of topographic change downwind (northeast) of the sandbar (fig. 35; table 61). Within the archaeological site, topographic changes were minor with erosion in the northern part of the site and slightly more deposition in the

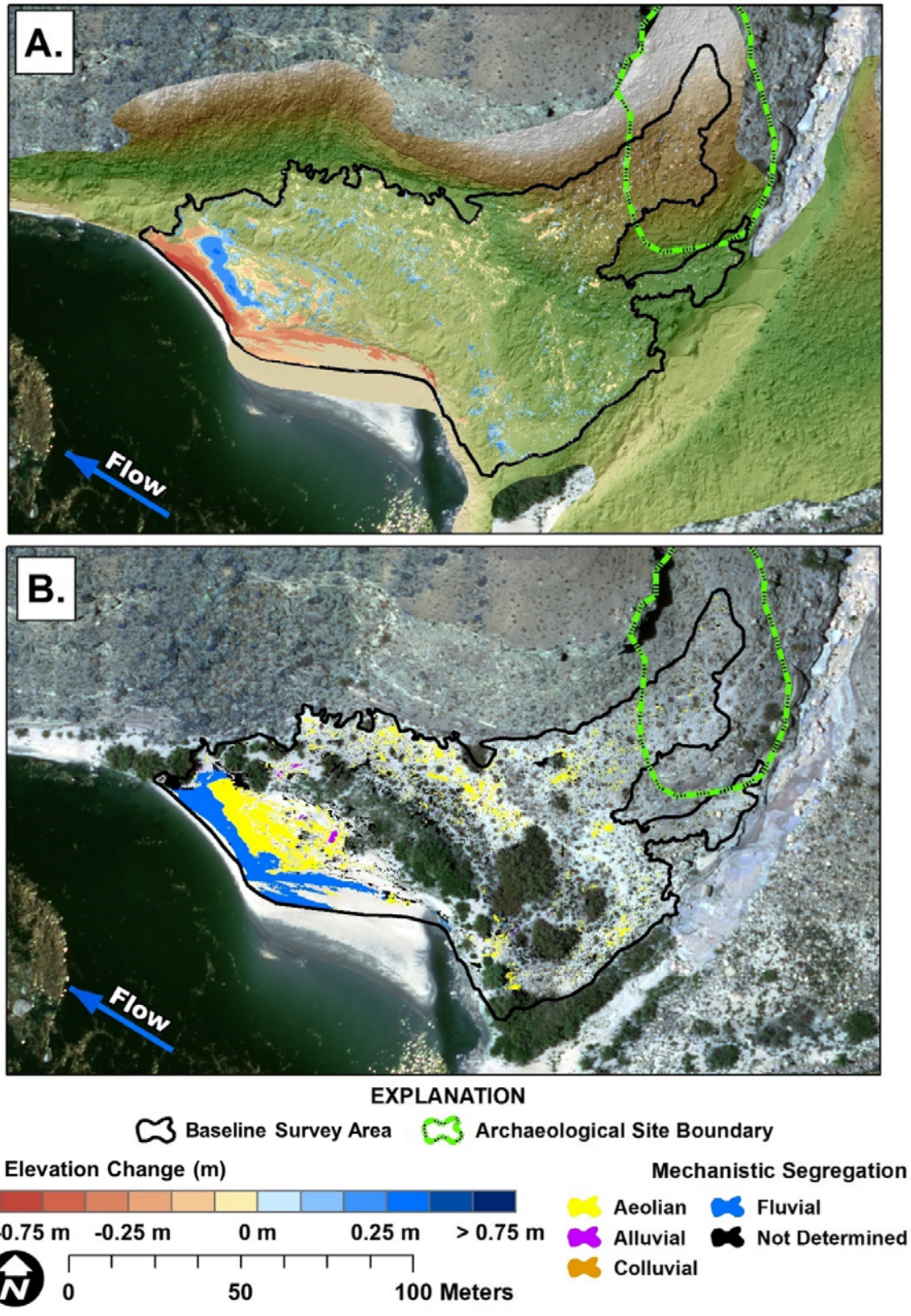

Figure 35. Maps showing change detection results between May 2019 and June 2020 for monitoring location EGC-7, eastern Grand Canyon, Arizona. *A*, Shaded relief showing elevation change results, in meters (m). Changes are with the 95-percent confidence interval. *B*, Results of automated geomorphic classification changes after Kasprak and others (2017). Aerial image collected by Grand Canyon Monitoring and Research Center (Durning and others, 2018).

Table 60. Results of change detection between May 2019 and June 2020 for the baseline survey area at monitoring location EGC-7, eastern Grand Canyon, Arizona.

[The archaeological site boundary is included in the above maximum flood elevation subdivision. m^2, square meter; m^3, cubic meter; %, percent]

Spatial subdivision	Survey area (m^2)	Area (m^2)			Volume (m^3)			Percent imbalance (%)
		Erosion	Deposition	Total	Erosion	Deposition	Net	
Baseline survey area	9,008.71	923.92	771.81	1,695.73	186.03	57.61	−128.42	−26.4
Below maximum flood elevation	3,252.44	611.27	429.23	1,040.50	174.37	38.59	−135.78	−31.9
Above maximum flood elevation	5,756.26	312.65	342.59	655.23	11.67	19.02	7.35	12.0
Archaeological site boundary	820.88	20.19	23.12	43.30	0.88	1.60	0.72	14.6

Table 61. Results of change detection by geomorphic mechanism between May 2019 and June 2020 at monitoring location EGC-7, eastern Grand Canyon, Arizona.

[NA indicates mechanisms not identified in the survey. m^2, square meter; m^3, cubic meter; %, percent]

Spatial subdivision	Area (m^2)			Volume (m^3)			Percent imbalance (%)
	Erosion	Deposition	Total	Erosion	Deposition	Net	
Baseline survey area							
Fluvial	395.82	4.19	400.01	147.54	0.29	−147.26	−49.8
Aeolian	299.90	370.40	670.30	17.97	30.94	12.96	13.3
Alluvial	14.73	1.64	16.36	0.68	0.08	−0.60	−39.5
Colluvial	0.11	0.26	0.37	0.01	0.03	0.02	35.3
Indeterminate	213.36	395.33	608.69	19.83	26.28	6.45	7.0
Archaeological site boundary							
Fluvial	NA	NA	NA	NA	NA	NA	NA
Aeolian	5.90	7.51	13.40	0.24	0.51	0.27	18.0
Alluvial	0.63	0.01	0.64	0.04	0.00	−0.04	−49.1
Colluvial	0.00	0.11	0.11	0.00	0.02	0.02	50.0
Indeterminate	13.66	15.50	29.16	0.60	1.07	0.47	14.1

southern part of the site, leading to net deposition (fig. 35; table 61). Aeolian and indeterminate processes were responsible for much of the measured changes within the site (fig. 35; table 61).

Among the two repeat survey periods, volumetric changes in sediment storage for the baseline survey area at monitoring location EGC-7 showed significant fluvial erosion and comparatively minor deposition by aeolian and indeterminate processes above the area inundated by controlled floods. This resulted in a net reduction in sediment storage between 2016 and 2020 of 128.1 m^3 for the baseline survey area (fig. 35).

In the archaeological site, $DoD_{2016–2019}$ showed negative changes and $DoD_{2019–2020}$ showed positive changes in sediment storage resulting in net sediment deposition or burial of 0.4 m^3. Many of the topographic changes for both detection intervals in the archaeological site were indeterminate as a result of their dispersed spatial distribution, though some changes in $DoD_{2019–2020}$ were attributed to aeolian processes. The indeterminate changes are likely a result of multiple geomorphic agents, including rainfall runoff, sediment trapping by vegetation, and slope creep as evidenced by visible indicators of runoff within walking trails and animal pathways, topographic changes along the base of plants, and presence of loose sediment on slopes near the angle of repose.

Areas of repeat change were documented throughout the survey area, though they were particularly concentrated on the sandbar, where erosion occurred along the edge of the river and deposition occurred upslope at the base of a stand of arrowweed (*Plucea sericea*; fig. 36). Outside of the sandbar, most of the change was recorded in only a single interval, though repeat erosion was measured along the gullies west of the archaeological site and deposition occurred where the gullies terminate within the open sand downwind of the arrowweed above the sandbar.

Monitoring Location CGC-1

Monitoring location CGC-1 is located in central Grand Canyon on river left. This is a long-term monitoring location with previous TLS surveys and weather station records (Draut and others, 2009, 2010; Collins and others, 2009, 2012, 2016; Dealy and others, 2014; Caster and others, 2014, 2018; East and others, 2016) covering one archaeological site, B:10:0225, and the surrounding landscape. Site B:10:0225 is classified as aeolian type 2c and drainage type 4, owing to vegetation on the sandbar and the location of the site at the base of a steep rocky ledge with an incised gully grading to the river. It was previously surveyed using TLS in September 2007 and 2010 and those results are synthesized by Collins and others (2012, 2016). During the 2007–2010 survey period, little change occurred within the boundaries of the archaeological site. However, significant topographic changes in the surrounding landscape were concentrated in, and adjacent to, a gully that incised after a single rainfall event in August 2007 (Collins and others, 2012; 2016). This site had a baseline survey area of approximately 4,103 m^2 that was covered during five surveys between September 2010 and May 2017 (figs. 37–40; tables 62–73).

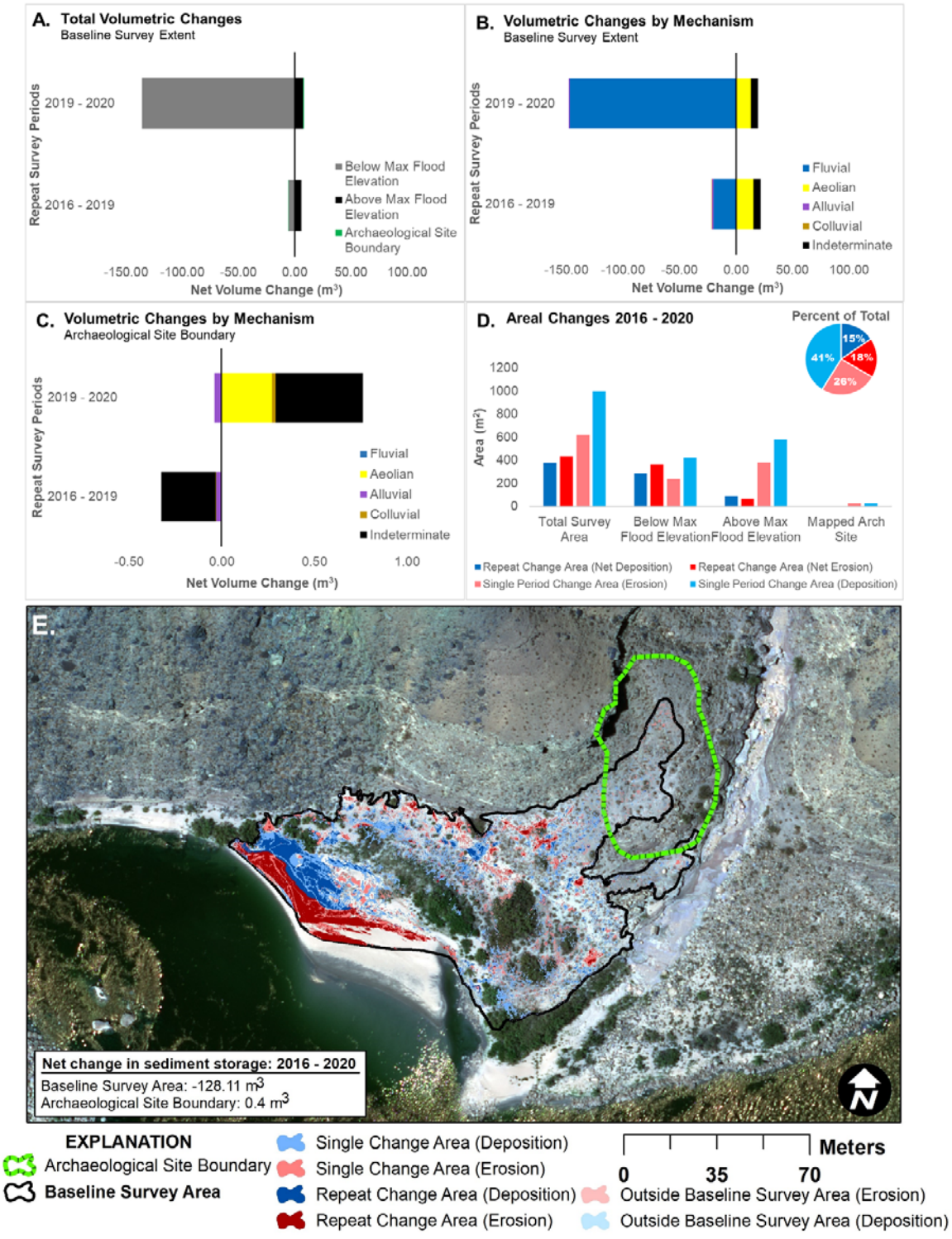

Figure 36. Plots of net volumetric (in cubic meters [m^3]) and areal (in square meters [m^2]) change in sediment storage between May 2016 and June 2020 for monitoring location EGC-7, eastern Grand Canyon, Arizona. *A*, Change results for the baseline survey area by spatial subdivision. *B*, Change results for the baseline survey area by geomorphic mechanism. *C*, Change results within the boundary of archaeological site B:14:0105 by geomorphic mechanism. Net volumetric changes to the left of the zero line indicate erosion and changes to the right of the zero line indicate deposition. *D*, Plot of change by location with regard to the regulated flood stage elevation (which occurs at a flow rate of 45,000 cubic feet per second) and the archaeological site. *E*, Map of areas that have repeat and single changes. Area of topographic change, net change direction (erosion or deposition), and net change in sediment storage were determined from the summation of all six digital elevation models of difference (DoDs). Repeat change area refers to pixels that have significant change in at least two DoDs. Single period change area refers to pixels that have significant change in only one DoD. Aerial image collected by Grand Canyon Monitoring and Research Center (Durning and others, 2018).

During the $DoD_{2010–2013}$ interval, net volumetric change within the baseline survey area was erosional, particularly above the maximum regulated flood elevation along an aeolian dune crest superimposed on an interfluve at the northeastern edge of the site (fig. 37; table 62). Net volumetric changes were also erosional in the archaeological site and associated feature (tables 62 and 63). Within the archaeological site boundary and the baseline survey area, aeolian processes were the dominant mechanism of change (table 64).

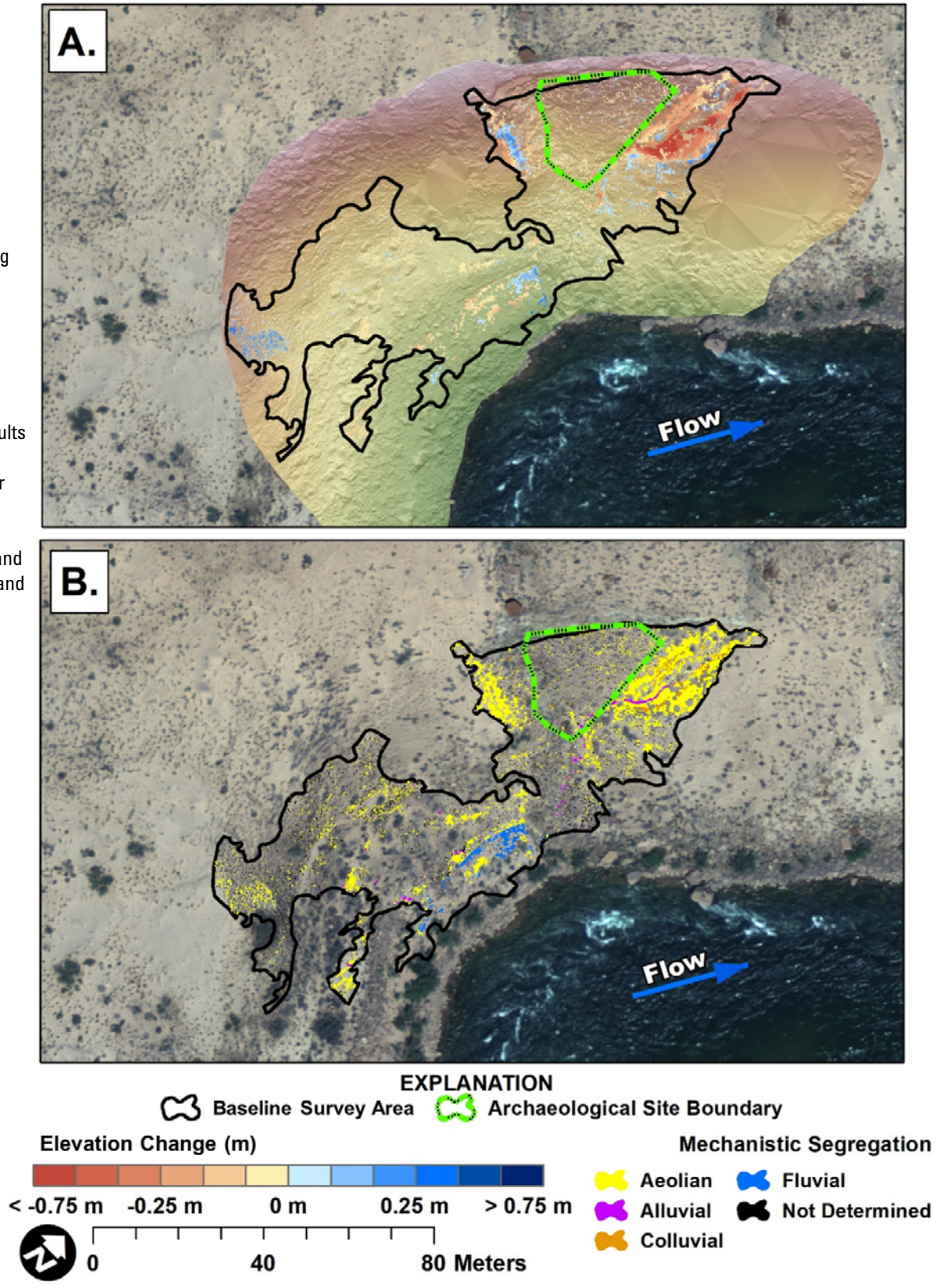

Figure 37. Maps showing change detection results between September 2010 and May 2013 for monitoring location CGC-1, central Grand Canyon, Arizona. *A*, Shaded relief showing elevation change results, in meters (m). Changes are within the 95-percent confidence interval. *B*, Results of automated geomorphic classification changes after Kasprak and others (2017). Aerial image collected by Grand Canyon Monitoring and Research Center (Durning and others, 2018).

Table 62. Results of change detection between September 2010 and May 2013 for the baseline survey area at monitoring location CGC-1, central Grand Canyon, Arizona.

[The archaeological site boundary is included in the above maximum flood elevation subdivision. m^2, square meter; m^3, cubic meter; %, percent]

Spatial subdivision	Survey area (m^2)	Area (m^2)			Volume (m^3)			Percent imbalance (%)
		Erosion	Deposition	Total	Erosion	Deposition	Net	
Baseline survey area	4,103.28	507.91	167.45	675.36	80.91	10.50	−70.40	−38.5
Below maximum flood elevation	379.57	30.27	21.39	51.65	1.62	1.50	−0.13	−2.0
Above maximum flood elevation	3,723.71	477.65	150.68	628.32	79.28	9.76	−69.52	−39.0
Archaeological site boundary	515.56	32.75	16.77	49.52	1.55	0.74	−0.81	−17.7

Table 63. Results of change detection between September 2010 and May 2013 for mapped archaeological features at site B:10:0225, central Grand Canyon, Arizona.

[Feature + buffer is inclusive of the feature area and a surrounding 1-meter-wide buffer. m^2, square meter; m^3, cubic meter; %, percent]

Spatial subdivision	Survey area (m^2)	Area (m^2)			Volume (m^3)			Percent imbalance (%)
		Erosion	Deposition	Total	Erosion	Deposition	Net	
Feature 1	0.22	0.07	0.00	0.07	0.00	0.00	0.00	−48.5
Feature 1 + buffer	7.19	0.71	0.52	1.23	0.03	0.02	−0.01	−8.1

Table 64. Results of change detection by geomorphic mechanism between September 2010 and May 2013 at monitoring location CGC-1, central Grand Canyon, Arizona.

[NA indicates mechanisms not identified in the survey. m^2, square meter; m^3, cubic meter; %, percent]

Spatial subdivision	Area (m^2)			Volume (m^3)			Percent imbalance (%)
	Erosion	Deposition	Total	Erosion	Deposition	Net	
Baseline survey area							
Fluvial	18.39	15.44	33.82	1.00	1.00	0.00	0.0
Aeolian	345.30	114.00	459.30	60.08	7.87	−52.21	−38.4
Alluvial	18.32	1.24	19.56	5.96	0.08	−5.88	−48.7
Colluvial	26.67	4.13	30.80	8.80	0.33	−8.47	−46.4
Indeterminate	99.23	54.03	153.26	5.06	2.72	−2.34	−15.1
Archaeological site boundary							
Fluvial	NA	NA	NA	NA	NA	NA	NA
Aeolian	16.47	8.17	24.65	0.74	0.40	−0.34	−14.9
Alluvial	1.73	0.05	1.78	0.22	0.00	−0.22	−48.4
Colluvial	1.10	0.25	1.35	0.07	0.02	−0.05	−30.3
Indeterminate	13.59	8.33	21.92	0.53	0.32	−0.21	−12.4

Net volumetric change for the $DoD_{2013–2014}$ was erosional in the baseline survey area, the archaeological site, and feature (fig. 38; tables 65 and 66). Wind was the most common geomorphic agent of change, both in the archaeological site and the baseline survey area (table 67). Similar to the previous interval, erosion was most pronounced on the northeastern edge of the archaeological site (fig. 38).

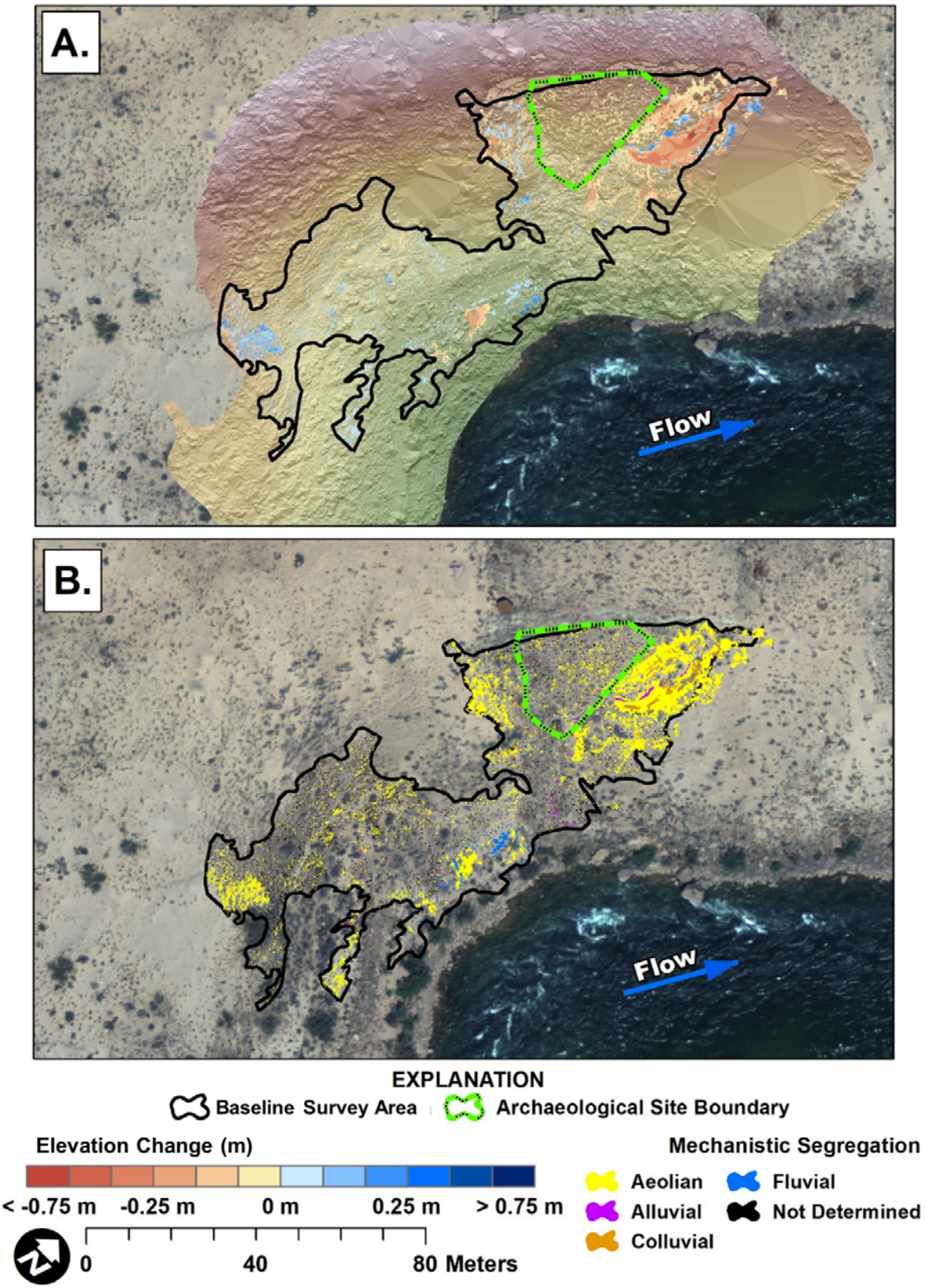

Figure 38. Maps showing change detection results between May 2013 and May 2014 for monitoring location CGC-1, central Grand Canyon, Arizona. *A*, Shaded relief showing elevation change results, in meters (m). Changes are within the 95-percent confidence interval. *B*, Results of automated geomorphic classification changes after Kasprak and others (2017). Aerial image collected by Grand Canyon Monitoring and Research Center (Durning and others, 2018).

Table 65. Results of change detection between May 2013 and May 2014 for the baseline survey area at monitoring location CGC-1, central Grand Canyon, Arizona.

[The archaeological site boundary is included in the above maximum flood subdivision. m^2, square meter; m^3, cubic meter; %, percent]

Spatial subdivision	Survey area (m^2)	Area (m^2)			Volume (m^3)			Percent imbalance (%)
		Erosion	Deposition	Total	Erosion	Deposition	Net	
Baseline survey area	4,103.28	536.69	274.80	811.49	48.38	13.73	−34.64	−27.9
Below maximum flood elevation	379.57	33.60	31.19	64.78	2.32	1.99	−0.33	−3.9
Above maximum flood elevation	3,723.71	479.29	267.67	746.96	45.93	13.46	−32.47	−27.3
Archaeological site boundary	515.56	57.40	7.13	64.53	2.45	0.27	−2.18	−40.1

Table 66. Results of change detection between May 2013 and May 2014 for mapped archaeological features at site B:10:0225, central Grand Canyon, Arizona.

[Feature + buffer is inclusive of the feature area and a surrounding 1-meter-wide buffer. m^2, square meter; m^3, cubic meter; %, percent; NA, not applicable]

Spatial subdivision	Survey area (m^2)	Area (m^2)			Volume (m^3)			Percent imbalance (%)
		Erosion	Deposition	Total	Erosion	Deposition	Net	
Feature 1	0.22	0.00	0.00	0.00	0.00	0.00	0.00	NA
Feature 1 + buffer	7.19	1.39	0.02	1.40	0.06	0.00	−0.06	−49.2

Table 67. Results of change detection by geomorphic mechanism between May 2013 and May 2014 at monitoring location CGC-1, central Grand Canyon, Arizona.

[NA indicates mechanisms not identified in the survey. m^2, square meter; m^3, cubic meter; %, percent]

Spatial subdivision	Area (m^2)			Volume (m^3)			Percent imbalance (%)
	Erosion	Deposition	Total	Erosion	Deposition	Net	
Baseline survey area							
Fluvial	5.49	14.17	19.65	0.44	0.68	0.24	10.8
Aeolian	378.93	165.28	544.21	37.49	9.69	−27.80	−29.5
Alluvial	8.94	4.53	13.47	0.75	0.19	−0.56	−29.8
Colluvial	27.36	5.85	33.21	5.98	0.38	−5.60	−44.1
Indeterminate	92.18	109.03	201.21	3.59	4.51	0.92	5.7
Archaeological site boundary							
Fluvial	NA	NA	NA	NA	NA	NA	NA
Aeolian	30.23	2.59	32.81	1.28	0.10	−1.18	−42.5
Alluvial	0.96	0.06	1.02	0.10	0.00	−0.10	−48.2
Colluvial	1.29	0.40	1.69	0.12	0.02	−0.10	−36.4
Indeterminate	14.35	2.63	16.98	0.60	0.10	−0.50	−35.8

Net volumetric change in the $DoD_{2014–2016}$ was predominantly depositional in the baseline survey area, the archaeological site, and feature (fig. 39; tables 68–70). Aeolian processes were the most common mechanism of change, though both colluvial processes, in the form of backwasting of gully walls, and fluvial processes were also important (fig. 39; table 70). Like the previous intervals, erosion was concentrated at the northeastern edge of the archaeological site (fig. 39). Deposition was spatially dispersed throughout the survey, though areas of greater depositional volume were concentrated downslope of the large dune field to the south and around the gullies on either side of the archaeological site (fig. 39).

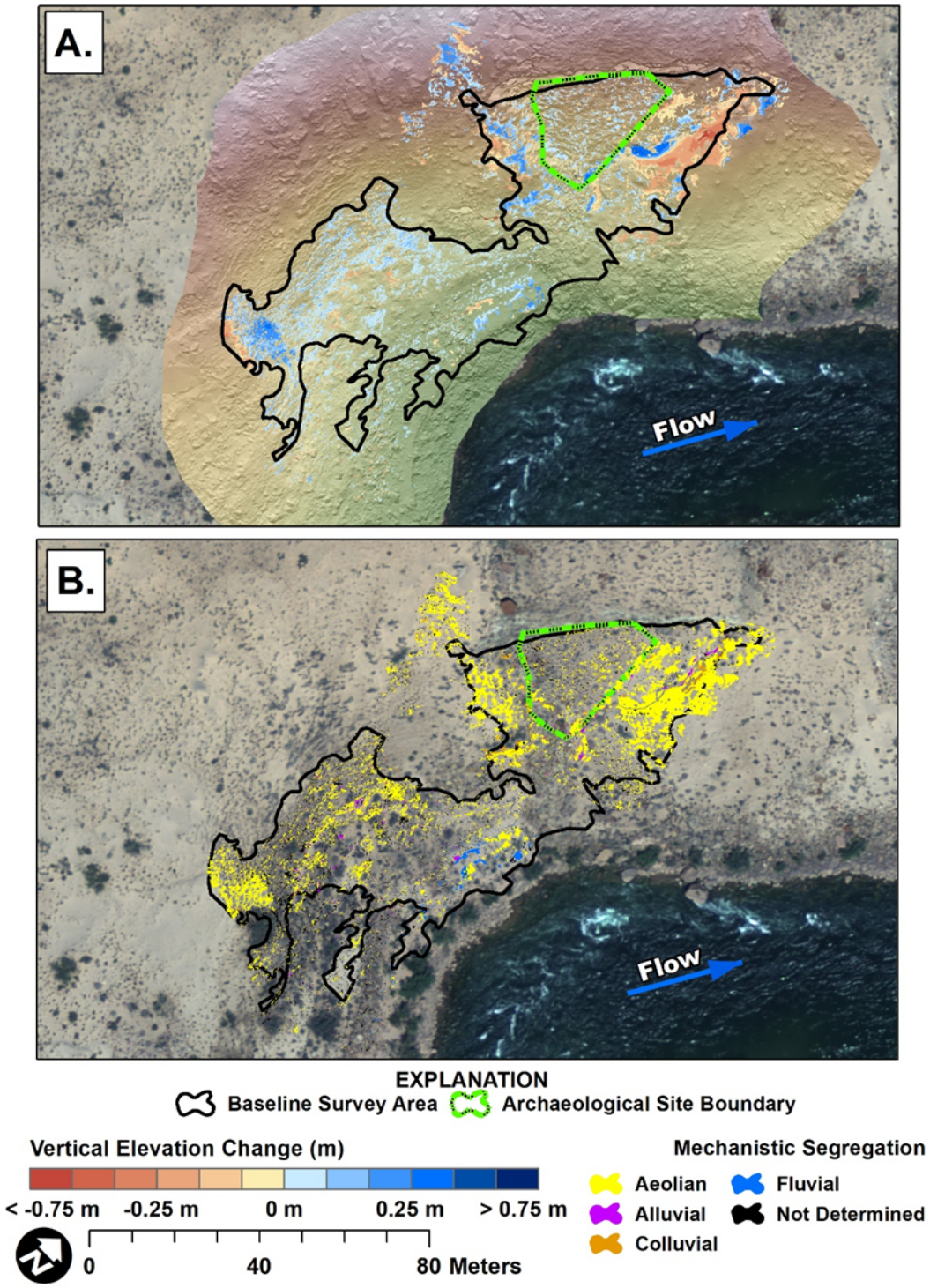

Figure 39. Maps showing change detection results between May 2014 and May 2016 for monitoring location CGC-1, central Grand Canyon, Arizona. *A*, Shaded relief showing elevation change results, in meters (m). Changes are within the 95-percent confidence interval. *B*, Results of automated geomorphic classification changes after Kasprak and others (2017). Aerial image collected by Grand Canyon Monitoring and Research Center (Durning and others, 2018).

Table 68. Results of change detection between May 2014 and May 2016 for the baseline survey area at monitoring location CGC-1, central Grand Canyon, Arizona.

[The archaeological site boundary is included in the above maximum flood elevation subdivision. m^2, square meter; m^3, cubic meter; %, percent]

Spatial subdivision	Survey area (m^2)	Area (m^2)			Volume (m^3)			Percent imbalance (%)
		Erosion	Deposition	Total	Erosion	Deposition	Net	
Baseline survey area	4,103.28	291.26	560.85	852.11	35.39	37.33	1.93	1.3
Below maximum flood elevation	379.57	8.89	40.16	49.05	0.46	2.37	1.90	33.6
Above maximum flood elevation	3,723.71	282.37	520.69	803.06	34.93	34.96	0.03	0.0
Archaeological site boundary	515.56	9.33	60.87	70.20	0.58	3.47	2.88	35.6

Table 69. Results of change detection between May 2014 and May 2016 for mapped archaeological features at site B:10:0225, central Grand Canyon, Arizona.

[Feature + buffer is inclusive of the feature area and a surrounding 1-meter-wide buffer. m^2, square meter; m^3, cubic meter; %, percent]

Spatial subdivision	Survey area (m^2)	Area (m^2)			Volume (m^3)			Percent imbalance (%)
		Erosion	Deposition	Total	Erosion	Deposition	Net	
Feature 1	0.22	0.00	0.01	0.01	0.00	0.00	0.00	50.0
Feature 1 + buffer	7.19	0.00	0.96	0.96	0.00	0.04	0.04	49.9

Table 70. Results of change detection by geomorphic mechanism between May 2014 and May 2016 at monitoring location CGC-1, central Grand Canyon, Arizona.

[NA indicates mechanisms not identified in the survey. m^2, square meter; m^3, cubic meter; %, percent]

Spatial subdivision	Area (m^2)			Volume (m^3)			Percent imbalance (%)
	Erosion	Deposition	Total	Erosion	Deposition	Net	
Baseline survey area							
Fluvial	5.52	12.97	18.49	0.29	0.85	0.56	24.6
Aeolian	227.20	398.37	625.57	29.21	28.85	−0.35	−0.3
Alluvial	8.15	10.87	19.02	0.63	0.52	−0.11	−4.8
Colluvial	12.42	18.48	30.89	2.70	1.52	−1.18	−14.0
Indeterminate	37.77	120.38	158.15	2.43	5.62	3.18	19.8
Archaeological site boundary							
Fluvial	NA	NA	NA	NA	NA	NA	NA
Aeolian	5.37	37.26	42.63	0.38	2.43	2.05	36.4
Alluvial	0.36	1.46	1.82	0.03	0.08	0.05	22.9
Colluvial	0.21	2.92	3.13	0.02	0.17	0.16	42.0
Indeterminate	1.48	12.43	13.91	0.08	0.55	0.48	37.8

In the $DoD_{2016–2017}$, net volumetric change was erosional in the baseline survey area, particularly adjacent to the northeastern part of the archaeological site (fig. 40; table 71). Consistent with the previous interval, net volumetric change in the archaeological site and feature were depositional (fig. 40; tables 71 and 72). Aeolian processes were responsible for most of the changes observed in the baseline survey area and the archaeological site (fig. 40; table 73).

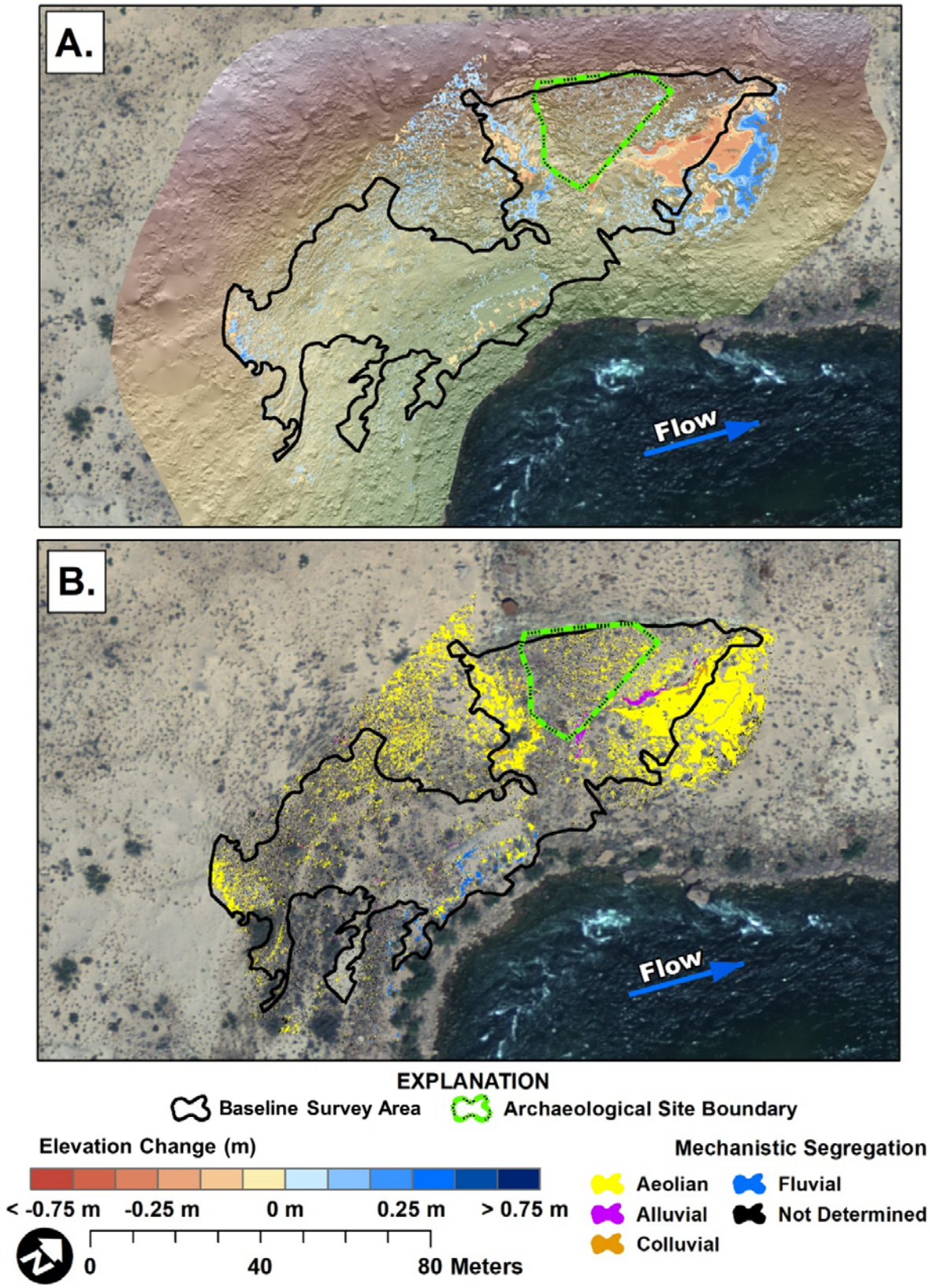

Figure 40. Maps showing change detection results between May 2016 and May 2017 for monitoring location CGC-1, central Grand Canyon, Arizona. *A*, Shaded relief showing elevation change results, in meters (m). Changes are within the 95-percent confidence interval. *B*, Results of automated geomorphic classification changes after Kasprak and others (2017). Aerial image collected by Grand Canyon Monitoring and Research Center (Durning and others, 2018).

Table 71. Results of change detection between May 2016 and May 2017 for the baseline survey area at monitoring location CGC-1, central Grand Canyon, Arizona.

[The archaeological site boundary is included in the above maximum flood elevation subdivision. m^2, square meter; m^3, cubic meter; %, percent]

Spatial subdivision	Survey area (m^2)	Area (m^2)			Volume (m^3)			Percent imbalance (%)
		Erosion	Deposition	Total	Erosion	Deposition	Net	
Baseline survey area	4,103.28	353.89	472.43	826.31	31.29	18.77	−12.52	−12.5
Below maximum flood elevation	379.57	29.09	22.71	51.79	1.43	0.96	−0.47	−9.7
Above maximum flood elevation	3,723.71	324.80	449.72	774.52	29.87	17.81	−12.06	−12.6
Archaeological site boundary	515.56	13.95	66.54	80.49	0.76	2.18	1.42	24.3

Table 72. Results of change detection between May 2016 and May 2017 for mapped archaeological features at site B:10:0225, central Grand Canyon, Arizona.

[Feature + buffer is inclusive of the feature area and a surrounding 1-meter-wide buffer. m^2, square meter; m^3, cubic meter; %, percent]

Spatial subdivision	Survey area (m^2)	Area (m^2)			Volume (m^3)			Percent imbalance (%)
		Erosion	Deposition	Total	Erosion	Deposition	Net	
Feature 1	0.22	0.11	0.08	0.19	0.00	0.00	0.00	−4.2
Feature 1 + buffer	7.19	0.54	1.11	1.64	0.02	0.03	0.02	15.6

Table 73. Results of change detection by geomorphic mechanism between May 2016 and May 2017 at monitoring location CGC-1, central Grand Canyon, Arizona.

[NA indicates mechanisms not identified in the survey. m^2, square meter; m^3, cubic meter; %, percent]

Spatial subdivision	Area (m^2)			Volume (m^3)			Percent imbalance (%)
	Erosion	Deposition	Total	Erosion	Deposition	Net	
Baseline survey area							
Fluvial	11.18	11.44	22.62	0.57	0.48	−0.09	−4.1
Aeolian	247.75	305.85	553.60	22.61	13.08	−9.53	−13.4
Alluvial	21.65	2.75	24.39	4.38	0.11	−4.27	−47.6
Colluvial	11.18	15.58	26.75	1.65	0.72	−0.93	−19.7
Indeterminate	62.13	136.82	198.95	2.08	4.38	2.30	17.8
Archaeological site boundary							
Fluvial	NA	NA	NA	NA	NA	NA	NA
Aeolian	6.76	38.70	45.46	0.28	1.33	1.05	32.6
Alluvial	2.78	0.11	2.89	0.30	0.01	−0.30	−48.3
Colluvial	0.27	1.81	2.08	0.03	0.06	0.04	20.2
Indeterminate	3.98	24.02	27.99	0.14	0.73	0.58	33.6

Among the four DoDs from 2010 to 2017, aeolian processes were consistently the most important mechanism of change, though alluvial and colluvial erosion were also important contributors (fig. 41). Changes in sediment storage by these mechanisms were consistently erosional. The net change in sediment storage between 2010 and 2017 for the baseline survey area was 112.1 m^3. Areas of repeat change were documented throughout the survey area, but the greatest and most consistent loss of sediment was along the gullies on either side of the archaeological site and just downslope of the large dune field located to the south of the survey (fig. 41). Single interval changes were more spatially dispersed and contributed less to total change in sediment storage compared to areas of repeat changes (fig. 41). In the archaeological site, the net change in sediment storage was 1.3 m^3, owing to aeolian sediment deposition.

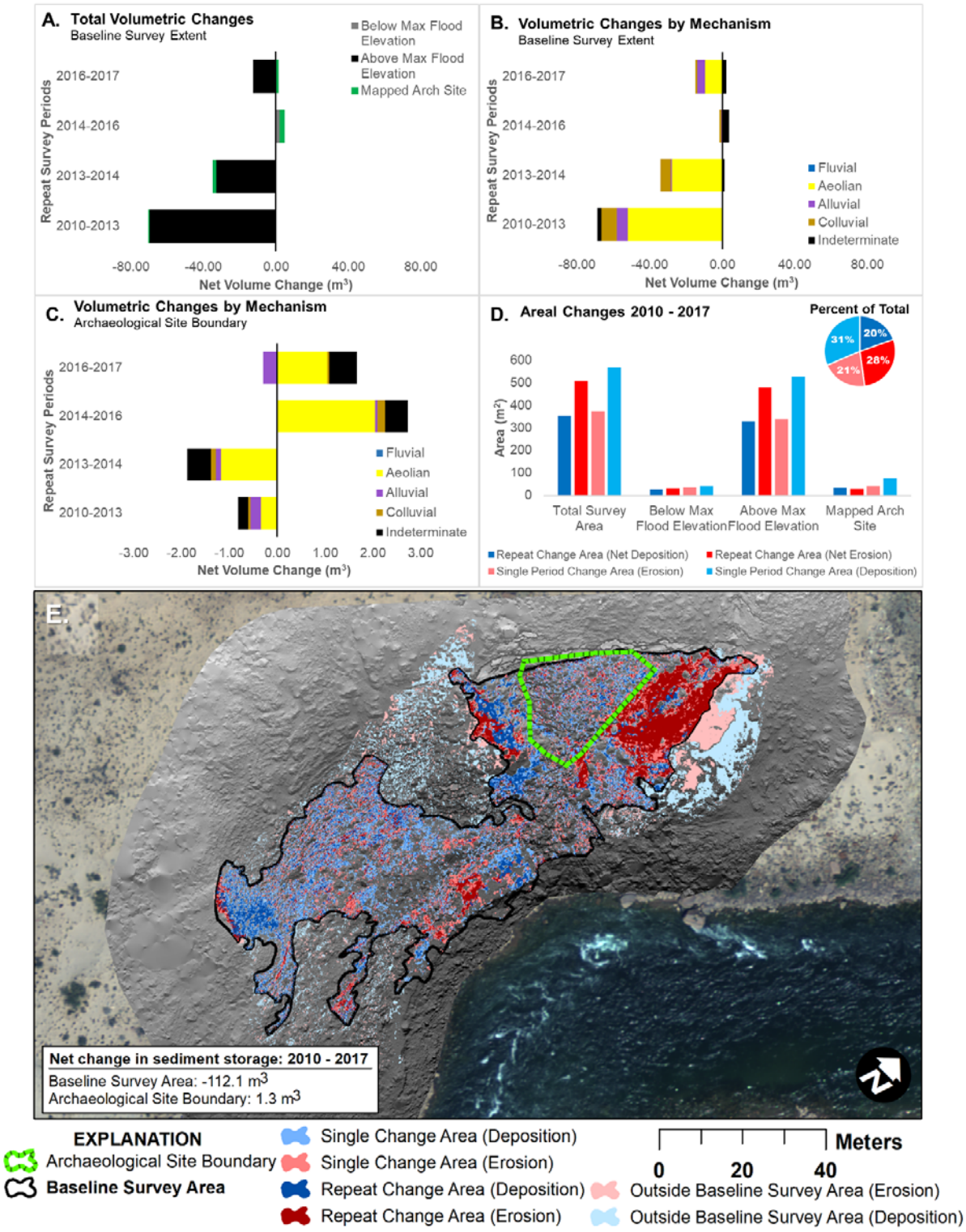

Figure 41. Plots of net volumetric (in cubic meters [m^3]) and areal (in square meters [m^2]) change in sediment storage between September 2010 and June 2020 for monitoring location CGC-1, central Grand Canyon, Arizona. *A*, Change results for the baseline survey area by spatial subdivision. *B*, Change results for the baseline survey area by geomorphic mechanism. *C*, Change results within the boundary of archaeological site B:10:0125 by geomorphic mechanism. Net volumetric changes to the left of the zero line indicate erosion and changes to the right of the zero line indicate deposition. *D*, Plot of change by location with regard to the regulated flood stage elevation (which occurs at a flow rate of 45,000 cubic feet per second) and the archaeological site. *E*, Map of areas that have repeat and single changes. Area of topographic change, net change direction (erosion or deposition), and net change in sediment storage were determined from the summation of all six digital elevation models of difference (DoDs). Repeat change area refers to pixels that have significant change in at least two DoDs. Single period change area refers to pixels that have significant change in only one DoD. Aerial image collected by Grand Canyon Monitoring and Research Center (Durning and others, 2018).

Monitoring Location CGC-3

Monitoring location CGC-3 is in central Grand Canyon on river left and was selected by the NPS as a vegetation management area in 2019. Management consisted of removing riparian vegetation that was growing on the sandbar; the vegetation created a barrier to aeolian transport of sand from the sandbar toward archaeological site B:13:0002. Vegetation management was conducted in April 2019 and repeated in September 2020. We surveyed monitoring location CGC-3 in May 2019 and again in June 2020 for a baseline survey area of 27,225 m^2 that extended from the downstream sandbar to archaeological site B:13:0002 upstream of a side canyon tributary within land managed by the Hualapai Tribe (fig. 42). The original NPS map of the archaeological site placed it further from the Colorado River within the side canyon tributary, though field observations during the 2019 survey identified previously documented site components 50 m closer to the river than indicated by the NPS map (fig. 42). Here we report both locations as two components of the same site as some cultural material may have been present within both areas. Site B:13:0002 is an aeolian type 4 and drainage type 3 site, owing to the lack of a direct upwind sandbar and two gullies extending from the northern part of the site into the side canyon tributary.

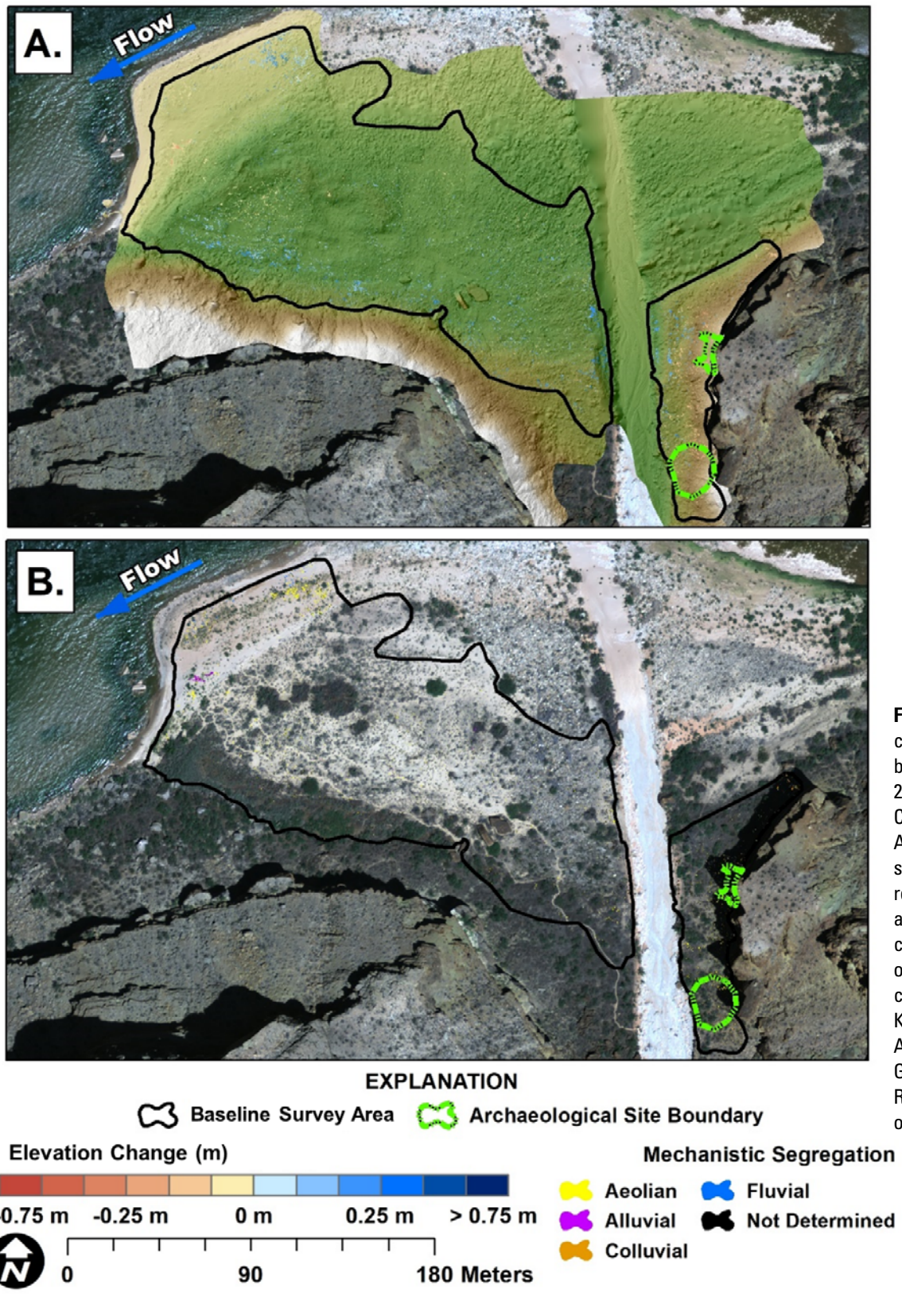

Figure 42. Maps showing change detection results between May 2019 and June 2020 for monitoring location CGC-3, central Grand Canyon, Arizona. *A*, Shaded relief showing elevation change results, in meters (m). Changes are within the 95-percent confidence interval. *B*, Results of automated geomorphic classification changes after Kasprak and others (2017). Aerial image collected by Grand Canyon Monitoring and Research Center (Durning and others, 2018).

Table 74. Results of change detection between May 2019 and June 2020 for the change detection area at monitoring location CGC-3, central Grand Canyon, Arizona.

[The archaeological site boundary is included in the above maximum flood elevation subdivision. m^2, square meter; m^3, cubic meter; %, percent]

Spatial subdivision	Survey area (m^2)	Area (m^2)			Volume (m^3)			Percent imbalance (%)
		Erosion	Deposition	Total	Erosion	Deposition	Net	
Baseline survey area	27,224.69	261.40	560.94	822.34	18.35	51.13	32.78	23.6
Below maximum flood elevation	3,100.24	38.37	75.73	114.10	2.60	6.95	4.35	22.8
Above maximum flood elevation (upstream)	3,665.44	105.49	64.64	170.13	9.48	6.26	−3.22	−10.2
Above maximum flood elevation (downstream)	20,459.02	117.55	420.57	538.12	6.27	37.92	31.65	35.8
Archaeological site boundary	487.48	19.38	2.41	21.79	1.91	0.22	−1.69	−39.6

Table 75. Results of change detection by geomorphic mechanism between May 2019 and June 2020 at monitoring location CGC-3, central Grand Canyon, Arizona.

[NA indicates mechanisms not identified in the survey. m^2, square meter; m^3, cubic meter; %, percent]

Spatial subdivision	Area (m^2)			Volume (m^3)			Percent imbalance (%)
	Erosion	Deposition	Total	Erosion	Deposition	Net	
Baseline survey area							
Fluvial	2.81	6.49	9.30	0.13	0.75	0.62	35.0
Aeolian	50.84	87.10	137.94	3.43	7.88	4.45	19.7
Alluvial	8.73	4.14	12.88	0.66	0.27	−0.38	−20.6
Colluvial	8.56	1.82	10.38	1.01	0.26	−0.75	−29.4
Indeterminate	190.46	461.40	651.85	13.13	41.97	28.84	26.2
Archaeological site boundary (B:13:0002)							
Fluvial	NA	NA	NA	NA	NA	NA	NA
Aeolian	3.34	0.00	3.34	0.31	0.00	−0.31	−50.0
Alluvial	0.00	0.16	0.16	0.00	0.01	0.01	50.0
Colluvial	1.44	0.03	1.47	0.15	0.00	−0.15	−48.1
Indeterminate	14.60	2.22	16.82	1.45	0.21	−1.24	−37.5

Between the 2019 and 2020 surveys, the net volumetric change for the baseline survey area was depositional for the part downstream of the tributary channel and erosional for the part upstream of the tributary channel (table 74). Net volumetric change was deposition for the archaeological site (table 74). On the upstream part of the baseline survey area, the greatest areal cover of topographic changes was attributed to both aeolian and indeterminant processes (table 75). Much of the indeterminant erosion was along the steep talus slope to the south of the baseline survey area and areas of deposition were located along the base of the slope (fig. 42). These changes are interpreted as runoff and slope-wash erosion that were deposited along the southern edge of the dune field and subsequently reworked by wind; the dominant wind direction interpreted from dune morphology and wind ripples is south by southeast. Similarly, topographic changes in the archaeological site and upstream baseline survey area were along the relatively steep slopes of mixed alluvium and talus below the canyon walls that were primarily categorized as from indeterminant processes but interpreted as slope wash (fig. 42; table 75).

Monitoring Location WGC-1

Monitoring location WGC-1 is located in western Grand Canyon on river right and is a long-term monitoring location with previous TLS surveys and weather station records (Draut and others, 2009, 2010; Collins and others, 2012; Dealy and others, 2014; Caster and others, 2014, 2018; East and others, 2016). Site WGC-1 was previously surveyed using TLS in May 2006, May 2007, September 2007, and September 2010. Collins and others (2012, 2016) synthesized those previous monitoring results, showing that topographic changes were predominantly erosional from 2006 to 2010 owing to alluvial and aeolian processes. However, topographic change from 2007 to 2010 in the associated archaeological site, G:03:0072, had areas of aeolian deposition. Site G:03:0072 is classified as aeolian type 1, with wind records indicating a predominant wind direction from the south by southeast that transports sand from the sandbar to the north by northwest. Several incised gullies channelize excess rainfall runoff from the archaeological site into the side canyon tributary to the west as well as to the active Colorado River channel to the east by southeast, making it drainage type 4.

Monitoring location WGC-1 has a baseline survey area of approximately 2,904 m^2 that was covered during all seven surveys between 2010 and 2020 and an expanded baseline survey area of 3,711 m^2 covered between 2013 and 2020 (figs. 43–48; tables 76–93). Change detection results focus on the baseline survey area, though topographic changes within the full overlapping survey coverage area for each interval after 2010 are also included in the cultural feature results (tables 80, 83, 86, 89, and 92) and visually presented in each associated figure (figs. 43–48).

In the $DoD_{2010–2013}$, net volumetric change in the baseline survey area and archaeological site was erosional, with the greatest proportion between features 11 and 2 (fig. 43; tables 76 and 77). Most change was categorized as indeterminate, possibly representing cumulative effects of interacting fluvial and aeolian processes (table 78). Aeolian changes also affected a substantial spatial extent and were primarily concentrated in the southwestern part of the site near features 11 and 12 (fig. 43; table 78).

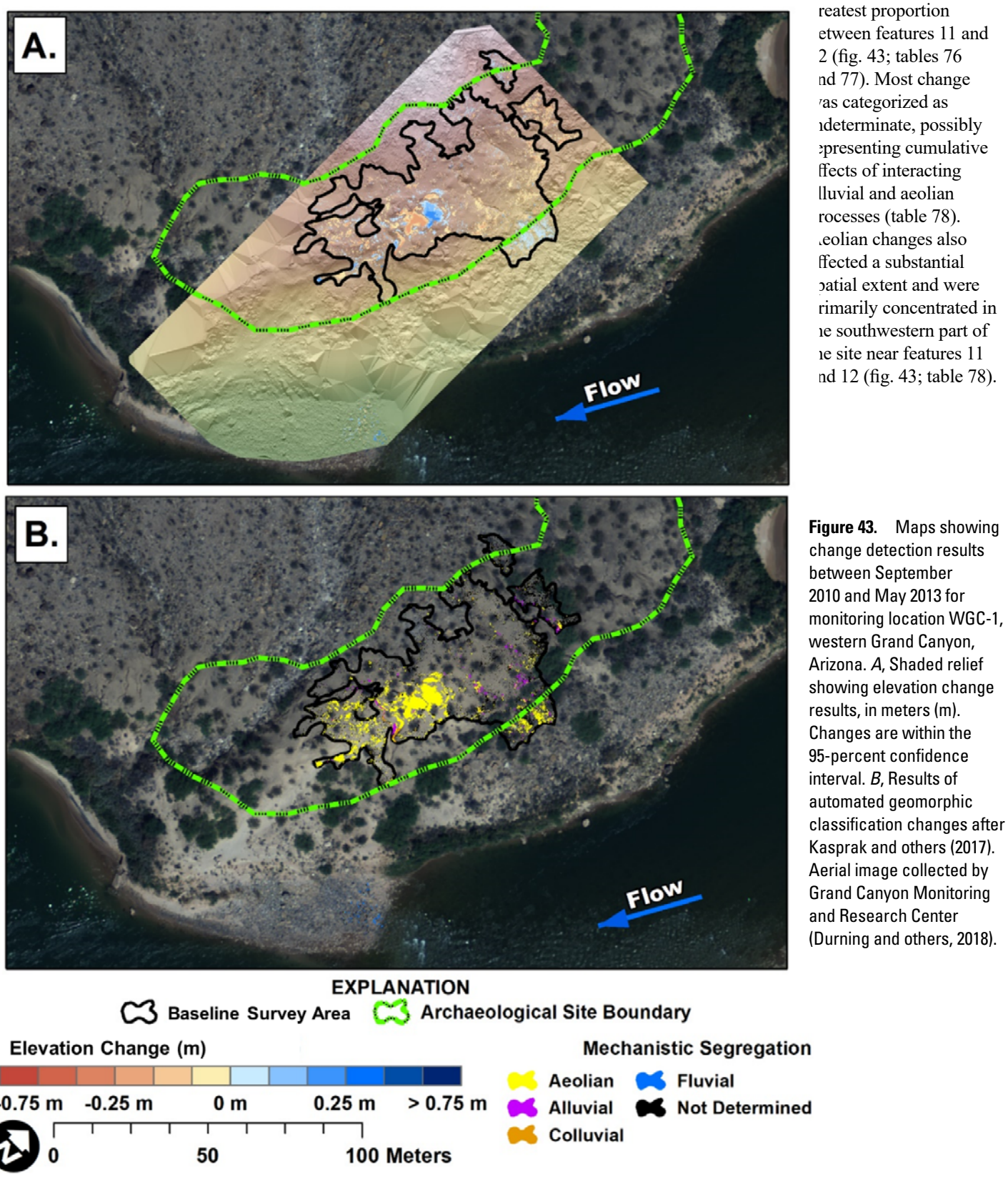

Figure 43. Maps showing change detection results between September 2010 and May 2013 for monitoring location WGC-1, western Grand Canyon, Arizona. *A*, Shaded relief showing elevation change results, in meters (m). Changes are within the 95-percent confidence interval. *B*, Results of automated geomorphic classification changes after Kasprak and others (2017). Aerial image collected by Grand Canyon Monitoring and Research Center (Durning and others, 2018).

Table 76. Results of change detection between September 2010 and May 2013 for the baseline survey area at monitoring location WGC-1, western Grand Canyon, Arizona.

[The archaeological site boundary is included in the above maximum flood elevation subdivision. NA represents areas outside of the baseline survey. m^2, square meter; m^3, cubic meter; %, percent]

Spatial subdivision	Survey area (m^2)	Area (m^2)			Volume (m^3)			Percent imbalance (%)
		Erosion	Deposition	Total	Erosion	Deposition	Net	
Baseline survey area	2,903.56	342.54	220.25	562.80	20.00	9.85	−10.15	−17.0
Below maximum flood elevation	NA	NA	NA	NA	NA	NA	NA	NA
Above maximum flood elevation	2,903.56	342.54	220.25	562.80	20.00	9.85	−10.15	−17.0
Archaeological site boundary	2,714.95	335.05	167.16	502.21	19.60	8.02	−11.58	−21.0

Table 77. Results of change detection between September 2010 and May 2013 for mapped archaeological features at site G:03:0072, western Grand Canyon, Arizona.

[Feature + buffer is inclusive of the feature area and a surrounding 1-meter-wide buffer. m^2, square meter; m^3, cubic meter; %, percent]

Spatial subdivision	Survey area (m^2)	Area (m^2)			Volume (m^3)			Percent imbalance (%)
		Erosion	Deposition	Total	Erosion	Deposition	Net	
Feature 6	3.90	1.23	0.06	1.29	0.08	0.00	−0.08	−46.3
Feature 6 + buffer	13.05	4.73	0.11	4.84	0.29	0.01	−0.28	−48.2
Feature 7	1.46	0.11	0.01	0.12	0.00	0.00	0.00	−44.2
Feature 7 + buffer	9.03	0.43	0.01	0.44	0.01	0.00	−0.01	−48.2
Feature 8	1.93	0.21	0.07	0.28	0.01	0.00	−0.01	−30.5
Feature 8 + buffer	9.89	1.30	0.33	1.63	0.05	0.01	−0.04	−35.2
Feature 9	7.84	0.70	0.07	0.77	0.04	0.00	−0.04	−45.3
Feature 9 + buffer	19.04	0.86	0.44	1.30	0.04	0.02	−0.03	−22.8
Feature 10	2.92	0.30	0.00	0.30	0.01	0.00	−0.01	−50.0
Feature 10 + buffer	12.29	0.85	0.00	0.85	0.04	0.00	−0.04	−50.0
Feature 11	1.10	0.62	0.00	0.62	0.07	0.00	−0.07	−50.0
Feature 11 + buffer	8.03	2.57	0.55	3.11	0.31	0.03	−0.28	−41.8
Feature 12	1.37	0.25	0.01	0.26	0.01	0.00	−0.01	−46.0
Feature 12 + buffer	8.74	1.35	0.22	1.56	0.05	0.01	−0.05	−39.1
Feature 15	2.00	0.08	0.01	0.09	0.00	0.00	0.00	−35.1
Feature 15 + buffer	10.32	0.44	0.03	0.47	0.01	0.00	−0.01	−44.7

Table 78. Results of change detection by geomorphic mechanism between September 2010 and May 2013 at monitoring location WGC-1, western Grand Canyon, Arizona.

[NA indicates mechanisms not identified in the survey. m^2, square meter; m^3, cubic meter; %, percent]

Spatial subdivision	Area (m^2)			Volume (m^3)			Percent imbalance (%)
	Erosion	Deposition	Total	Erosion	Deposition	Net	
Baseline survey area							
Fluvial	NA	NA	NA	NA	NA	NA	NA
Aeolian	135.37	120.80	256.18	8.59	6.07	−2.52	−8.6
Alluvial	19.22	7.81	27.03	0.95	0.37	−0.58	−22.0
Colluvial	6.99	1.90	8.89	1.06	0.14	−0.92	−38.0
Indeterminate	180.97	89.74	270.71	9.40	3.27	−6.13	−24.2
Archaeological site boundary							
Fluvial	NA	NA	NA	NA	NA	NA	NA
Aeolian	134.90	92.39	227.29	8.57	5.13	−3.44	−12.5
Alluvial	18.51	6.64	25.15	0.91	0.32	−0.59	−23.9
Colluvial	6.94	1.74	8.68	1.06	0.13	−0.93	−38.8
Indeterminate	174.70	66.40	241.09	9.06	2.43	−6.63	−28.9

Net volumetric change for the $DoD_{2013–2014}$ was erosional in the extended baseline survey area (larger after 2013) and the archaeological site (fig. 44; table 79). Within the archaeological site boundary, features 6, 7, 10, and 15 incurred net deposition (table 80). Wind was the most significant geomorphic agent during this interval, with areas of change concentrated in the southwestern part of the archaeological site and the baseline survey area (fig. 44; table 81). Topographic changes within the northern part of the site were primarily alluvial erosion associated with gullies around features 7, 8, 9, and 10 (fig. 44).

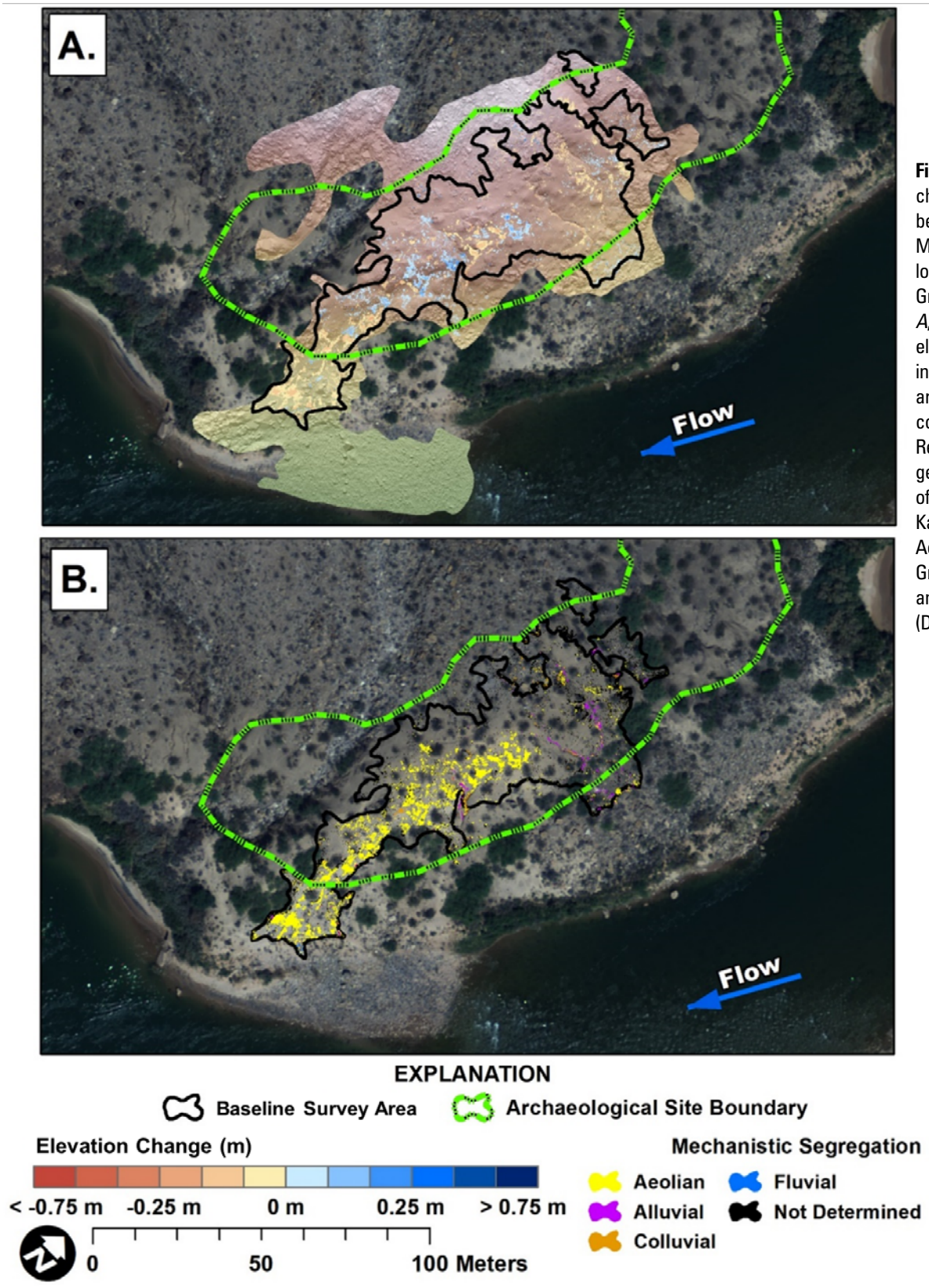

Figure 44. Maps showing change detection results between May 2013 and May 2014 for monitoring location WGC-1, western Grand Canyon, Arizona. *A*, Shaded relief showing elevation change results, in meters (m). Changes are within the 95-percent confidence interval. *B*, Results of automated geomorphic classification of threshold changes after Kasprak and others (2017). Aerial image collected by Grand Canyon Monitoring and Research Center (Durning and others, 2018).

Table 79. Results of change detection between May 2013 and May 2014 for the baseline survey area at monitoring location WGC-1, western Grand Canyon, Arizona.

[The archaeological site boundary is included in the above maximum flood elevation subdivision. m^2, square meter; m^3, cubic meter; %, percent]

Spatial subdivision	Survey area (m^2)	Area (m^2)			Volume (m^3)			Percent imbalance (%)
		Erosion	Deposition	Total	Erosion	Deposition	Net	
Baseline survey area	3,711.00	323.06	261.79	584.85	14.21	10.73	−3.47	−7.0
Below maximum flood elevation	9.46	1.80	0.21	2.01	0.12	0.01	−0.10	−40.3
Above maximum flood elevation	3,701.55	321.26	261.58	582.84	14.09	10.72	−3.37	−6.8
Archaeological site boundary	3,167.29	226.13	236.13	462.27	10.18	9.71	−0.47	−1.2

Table 80. Results of change detection between May 2013 and May 2014 for mapped archaeological features at site G:03:0072, western Grand Canyon, Arizona.

[Results are presented for two inclusive subdivisions. The largest overlapping area represents all significant topographic change within the DEM of difference and the baseline survey area represents a subset of significant changes relative to the baseline survey. Feature + buffer is inclusive of the feature area and a surrounding 1-meter-wide buffer. DEM, digital elevation model; m^2, square meter; m^3, cubic meter; %, percent]

Spatial subdivision	Survey area (m^2)	Area (m^2)			Volume (m^3)			Percent imbalance (%)
		Erosion	Deposition	Total	Erosion	Deposition	Net	
Largest overlapping area								
Feature 6	3.90	0.08	0.35	0.43	0.00	0.02	0.01	31.6
Feature 6 + buffer	13.05	0.39	1.32	1.71	0.02	0.05	0.04	28.1
Feature 7	1.46	0.00	0.28	0.28	0.00	0.01	0.01	50.0
Feature 7 + buffer	9.03	0.00	2.32	2.32	0.00	0.07	0.07	50.0
Feature 8	1.93	0.45	0.00	0.45	0.01	0.00	−0.01	−50.0
Feature 8 + buffer	9.89	1.65	0.01	1.65	0.06	0.00	−0.06	−49.8
Feature 9	7.84	0.61	0.04	0.65	0.02	0.00	−0.02	−40.8
Feature 9 + buffer	19.04	1.56	0.10	1.66	0.06	0.00	−0.05	−43.8
Feature 10	2.92	0.00	0.13	0.13	0.00	0.00	0.00	50.0
Feature 10 + buffer	12.29	0.07	0.41	0.48	0.00	0.01	0.01	35.2
Feature 11	1.10	0.49	0.00	0.49	0.02	0.00	−0.02	−50.0
Feature 11 + buffer	8.03	1.47	0.12	1.59	0.08	0.00	−0.08	−45.5
Feature 12	1.37	0.36	0.00	0.36	0.01	0.00	−0.01	−50.0
Feature 12 + buffer	8.74	1.01	0.05	1.06	0.03	0.00	−0.03	−45.6
Feature 15	2.00	0.00	0.16	0.16	0.00	0.00	0.00	50.0
Feature 15 + buffer	10.32	0.00	0.92	0.93	0.00	0.03	0.03	49.7
Baseline survey area								
Feature 6	3.90	0.08	0.35	0.43	0.00	0.02	0.01	31.6
Feature 6 + buffer	13.05	0.37	1.32	1.69	0.01	0.05	0.04	28.7
Feature 7	1.46	0.00	0.28	0.28	0.00	0.01	0.01	50.0
Feature 7 + buffer	9.03	0.00	2.32	2.32	0.00	0.07	0.07	50.0
Feature 8	1.93	0.45	0.00	0.45	0.01	0.00	−0.01	−50.0
Feature 8 + buffer	9.89	1.65	0.01	1.65	0.06	0.00	−0.06	−49.8
Feature 9	7.84	0.61	0.03	0.63	0.02	0.00	−0.02	−45.2
Feature 9 + buffer	19.04	1.53	0.06	1.59	0.05	0.00	−0.05	−46.4
Feature 10	2.92	0.00	0.13	0.13	0.00	0.00	0.00	50.0
Feature 10 + buffer	12.29	0.07	0.41	0.48	0.00	0.01	0.01	35.2

Table 80. Results of change detection between May 2013 and May 2014 for mapped archaeological features at site G:03:0072, western Grand Canyon, Arizona.—Continued

Spatial subdivision	Survey area (m^2)	Area (m^2)			Volume (m^3)			Percent imbalance (%)
		Erosion	Deposition	Total	Erosion	Deposition	Net	
Baseline survey area—continued								
Feature 11	1.10	0.49	0.00	0.49	0.02	0.00	−0.02	−50.0
Feature 11 + buffer	8.03	1.47	0.12	1.59	0.08	0.00	−0.08	−45.5
Feature 12	1.37	0.36	0.00	0.36	0.01	0.00	−0.01	−50.0
Feature 12 + buffer	8.74	1.01	0.05	1.06	0.03	0.00	−0.03	−45.6
Feature 15	2.00	0.00	0.16	0.16	0.00	0.00	0.00	50.0
Feature 15 + buffer	10.32	0.00	0.92	0.93	0.00	0.03	0.03	49.7

Table 81. Results of change detection by geomorphic mechanism between May 2013 and May 2014 at monitoring location WGC-1, western Grand Canyon, Arizona.

[NA indicates mechanisms not identified in the survey. m^2, square meter; m^3, cubic meter; %, percent]

Spatial subdivision	Area (m^2)			Volume (m^3)			Percent imbalance (%)
	Erosion	Deposition	Total	Erosion	Deposition	Net	
Baseline survey area							
Fluvial	1.27	0.09	1.36	0.09	0.01	−0.08	−40.8
Aeolian	180.87	160.82	341.68	7.92	6.88	−1.04	−3.5
Alluvial	17.60	7.02	24.61	0.89	0.32	−0.57	−23.6
Colluvial	13.48	3.08	16.56	1.20	0.29	−0.91	−30.6
Indeterminate	109.69	90.58	200.27	4.09	3.23	−0.87	−5.9
Archaeological site boundary							
Fluvial	NA	NA	NA	NA	NA	NA	NA
Aeolian	106.30	150.18	256.48	4.88	6.43	1.55	6.8
Alluvial	15.42	3.76	19.19	0.79	0.19	−0.60	−30.8
Colluvial	11.92	2.87	14.79	1.08	0.27	−0.81	−29.7
Indeterminate	92.43	79.19	171.62	3.42	2.82	−0.61	−4.9

Net volumetric change in the $DoD_{2014–2016}$ was erosional for the expanded baseline survey area, but the archaeological site area incurred net deposition (table 82). Despite positive changes in sediment storage for the archaeological site, features 6 and 15 exhibited the greatest erosion of any interval (fig. 45; table 83). Aeolian processes were the most laterally extensive mechanism of change, but colluvial processes—specifically backwasting of gully walls—produced the greatest net erosional change (fig. 45; table 84). Colluvial changes were primarily associated with a large gully near feature 11 and a smaller gully near features 10 and 15 (fig. 45). For the sandbar southeast of the extended baseline survey area, previously buried river cobbles were exposed by fluvial erosion of overlying flood sediment.

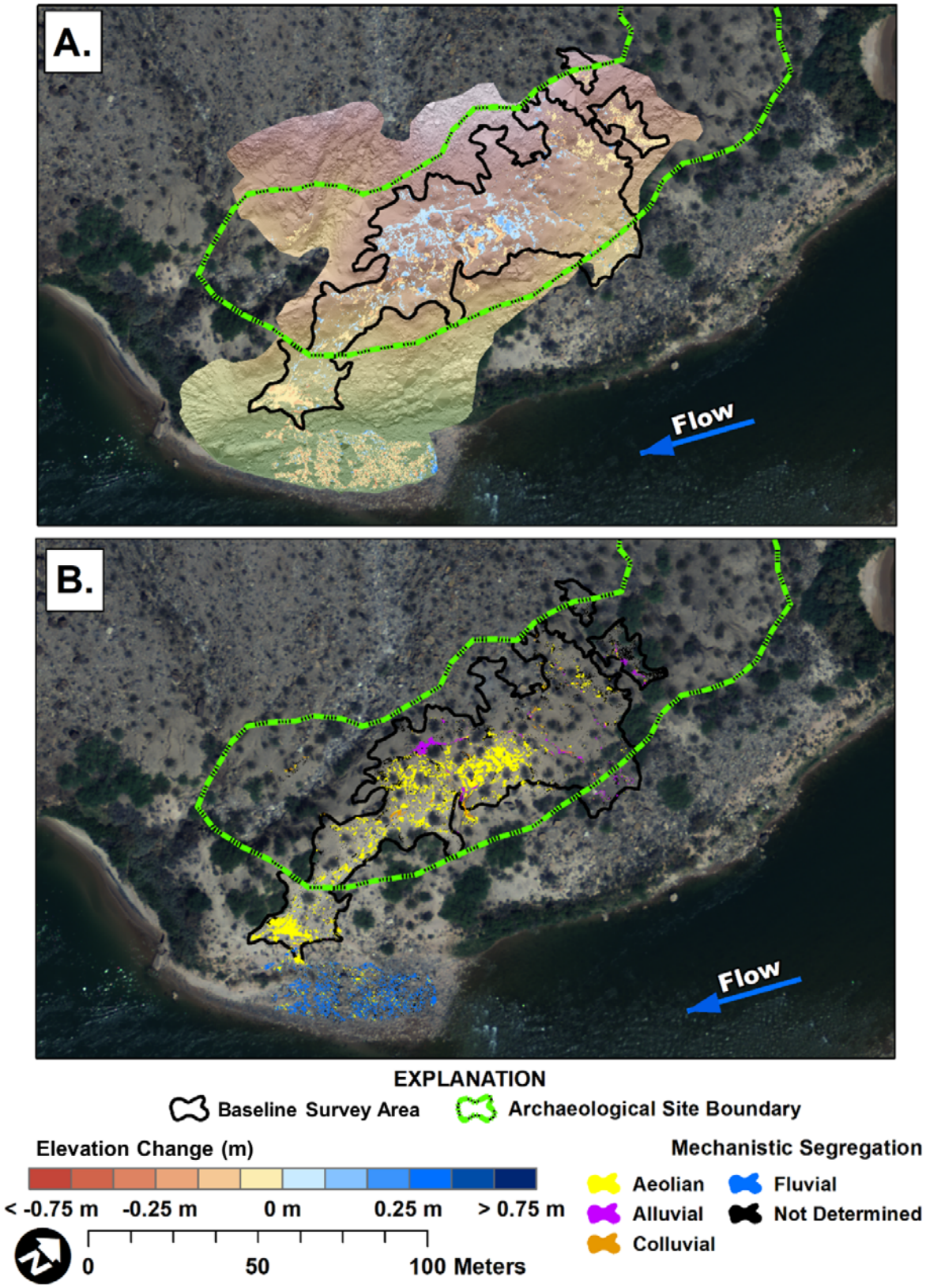

Figure 45. Maps showing change detection results between May 2014 and May 2016 for monitoring location WGC-1, western Grand Canyon, Arizona. *A*, Shaded relief showing elevation change results, in meters (m). Changes are within the 95-percent confidence interval. *B*, Results of automated geomorphic classification changes after Kasprak and others (2017). Aerial image collected by Grand Canyon Monitoring and Research Center (Durning and others, 2018).

Table 82. Results of change detection between May 2014 and May 2016 for the baseline survey area at monitoring location WGC-1, western Grand Canyon, Arizona.

[The archaeological site boundary is included in the above maximum flood elevation subdivision. m^2, square meter; m^3, cubic meter; %, percent]

Spatial subdivision	Survey area (m^2)	Area (m^2)			Volume (m^3)			Percent imbalance (%)
		Erosion	Deposition	Total	Erosion	Deposition	Net	
Baseline survey area	3,711.00	278.13	285.82	563.95	13.55	11.53	−2.02	−4.0
Below maximum flood elevation	9.46	3.27	0.00	3.27	0.22	0.00	−0.22	−50.0
Above maximum flood elevation	3,701.55	274.86	285.82	560.68	13.33	11.53	−1.80	−3.6
Archaeological site boundary	3,167.29	202.20	274.23	476.43	10.07	11.04	0.97	2.3

Table 83. Results of change detection between May 2014 and May 2016 for mapped archaeological features at site G:03:0072, western Grand Canyon, Arizona.

[Results are presented for two inclusive subdivisions. The largest overlapping area represents all significant topographic change within the DEM of difference and the baseline survey area represents a subset of significant changes relative to the baseline survey. Feature + buffer is inclusive of the feature area and a surrounding 1-meter-wide buffer. DEM, digital elevation model; m^2, square meter; m^3, cubic meter; %, percent]

Spatial subdivision	Survey area (m^2)	Area (m^2)			Volume (m^3)			Percent imbalance (%)
		Erosion	Deposition	Total	Erosion	Deposition	Net	
Largest overlapping area								
Feature 6	3.90	2.36	0.00	2.36	0.11	0.00	−0.11	−50.0
Feature 6 + buffer	13.05	8.22	0.00	8.22	0.36	0.00	−0.36	−50.0
Feature 7	1.46	0.26	0.00	0.26	0.01	0.00	−0.01	−50.0
Feature 7 + buffer	9.03	1.56	0.00	1.56	0.04	0.00	−0.04	−50.0
Feature 8	1.93	0.00	0.17	0.17	0.00	0.01	0.01	50.0
Feature 8 + buffer	9.89	0.05	0.17	0.22	0.00	0.01	0.00	24.9
Feature 9	NA	NA	NA	NA	NA	NA	NA	NA
Feature 9 + buffer	NA	NA	NA	NA	NA	NA	NA	NA
Feature 10	2.92	0.02	0.03	0.05	0.00	0.00	0.00	27.3
Feature 10 + buffer	12.29	0.02	0.45	0.47	0.00	0.02	0.02	48.1
Feature 11	1.10	0.41	0.01	0.42	0.03	0.00	−0.03	−49.6
Feature 11 + buffer	8.03	1.14	1.13	2.27	0.08	0.05	−0.04	−13.6
Feature 12	1.37	0.05	0.02	0.07	0.00	0.00	0.00	−16.5
Feature 12 + buffer	8.74	0.56	1.17	1.74	0.02	0.04	0.02	20.2
Feature 15	2.00	0.75	0.00	0.75	0.02	0.00	−0.02	−50.0
Feature 15 + buffer	10.32	4.38	0.00	4.38	0.15	0.00	−0.15	−50.0
Baseline survey area								
Feature 6	3.90	2.36	0.00	2.36	0.11	0.00	−0.11	−50.0
Feature 6 + buffer	13.05	8.22	0.00	8.22	0.36	0.00	−0.36	−50.0
Feature 7	1.46	0.26	0.00	0.26	0.01	0.00	−0.01	−50.0
Feature 7 + buffer	9.03	1.56	0.00	1.56	0.04	0.00	−0.04	−50.0
Feature 8	1.93	0.00	0.17	0.17	0.00	0.01	0.01	50.0
Feature 8 + buffer	9.89	0.05	0.17	0.22	0.00	0.01	0.00	24.9
Feature 9	NA	NA	NA	NA	NA	NA	NA	NA
Feature 9 + buffer	NA	NA	NA	NA	NA	NA	NA	NA
Feature 10	2.92	0.02	0.03	0.05	0.00	0.00	0.00	27.3
Feature 10 + buffer	12.29	0.02	0.45	0.47	0.00	0.02	0.02	48.1
Feature 11	1.10	0.41	0.01	0.42	0.03	0.00	−0.03	−49.6
Feature 11 + buffer	8.03	1.14	1.13	2.27	0.08	0.05	−0.04	−13.6
Feature 12	1.37	0.05	0.02	0.07	0.00	0.00	0.00	−16.5
Feature 12 + buffer	8.74	0.56	1.17	1.74	0.02	0.04	0.02	20.2
Feature 15	2.00	0.75	0.00	0.75	0.02	0.00	−0.02	−50.0
Feature 15 + buffer	10.32	4.38	0.00	4.38	0.15	0.00	−0.15	−50.0

Table 84. Results of change detection by geomorphic mechanism between May 2014 and May 2016 at monitoring location WGC-1, western Grand Canyon, Arizona.

[NA indicates mechanisms not identified in the survey. m^2, square meter; m^3, cubic meter; %, percent]

Spatial subdivision	Area (m^2)			Volume (m^3)			Percent imbalance (%)
	Erosion	Deposition	Total	Erosion	Deposition	Net	
Baseline survey area							
Fluvial	0.99	0.00	0.99	0.04	0.00	−0.04	−50.0
Aeolian	162.56	175.86	338.42	7.59	6.97	−0.62	−2.1
Alluvial	12.91	24.13	37.04	0.82	0.99	0.17	4.7
Colluvial	12.86	3.81	16.67	1.65	0.29	−1.36	−35.0
Indeterminate	88.41	81.82	170.23	3.43	3.28	−0.16	−1.2
Archaeological site boundary							
Fluvial	NA	NA	NA	NA	NA	NA	NA
Aeolian	91.74	156.29	248.03	4.49	6.34	1.86	8.6
Alluvial	8.24	20.64	28.88	0.57	0.84	0.27	9.5
Colluvial	11.04	2.86	13.90	1.49	0.23	−1.26	−36.6
Indeterminate	63.19	62.87	126.06	2.56	2.62	0.06	0.5

For the $DoD_{2016–2017}$, net volumetric change was depositional in the expanded baseline survey area (fig. 46; tables 85 and 86). Net change in the archaeological site was also depositional, though erosion occurred in features 1 and 8. Deposition >0.1 m^3 occurred at features 6 and 15 (fig. 46; table 86). Similar to $DoD_{2010–2013}$, aeolian changes had the greatest spatial coverage but the largest net volume changes were classified as indeterminate (table 87). Much of the indeterminate topographic changes were deposition within the northern part of the extended baseline survey area along flat terrain between gullies. These areas were vegetated by grasses and partially covered with biological soil crust that may have trapped sediment transported by wind or runoff. South of the extended baseline survey area, flood deposits were observed in 2017 on the sandbar that covered a portion of the exposed gravel noted in the 2016 survey.

Table 85. Results of change detection between May 2016 and May 2017 for the baseline survey area at monitoring location WGC-1, western Grand Canyon, Arizona.

[The archaeological site boundary is included in the above maximum flood elevation subdivision. m^2, square meter; m^3, cubic meter; %, percent]

Spatial subdivision	Survey area (m^2)	Area (m^2)			Volume (m^3)			Percent imbalance (%)
		Erosion	Deposition	Total	Erosion	Deposition	Net	
Baseline survey area	3,711.00	196.53	502.22	698.75	8.10	19.53	11.44	20.7
Below maximum flood elevation	9.46	0.06	6.68	6.74	0.00	0.37	0.37	49.5
Above maximum flood elevation	3,701.55	196.47	495.54	692.01	8.09	19.16	11.07	20.3
Archaeological site boundary	3,167.29	178.35	451.61	629.96	7.37	17.33	9.96	20.1

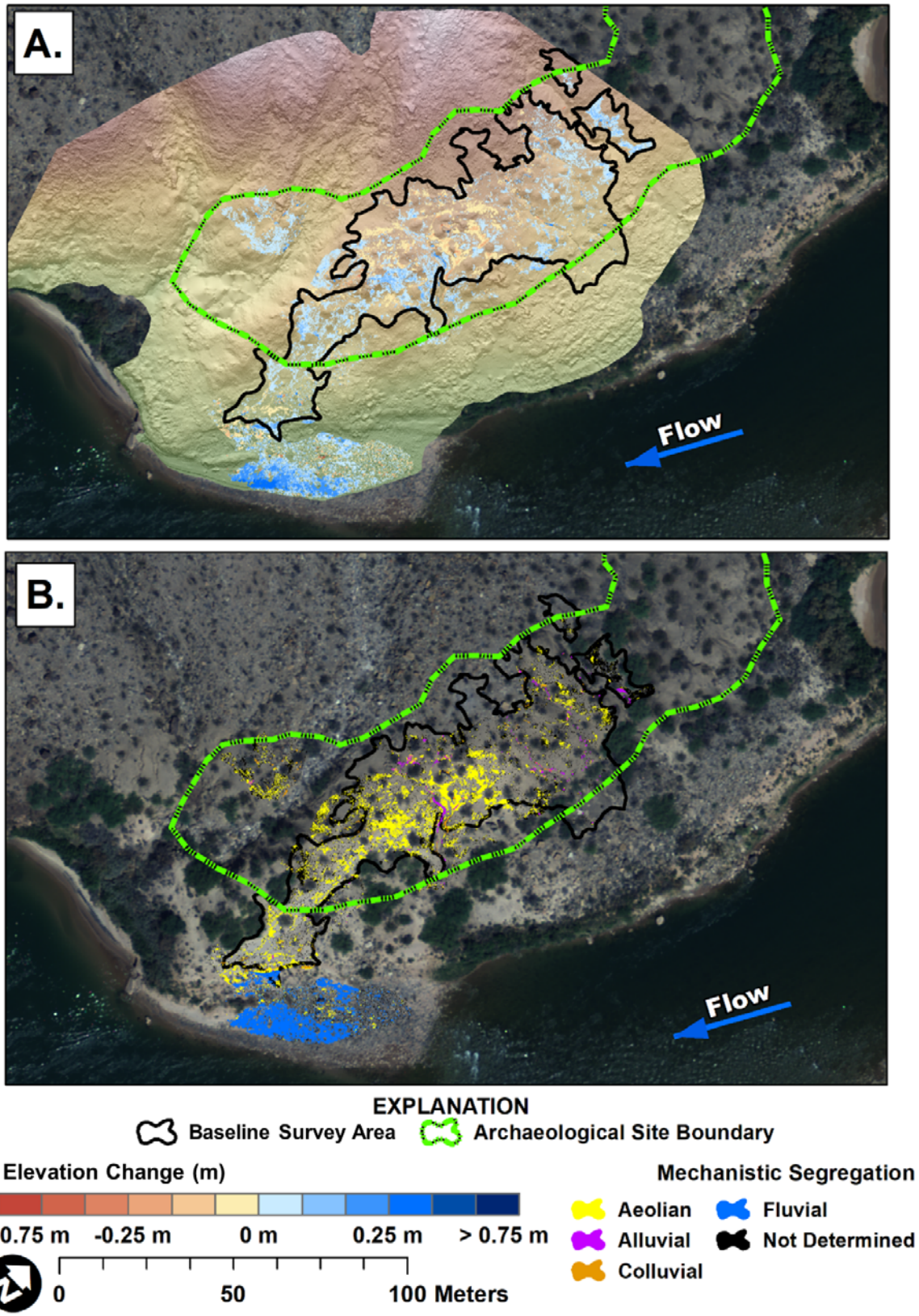

Figure 46. Maps showing change detection results between May 2016 and May 2017 for monitoring location WGC-1, western Grand Canyon, Arizona. *A*, Shaded relief showing elevation change results, in meters (m). Changes are within the 95-percent confidence interval. *B*, Results of automated geomorphic classification changes after Kasprak and others (2017). Aerial image collected by Grand Canyon Monitoring and Research Center (Durning and others, 2018).

Table 86. Results of change detection between May 2016 and May 2017 for mapped archaeological features at site G:03:0072, western Grand Canyon, Arizona.

[Results are presented for two inclusive subdivisions. The largest overlapping area represents all significant topographic change within the DEM of difference and the baseline survey area represents a subset of significant changes relative to the baseline survey. Feature + buffer is inclusive of the feature area and a surrounding 1-meter-wide buffer. DEM, digital elevation model; m^2, square meter; m^3, cubic meter; %, percent]

Spatial subdivision	Survey area (m^2)	Area (m^2)			Volume (m^3)			Percent imbalance (%)
		Erosion	Deposition	Total	Erosion	Deposition	Net	
Largest overlapping area								
Feature 6	3.90	0.00	1.85	1.85	0.00	0.10	0.10	50.0
Feature 6 + buffer	14.16	0.01	6.51	6.51	0.00	0.32	0.32	49.9
Feature 7	1.46	0.00	0.46	0.46	0.00	0.02	0.02	50.0
Feature 7 + buffer	9.03	0.00	2.90	2.90	0.00	0.07	0.07	50.0
Feature 8	1.93	0.11	0.02	0.13	0.01	0.00	−0.01	−39.5
Feature 8 + buffer	10.15	0.61	0.34	0.94	0.02	0.01	−0.01	−21.1
Feature 9	NA	NA	NA	NA	NA	NA	NA	NA
Feature 9 + buffer	NA	NA	NA	NA	NA	NA	NA	NA
Feature 10	2.92	0.02	0.07	0.09	0.00	0.00	0.00	37.5
Feature 10 + buffer	12.29	0.21	0.60	0.81	0.01	0.02	0.01	16.8
Feature 11	1.10	0.33	0.03	0.37	0.02	0.00	−0.02	−46.6
Feature 11 + buffer	8.03	1.43	0.73	2.16	0.10	0.02	−0.08	−34.9
Feature 12	1.37	0.04	0.02	0.06	0.00	0.00	0.00	−14.7
Feature 12 + buffer	8.74	0.84	1.38	2.21	0.03	0.04	0.01	9.2
Feature 13	0.90	0.01	0.25	0.26	0.00	0.01	0.01	47.1
Feature 13 + buffer	7.48	0.05	1.41	1.45	0.00	0.04	0.04	47.0
Feature 14	1.30	0.00	0.00	0.00	0.00	0.00	0.00	0.0
Feature 14 + buffer	6.56	0.00	0.23	0.23	0.00	0.01	0.01	50.0
Feature 15	2.00	0.00	0.73	0.73	0.00	0.02	0.02	50.0
Feature 15 + buffer	10.32	0.00	4.64	4.64	0.00	0.15	0.15	50.0
Baseline survey area								
Feature 6	3.90	0.00	1.85	1.85	0.00	0.10	0.10	50.0
Feature 6 + buffer	14.16	0.01	6.51	6.51	0.00	0.32	0.32	49.9
Feature 7	1.46	0.00	0.46	0.46	0.00	0.02	0.02	50.0
Feature 7 + buffer	9.03	0.00	2.90	2.90	0.00	0.07	0.07	50.0
Feature 8	1.93	0.11	0.02	0.13	0.01	0.00	−0.01	−39.5
Feature 8 + buffer	10.15	0.61	0.34	0.94	0.02	0.01	−0.01	−21.1
Feature 9	8.73	NA	NA	NA	NA	NA	NA	NA
Feature 9 + buffer	22.51	NA	NA	NA	NA	NA	NA	NA
Feature 10	2.92	0.02	0.07	0.09	0.00	0.00	0.00	37.5
Feature 10 + buffer	12.29	0.21	0.60	0.81	0.01	0.02	0.01	16.8
Feature 11	1.10	0.33	0.03	0.37	0.02	0.00	−0.02	−46.6
Feature 11 + buffer	8.03	1.43	0.73	2.16	0.10	0.02	−0.08	−34.9
Feature 12	1.37	0.04	0.02	0.06	0.00	0.00	0.00	−14.7
Feature 12 + buffer	8.74	0.84	1.38	2.21	0.03	0.04	0.01	9.2
Feature 13	NA	NA	NA	NA	NA	NA	NA	NA
Feature 13 + buffer	NA	NA	NA	NA	NA	NA	NA	NA
Feature 14	NA	NA	NA	NA	NA	NA	NA	NA
Feature 14 + buffer	NA	NA	NA	NA	NA	NA	NA	NA
Feature 15	2.00	0.00	0.73	0.73	0.00	0.02	0.02	50.0
Feature 15 + buffer	10.32	0.00	4.64	4.64	0.00	0.15	0.15	50.0

Table 87. Results of change detection by geomorphic mechanism between May 2016 and May 2017 at monitoring location WGC-1, western Grand Canyon, Arizona.

[NA indicates mechanisms not identified in the survey. m^2, square meter; m^3, cubic meter; %, percent]

Spatial subdivision	Area (m^2)			Volume (m^3)			Percent imbalance (%)
	Erosion	Deposition	Total	Erosion	Deposition	Net	
Baseline survey area							
Fluvial	0.06	5.37	5.43	0.00	0.31	0.30	49.4
Aeolian	133.41	250.78	384.19	5.12	9.50	4.38	15.0
Alluvial	9.24	19.48	28.71	0.61	1.04	0.42	12.8
Colluvial	5.16	6.20	11.35	0.68	0.62	−0.07	−2.6
Indeterminate	48.66	220.44	269.10	1.67	8.08	6.41	32.9
Archaeological site boundary							
Fluvial	NA	NA	NA	NA	NA	NA	NA
Aeolian	121.07	220.10	341.17	4.63	8.22	3.59	14.0
Alluvial	8.75	19.42	28.16	0.59	1.03	0.44	13.7
Colluvial	4.74	4.87	9.61	0.64	0.45	−0.19	−8.5
Indeterminate	43.80	207.26	251.06	1.52	7.63	6.11	33.4

Beginning in 2019, the NPS began annual vegetation management at monitoring location WGC-1 to remove riparian plants south of the extended baseline survey area along a steep bank located upslope of the downstream part of the sandbar; the plants created a barrier to aeolian transport of sand from the sandbar toward the archaeological site. In May 2019, we surveyed monitoring location WGC-1 after that year's vegetation management effort. In the $DoD_{2017–2019}$, net volumetric change was erosional in the expanded baseline survey area and archaeological site (fig. 47; table 88). Within the archaeological site, features 8 and 9 incurred sediment deposition though much of the area surrounding the other features experienced erosion (table 89). Within both the archaeological site and the extended baseline survey area, aeolian processes were responsible for a large area of topographic change, though the net change in sediment storage was relatively small (table 90). Indeterminate processes contributed to the greatest net loss in sediment storage. In general, indeterminate erosion was spatially dispersed throughout the extended baseline survey area and is interpreted as wind scour. Indeterminate deposition was primarily concentrated along the bases of plants and is interpreted as a mix of sediment transported by wind and runoff (fig. 47). Colluvial erosion was also an important contributor of change in sediment storage (table 90). These changes were associated with alluvial processes and backwasting within three gullies in the north and central parts of the extended baseline survey area as well as slumping near the weather station in the central part of the site.

Table 88. Results of change detection between May 2017 and May 2019 for the baseline survey area at monitoring location WGC-1, western Grand Canyon, Arizona.

[The archaeological site boundary is included in the above maximum flood elevation subdivision. m^2, square meter; m^3, cubic meter; %, percent]

Spatial subdivision	Survey area (m^2)	Area (m^2)			Volume (m^3)			Percent imbalance (%)
		Erosion	Deposition	Total	Erosion	Deposition	Net	
Baseline survey area	3,711.00	451.50	379.36	830.86	22.72	18.09	−4.62	−5.7
Below maximum flood elevation	9.46	2.64	3.39	6.03	0.16	0.17	0.01	1.1
Above maximum flood elevation	3,701.55	448.87	375.97	824.84	22.56	17.92	−4.63	−5.7
Archaeological site boundary	3,167.29	379.20	349.68	728.87	19.98	16.73	−3.25	−4.4

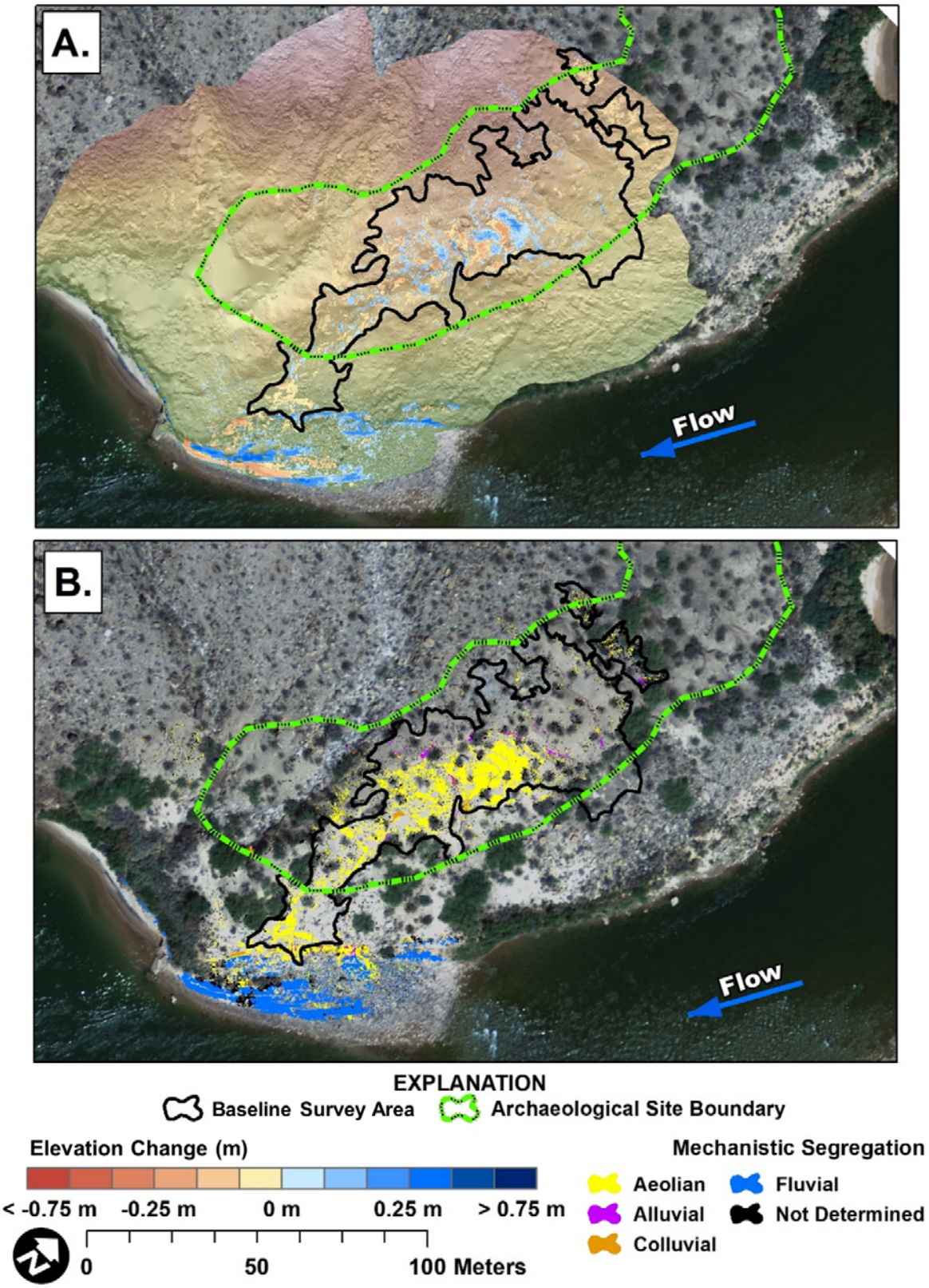

Figure 47. Maps showing change detection results between May 2017 and May 2019 for monitoring location WGC-1, western Grand Canyon, Arizona. *A*, Shaded relief showing elevation change results, in meters (m). Changes are within the 95-percent confidence interval. *B*, Results of automated geomorphic classification of threshold changes after Kasprak and others (2017). Aerial image collected by Grand Canyon Monitoring and Research Center (Durning and others, 2018).

Table 89. Results of change detection between May 2017 and May 2019 for mapped archaeological features at site G:03:0072, western Grand Canyon, Arizona.

[Results are presented for two inclusive subdivisions. The largest overlapping area represents all significant topographic change within the DEM of difference and the baseline survey area represents a subset of significant changes relative to the baseline survey. Feature + buffer is inclusive of the feature area and a surrounding 1-meter-wide buffer. DEM, digital elevation model; m^2, square meter; m^3, cubic meter; %, percent]

Spatial subdivision	Survey area (m^2)	Area (m^2)			Volume (m^3)			Percent imbalance (%)
		Erosion	Deposition	Total	Erosion	Deposition	Net	
Largest overlapping area								
Feature 6	3.90	1.24	0.00	1.24	0.05	0.00	−0.05	−50.0
Feature 6 + buffer	14.16	3.88	0.03	3.91	0.16	0.00	−0.15	−49.0
Feature 7	1.46	0.01	0.00	0.01	0.00	0.00	0.00	−50.0
Feature 7 + buffer	9.03	0.16	0.00	0.16	0.00	0.00	0.00	−50.0
Feature 8	1.93	0.00	0.31	0.31	0.00	0.01	0.01	50.0
Feature 8 + buffer	10.15	0.02	0.74	0.76	0.01	0.03	0.01	14.4
Feature 9	8.73	0.04	0.15	0.19	0.00	0.00	0.00	30.9
Feature 9 + buffer	22.51	0.05	0.36	0.41	0.00	0.01	0.01	35.8
Feature 10	2.92	0.02	0.00	0.02	0.00	0.00	0.00	−50.0
Feature 10 + buffer	12.29	0.21	0.15	0.36	0.01	0.01	0.00	−10.0
Feature 11	1.10	0.90	0.01	0.91	0.06	0.00	−0.06	−49.5
Feature 11 + buffer	8.03	3.08	1.20	4.28	0.25	0.04	−0.21	−36.7
Feature 12	1.37	0.00	0.00	0.00	0.00	0.00	0.00	NA
Feature 12 + buffer	8.74	1.77	0.31	2.07	0.09	0.01	−0.08	−39.2
Feature 13	0.90	0.13	0.00	0.13	0.00	0.00	0.00	−50.0
Feature 13 + buffer	7.48	0.43	0.14	0.57	0.01	0.00	−0.01	−28.9
Feature 14	1.30	0.00	0.00	0.00	0.00	0.00	0.00	0.0
Feature 14 + buffer	6.56	0.46	0.04	0.50	0.01	0.00	−0.01	−41.3
Feature 15	2.00	0.00	0.00	0.00	0.00	0.00	0.00	NA
Feature 15 + buffer	10.32	0.06	0.00	0.06	0.00	0.00	0.00	−50.0
Baseline survey area								
Feature 6	3.90	1.24	0.00	1.24	0.05	0.00	−0.05	−50.0
Feature 6 + buffer	14.16	3.88	0.03	3.91	0.16	0.00	−0.15	−49.0
Feature 7	1.46	0.01	0.00	0.01	0.00	0.00	0.00	−50.0
Feature 7 + buffer	9.03	0.16	0.00	0.16	0.00	0.00	0.00	−50.0
Feature 8	1.93	0.00	0.31	0.31	0.00	0.01	0.01	50.0
Feature 8 + buffer	10.15	0.02	0.74	0.76	0.01	0.03	0.01	14.4
Feature 9	8.73	0.04	0.15	0.19	0.00	0.00	0.00	30.9
Feature 9 + buffer	22.51	0.05	0.36	0.41	0.00	0.01	0.01	35.8
Feature 10	2.92	0.02	0.00	0.02	0.00	0.00	0.00	−50.0
Feature 10 + buffer	12.29	0.21	0.15	0.36	0.01	0.01	0.00	−10.0
Feature 11	1.10	0.90	0.01	0.91	0.06	0.00	−0.06	−49.5
Feature 11 + buffer	8.03	3.08	1.20	4.28	0.25	0.04	−0.21	−36.7
Feature 12	1.37	0.00	0.00	0.00	0.00	0.00	0.00	NA
Feature 12 + buffer	8.74	1.77	0.31	2.07	0.09	0.01	−0.08	−39.2
Feature 13	NA	NA	NA	NA	NA	NA	NA	NA
Feature 13 + buffer	NA	NA	NA	NA	NA	NA	NA	NA
Feature 14	NA	NA	NA	NA	NA	NA	NA	NA
Feature 14 + buffer	NA	NA	NA	NA	NA	NA	NA	NA
Feature 15	2.00	0.00	0.00	0.00	0.00	0.00	0.00	NA
Feature 15 + buffer	10.32	0.06	0.00	0.06	0.00	0.00	0.00	−50.0

Table 90. Results of change detection by geomorphic mechanism between May 2017 and May 2019 at monitoring location WGC-1, western Grand Canyon, Arizona.

[NA indicates mechanisms not identified in the survey. m^2, square meter; m^3, cubic meter; %, percent]

Spatial subdivision	Area (m^2)			Volume (m^3)			Percent imbalance (%)
	Erosion	Deposition	Total	Erosion	Deposition	Net	
Baseline survey area							
Fluvial	0.75	0.00	0.75	0.04	0.00	−0.04	−50.0
Aeolian	263.85	266.80	530.64	13.85	13.05	−0.79	−1.5
Alluvial	8.32	16.85	25.17	0.41	0.99	0.58	20.7
Colluvial	12.25	3.54	15.78	1.49	0.31	−1.18	−32.9
Indeterminate	166.23	92.29	258.52	6.93	3.74	−3.18	−14.9
Archaeological site boundary							
Fluvial	NA	NA	NA	NA	NA	NA	NA
Aeolian	207.21	246.57	453.77	11.79	12.13	0.34	0.7
Alluvial	8.07	15.85	23.92	0.40	0.93	0.53	20.0
Colluvial	11.80	3.26	15.06	1.44	0.28	−1.16	−33.8
Indeterminate	152.03	84.10	236.13	6.35	3.40	−2.95	−15.1

We resurveyed monitoring location WGC-1 in June 2020 prior to vegetation management conducted by NPS in September 2020. In the $DoD_{2019–2020}$, net volumetric change was depositional in the expanded baseline and archaeological site (fig. 48; table 91). Within the archaeological site, the area surrounding features were relatively stable with almost no detectable change, although the area surrounding feature 15 had net topographic change about four times greater than the other features (−0.04 m^3; table 92). As with previous change detection intervals, aeolian and indeterminate processes were responsible for much of the measured topographic changes (table 93). Aeolian processes were dominantly erosional, associated with indistinct dunes migrating from south to north across the extended survey area. Topographic changes attributed to indeterminate processes were less concentrated (fig. 48). As in the $DoD_{2017–2019,}$ these topographic changes were associated with vegetation and biological soil crusts, possibly representing sediment trapping by these biotic communities. South of the extended baseline survey area, a portion of the sediment deposited on the sandbar in 2017 was removed by fluvial processes, including an area adjacent to vegetation management operations (fig. 48).

Table 91. Results of change detection between May 2019 and June 2020 for the baseline survey area at monitoring location WGC-1, western Grand Canyon, Arizona.

[The archaeological site boundary is included in the above maximum flood elevation subdivision. m^2, square meter; m^3, cubic meter; %, percent]

Spatial subdivision	Survey area (m^2)	Area (m^2)			Volume (m^3)			Percent imbalance (%)
		Erosion	Deposition	Total	Erosion	Deposition	Net	
Baseline survey area	3,711.00	225.90	247.85	473.75	10.04	12.46	2.42	5.4
Below maximum flood elevation	9.46	0.14	0.59	0.73	0.00	0.03	0.03	36.4
Above maximum flood elevation	3,701.55	225.76	247.26	473.02	10.04	12.43	2.39	5.3
Archaeological site boundary	3,167.29	181.58	238.94	420.52	8.22	12.03	3.81	9.4

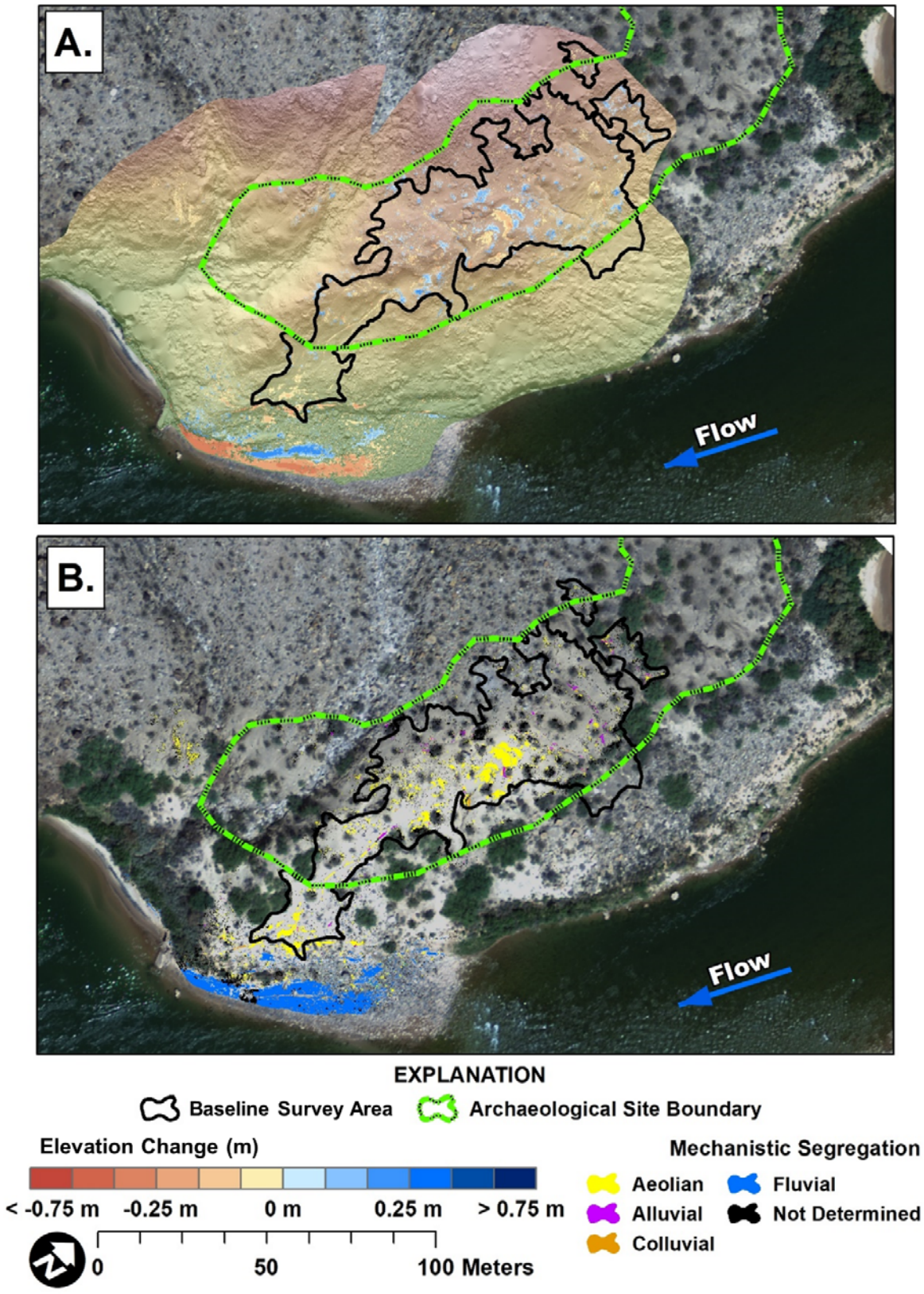

Figure 48. Maps showing change detection results between May 2019 and June 2020 for monitoring location WGC-1, western Grand Canyon, Arizona. *A*, Shaded relief showing elevation change results, in meters (m). Changes are within the 95-percent confidence interval. *B*, Results of automated geomorphic classification of threshold changes after Kasprak and others (2017). Aerial image collected by Grand Canyon Monitoring and Research Center (Durning and others, 2018).

Table 92. Results of change detection between May 2019 and June 2020 for mapped archaeological features at site G:03:0072, western Grand Canyon, Arizona.

[Results are presented for two inclusive subdivisions. The largest overlapping area represents all significant topographic change within the DEM of difference and the baseline survey area represents a subset of significant changes relative to the baseline survey. Feature + buffer is inclusive of the feature area and a surrounding 1-meter-wide buffer. DEM, digital elevation model; m^2, square meter; m^3, cubic meter; %, percent]

Spatial subdivision	Survey area (m^2)	Area (m^2)			Volume (m^3)			Percent imbalance (%)
		Erosion	Deposition	Total	Erosion	Deposition	Net	
Largest overlapping area								
Feature 6	3.90	0.04	0.00	0.04	0.00	0.00	0.00	−50.0
Feature 6 + buffer	14.16	0.26	0.14	0.40	0.01	0.01	0.00	−2.6
Feature 7	1.46	0.08	0.00	0.08	0.00	0.00	0.00	−50.0
Feature 7 + buffer	9.03	0.23	0.00	0.23	0.01	0.00	−0.01	−50.0
Feature 8	1.93	0.14	0.32	0.46	0.00	0.01	0.01	19.1
Feature 8 + buffer	10.15	0.14	0.32	0.46	0.01	0.01	0.01	18.7
Feature 9	8.73	0.23	0.01	0.24	0.01	0.00	−0.01	−45.1
Feature 9 + buffer	22.51	0.42	0.09	0.50	0.01	0.00	−0.01	−33.3
Feature 10	2.92	0.03	0.00	0.03	0.00	0.00	0.00	−50.0
Feature 10 + buffer	12.29	0.05	0.18	0.23	0.00	0.01	0.00	31.9
Feature 11	1.10	0.09	0.04	0.13	0.00	0.00	0.00	−30.7
Feature 11 + buffer	8.03	0.30	0.45	0.75	0.02	0.02	0.00	−4.6
Feature 12	1.37	0.00	0.00	0.00	0.00	0.00	0.00	NA
Feature 12 + buffer	8.74	0.25	0.26	0.51	0.01	0.01	0.00	−5.9
Feature 13	0.90	0.02	0.01	0.02	0.00	0.00	0.00	−28.4
Feature 13 + buffer	7.48	0.12	0.01	0.13	0.00	0.00	0.00	−41.4
Feature 14	1.30	0.00	0.00	0.00	0.00	0.00	0.00	0.0
Feature 14 + buffer	6.56	0.01	0.31	0.32	0.00	0.01	0.01	47.5
Feature 15	2.00	0.30	0.00	0.30	0.01	0.00	−0.01	−50.0
Feature 15 + buffer	10.32	1.57	0.01	1.59	0.04	0.00	−0.04	−49.2
Baseline survey area								
Feature 6	3.90	0.04	0.00	0.04	0.00	0.00	0.00	−50.0
Feature 6 + buffer	14.16	0.26	0.14	0.40	0.01	0.01	0.00	−2.6
Feature 7	1.46	0.08	0.00	0.08	0.00	0.00	0.00	−50.0
Feature 7 + buffer	9.03	0.23	0.00	0.23	0.01	0.00	−0.01	−50.0
Feature 8	1.93	0.14	0.32	0.46	0.00	0.01	0.01	19.1
Feature 8 + buffer	10.15	0.14	0.32	0.46	0.01	0.01	0.01	18.7
Feature 9	8.73	0.23	0.01	0.24	0.01	0.00	−0.01	−45.1
Feature 9 + buffer	22.51	0.42	0.09	0.50	0.01	0.00	−0.01	−33.3
Feature 10	2.92	0.03	0.00	0.03	0.00	0.00	0.00	−50.0
Feature 10 + buffer	12.29	0.05	0.18	0.23	0.00	0.01	0.00	31.9
Feature 11	1.10	0.09	0.04	0.13	0.00	0.00	0.00	−30.7
Feature 11 + buffer	8.03	0.30	0.45	0.75	0.02	0.02	0.00	−4.6
Feature 12	1.37	0.00	0.00	0.00	0.00	0.00	0.00	NA
Feature 12 + buffer	8.74	0.25	0.26	0.51	0.01	0.01	0.00	−5.9
Feature 13	NA	NA	NA	NA	NA	NA	NA	NA
Feature 13 + buffer	NA	NA	NA	NA	NA	NA	NA	NA
Feature 14	NA	NA	NA	NA	NA	NA	NA	NA
Feature 14 + buffer	NA	NA	NA	NA	NA	NA	NA	NA
Feature 15	2.00	0.30	0.00	0.30	0.01	0.00	−0.01	NA
Feature 15 + buffer	10.32	1.57	0.01	1.59	0.04	0.00	−0.04	−49.2

Table 93. Results of change detection by geomorphic mechanism between May 2019 and June 2020 at monitoring location WGC-1, western Grand Canyon, Arizona.

[NA indicates mechanisms not identified in the survey. m^2, square meter; m^3, cubic meter; %, percent]

Spatial subdivision	Area (m^2)			Volume (m^3)			Percent imbalance (%)
	Erosion	Deposition	Total	Erosion	Deposition	Net	
Baseline survey area							
Fluvial	0.14	0.52	0.66	0.00	0.03	0.02	35.7
Aeolian	121.15	78.38	199.53	5.65	3.53	−2.12	−11.5
Alluvial	11.75	8.68	20.43	0.59	0.45	−0.15	−7.0
Colluvial	2.39	0.25	2.64	0.44	0.03	−0.41	−43.4
Indeterminate	90.48	160.03	250.50	3.36	8.43	5.07	21.5
Archaeological site boundary							
Fluvial	NA	NA	NA	NA	NA	NA	NA
Aeolian	89.24	75.63	164.87	4.31	3.42	−0.89	−5.8
Alluvial	10.83	8.68	19.51	0.56	0.45	−0.12	−5.9
Colluvial	2.38	0.25	2.63	0.44	0.03	−0.41	−43.4
Indeterminate	79.14	154.38	233.51	2.91	8.14	5.23	23.7

Between 2010 and 2020, volumetric change for site G:03:0072 vacillated between erosion and deposition: substantial net erosion occurred in the $DoD_{2010–2013}$, net deposition in the $DoD_{2016–2017}$, net erosion in the $DoD_{2017–2019}$, and net deposition in the $DoD_{2019–2020}$ (fig. 49). The net change in sediment storage from 2010 to 2020 was −6.4 m^3. Change in the archaeological site generally followed the same trend as within the baseline survey area, as they covered much of the same area excluding the locations below the maximum regulated flood inundation elevation (fig. 49). The net change in sediment storage in the archaeological site was −0.51 m^3 between 2010 and 2020. During the first and last DoD intervals, aeolian changes typically covered the largest area, whereas colluvial changes along gully margins produced larger volumetric changes across smaller areas (tables 76–93). Repeat change, specifically for deposition, covered a slightly larger areal extent in comparison to single interval changes (fig. 49). Both repeat and single interval changes were most concentrated near the center of the survey area and alternated spatially with the dominant wind direction toward the north associated with small dune crests and troughs (fig. 49). In the northern part of the extended baseline survey area, repeat change was dominantly erosion that was associated with gullies and the hillslopes adjacent to gullies. South of the archaeological site, repeat changes were also erosional, with most classified as aeolian transport of sand.

Monitoring Location WGC-2

Monitoring location WGC-2 is located in western Grand Canyon on river left within land managed by the Hualapai Tribe. This monitoring location contains one archaeological site, G:03:0041, that was categorized as an aeolian type 3 and drainage type 4 site owing to no upwind sandbar and presence of gullies that run through the site into both the side canyon tributary as well as the Colorado River. Site G:03:0041 was previously surveyed using TLS in May 2006, May 2007, and September 2007; those results are detailed by Collins and others (2009). Between May 2006 and September 2007, much of the surveyed area experienced little topographic change except for minor gully erosion from a sandy surface at the base of rock talus in the northeastern part of the 2006 and 2007 surveys and deposition from slope wash on a lower elevation surface to the south. In June 2020, we resurveyed monitoring location WGC-2 covering a larger area, including a portion of the downstream aeolian dune, the side canyon tributary, and additional gully networks upstream of the archaeological site (fig. 50). The overlapping area between the 2007 and 2020 surveys was 4,914 m^2, which contained the entire archaeological site, and is presented here as the baseline survey area.

In the $DoD_{2007–2020}$, net volume change in sediment storage for the baseline survey area was erosional and net volume change in the archaeological site was depositional (fig. 50; table 94). The largest percentage of these topographic changes were attributed to aeolian processes for both the baseline survey area and the archaeological site (table 94). Within the baseline survey area, a large volume of erosion by wind was attributed to a migrating dune downstream of the side canyon tributary (table 95). Within the upstream portion of the baseline survey area and the archaeological site, alluvial and aeolian processes appeared to be intermixed (fig. 50). Similar to Collins and other's (2009) findings, there was significant erosion within at least two gullies in the archaeological site boundary. This erosion included slumping at the head of a gully

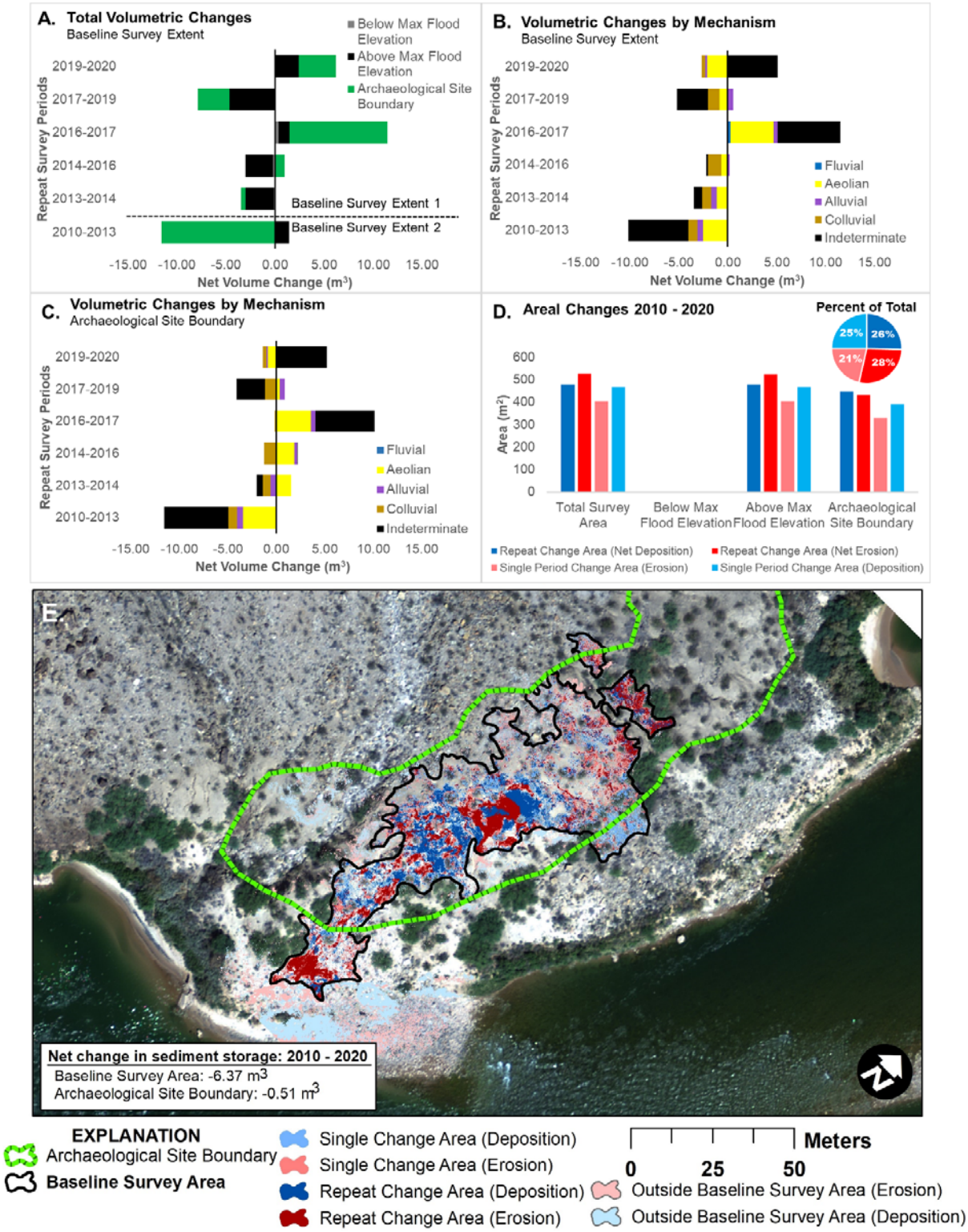

Figure 49. Plots of net volumetric (in cubic meters [m^3]) and areal (in square meters [m^2]) change in sediment storage between September 2010 and June 2020 for monitoring location WGC-1, western Grand Canyon, Arizona. *A*, Change results for the baseline survey area by spatial subdivision. *B*, Change results for the baseline survey area by geomorphic mechanism. *C*, Change results within the boundary of archaeological site G:03:0072 by geomorphic mechanism. Net volumetric changes to the left of the zero line indicate erosion and changes to the right of the zero line indicate deposition. *D*, Plot of change by location with regard to the regulated flood stage elevation (which occurs at a flow rate of 45,000 cubic feet per second) and the archaeological site. *E*, Map of areas that have repeat and single changes. Area of topographic change, net change direction (erosion or deposition), and net change in sediment storage were determined from the summation of all six digital elevation models of difference (DoDs). Repeat change area refers to pixels that have significant change in at least two DoDs. Single period change area refers to pixels that have significant change in only one DoD. Aerial image collected by Grand Canyon Monitoring and Research Center (Durning and others, 2018).

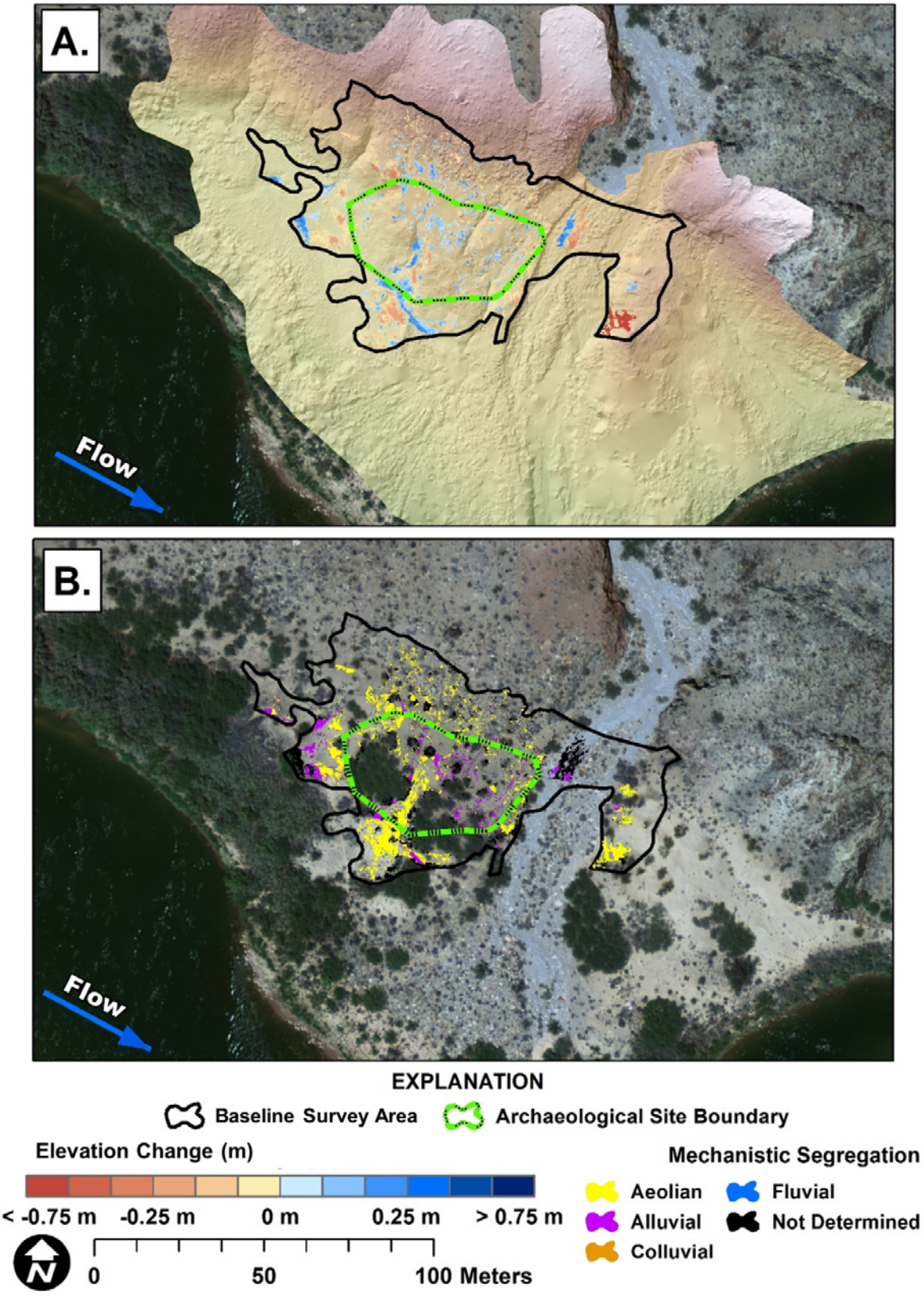

Figure 50. Maps showing change detection results between September 2007 and June 2020 for monitoring location WGC-2, western Grand Canyon, Arizona. *A*, Shaded relief showing elevation change results, in meters (m). Changes are within the 95-percent confidence interval. *B*, Results of automated geomorphic classification changes after Kasprak and others (2017). Aerial image collected by Grand Canyon Monitoring and Research Center (Durning and others, 2018).

Table 94. Results of change detection between September 2007 and June 2020 for the baseline survey area at monitoring location WGC-2, western Grand Canyon, Arizona.

[The archaeological site boundary is included in the above maximum flood elevation subdivision. NA indicates areas outside of the baseline survey. m^2, square meter; m^3, cubic meter; %, percent]

Spatial subdivision	Survey area (m^2)	Area (m^2)			Volume (m^3)			Percent imbalance (%)
		Erosion	Deposition	Total	Erosion	Deposition	Net	
Baseline survey area	4,914.61	413.80	377.80	791.60	59.55	26.95	−32.60	−18.8
Below maximum flood elevation	NA	NA	NA	NA	NA	NA	NA	NA
Above maximum flood elevation	4,914.61	413.80	377.80	791.60	59.55	26.95	−32.60	−18.8
Archaeological site boundary	1,408.94	72.34	161.57	233.92	5.01	9.92	4.91	16.4

Table 95. Results of change detection by geomorphic mechanism between September 2007 and June 2020 at monitoring location WGC-2, western Grand Canyon, Arizona.

[NA indicates mechanisms not identified in the survey. m^2, square meter; m^3, cubic meter; %, percent]

Spatial subdivision	Area (m^2)			Volume (m^3)			Percent imbalance (%)
	Erosion	Deposition	Total	Erosion	Deposition	Net	
Baseline survey area							
Fluvial	NA	NA	NA	NA	NA	NA	NA
Aeolian	252.83	145.90	398.72	42.39	8.99	−33.40	−32.5
Alluvial	33.21	73.64	106.84	2.55	5.22	2.67	17.2
Colluvial	2.57	0.93	3.50	0.84	0.06	−0.78	−43.4
Indeterminate	125.20	157.33	282.53	13.78	12.68	−1.09	−2.1
Archaeological site boundary							
Fluvial	NA	NA	NA	NA	NA	NA	NA
Aeolian	39.20	63.39	102.59	2.84	3.72	0.88	6.7
Alluvial	9.95	34.56	44.51	0.50	1.94	1.44	29.6
Colluvial	0.95	0.10	1.05	0.19	0.01	−0.19	−47.2
Indeterminate	22.24	63.53	85.77	1.48	4.25	2.77	24.2

near the northwestern archaeological site boundary that appeared to have removed a survey control benchmark used during the 2006 and 2007 surveys. At least a portion of the eroded material appeared to be redeposited downslope, where the landscape flattened and gully channels became less defined (fig. 50).

Discussion

The 23 monitoring locations and 30 associated archaeological sites detailed in this report are part of a monitoring program designed to assess how Colorado River management actions, primarily those regarding flow regulation from Glen Canyon Dam, affect archaeological sites in Grand Canyon. As part of this monitoring program, sites were classified using two geomorphic systems that have evolved out of decades of research on rainfall runoff processes and windblown sediment transport at archaeological sites in Grand Canyon (Hereford and others, 1993; Draut and Rubin, 2008; Draut, 2012; Collins and others, 2009, 2012, 2016; East and others, 2016, 2017). These geomorphic classification systems, as well as supporting monitoring data, have been presented in previous reports (Leap and others, 2000; East and others, 2016, 2017). We have updated the geomorphic classifications for 30 archaeological sites, one of which, C:06:0003, has two loci with differing classifications (C:06:0003A and C:06:0003B; appendix 1). For clarity, we present both loci as different sites. Hereafter, we report 31 geomorphic site classifications representing 30 individual sites, one of which, C:06:0003, is split into two spatially discrete loci (table 96; appendix 1).

Synthesis of Geomorphic Site Classifications

The aeolian and drainage geomorphic classifications (defined in detail in the Methods section) provide the framework for predicting mechanisms of sediment erosion and deposition in the archaeological sites studied here as well as other Grand Canyon Colorado River corridor sites that have not been monitored using lidar topographic surveys. For this reason, archaeological sites were sampled to select a diversity of classification combinations. Of the 31 geomorphic site classifications reported here, seven are aeolian type 1 sites (table 96) that exhibit connectivity to the modern active channel of the Colorado River by way of recent fluvial deposition on an upwind sandbar and a pathway for aeolian

sediment transport from the sandbar to the archaeological site that is not obstructed by riparian vegetation or topography. These sites are expected to have the greatest potential for aeolian sediment resupply from sandbars rebuilt by high-flow experiments (HFEs). Aeolian sediment deposition on archaeological sites aids in site preservation, as burial by sediment reduces physical and chemical weathering of cultural material exposed at the ground surface (Butzer, 1982; Ferring, 1986). Aeolian type 1 sites are thus places within the larger Colorado River ecosystem that are especially sensitive to adjustments in river management that affects sediment as well as vegetation resources (East and others, 2016).

Aeolian type 2 sites can also be affected by river management, though effects may be muted by existing vegetative or topographic barriers to aeolian sediment transport from active river channel bars. There are four aeolian type 2a and two aeolian type 2b sites surveyed as part of the present monitoring program (table 96). For seven of these sites, both vegetative and topographic barriers to aeolian sediment transport were present (aeolian type 2c; table 96). Ten aeolian type 3 sites were included in monitoring, representing locations that no longer have an upwind unvegetated river sandbar to serve as a source for aeolian sediment transport toward the archaeological site (table 96), although the presence of widespread aeolian deposits of Colorado River sand imply that there was a historical proximal sediment source.

In the drainage classification results, more than half of the geomorphic site classifications (18 of 31) have mature drainage type 3 and 4 gully networks that have incised to their local base level elevation of either the side canyon tributary channel or the Colorado River (table 96). Drainage type 3 and 4 sites tend to represent terminal states with gullies that may be subject to future lateral erosion but have limited potential for state transitions to a lower order drainage type. The 13 drainage type 1 and 2 sites have comparatively less mature drainage networks that have not yet incised to the channel of the Colorado River or side canyon tributary (table 96). These lower order drainage type sites are sensitive to changes in the external sediment supply, precipitation regimes, or erosion of the river or tributary channels that could contribute to future gully incision.

Three of the four archaeological sites with three or more repeat topographic surveys between 2010 and 2020 (sites C:05:0031, C:013:0321, and B:10:0225), show cumulative increases in sediment storage from 2010 to 2017; sites C:05:0031 and C:13:0321 continue that trend through 2020 (fig. 51). The fourth site, G:03:0072, showed cumulative increases in sediment storage since 2013, though net storage volume has remained below the 2010 baseline survey. These changes in sediment storage indicate that the influx of sediment to those sites exceeded sediment efflux out of those sites. These results are consistent with previously reported findings for aeolian dune fields surrounding the sites (Sankey and others, 2018b) and are evidence that these sites were resupplied with windblown sand from upwind sandbars.

Though lacking the same level of temporal data resolution as the four sites that have multiple repeat surveys, four additional sites that have TLS data from 2010 or earlier were resurveyed for this report. One of these sites, G:03:0041 also showed an increase in sediment storage whereas the other three (C:13:0006, C:13:0346, and C:13:0348) showed net loss of sediment storage. Increases in sediment storage between 2007 and 2020 for site G:03:0041, an aeolian type 3 site, were consistent with Collins and others (2009), who reported that sedimentation occurred from alluvial and colluvial material transported from higher elevation landforms as well as reworking of sediment by wind. Vegetation surrounding the site creates a barrier to aeolian sediment transport of sand from the river channel, but also protects the site from wind erosion. These additional factors seemed to reduce the potential for further degradation of the site condition. The other two aeolian type 3 archaeological sites (C:13:0346 and C:13:0348) were drainage type 2 sites that showed net erosion by wind and gullying between 2010 and 2020, consistent with the 2006, 2007, and 2010 results reported by Collins and others (2009, 2012). Site C:13:0006, an aeolian type 2c and drainage type 3 site, showed a long-term decrease in sediment storage, perhaps owing to the topographic barrier that impedes aeolian sediment transport from the upwind sandbar to the site. In these three cases, the lack of an upwind sediment source appeared to contribute to a more degraded site condition throughout the monitoring period.

Table 96. Summary of the number of geomorphic site classifications that were updated for Colorado River corridor archaeological sites within this study.

[Updated aeolian and drainage type classes are reported by monitoring location and archaeological site in appendix 1]

Aeolian type	Drainage type				Total
	1	2	3	4	
1	1	2	1	3	7
2a	0	1	1	2	4
2b	1	0	1	0	2
2c	0	1	4	2	7
3	3	4	0	3	10
4	0	0	1	0	1
Total	5	8	8	10	31

Synthesis of Geomorphic Change

Geomorphic change in archaeological sites is inferred through changes in sediment storage measured between repeat topographic surveys and observed differences in the drainage and aeolian geomorphic site classifications. The magnitudes of volumetric changes in sediment storage measured at the same site over multiple years are useful metrics to track erosion, deposition, and sediment transport. However, differences in volumetric changes in sediment storage (for example, fig. 51*A*) are not easily compared from one location to another, as archaeological sites can cover substantially different geographic extents and were surveyed repeatedly at different time intervals. To make change detection results more comparable among sites, we normalized volumetric change in

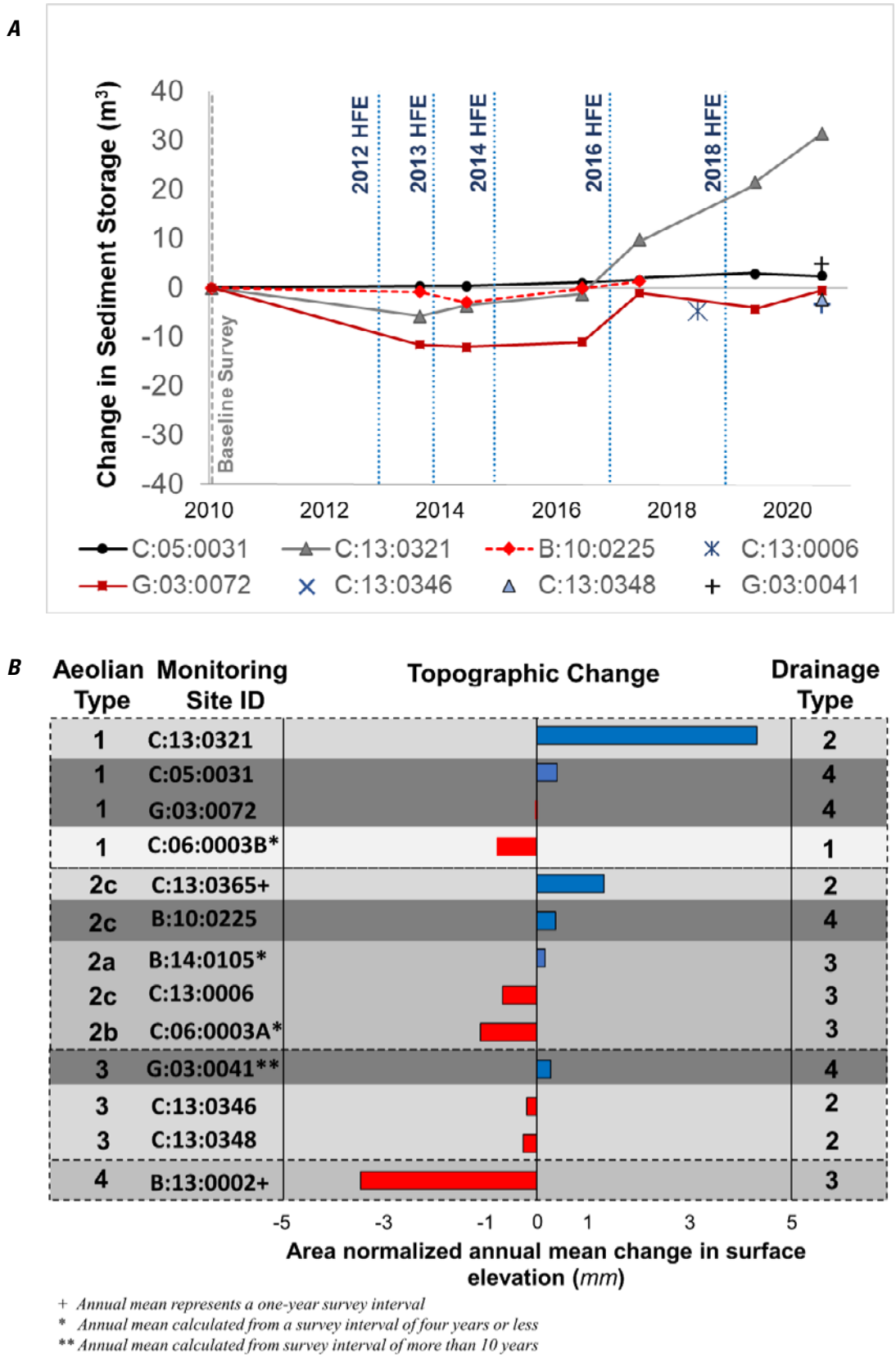

Figure 51. Summary plots of changes in sediment storage between 2010 and 2020 for Colorado River corridor archaeological sites that have repeat surveys. Changes in sediment storage represent the summation of detected volumetric changes from high-resolution digital elevation models of difference (DoDs). *A*, Net volumetric change (in cubic meters [m^3]) in sediment storage calculated as the sum of net volume changes of all survey intervals after the 2010 baseline survey (zero net change) for all sites except site G:03:0041, which had a 2007 baseline survey. Though sites C:13:0006, C:13:0346, C:13:0348, and G:03:0041 lack the same temporal resolution as the other four sites, results are shown for purposes of discussion about differing aeolian and drainage classification types. Blue dashed lines show when high-flow experiments (HFEs) occurred. *B*, Mean annual change in surface elevation (in millimeters [mm]) normalized by area. Mean annual changes for sites C:13:0365 and B:13:0002 represent a survey interval of only 1 year, sites C:06:0003A, C:06:0003B, and B:14: 0105 have a survey interval of 3 to 4 years, and all other sites have a survey interval of 7 or more years.

sediment storage (in cubic meters [m^3]) by dividing it by the number of years between survey intervals and dividing the result by site area (in square meters [m^2]) to produce an area-normalized mean annual change in surface elevation (expressed in millimeters [mm]) (Collins and others, 2012; fig. 51*B*). Eight of the 13 sites that have repeat surveys had a maximum survey interval of at least 7 years, one site (B:14:0105) had a maximum survey interval of 4 years, two sites (C:06:0003A and C:06:0003A) had a maximum survey interval of 3 years, and two sites (C:13:0365 and B:13:0002) had a maximum survey interval of only 1 year. Of these 13 sites, four were aeolian type 1 and two aeolian type 1 sites were drainage type 4. Though the other three aeolian type 1 sites had positive to near-neutral average annual changes in sediment storage, site C:06:0003B exhibited a greater proportion of erosion (fig. 51). This was expected as site C:06:0003B was further from aeolian and hillslope sediment sources than any of the other sites and therefore had a lower potential for external resupply of sediment during the 3-year survey interval. The other three sites all had a greater potential to be resupplied with windblown river-sourced sediment as well as sediment from higher elevation landforms. In contrast, site C:13:0321 was closer to the active river channel and an upwind sandbar compared to the other sites and had the greatest recorded average wind strength and directional consistency (Collins and others, 2016; East and others, 2016; Sankey and others, 2018b), which likely contributed to its greater volume of deposition (fig. 51). Site C:13:0321 was thus particularly sensitive in terms of geomorphic response to river management actions, such as controlled flooding from HFEs (East and others, 2016; Sankey and others, 2018b).

In addition to the four aeolian type 1 sites, there were five type 2 sites, three type 3 sites, and one type 4 site (fig. 51). Five of the nine sites experienced a net loss in sediment storage and four showed net gains in sediment storage (fig. 51). The sites that gained sediment (B:10:0225, B:14:0105, C:13:0365, and G:03:0041), as well as sites C:13:0346 and C:13:0348, which lost sediment, were similar in that they are located in areas with active aeolian sediment and are also downslope from higher elevation landforms that shed sediment during rainfall-runoff events. Of these sites, site C:13:0365 had the greatest increase in sediment storage, though this site only had a 1-year survey interval, precluding definitive inferences regarding longer term sediment dynamics at the site. This monitoring location had an active aeolian dune on the downstream part of the sandbar, open unvegetated sand upwind of the archaeological site, and a mix of talus and unconsolidated sediment on the nearby higher elevation landform that may have made this location better positioned to be resupplied with sediment from both aeolian and hillslope processes.

In agreement with previous work by East and others (2016), the topographic changes measured at aeolian type 1 sites appear to be more strongly influenced by wind and the connectivity between sandbars and the landscape directly downwind. Sites with barriers to sediment transport or loss of aeolian sand sources are still influenced by wind, but the dominant source of incoming sediment is from higher elevation landforms. Without connectivity to either upwind or hillslope sources of sediment supply, sites appear to be more likely to erode and thus degrade.

There are 12 monitoring locations that have been surveyed once and lack a repeat survey at the time of this report. These locations and associated archaeological sites will be quantitatively evaluated for topographic change during future investigations. However, some inferences can be made about predicted geomorphic changes by looking at deviations in the updated classifications within this report from previous drainage type classifications completed in 2000 by Leap and others (2000) and aeolian type classifications completed for 1973 data by East and others (2016). A conceptual framework for interpretation of geomorphic classification type changes was demonstrated for archaeological sites along the Colorado River in Glen Canyon National Recreation Area by East and others (2017). In that framework, changes from lower numerical values to higher numerical values in both the aeolian and drainage classifications (for example, aeolian type 1 to aeolian type 2a and drainage type 1 to drainage type 2) represent decreased influx of river sediment via aeolian transport and increased gullying from overland flow erosion, and thus are interpreted as a transition to a more degraded state.

Here, we summarize those changes in classifications for the 31 archaeological sites within the 23 monitoring locations as increases, decreases, or no change with regard to previously reported values (Leap and others, 2000; East and others, 2016; table 97). Within the updated classifications, both the aeolian and drainage type increased at seven archaeological sites (table 97): A:16:0004, B:10:0225, C:05:0237, C:13:0006, C:13:0069, G:03:0032, and G:03:0044. In all seven cases, class changes were associated with growth of a riparian vegetative barrier and the incision of gullies to the active Colorado River channel, and indicate that the geomorphic condition of the seven sites degraded.

Table 97. Summary of changes in aeolian and drainage classifications for Colorado River corridor archaeological sites.

[Updated aeolian and drainage type classes are reported by monitoring location and archaeological site in appendix 1. Aeolian type changes occurred between 1973 and 2012 (East and others, 2016). Drainage type changes occurred between 2000 (Leap and others, 2000) and 2018. Increase indicates a change from lower to higher number aeolian or drainage type and decrease indicates the opposite direction of change (for example, type 1 to type 2a is an increase, type 2c to type 2b is a decrease). Not determined indicates that no previous drainage classification was available. The 31 geomorphic classifications represent 30 archaeological sites, one of which is divided into two loci]

Aeolian type	Drainage type				Total
	Increase	Decrease	No change	Not determined	
Increase	7	2	9	3	21
Decrease	0	0	0	0	0
No change	0	1	5	4	10
Total	7	3	14	7	31

One archaeological site, G:03:0032, exhibited an increase in aeolian type number with a decrease in drainage type number (table 97; appendix 1). These changes are because of an increase in riparian vegetation that reduced sediment transport by wind and may also be partly responsible for diverting a gully from terminating at the river (drainage type 4) to instead terminating at the side canyon tributary channel (drainage type 3; appendix 1). These changes indicate that site G:03:0032 transitioned to a more degraded geomorphic site condition.

Nine classified sites (B:10:0237, C:13:0393, C:13:0005, A:15:0005, C:13:0365, C:13:0346, C:13:0348, G:03:0058, and G:03:0041) transitioned to higher aeolian type numbers without apparent changes in drainage classification and thus indicate a more degraded geomorphic condition (table 97). Of these nine sites, all had upwind river channel bars that were overgrown with riparian vegetation and were subjected to other changes in the river shoreline after 1973. Site C:13:0393 transitioned from aeolian type 1 to 2a between 1984 and 1996 and then to aeolian type 3 in the most recent interval, likely exhibiting the most significant reduction in fluvial-aeolian sediment connectivity among the sites monitored in this report. Two sites (A:15:0005 and C:13:0365) incurred an increase in riparian vegetation and transitioned from aeolian type 2b with topographic barriers to aeolian type 2c with topographic and vegetative barriers to aeolian sediment transport.

Three classified sites (B:14:0105, C:13:0321, and G:03:0080) decreased in drainage type (table 97; appendix 1). Sites B:14:0105 and G:03:0080 transitioned from drainage type 4 to 3, owing to alteration of gullies by the expansion of riparian vegetation. This change resulted in the existing side canyon channel-based gullies becoming the most significant gullies at the site and likely does not represent a marked improvement in the site condition. Site C:13:0321 transitioned from a drainage type 4 to a type 2 owing to differing interpretation of run-off pathways as originally classified by Leap and others (2002). This change in classification does not represent a change in the geomorphic condition of the site.

There were five classified archaeological sites, including two with reported change detection results (C:05:0031 and G:03:0072), that exhibited no changes in geomorphic classification and thus are interpreted as having stable geomorphic site conditions. Three of the five sites are drainage type 4 (C:05:0031, B:15:0138, and G:03:0072) with existing gullies that could be subject to future lateral erosion but have limited potential for state transitions to a lower order drainage type. However, the other two of the five sites (B:14:0095 and C:13:0092) are drainage type 1 or 2 and thus have less mature drainage networks with gullies that could incise to the river or side canyon tributary channels in the future. Site B:14:0095 is aeolian type 1 and thus retains some sediment connectivity with an upwind sandbar. Though site B:14:0095 is interpreted as stable at present, it is expected to be particularly sensitive to river management of controlled flooding by HFEs that may influence sediment availability in the future.

Conclusion

This report is a comprehensive synthesis of high-resolution topographic monitoring data from 2010 to 2020 for a set of archaeological sites along the Colorado River in Grand Canyon. Some of the data have been reported in previous publications, whereas some of the data are new and reported here for the first time. These data cover a sample of a much larger population of Colorado River archaeological sites in Grand Canyon that are being qualitatively monitored by a separate National Park Service (NPS) program. Within this report, we present monitoring data collected for 30 archaeological sites at 23 monitoring locations using ground-based light detection and ranging (lidar). We produced 5-centimeter-resolution DEMs at each site as a baseline for assessing changes in the geomorphic condition of archaeological sites in relation to operations of Glen Canyon Dam. Ground-based lidar surveys were repeated at 11 monitoring locations, permitting us to quantitatively assess topographic changes that are primarily related to changes in the erosion, deposition, and storage of river sediment. In general, sediment transport by wind and river processes were the dominant mechanisms of identifiable changes and highlight that the connectivity, or transfer, of sediment between riverine and upland environments is important for the geomorphic condition of many archaeological sites within the Colorado River corridor.

To complement the NPS monitoring program, the quantitative high-resolution topographic monitoring results presented in this report focus on sites sampled by geomorphic context, using previous geomorphic classification frameworks, including the aeolian classification, which characterizes the potential for sediment transport by wind between sandbars and archaeological sites, and the drainage classification, which characterizes the potential for erosion by local rainfall runoff and gullying at archaeological sites (East and others, 2016, 2017). For the 30 archaeological sites within this report, we present 31 unique geomorphic site classifications that were updated to qualitatively identify important changes in site geomorphic condition that have occurred since the original classifications were conducted more than a decade ago. Changes in geomorphic classifications can be related to Colorado River management (East and others, 2016, 2017). We found that five of the sites did not change in either aeolian or drainage classifications, four sites were not previously classified by drainage type with no change in aeolian classification, and 22 of the sites changed in one or both classifications. Of the sites that changed classification, most (21 out of 22) transitioned to a more degraded geomorphic condition.

The monitoring records contained within this report provide a foundation for future monitoring of landscape changes at these and other archaeological sites based on the use of repeated high-resolution topographic surveys. These detailed datasets and quantitative measurements are expected to provide helpful insights

to managers of cultural resources along the Colorado River in Grand Canyon about the rates, volumes, and extents of changes that can be attributed to geomorphic processes, some of which are directly related to current dam operations. Our results provide a baseline record of measured topographic changes for assessing significant effects on cultural resource integrity over time and to help plan future risk management and mitigation strategies. The long-term topographic survey and change detection datasets acquired for monitoring the dynamic geomorphic condition of archaeological sites also provide a unique record of sediment transfer among coupled fluvial, aeolian, and alluvial (hillslope or rainfall-runoff) systems that is likely to be relevant to other river valleys in addition to the Colorado River in Grand Canyon.

References Cited

Butzer, K.W., 1982, Archaeology as Human Ecology: Cambridge University Press, 380 p., https://doi.org/10.1017/CBO9780511558245.

Caster, J.J., Dealy, T., Andrews, T., Fairley, H., Draut, A., and Sankey, J.B., 2014, Meteorological data for selected sites along the Colorado River Corridor, Arizona, 2011–13: U.S. Geological Survey Open-File Report 2014–1247, 56 p., https://doi.org/10.3133/ofr20141247.

Caster, J.J., and Sankey, J.B., 2016, Variability in rainfall at monitoring stations and derivation of a long-term rainfall intensity record in the Grand Canyon region, Arizona, USA: U.S. Geological Survey Scientific Investigations Report 2016–5012, 38 p., https://doi.org/10.3133/sir20165012.

Caster, J.J., Sankey, J.B., and Fairley, H., 2018, Meteorological data for selected sites along the Colorado River corridor, Arizona, 2014–2015: U.S. Geological Survey data release, https://doi.org/10.5066/F7DZ0771.

Collins, B.D., Bedford, D.R., Corbett, S.C., Cronkite-Ratcliff, C., and Fairley, H.C., 2016, Relations between rainfall–runoff-induced erosion and aeolian deposition at archaeological sites in a semi-arid dam-controlled river corridor: Earth Surface Processes and Landforms, v. 41, no. 7, p. 899–917, https://doi.org/10.1002/esp.3874.

Collins, B.D., Brown, K.M., and Fairley, H.C., 2008, Evaluation of terrestrial LIDAR for monitoring geomorphic change at archeological sites in Grand Canyon National Park, Arizona: U.S. Geological Survey Open-File Report 2008–1384, 60 p., https://doi.org/10.3133/ofr20081384.

Collins, B.D., Corbett, S.C., Fairley, H.C., Minasian, D., Kayen, R., Dealy, T.P., and Bedford, D.R., 2012, Topographic change detection at select archeological sites in Grand Canyon National Park, Arizona, 2007–2010: U.S. Geological Survey Scientific Investigations Report 2012–5133, p., https://doi.org/10.3133/sir20125133.

Collins, B.D., Minasian, D.L., and Kayen, R., 2009, Topographic change detection at select archeological sites in Grand Canyon National Park, Arizona, 2006-2007: U.S. Geological Survey Scientific Investigations Report 2009–5116, 59 p., https://doi.org/10.3133/sir20095116.

Cook, T., East, A., Fairley, H., and Sankey, J.B., 2019, Managing sand along the Colorado River to protect cultural sites downstream of Glen Canyon Dam: U.S. Geological Survey Fact Sheet 2019–3054, 6 p., https://doi.org/10.3133/fs20193054.

Dealy, T.P., Draut, A.E., and Fairley, H.C., 2014, 2010 weather and aeolian sand-transport data from the Colorado River corridor, Grand Canyon, Arizona: U.S. Geological Survey Open-File Report 2014–1135, 90 p., https://doi.org/10.3133/ofr20141135.

Draut, A.E., 2012, Effects of river regulation on aeolian landscapes, Colorado River, southwestern USA: Journal of Geophysical Research Earth Surface, v. 117, 22 p., https://doi.org/10.1029/2011JF002329.

Draut, A.E., Sondossi, H.A., Dealy, T.P., Hazel, J.E., Jr., Fairley, H.C., and Brown, C.R., 2010, 2009 weather and aeolian sand-transport data from the Colorado River corridor, Grand Canyon, Arizona: U.S. Geological Survey Open-File Report 2010–1166, 98 p., https://doi.org/10.3133/ofr20101166.

Draut, A.E., Sondossi, H.A., Hazel, J.E., Jr., Andrews, T., Fairley, H.C., Brown, C.R., and Vanaman, K.M., 2009, 2008 weather and aeolian sand-transport data from the Colorado River corridor, Grand Canyon, Arizona: U.S. Geological Survey Open-File Report 2009–1190, 98 p., https://doi.org/10.3133/ofr20091190.

Draut, A.E., and Rubin, D.M., 2008, The role of eolian sediment in the preservation of archeologic sites along the Colorado River corridor in Grand Canyon National Park, Arizona: U.S. Geological Survey Professional Paper 1756, 71 p., https://doi.org/10.3133/ofr20071001.

Durning, L.E., Sankey, J.B., Bedford, A., and Sankey, T.T., 2018, Riparian species vegetation classification data for the Colorado River within Grand Canyon derived from 2013 airborne imagery: U.S. Geological Survey data release, https://doi.org/10.5066/F7K64GJF.

East, A.E., Collins, B.D., Sankey, J.B., Corbett, S.C., Fairley, H.C., and Caster, J., 2016, Conditions and processes affecting sand resources at archeological sites in the Colorado River corridor below Glen Canyon Dam, Arizona: U.S. Geological Survey Professional Paper 1825, 104 p., https://doi.org/10.3133/pp1825.

East, A.E., Sankey, J.B., Fairley, H.C., Caster, J.J., and Kasprak, A., 2017, Modern landscape processes affecting archaeological sites along the Colorado River corridor downstream of Glen Canyon Dam, Glen Canyon National Recreation Area, Arizona: U.S. Geological Survey Scientific Investigations Report 2017–5082, 22 p., https://doi.org/10.3133/sir20175082.

Fairley, H.C., and Sondossi, H., 2010, Applying an ecosystem framework to evaluate archaeological site condition along the Colorado River in Grand Canyon National Park, Arizona, *in* Melis, T.S., Hamill, J.F., Bennett, G.E., Coggins, L.G., Jr., Grams, P.E., Kennedy, T.A., Kubly, D.M., and Ralston, B.E., eds., Proceedings of the Colorado River Basin Science and Resource Management Symposium, November 18–20, 2008, Scottsdale, Arizona: U.S. Geological Survey Scientific Investigations Report 2010–5135, 372 p., https://doi.org/10.3133/sir20105135.

Ferring, C.R., 1986, Rates of fluvial sedimentation—Implications for archaeological variability: Geoarchaeology, v. 1, no. 3, p. 259–274, https://doi.org/10.1002/gea.3340010303.

Grams, P.E., Topping, D.J., Schmidt, J.C., Hazel, J.E., and Kaplinski, M., 2013, Linking morphodynamic response with sediment mass balance on the Colorado River in Marble Canyon—Issues of scale, geomorphic setting, and sampling design: Journal of Geophysical Research Earth Surface, v. 118, no. 2, p. 361–381, https://doi.org/10.1002/jgrf.20050.

Hazel, J.E., Jr., Grams, P.E., Schmidt, J.C., and Kaplinski, M., 2010, Sandbar response in Marble and Grand Canyons, Arizona, following the 2008 high-flow experiment on the Colorado River: U.S. Geological Survey Scientific Investigations Report 2010–5015, 52 p., https://doi.org/10.3133/sir20105015.

Hereford, R., Fairley, H.C., Thompson, K.S., and Balsom, J.R., 1993, Surficial geology, geomorphology, and erosion of archeologic sites along the Colorado River, eastern Grand Canyon, Grand Canyon National Park, Arizona: U.S. Geological Survey Open-File Report 93–517, 46 p., https://doi.org/10.3133/ofr93517.

Kasprak, A., Caster, J., Bangen, S.G., and Sankey, J.B., 2017, Geomorphic process from topographic form—Automating the interpretation of repeat survey data in river valleys: Earth Surface Processes and Landforms, v. 42, p. 1,872–1,883, https://doi.org/10.1002/esp.4143.

Kasprak, A., Sankey, J.B., Buscombe, D., Caster, J., East, A.E., and Grams, P.E., 2018, Quantifying and forecasting changes in the areal extent of river valley sediment in response to altered hydrology and land cover: Progress in Physical Geography; Earth and Environment, p. 739–764, https://doi.org/10.1177/0309133318795846.

Kasprak, A., Sankey, J.B., and Butterfield, B.J., 2021, Future regulated flows of the Colorado River in Grand Canyon foretell decreased areal extent of sediment and increases in riparian vegetation: Environmental Research Letters, v. 16, no. 1, article no. 014029, https://doi.org/10.1088/1748-9326/abc9e4.

Leap, L.M., Kunde, J.L., Hubbard, D.C., Andrews, N., Downum, C.E., Miler, A., and Balsom, J.R., 2000, Grand Canyon Monitoring Project 1992–1999—Synthesis and Annual Monitoring Report FY99: [Report prepared for] Bureau of Reclamation Grand Canyon National Park River Corridor Monitoring Project Report No. 66, 285 p.

Magirl, C.S., Breedlove, M.J., Webb, R.H., and Griffiths, P.G., 2008, Modeling water-surface elevations and virtual shorelines for the Colorado River in Grand Canyon, Arizona: U.S. Geological Survey Scientific Investigations Report 2008–5075, 32 p., https://doi.org/10.3133/sir20085075.

Norman, L.M., Sankey, J.B., Dean, D., Caster, J., DeLong, S., DeLong, W., and Pelletier, J.D., 2017, Quantifying geomorphic change at ephemeral stream restoration sites using a coupled-model approach: Geomorphology, v. 283, no. 15, p. 1–16, https://doi.org/10.1016/j.geomorph.2017.01.017.

Sankey, J.B., Kasprak, A., Caster, J., East, A.E., and Fairley, H.C., 2018a, The response of source-bordering aeolian dunefields to sediment-supply changes 1—Effects of wind variability and river-valley morphodynamics: Aeolian Research, v. 32, p. 228–245, https://doi.org/10.1016/j.aeolia.2018.02.005.

Sankey, J.B., Caster, J., Kasprak, A., and East, A.E., 2018b, The response of source-bordering aeolian dunefields to sediment-supply changes 2—Controlled floods of the Colorado River in Grand Canyon, Arizona, USA: Aeolian Research, v. 32, p. 154–169, https://doi.org/10.1016/j.aeolia.2018.02.004.

Sankey J.B., and Draut A.E., 2014, Gully annealing by aeolian sediment—Field and remote-sensing investigation of aeolian–hillslope–fluvial interactions, Colorado River corridor, Arizona, USA: Geomorphology, v. 220, no. 1, p. 68–80, https://doi.org/10.1016/j.geomorph.2014.05.028.

U.S. Department of the Interior, 1996, Operation of Glen Canyon Dam Final Environmental Statement: Bureau of Reclamation Upper Colorado Region FES 95-98, 15 p., accessed September 16, 2020, at https://www.usbr.gov/uc/envdocs/rod/Oct1996_OperationGCD_ROD.pdf.

U.S. Department of the Interior, 2016, Record of Decision for the Glen Canyon Dam Long-Term Experimental and Management Plan Final Environmental Impact Statement: Bureau of Reclamation Upper Colorado Region FES 2016, 195 p., accessed September 16, 2020, at http://ltempeis.anl.gov/documents/docs/LTEMP_ROD.pdf.

Wheaton, J.M., Brasington, J., Darby, S.E., and Sear, D.A., 2010, Accounting for uncertainty in DEMs from repeat topographic surveys—Improved sediment budgets: Earth Surface Processes and Landforms, v. 35, p. 136– 156, https://doi.org/10.1002/esp.1886.

Appendix 1. Summary of Monitoring Activity and Site Classifications

Table 1.1. Summary of Grand Canyon corridor monitoring locations and associated archaeological sites surveyed between 2010 and 2020 in this report.

[The aeolian and drainage classification values are the most recent designation determined during fieldwork between 2010 and 2022. Classification values in parentheses are aeolian type classifications from 1973 determined by East and others (2016) and drainage type classifications from 2000 determined by Leap and others (2000); values are only given for those sites that changed type. lidar, light detection and ranging; NPS, National Park Service]

Monitoring location	Archaeological site	Aeolian type classification (previous classification)	Drainage type classification (previous classification)	Monitoring Activity
NMC-1[a]	C:06:0003A	2b	3	Lidar survey (spring 2017, summer 2020)
NMC-1[a]	C:06:0003B	1	1	Lidar survey (spring 2017, summer 2020)
CMC-1[a]	C:05:0031	1	4	Weather station (2007–2018), lidar survey (fall 2010, fall 2013, spring 2014, spring 2016, spring 2017, spring 2019, summer 2020), NPS vegetation management (spring 2019, fall 2020)
CMC-2	C:05:0037	2a (1)	4 (2)	Lidar survey (spring 2017, spring 2018)
SMC-1[a]	C:13:0006	2c (2b)	3 (2)	Weather station (2008–2011), lidar survey (fall 2010, spring 2018)
SMC-2	C:13:0365	2c (2b)	2	Weather station (2008–2011), lidar survey (spring 2018, spring 2019)
EGC-1	C:13:0321	1	2 (4)	Weather station (2007–2020), lidar survey (fall 2010, fall 2013, spring 2014, spring 2016, spring 2017, spring 2019, summer 2020), NPS vegetation management (spring 2019, fall 2020)
EGC-1	C:13:0009	1	3	Lidar survey (spring 2019, summer 2020)
EGC-1	C:13:0092	3	1	Lidar survey (spring 2019, summer 2020)
EGC-2	C:13:0346	3 (1)	2	Weather station (2007–2020; same as EGC-1), lidar survey (fall 2010, summer 2020)
EGC-2	C:13:0348	3 (1)	2	Lidar survey (fall 2010, summer 2020)
EGC-3	C:13:0069	2a (1)	4 (2)	Lidar survey (spring 2018)
EGC-4	C:13:0005	3 (2b)	2	Lidar survey (spring 2018)
EGC-4	C:13:0393	3 (1)	1	Lidar survey (spring 2018)
EGC-4	C:13:0392	3 (2b)	1	Lidar survey (spring 2018)
EGC-5	B:16:0911	2c (2b)	3	Lidar survey (summer 2020)
EGC-6	B:15:0138	1	4	Lidar survey (spring 2016)
EGC-7[a]	B:14:0105	2a (1)	3 (4)	Lidar survey (spring 2016, spring 2019, summer 2020), NPS vegetation management (spring 2019, fall 2020)
EGC-8	B:14:0094	2b	1	Lidar survey (spring 2018)
EGC-8	B:14:0095	1	2	Lidar survey (spring 2018)
CGC-1[a]	B:10:0225	2c (1)	4 (1)	Weather station (2007–2020), lidar survey (fall 2010, fall 2013, spring 2014, spring 2016, spring 2017)
CGC-2	B:10:0237	2a (1)	2	Lidar survey (spring 2017)
CGC-3[a]	B:13:0002	4 (3)	3	Lidar survey (spring 2019, summer 2020)
WGC-1[a]	G:03:0072	1	4	Weather station (2007–2020), lidar survey (fall 2010, fall 2013, spring 2014, spring 2016, spring 2017, spring 2019, summer 2020), NPS vegetation management (spring 2019, fall 2020)
WGC-2[a]	G:03:0041	3 (2b)	4	Lidar survey (fall 2007, summer 2020)
WGC-3	A:16:0004	2c (2b)	4 (2)	Lidar survey (spring 2018)
WGC-4	A:15:0005	2c (2b)	4	Lidar survey (spring 2016)
WGC-5	G:03:0032	3 (2b)	4 (2)	Lidar survey (spring 2018)
WGC-5	G:03:0044	3 (1)	4 (2)	Lidar survey (spring 2018)
WGC-6	G:03:0058	3 (1)	2	Lidar survey (spring 2016)
WGC-7	G:03:0080	2c (2b)	3 (4)	Lidar survey (spring 2018)

[a]Location was surveyed using terrestrial lidar more than once during the reporting period.

Table 1.2. Summary of previous monitoring activity not covered in this report.

[The aeolian and drainage classification values are the most recent designation determined during fieldwork between 2010 and 2022. Classification values in parentheses are aeolian type classifications from 1973 determined by East and others (2016) and drainage type classifications from 2000 determined by Leap and others (2000); values are only given for those sites that changed type. lidar, light detection and ranging]

Monitoring location	Archaeological site	Aeolian type classification (previous classification)	Drainage type classification (previous classification)	Monitoring activity
SMC-1[a]	C:13:0006	2c (2b)	3 (2)	Lidar survey (spring 2006, spring 2007, fall 2007, spring 2010)
EGC-1[a]	B:10:0225	2c (1)	4 (1)	Lidar survey (spring 2010)
CGC-1[a]	C:13:0321	1	2 (4)	Lidar survey (fall 2007)
WGC-1[a]	G:03:0072	1	4	Lidar survey (spring 2010)
ND-1	C:13:0099	4 (1)	4	Weather station (2007–2011), lidar survey (spring 2006, spring 2007, fall 2007, spring 2010, fall 2010)
ND-1	C:13:0334	4	4	Lidar survey (spring 2010, fall 2010)
ND-1	C:13:0336	4 (1)	4 (2)	Lidar survey (spring 2006, spring 2007, spring 2010, fall 2010)
EGC-2[a]	C:13:0346	3 (1)	2	Lidar survey (spring 2006, spring 2007, fall 2007)
EGC-2[a]	C:13:0348	3 (1)	2	Lidar survey (spring 2006, spring 2007, fall 2007)
WGC-2[a]	G:03:0041	3 (2b)	4	Lidar survey (spring 2006, spring 2007)
ND-4	G:03:0002	3 (2b)	4	Lidar survey (spring 2006, spring 2007, fall 2007)

[a]Monitoring activity from 2010 or later included in table 1.1.

References Cited

East, A.E., Collins, B.D., Sankey, J.B., Corbett, S.C., Fairley, H.C., and Caster, J., 2016, Conditions and processes affecting sand resources at archeological sites in the Colorado River corridor below Glen Canyon Dam, Arizona: U.S. Geological Survey Professional Paper 1825, 104 p., https://doi.org/10.3133/pp1825.

Leap, L.M., Kunde, J.L., Hubbard, D.C., Andrews, N., Downum, C.E., Miler, A., and Balsom, J.R., 2000, Grand Canyon Monitoring Project 1992–1999—Synthesis and Annual Monitoring Report FY99: [Report prepared for] Bureau of Reclamation Grand Canyon National Park River Corridor Monitoring Project Report No. 66, 285 p.

Moffett Field Publishing Science Center
Manuscript approved October 18, 2022
Edited by Monica Erdman
Layout by Cory Hurd

ISSN 2331-1258 (online)
https://doi.org/10.3133/ofr20221097